USC
UNIVERSIDADE
DE SANTIAGO
DE COMPOSTELA

TESE DE DOUTORAMENTO

CONTRIBUTIONS TO MATHEMATICAL ANALYSIS OF NON-LINEAR MODELS WITH APPLICATIONS IN POPULATION DYNAMICS

Cristina Lois Prados

ESCOLA DE DOUTORAMENTO INTERNACIONAL DA UNIVERSIDADE DE SANTIAGO DE COMPOSTELA

PROGRAMA DE DOUTORAMENTO EN MATEMÁTICAS

SANTIAGO DE COMPOSTELA

2021

USC
UNIVERSIDADE
DE SANTIAGO
DE COMPOSTELA

USC
UNIVERSIDADE
DE SANTIAGO
DE COMPOSTELA

DECLARACIÓN DA AUTORA DA TESE

CONTRIBUTIONS TO MATHEMATICAL ANALYSIS OF NON-LINEAR MODELS WITH APPLICATIONS IN POPULATION DYNAMICS

Dna. Cristina Lois Prados

Presento a miña tese, seguindo o procedemento axeitado ao Regulamento, e declaro que:

1. A tese abarca os resultados da elaboración do meu traballo.

2. De ser o caso, na tese faise referencia ás colaboracións que tivo este traballo.

3. Confirmo que a tese non incorre en ningún tipo de plaxio doutros/as autores/as nin de traballos presentados por min para a obtención doutros títulos.

4. A tese é a versión definitiva presentada para a súa defensa e coincide a versión impresa coa presentada en formato electrónico.

E comprométome a presentar o Compromiso Documental de Supervisión no caso de que o orixinal non estea na Escola.

En Santiago de Compostela, a 21 de xuño de 2021.

Asdo. Cristina Lois Prados

USC
UNIVERSIDADE
DE SANTIAGO
DE COMPOSTELA

AUTORIZACIÓN DOS DIRECTORES/TITORA DA TESE

CONTRIBUTIONS TO MATHEMATICAL ANALYSIS OF NON-LINEAR MODELS WITH APPLICATIONS IN POPULATION DYNAMICS

D. Eduardo Liz Marzán,
Dna. Rosana Rodríguez López

INFORMAN:

Que a presente tese se corresponde co traballo realizado por Dna. Cristina Lois Prados, baixo a nosa dirección/titorización, e autorizamos a súa presentación, considerando que reúne os requisitos esixidos no Regulamento de Estudos de Doutoramento da USC, e que como directores/titora desta non incorren nas causas de abstención establecidas na Lei 40/2015.

De acordo co indicado no Regulamento de Estudos de Doutoramento da USC, declaramos tamén que a presente tese de doutoramento é idónea para ser defendida en base á modalidade Monográfica con reprodución de publicacións, nas que a participación da doutoranda foi decisiva para a súa elaboración e as publicacións axústanse ao Plan de Investigación.

En Vigo/Santiago de Compostela, a 21 de xuño de 2021.

Asdo. Eduardo Liz Marzán

Asdo. Rosana Rodríguez López

USC
UNIVERSIDADE
DE SANTIAGO
DE COMPOSTELA

Aos meus pais,
que, ensinándome e apoiándome,
conseguiron que chegara ata aquí.

USC
UNIVERSIDADE
DE SANTIAGO
DE COMPOSTELA

ACKNOWLEDGEMENTS / AGRADECEMENTOS

PERSONAL / PERSOAL

Esta tese de doutoramento non é só o resultado do esforzo realizado durante estes catro últimos anos, eu tamén a considero o reflexo do camiño percorrido da man dos que me foron acompañando dende os meus inicios e, por suposto, daqueles que se foron unindo, e son eles aos que van dedicadas as seguintes liñas.

Xa fai moito tempo que as miñas primas saben do meu gusto polas Matemáticas, pois parece que cando era unha nena recitaba a táboa de multiplicar en voz alta e tamén lles pedía que me puxeran exercicios de cálculo (seguro que isto non é o peor que tiñan que aguantar...). Sen embargo, a miña primeira vocación foi ser profesora de Educación Física. Tal vez o motivo era que nesa materia non tiñamos deberes. A verdade é que non me gustaba moito traer tarefas para a casa, seguro que os meus pais o poden corroborar, pois teñen pasado horas e horas sentados comigo para que as fixera. A eles teño que agradecerlles toda a dedicación que me prestaron, coa que conseguiron que mellorara as miñas calidades como estudante.

Foi en Bacharelato cando me decatei de que a miña paixón eran as Matemáticas. No primeiro curso, a profesora trataba de ensinarnos a esencia desta ciencia exacta, conseguindo así espertar o meu gusto por ela. No segundo ano mudou o profesor, pero non o meu interese, que se pode dicir que se viu reforzado. A Juan Antonio e a Jose Jorge (Jota) teño que darlles as grazas por orientarme e apoiarme nos meus últimos anos de instituto, pero tamén por acompañarme na miña etapa universitaria.

Agora vén un dos piares fundamentais que sustentan a miña etapa na universidade, sen o que estou segura de que moitos dos éxitos académicos conseguidos non serían posibles. Son os compañeiros que estiveron ao meu carón nos primeiros anos que pasamos na nosa segunda casa, a Facultade de Matemáticas. Estou falando dos integrantes do "Grupo Abierto" ou "Grupo Haveliano" e as rapazas do grupo "Aplicadas". Mención especial para Pilar, Ángela e Uzal. Este piar aumentou de tamaño no ecuador da carreira, cando a promoción 2012/2016 se converteu nunha piña que atopou a maneira de desfrutar do ano máis duro destes estudos. Que bos recordos! Non me esquezo de Rosana e Fernando Costal, os profesores que fixeron que me interesara pola Análise Matemática e as Ecuacións Diferenciais. Tamén quero destacar neste momento o apoio dos meus pais e a miña madriña, que sempre confiaron na miña elección e fixeron todo o que estaba nas súas mans para que esta etapa fora posible.

Tras o Grao en Matemáticas, estudei o Máster en Matemáticas e o que veu despois supoño que o podedes imaxinar. Teño que agradecer a todas esas per-

soas que me animaron a escoller este camiño enriquecedor. En especial, a miña codirectora Rosana, que sempre confiou en min, que me deu liberdade nas miñas eleccións e que me apoiou en todas elas. Tamén, aos meus compañeiros de promoción no doutoramento, que se animaron a compartir esta experiencia xuntos. E non me esquezo da Lorena, a compañeira de piso que me insistía (case) todos os días en que escollera este camiño e á que llo agradezo de corazón.

Para rematar toca falar destes últimos catro anos nos estudos de Doutoramento, nos que tiven moita sorte de estar rodeada de xente marabillosa.

Non atopo palabras para expresar o meu agradecemento cara aos meus codirectores de tese, Rosana e Eduardo. Rosana, presente en todas as miñas etapas na universidade, sempre está pendente dos seus alumnos de doutoramento, tratando de axudarnos e aconsellarnos en todo o que está na súa man e dedicándonos todo o tempo que ten (e tamén o que non ten). Foi con ela coa que me iniciei na investigación na teoría de punto fixo, compartindo comigo a súa experiencia na obtención ou xeneralización deste tipo de resultados. Eduardo deume toda a súa confianza sen case coñecerme e sen a súa axuda non tería obtido os mesmos froitos no ámbito da teoría cualitativa dos sistemas dinámicos. Ademais, unha das cousas que máis valoro del é que pouco a pouco me foi ensinando moitos dos seus grandes valores, tanto profesionais coma persoais. Grazas de verdade por todo o compartido, o tempo adicado, o que me tedes ensinado e as oportunidades brindadas. At this moment, I would also like to dedicate some words to the professors responsible of my research stays in Germany and Romania. I am very grateful to both Frank and Radu for the hospitality I received during my visits, also to their colleagues, specially to Matthew and Adriana, that made me feel as part of their group. When I went to Germany, I was starting to work with discrete-time dynamical systems and Frank introduced me on the more ecology-oriented part of my research work. We met many times to think about the ecological aspects of our joint research and he also recommended me some key references in fisheries management. In Romania, with Radu, we worked in the framework of fixed point theory and I learned a lot of things from him. We met almost every day at the department to think, investigate and work together. I also have a collection of good memories of the meals and travels we shared. Aproveito tamén para agradecer aos profesores que sen dubidalo apoiaron as miñas solicitudes da beca FPU.

Síntome afortunada por ter sufrido e desfrutado a miña etapa no doutoramento rodeada de xente estupenda: os meus compañeiros de doutoramento e achegados, os profesores e outros traballadores da Facultade e, por suposto, os alumnos. Aos compañeiros de doutoramento quero agradecerlles todos os bos consellos e o gran apoio que me deron, a grata compañía que me fixeron, tanto na Facultade coma nos congresos, e os momentos de diversión dos que desfrutamos xuntos (ceas, excursións, pachangas, etc.). En particular, quero mencionar a Pilar, Laura, Uzal, Dani, Sebas e Óscar. Aos profesores e demais traballadores doulles as grazas polo trato recibido, dá gusto ir á cafetería para desconectar e saír cun sorriso, tamén dar clase con profesores que che axudan

e valoran o teu traballo, e agradécese a eficiencia dos traballadores que xestionan a Facultade. Aquí non me esquezo de Alberto, ao que coñecín mellor grazas a impartir unha materia con el, co que compartimos moi bos momentos nas comidas e a quen lle agradezo a confianza depositada en min. Por último, penso que tiven moita sorte cos alumnos que me tocaron, xente traballadora e con ganas de aprender, pero tamén boas persoas ás que dá gusto atoparse pola Facultade.

Xa para rematar, non me esquezo da miña familia e amigos, que sei que pensan que non teñen moito que ver nisto, pero a verdade é que non poido evitar emocionarme ao pensar neles neste momento. Eles son os que máis me aturaron cando tiña un mal día (e probablemente as veces non foi unha tarefa sinxela), xa sabedes que cando hai confianza... Tamén os que conseguiron facerme desconectar, rir, desfrutar, desafogar e devolverme as enerxías que foron tan necesarias ao longo desta etapa. Non sabedes o que valoro o interese que tedes mostrado por seguir os meus avances en algo que vos queda lonxe, tamén a vosa preocupación e o ánimo recibido. Quero citar aquí aos meus pais, ás miñas avoas, aos meus tíos, ás miñas primas Rocío, Rebeca e Laura, a Antonio (o meu adestrador de Bádminton) e aos meus amigos de Cedeira (especialmente a Uxía, Goretti, Iván, Sergio, Luís e Inés). Por último, vou falar dunha das persoas máis importantes para min nesta etapa, Diego. Sempre confiando en min, tamén interesado na miña investigación e nas miñas labores docentes, e sempre disposto a escoitarme falar de temas do doutoramento que me preocupaban, para darme a súa opinión e apoiarme cando máis o necesitaba. Sen dúbida, a persoa que mellor coñece o transcurso desta etapa e a quen lle dedico un agradecemento especial nesta tese.

PUBLICATIONS / PUBLICACIÓNS

We are grateful to the Editors and the anonymous Referees that participated in the reviewing process of the articles being part of this PhD thesis. They have made interesting and helpful comments or suggestions which helped to improve the quality of the manuscript. In addition:

Lois-Prados, Precup, and Rodríguez-López (2020) thank the anonymous referee for suggesting to give a more general application to systems instead of a single equation, and also for giving us the idea to apply the results to boundary value problems for PDEs, a topic for possible future research. We also acknowledge Dr. Daniel Cao Labora for his idea for the proof of Theorem 2.2.

Liz and Lois-Prados (2020a) also thank Dr. Paweł J. Mitkowski for providing the crucial reference (Lasota, 1977).

Liz and Lois-Prados (2020b) acknowledge the anonymous referees for mentioning some useful references. We also thank professor Frank M. Hilker for his constructive comments on a first version of the manuscript.

Last but not least, I would like to thank the institutions that provided me financial support through my PhD studies; without these facilities the PhD experience may have never become real.

During this period, I was recruited under several contracts:

- Research support technician contract funded by *Consolidación e Estructuración Redes* 2016 *GI*-1561 *IEMATH-GALICIA*, from October 3rd, 2017 to April 15th, 2018.
- Research support technician contract funded by *Consolidación e Estructuración* 2015 *GRC GI*-1561 *Ecuacións Diferenciais Non Lineais EDNL*, from April 16th, 2018 to May 30th, 2018.
- PhD scholarship ED481A–2018/080 funded by *Xunta de Galicia (Spain)*, from May 31th, 2018 to September 22nd, 2019.
- PhD scholarship FPU18/00719 funded by *Ministerio de Ciencia, Innovación y Universidades (Spain)*, from September 23rd, 2019 to the date of defense of this thesis.

My research work was also supported by the projects MTM2016–75140–P (Agencia Estatal de Investigación and FEDER) and ED431C2019/02 (Xunta de Galicia), in particular, they gave me the possibility to attend many conferences on the topics of my thesis.

I have already mentioned that I fortunately had the opportunity to spent some months working with two outstanding researchers at international institutions, where I really improved my research skills:

- The research stay supervised by professor Frank M. Hilker at the Institute of Environmental Systems Research (Osnabrück University, Germany) for a period of one month and a half was supported by Osnabrück University. The basis of the research work in (Lois-Prados and Hilker, submitted) was conducted during that period.
- The research stay supervised by professor Radu Precup at the Department of Mathematics (Babeş-Bolyai University, Romania) for a period of three months was supported by the PhD scholarship ED481A–2018/080. During this period, we developed the research in (Lois-Prados, Precup, and Rodríguez-López, 2020) and (Lois-Prados and Precup, 2020).

ABSTRACT

The PhD thesis contains two different research topics, both related with the application of mathematical analysis to non-linear models. On the one hand, we deal with the development of fixed-point theory techniques and their applications to boundary or initial value problems for ordinary differential equations. On the other hand, by means of the qualitative theory of dynamical systems, we study the dynamics of smooth and non-smooth discrete-time population models combining analytical results and numerical tools. We provide now a brief description of the contents of each research line, while a more detailed information for each chapter is given in the Preface.

In fixed point theory, there exist a huge amount of generalizations of the Theorem of Krasnosel'skii in cones, whose proofs normally make use of topological results, such as those corresponding to degree theory. In this monograph, we try to generalize this result by means of the classical theory. Furthermore, we have realized that fixed-point theorems, which allow to prove the existence and to localize solutions to boundary or initial value problems for differential equations, have been applied to a wide range of problems in different fields, however we found a gap in their application to some particular population models, where we provide some contributions.

In the framework of discrete-time one-dimensional dynamical systems, we pay special attention to the influence of parameters on population asymptotic dynamics. In particular, we are interested in determining parameter values such that all initial conditions converge to an equilibrium (global stability); as well as those that produce qualitative changes on the asymptotic dynamics (bifurcations) or other interesting features, such as multi-stability, extinction windows, hydra effect, etc. One issue of particular interest is the study of bifurcations in continuous and discontinuous piecewise-smooth systems arising from the application of protective fisheries management policies. They involve border- and boundary-collision bifurcations, basin boundary metamorphoses and the well-known smooth bifurcations. We also consider a smooth model for blood cell production, which can be used for modeling populations with adult survivorship. In this case, we completely determine the stability of fixed points and find some interesting features in the bifurcation diagrams, such as different ways in which a sudden collapse occurs.

A tese doutoral contén o desenvolvemento de dúas liñas de investigación dentro da rama da análise matemática dos modelos non lineares. Por unha banda, trabállase no desenvolvemento de técnicas de punto fixo e na súa aplicación a problemas de fronteira ou de valor inicial para ecuacións diferenciais ordinarias. Por outra banda, facendo uso da teoría cualitativa dos sistemas dinámicos discretos, estudamos a dinámica de modelos de poboación, regulares e non regulares, mediante resultados analíticos e ferramentas numéricas. No que segue, facemos unha breve descrición dos contidos de cada liña de investigación, mentres que unha información detallada por capítulos pode consultarse o Resumo Estendido.

Dentro da teoría de punto fixo, é ben coñecido o Teorema de Krasnosel'skii en conos, do que hoxe en día existen un gran número de xeneralizacións cuxas probas se realizan en certa medida facendo uso de recursos topolóxicos como a teoría do grao. Neste documento, intentaremos establecer xeneralizacións deste resultado a través de resultados clásicos da análise matemática. No que respecta ás aplicacións, este tipo de resultados úsase para probar a existencia e localizar solucións a problemas de fronteira. A pesar de que a variedade de problemas ós que se teñen aplicado é considerablemente ampla, percíbese unha carencia na literatura sobre a aplicación destes resultados a certos problemas de dinámica de poboacións, onde faremos algunha achega.

No contexto dos sistemas dinámicos discretos unidimensionais, poñemos especial atención á influencia dos parámetros no comportamento asintótico da poboación. En particular, estamos interesados en determinar os valores dos parámetros para os que todas as condicións iniciais converxen cara a un equilibrio (estabilidade global); así como aqueles para os que se producen cambios cualitativos na dinámica asintótica (bifurcacións) ou outros comportamentos interesantes, como multi-estabilidade, ventás de extinción, efecto hydra, etc. É de gran interese o estudo de bifurcacións en sistemas dinámicos regulares a anacos, continuos ou descontinuos, que proveñen de aplicar estratexias de pesca protectoras. Estas comprenden bifurcacións de tipo "border-collision" ou "boundary-collision", metamorfoses da cunca de atracción e as ben coñecidas bifurcacións regulares. Tamén se considera un modelo regular para a produción de glóbulos vermellos, que por outra banda pode ser considerado coma un modelo de poboación que inclúe supervivencia de adultos. Neste caso, fomos capaces de determinar a estabilidade dos puntos de equilibrio por completo, e tamén atopamos comportamentos interesantes nos diagramas de bifurcación, tales como diferentes formas nas que se produce un colapso.

PREFACE

The contents of the present thesis are the result of the work developed by Cristina Lois Prados during the PhD studies in Mathematics at the Universidade of Santiago de Compostela, in collaboration with her supervisors Eduardo Liz Marzán (Universidade de Vigo, Spain) and Rosana Rodríguez López (Universidade de Santiago de Compostela, Spain); and the professors responsible of two research stays, Frank M. Hilker (Osnabrück University, Germany) and Radu Precup (Babeş-Bolyai University, Romania).

The PhD thesis deals with two distinct research lines, both within the framework of mathematical analysis of non-linear models. The main differences appear in the type of equations we consider and the approach used. In Research Line I, we provide some generalizations of fixed point results that allow to improve the localization of solutions to initial or boundary value problems for different types of differential equations, in particular, for the ordinary ones; and we contribute to the application of fixed point theory to population models for this class of equations. In Research Line II, our main aim is to describe the asymptotic dynamics and bifurcations of some discrete-time one-dimensional dynamical systems. We follow a more applied-oriented approach, dealing with some population models arising in current fisheries management or blood cell production modeling.

As the topics of both research lines differ quite a lot, we have decided to write this monograph in two self-contained parts, each one with a separate list of references. Nevertheless, they follow a similar structure: they start with some preliminaries to establish the mathematical and notational framework of each part of the PhD thesis and finish with the conclusions and some future research lines. In between, we develop two chapters which comprise the central contents of our research.

In the following, we give a brief outline of the chapters for each of the research lines.

RESEARCH LINE I

The research within this line corresponds to that in the joint works with Rosana Rodríguez López and Radu Precup: (Lois-Prados, Precup, and Rodríguez-López, 2020; Lois-Prados and Rodríguez-López, 2020) (Chapter 2) and (Lois-Prados and Precup, 2020) (Chapter 3). The majority of the contents in this part of the thesis were compiled from the three mentioned research articles and reorganized in the different chapters. The preliminary notions and results stated and proved by other authors are mainly comprised in Chapter 1. Moreover, in Chapter 2 (Section 2.2 and Subsection 2.3.1), we have included some contents

developed by Cristina Lois Prados during her Master degree studies, since they are the starting point for new achievements in fixed point theory, see the initial paragraphs of the corresponding sections for further details. In this chapter, we have also added some extra information to the Introduction and to Sections 2.3 and 2.4. In Chapter 3, we have included additional background in the Introductory section and we have provided more insight on the problems found concerning the applicability when working with some well-known fixed point results and the model into consideration. The Discussion section is new in both Chapters 2 and 3.

The structure of Chapters 2 and 3 is similar, since both of them start with an Introduction and conclude with a Discussion; but differs in the central sections. In the introductory sections, we show the mathematical interest of our research and, in Chapter 3, we also include the mathematical formulation of the non-autonomous Lotka-Volterra type system that we will investigate. In the Discussion section, we highlight some relevant aspects of our study and we compare it with other related research works. The intermediate sections/subsections are devoted to show the contributions of our research work. In Chapter 2, we give or improve Krasnosel'skii type compression-expansion results for set contractions and conical domains determined by balls or star convex sets. In Chapter 3, we focus on the existence of positive periodic solutions to Lotka-Volterra systems with general prey growth and functional response of predators. We use an operator approach based on the homotopy version of Krasnosel'skii expansion fixed point theorem.

Chapter 1: Background definitions and results I

We start by presenting the mathematical framework where we will develop or apply fixed point theory techniques. We first consider an initial value problem for a simple first order differential equation, and we illustrate the procedure needed to apply the classical Krasnosel'skii compression-expansion fixed point result, showing the hypothesis that should be satisfied by the associated nonlinear operator. Then, we provide other examples of initial or boundary value problems that justify the necessity to generalize or replace some of the classical hypotheses owed to Krasnosel'skii.

We continue by stating the notions and results in which we have based our research work on fixed point theory. In Section 1.1, we recall some concepts and results related to compact maps and set contractions, that is, the regularity conditions required to the mappings involved. In Section 1.2, we include the Krasnosel'skii compression-expansion fixed point theorem and some of its generalizations. They are divided in two subsections, one for the generalizations in terms of the mapping hypotheses, and the other for those replacing the compression and expansion conditions.

Chapter 2: Krasnosel'skii type compression-expansion fixed point theorem for set contractions and star convex sets

In the framework of fixed point theory, many generalizations of the classical result due to Krasnosel'skii are known, so we begin with an introductory section, where we recall some extensions of this result in different directions, and we also compare two common approaches used in their proofs: direct arguments or topological degree.

One of the extensions consists in relaxing the conditions imposed on the mapping, working with set contractions instead of continuous and compact mappings. These results work for conical domains determined by balls or, equivalently, by the norm. Therefore, they are not useful to distinguish fixed points with the same norm. To overcome this necessity, we generalize these results to star convex sets that can be determined by functionals more general than a norm.

The first step for the generalization is given in Section 2.2, where we determine the conditions that we will require to the star convex sets. Then, in Section 2.3, we prove the main results. We first deal with the compressive case, where we adapt to this more general framework the proof developed by Potter. Then, the expansive case is reduced to the compressive one by means of a change of variable. We improve the existing result for balls and provide a new theorem for star convex sets. Finally, in Section 2.4, we look for functionals that define an admissible star convex set and, consequently, are appropriate replace the norm.

To illustrate the theory, we give an application to the initial value problem for a system of implicit first order differential equations.

We conclude the chapter with a discussion of our findings in the context of fixed point theory, with special attention to Krasnosel'skii type fixed point results. We begin explaining the relevance of the obtained generalizations of compression-expansion type results, we mention the complexity that may appear when dealing with set contractions and star convex sets and, we comment the utility of defining the localization domains by means of functionals.

Chapter 3: Applications of fixed point theory to periodic predator-prey differential equations

In the literature, there exist many several papers devoted to the study of the classical Lotka-Volterra equations and its generalizations. For instance, Tsvetkov (1996) considers the classical system with periodic coefficients and proves the existence of periodic solutions via the topological method of fixed point index. A different approach was developed in (Teixeira Alves and Hilker, 2017), where they include logistic prey growth and hunting cooperation between predators in the autonomous model and, by means of a qualitative study, they observe the presence of oscillations as a consequence of cooperation. Inspired by the

general formulation proposed by Teixeira Alves and Hilker (2017) and the periodicity of the model studied in (Tsvetkov, 1996), we consider the following non-autonomous Lotka-Volterra population model

$$\begin{cases} x' = a(t)xg(x) - \varphi(t,x,y)xy; \\ y' = -b(t)y + c(t)\varphi(t,x,y)xy; \end{cases}$$

for which we require some conditions to the functions a, b, c, g and φ, including periodicity in the time variable. For particular expressions of the prey growth g and the functional response φ, we recover the models consider by Teixeira Alves and Hilker (2017) and Tsvetkov (1996). As a continuation of their research work, we are also interested in the existence of periodic solutions.

To that purpose, we use an operator approach as in (Tsvetkov, 1996), but instead of applying topological methods, we use the homotopy version of Krasnosel'skii fixed point theorem. To our knowledge, for these particular predator-prey models, the application of fixed point results, whose hypotheses are given directly in terms of the mapping, has not been considered. Other more popular versions of Krasnosel'skii fixed point theorem have been applied to similar models, but they do not work for our particular formulation. Thus, we contribute to fill this gap in the literature.

In addition, we study some interesting properties of the localized solutions that can be seen as a small contribution to the qualitative study of this type of systems. We first state sufficient conditions to ensure that the periodic solution does not reduce to a steady state. Then, under uniqueness conditions, we prove that the nonconstant solutions are positive, therefore the prey and predator populations do not end in extinction.

To conclude, we summarize our main contributions, we compare our fixed point theory approach with other related research work and we comment some aspects of the preliminary qualitative study.

RESEARCH LINE II

The research within this part of the thesis corresponds to that in the joint works with Eduardo Liz Marzán and Frank M. Hilker: (Liz and Lois-Prados, 2020b), (Lois-Prados and Hilker, submitted) (Chapter 5) and (Liz and Lois-Prados, 2020a) (Chapter 6). The contents and results which had been previously developed by other authors are mainly comprised in Chapter 4 and small portions of Chapters 5 (Subsections 5.2.1 and 5.2.2) and 6 (Section 6.1). The preliminary contents in Chapter 4 were compiled from the literature and most of them do not appear in the three mentioned research articles. By contrast, the majority of Chapters 5 and 6 uses the contents of these three research works; in Chapter 5, we have included some extra information in the initial paragraphs of the Introduction section, and we have reorganized the distinct parts of the involved articles in order to get a similar structure for both of them; in Chapter 6, there is

a new subsection, where we describe in detail the different smooth bifurcations of fixed points.

We notice that Chapters 5 and 6 follow a similar structure: we start with an Introduction where we show several mathematical and biological motivations of the research study and, in this section of Chapter 6, we also include the mathematical formulation of the blood cell production model proposed by Lasota, while in Chapter 5 we just provide the ecological description of some fisheries management policies and shift their mathematical formalization to a separate section. The subsequent sections/subsections are devoted to determine the asymptotic dynamics of the models considered. For that purpose, we complement an analytical approach by means of the qualitative theory of dynamical systems with some numerical tools such as 1-parameter bifurcation diagrams. By using this information, we plot 2-parameter bifurcation diagrams, which give a global picture of the long-term dynamics with respect to the variation of two parameters. We conclude the chapters with a discussion section where we compare our study with other related research works. It is worth mentioning that, in Chapter 5, we consider general functions satisfying some typical conditions of discrete-time one-dimensional population maps, and we also work with some particular cases in order to obtain more information from analytical results and numerical simulations. However, in Chapter 6, we just deal with a case study, which is flexible enough to fulfill different typical conditions for population maps, depending on the choice of the parameters. For instance, the associated map can be monotone, unimodal or even bimodal.

Chapter 4: Background definitions and results II

We begin by introducing, in a mathematical and ecological context, the types of one-dimensional difference equations to be considered. In the mathematical setting, we distinguish between smooth and piecewise-smooth continuous or discontinuous equations. In the ecology context, particularly that of unmanaged single-species populations with discrete-time reproductive seasons, we recall different stock-recruitment relationships and we state some typical mathematical conditions fulfilled by the maps describing these relations.

Then, we present the notions and results we use to carry out the qualitative study of asymptotic dynamics. In Section 4.2, we recall some basic concepts that are useful when determining long-term dynamics of smooth and piecewise-smooth maps, then we state some auxiliary results which ensure global stability of an equilibrium. We use some prototypes of stock-recruitment models to illustrate their applicability. In Sections 4.3 and 4.4, we describe in detail a number of bifurcations and features of 1-parameter bifurcation diagrams which appear throughout the thesis. The bifurcations are local or global and the variety or complexity of local bifurcations increases when the regularity of the piecewise-smooth map is decreased. The features one can find in the anal-

ysis of bifurcation diagrams suggest unexpected dynamic behaviors which can have important consequences for the management of ecological systems.

Chapter 5: Combinations of constant quota and threshold based harvesting strategies

We study two discrete-time models for single-species populations subject to different harvesting rules. Both strategies combine constant catches to obtain predictable yield and a threshold or minimum biomass level to protect the population. In Section 5.1, we introduce these control rules in the context of fisheries management.

From this point of view, the simplest rule allows to harvest a maximum annual quota H if the population size after reproduction is above the threshold T; and, if it is below the threshold, no harvesting is applied. We refer to this strategy as threshold constant catch harvesting (TCC). If we require the additional condition that a minimum biomass level T must remain after harvesting, then the strategy becomes more protective and difficult to apply, we refer to it as precautionary threshold constant catch (PTCC).

Discrete-time mathematical models for these strategies lead in a natural way to piecewise-smooth maps, whose dynamics are challenging because multiple non-smooth bifurcations may appear. As the map associated to the TCC rule is discontinuous and that corresponding to PTCC is continuous, the qualitative study of TCC dynamics is more complex. Thus, we first study the PTCC rule in Section 5.3; then the TCC rule in Section 5.4. In both cases, we combine analytical and numerical results to provide a comprehensive overview of the dynamics, which depend on the two relevant harvesting parameters H and T.

In Section 5.3, we provide a thorough analytical description of dynamics and bifurcations for general compensatory population models. In the overcompensatory case, where we found more complicated dynamics, we explain the dynamical behavior in some regions on the 2-parameter plane (H, T), but we choose the Ricker model as a case study to give a global picture of the dynamics. In Section 5.4, the discontinuity of the map associated to TCC induces complex dynamical behavior for the strictly increasing compensatory case. Thus, we restrict our study to this type of stock-recruitment relations, for which we use the Beverton-Holt model as a particular example. For the TCC rule, we devote an additional subsection to the study of two frequently considered management objectives: average yield and harvest frequency.

We conclude the chapter with a discussion of our findings in the context of piecewise-smooth difference equations and harvesting control rules.

Chapter 6: Lasota discrete model for blood cell production

In an attempt to explain some experimental evidences of chaotic behavior in blood cell populations, Andrzej Lasota proposed in (Lasota, 1977) the following discrete-time one-dimensional model:

$$x_{n+1} = (1-\sigma)x_n + (cx_n)^\gamma e^{-x_n}, \quad n \in \mathbb{N} \cup \{0\}.$$

This model includes a destruction rate parameter $\sigma \in (0,1)$ and a gamma-Ricker function as a representation of the quantity of cells produced in the bone marrow. The gamma-Ricker map incorporates two other parameters $\gamma, c > 0$.

With the aim of explaining the influence of the destruction rate on the dynamics, Lasota fixed the parameter values as $c = 0.47$ and $\gamma = 8$, and chose some values for σ. These values allowed him to describe the dynamics in some relevant clinical cases: normal conditions ($\sigma = 0.1$: depending on the initial condition, solutions either go to extinction or converge to a positive equilibrium), non-severe disease ($\sigma = 0.4$: the positive equilibria are unstable and there is a 2-periodic attractor), and severe disease ($\sigma = 0.8$, where Lasota observed the presence of a 3-periodic orbit and, therefore, chaotic behavior).

In this chapter, we study the model in detail, by means of an analytical approach combined with some numerical simulations. In particular, we revisit the results which appear in the original paper, but we also discover new interesting phenomena. In the analytical part, we find sufficient conditions for extinction and stability (including a sharp global stability condition for $\gamma \leqslant 1$) depending on the involved parameters. Then, we show some 1-parameter bifurcation diagrams using either γ or σ as bifurcation parameters, while keeping $c = 0.47$ as in (Lasota, 1977). These diagrams allow us to discover the rich dynamics of the model, which exhibits features such as stability switches (bubbles), extinction windows, hydra effects and sudden collapses, among others. We also present a 2-parameter bifurcation diagram as an illustration that summarizes the long-term dynamics.

Finally, we compare our results with those in the previous work carried out by Lasota, and we additionally interpret them in the context of population dynamics. The considered equation is also suitable to model the dynamics of populations with discrete reproductive seasons, adult survivorship, overcompensatory density dependence and Allee effects. In this context, our results show the rich dynamics of this type of models and point out the subtle interplay between adult survivorship rates and strength of density dependence (including Allee effects).

USC
UNIVERSIDADE
DE SANTIAGO
DE COMPOSTELA

RESUMO ESTENDIDO

Os contidos desta tese de doutoramento son o resultado do traballo realizado pola autora Cristina Lois Prados durante os seus estudos correspondentes ao Programa de Doutoramento en Matemáticas da Universidade de Santiago de Compostela, en colaboración cos seus directores Eduardo Liz Marzán (Universidade de Vigo) e Rosana Rodríguez López (Universidade de Santiago de Compostela); así como cos profesores responsables das dúas estadías de investigación realizadas, Frank M. Hilker (Osnabrück University, Alemaña) e Radu Precup (Babeş-Bolyai University, Romanía).

Este documento comprende dúas liñas de investigación diferentes que se desenvolven no ámbito da análise matemática dos modelos non lineais. As maiores diferenzas obsérvanse no tipo de ecuacións que se consideran e na metodoloxía utilizada. Na Liña de Investigación I (Research Line I), mediante a xeneralización dalgúns resultados da teoría de punto fixo, mellórase a localización das solucións a problemas de valor inicial ou problemas de fronteira para diferentes tipos de ecuacións diferenciais, en particular, para as ordinarias; ademais contribúese á aplicación da teoría de punto fixo a modelos de poboación para esta clase de ecuacións. Na Liña de Investigación II (Research Line II), o noso obxectivo principal é describir o comportamento asintótico e as bifurcacións de algúns sistemas dinámicos discretos unidimensionais. Séguese unha metodoloxía máis aplicada, traballando con modelos de poboación que xorden na xestión de recursos pesqueiros ou no modelado da produción de glóbulos vermellos.

Dado que os contidos das liñas de investigación mencionadas son bastante diferentes, decidimos dividir este manuscrito en dúas partes autocontidas, que inclúen a súa propia lista de referencias. Sen embargo, seguen unha estrutura similar: comezan con algúns resultados preliminares que serven para sentar as bases matemáticas de cada parte da tese doutoral e rematan cunhas conclusións e algunhas ideas para continuar as liñas de investigación deste manuscrito. Os capítulos intermedios recollen os contidos centrais da investigación.

No que segue, damos unha breve descrición dos contidos dos capítulos correspondentes a cada liña de investigación.

LIÑA DE INVESTIGACIÓN I

A investigación levada a cabo nesta liña correspóndese cos traballos realizados conxuntamente con Rosana Rodríguez López e Radu Precup: (Lois-Prados, Precup e Rodríguez-López, 2020; Lois-Prados e Rodríguez-López, 2020) (Capítulo 2) e (Lois-Prados e Precup, 2020) (Capítulo 3). A maioría dos contidos desta parte da tese foron recompilados dos tres artigos mencionados e redistribuídos

nos diferentes capítulos. As nocións e os resultados preliminares previamente establecidos por outros autores están maioritariamente recollidos no Capítulo 1. Ademais, no Capítulo 2 (Sección 2.2 e Subsección 2.4), aparecen algúns contidos que Cristina Lois Prados desenvolveu durante os seus estudos de mestrado, dado que son a punto de partida de novas achegas no ámbito da teoría de punto fixo, para máis detalles véxanse os parágrafos iniciais das seccións correspondentes. Por outra banda, na Introdución e nas Seccións 2.3 e 2.4 deste capítulo, incluíuse información adicional á que aparece nos artigos. No Capítulo 3, tamén se amplía a descrición do contexto no que se desenvolve o traballo realizado (Sección 3.1) e ofrécense máis detalles sobre os problemas que aparecen ao aplicar versións coñecidas do resultado de punto fixo de Krasnosel'skii ao modelo que estamos a considerar. A Discusión é nova en ambos Capítulos 2 e 3.

A estrutura dos Capítulos 2 e 3 é similar, xa que ambos comezan cunha Introdución e rematan cunha Discusión, pero diferéncianse nas seccións centrais. Nas seccións introdutorias, abordamos o interese da nosa investigación dende un punto de vista matemático, no Capítulo 3 tamén se inclúe a formulación matemática do modelo non-autónomo de Lotka-Volterra co que imos traballar. Nas seccións de Discusión, destacamos os aspectos máis relevantes do estudo realizado e comparámolo con outras investigacións relacionadas. As seccións/subseccións intermedias amosan a investigación que se levou a cabo. No Capítulo 2, probamos ou melloramos resultados de punto fixo de tipo compresivo-expansivo de Krasnosel'skii para aplicacións contractivas e dominios cónicos determinados por bolas ou conxuntos estrelados. No Capítulo 3, centrámonos na existencia de solucións periódicas para modelos de tipo Lotka-Volterra con termo xenérico de predación. Facemos uso do operador non lineal asociado, que se atopa nas condicións do caso expansivo da versión homotópica do resultado clásico de Krasnosel'skii.

Capítulo 1: Definicións e resultados preliminares I

Comezamos presentando o contexto matemático no que se desenvolverán e aplicarán as técnicas de punto fixo. En primeira instancia, consideramos un problema de valor inicial para unha ecuación diferencial ordinaria sinxela e ilustramos o procedemento a seguir para aplicar o resultado clásico de Krasnosel'skii de tipo compresivo-expansivo, mostrando as hipóteses que debe verificar o operador non lineal asociado. Despois, engadimos outros exemplos de problemas de valor inicial ou de fronteira, que xustifican a necesidade de xeneralizar ou cambiar algunhas das hipóteses clásicas requiridas por Krasnosel'skii.

A continuación lembramos algunhas nocións e resultados nos que baseamos a nosa investigación no eido da teoría de punto fixo. Na Sección 1.1, establecemos conceptos e resultados relacionados con aplicacións compactas e contractivas, que son as condicións de regularidade que lles esiximos aos operadores.

Na Sección 1.2, incluímos o resultado de Krasnosel'skii de tipo compresivo-expansivo e algunhas das súas xeneralizacións. Dividímolas en dúas subsecións, unha para as xeneralizacións en termos das hipóteses sobre as aplicacións e outra para aquelas que modifican as condicións de compresión e expansión.

Capítulo 2: O teorema de punto fixo de Krasnosel'skii de tipo compresivo-expansivo para aplicacións contractivas e conxuntos estrelados

No ámbito da teoría de punto fixo, existen moitas xeneralizacións do resultado clásico de Krasnosel'skii, polo que comezamos cunha sección introdutoria, onde lembramos algunhas das extensións existentes en varias direccións, e tamén comparamos dúas técnicas comunmente utilizadas nas súas demostracións: argumentos directos e teoría do grado topolóxico.

Unha das extensións consiste en relaxar as condicións que se lle impoñen á aplicación, traballando con aplicacións contractivas en lugar de operadores continuos e compactos. Estes resultados son válidos para dominios cónicos determinados por bólas, ou de xeito equivalente, por normas. En consecuencia, estes resultados non serven para localizar puntos fixos coa mesma norma. Para paliar esta necesidade, obtivemos unha xeneralización destes resultados a conxuntos estrelados que poden vir dados por funcionais máis xerais que a norma.

O primeiro paso para dita xeneralización dáse na Sección 2.2, onde se determinan as condicións que lles imos esixir aos conxuntos estrelados. A continuación, na Sección 2.3, faise a demostración dos resultados principais. Trabállase en primeiro lugar co caso compresivo, no que se adapta a demostración de Potter a este ámbito máis xeral. Despois, na proba do caso expansivo faise unha redución ao caso compresivo mediante un cambio de variable. Neste caso, mellórase o resultado xa coñecido para bólas e conséguese un resultado novo para conxuntos estrelados. Finalmente, na Sección 2.4, búscanse funcionais que definan un destes conxuntos estrelados, e que en consecuencia, poidan ser usados para substituír a norma.

Para ilustrar esta teoría, aplicamos os resultados obtidos a un problema de valor inicial para un sistema de ecuacións diferenciais implícitas de primeira orde.

Rematamos este capítulo cunha discusión sobre as nosas achegas á teoría de punto fixo, con especial atención aos resultados do tipo dos de Krasnosel'skii. Comezamos explicando a relevancia que pode ter esta xeneralización dos resultados de tipo compresivo-expansivo, explicamos tamén cal é a complexidade que se presenta ao traballar con aplicacións e conxuntos máis xerais e, por último, poñemos en valor a posibilidade de definir os dominios de localización mediante funcionais.

Capítulo 3: Aplicacións da teoría de punto fixo a ecuacións diferenciais periódicas de tipo predador-presa

Podemos atopar na literatura unha ampla variedade de artigos nos que se estuda o modelo clásico de Lotka-Volterra e as súas xeneralizacións. Por exemplo, Tsvetkov (1996) considerou o sistema de ecuacións clásico con coeficientes periódicos e demostrou a existencia de solucións periódicas facendo uso dun método topolóxico coñecido como a teoría do índice. Unha técnica diferente foi aplicada en (Teixeira Alves e Hilker, 2017), onde se considerou unha modificación do modelo autónomo, con crecemento loxístico das presas e cooperación entre predadores para cazar e, mediante unha análise cualitativa, observaron a presenza de oscilacións como consecuencia da cooperación. Inspirados pola xeneralidade do modelo proposto por Teixeira Alves e Hilker (2017) e a periodicidade do modelo estudado en (Tsvetkov, 1996), consideramos o seguinte modelo de poboación non-autónomo e de tipo predador-presa

$$\begin{cases} x' = a(t)xg(x) - \varphi(t,x,y)xy; \\ y' = -b(t)y + c(t)\varphi(t,x,y)xy; \end{cases}$$

no que impoñemos certas condicións ás funcións a, b, c, g e φ, entre elas, a periodicidade con respecto á variable t. Baixo determinadas expresións do crecemento das presas g e a resposta funcional dos predadores φ, recuperamos os modelos de Teixeira Alves e Hilker (2017) e Tsvetkov (1996). Como continuación do seu traballo, estamos interesados na existencia de solucións periódicas.

Para realizar o estudo, comezamos seguindo os pasos de Tsvetkov (1996) e determinamos o operador non lineal asociado ao sistema, a continuación, en lugar de facer uso de métodos topolóxicos, aplicamos a versión homotópica do teorema de punto fixo de Krasnosel'skii. Ata onde sabemos, este tipo de formulación dos modelos predador-presa non fora anteriormente estudada mediante a aplicación de resultados de punto fixo cuxas hipóteses veñen dadas directamente en termos do operador. Outras versións máis coñecidas do Teorema de punto fixo de Krasnosel'skii si que se aplicaron a modelos similares, pero veremos que non funcionan coa nosa formulación. Polo tanto, co noso traballo, contribuímos a cubrir esta carencia.

A maiores, tamén estudamos algunhas propiedades interesantes das solucións localizadas, facendo así unha pequena contribución ao estudo cualitativo do sistema. En primeiro lugar, establecemos condicións suficientes que aseguran que as solucións periódicas non son puntos de equilibrio. A continuación, baixo condicións de unicidade de solución, vemos que estas solucións son positivas, polo que as poboacións de presas e predadores non se extinguirán.

Rematamos cun resumo das nosas principais contribucións, cunha comparación da nosa aplicación da teoría de punto fixo coa doutros traballos de investigación relacionados e cunha reflexión sobre o estudo cualitativo levado a cabo.

A liña de investigación desta parte da tese corresponde ós traballos levados a cabo en colaboración con Eduardo Liz Marzán e Frank M. Hilker: (Liz e Lois-Prados, 2020b; Lois-Prados e Hilker, env.) (Capítulo 5) e (Liz e Lois-Prados, 2020a) (Capítulo 6). Os contidos e resultados que foron previamente desenvolvidos por outros/as autores/as recóllense principalmente no Capítulo 4 e en pequenas partes dos Capítulos 5 (Subseccións 5.2.1 e 5.2.2) e 6 (Sección 6.1). Os resultados preliminares do Capítulo 4 foron recompilados a partir de diferentes referencias bibliográficas e moitos deles non aparecen nos tres artigos previamente mencionados. Pola contra, a meirande parte dos contidos dos Capítulos 5 e 6 aparecen nalgúns destes traballos; no Capítulo 5, inclúese algunha información adicional nos parágrafos iniciais da Introdución, por outra banda, reorganízanse os contidos dos artigos correspondentes para obter unha estrutura similar; no Capítulo 6, incluímos unha nova subsección onde se describen con detalle as bifurcacións regulares de puntos fixos.

Cabe mencionar que os Capítulos 5 e 6 seguen unha estrutura similar: ambos comezan cunha Introdución onde se mostran varios motivos de interese da investigación no ámbito biolóxico e matemático, no Capítulo 6 esta sección tamén inclúe a formulación matemática do modelo de produción de glóbulos vermellos proposto por Lasota, mentres que no Capítulo 5 só se dá a descrición ecolóxica dalgunhas estratexias de pesca, deixando pendente a súa formulación para a sección posterior. As seguintes seccións ou subseccións adícanse a determinar o comportamento asintótico dos distintos modelos. Para cumprir este propósito, acompañamos o estudo analítico realizado mediante a teoría cualitativa dos sistemas dinámicos con ferramentas numéricas coma os diagramas de bifurcación dun parámetro. Facendo uso desta información, construímos diagramas de bifurcación de dous parámetros, que nos ofrecen unha representación global da dinámica asintótica con respecto da variación de dous parámetros do modelo. Os capítulos conclúen cunha sección de discusión, na que se fai unha comparativa do estudo levado a cabo con outros traballos de investigación relacionados. Cabe mencionar que, no Capítulo 5, considéranse funcións xenéricas que cumpren condicións típicas das aplicacións asociadas a modelos de poboación en tempo discreto e trabállase con casos particulares co obxectivo de obter información extra mediante resultados analíticos ou simulacións numéricas. Sen embargo, no Capítulo 6, só se traballa cun modelo concreto, que é suficientemente flexible pois, en función da selección de parámetros, verificará distintas condicións habitualmente presentes nas funcións asociadas a modelos de poboación en tempo discreto. Por exemplo, a aplicación asociada pode ser monótona, unimodal ou incluso bimodal.

Capítulo 4: Definicións e resultados preliminares II

Comezamos introducindo, tanto no contexto matemático coma no ecolóxico, os tipos de ecuacións en diferenzas unidimensionais que imos considerar. No ámbito matemático, distinguiremos entre ecuacións regulares e regulares a anacos (continuas ou descontinuas). No marco ecolóxico, prestamos especial atención a poboacións dunha única especie con períodos reprodutivos estacionais en tempo discreto e que non se atopan baixo os efectos da explotación, para estas lembramos distintos tipos de relacións entre a poboación adulta e a súa descendencia e establecemos algunhas condicións matemáticas típicas das aplicacións asociadas a ditas relacións.

A continuación, presentamos as nocións e resultados que se utilizan para levar a cabo o estudo da dinámica asintótica. Na Sección 4.2, lembramos algúns conceptos básicos que son útiles para determinar o comportamento a longo prazo das solucións a ecuacións regulares e regulares a anacos, de seguido establecemos algúns resultados auxiliares que nos permiten xustificar a estabilidade global dun punto fixo ou de equilibrio. Para ver como se aplican estes resultados, facemos uso dalgúns prototipos de relacións entre adultos e a súa descendencia. Nas Seccións 4.3 e 4.4, describimos en detalle os distintos tipos de bifurcacións e comportamentos presentes en diagramas dun parámetro que atoparemos ao longo deste documento. As bifurcacións poden ser locais ou globais e a variedade e complexidade das bifurcacións locais medra ao reducirse a regularidade da aplicación asociada á ecuación en cuestión. Os comportamentos que se poden atopar mediante unha análise dos diagramas de bifurcación suxiren dinámicas inesperadas que poden ter importantes consecuencias na xestión de sistemas ecolóxicos.

Capítulo 5: Combinacións de estratexias de pesca constante e con límites

Neste apartado, estudamos dous modelos discretos para poboacións dunha única especie baixo os efectos de dúas estratexias de pesca diferentes. Ambas estratexias combinan cotas fixas que dan lugar a ganancias predicibles e un límite ou nivel mínimo de biomasa que protexe a poboación. Na Sección 5.1, introducimos estas estratexias no contexto pesqueiro.

Dende o punto de vista pesqueiro, a máis sinxela destas estratexias é a que permite pescar unha cota máxima anual H se o tamaño da poboación tras a reprodución é maior que un límite T e, se é máis pequeno que T, non se permite pescar. Referirémonos a esta estratexia como pesca de límite con cota fixa (TCC). Se, adicionalmente, esiximos que un nivel mínimo de biomasa T debe permanecer tras a pesca, entón a estratexia vólvese máis protectora e difícil de aplicar, referirémonos a ela como pesca preventiva de límite con cota fixa (PTCC).

Os modelos matemáticos discretos que describen estas estratexias conducen de maneira natural a aplicacións asociadas regulares a anacos, cuxo compor-

tamento dinámico é máis complexo, xa que poden aparecer múltiples bifurcacións non regulares. Como a aplicación asociada a TCC é descontinua e a de PTCC é continua, o estudo cualitativo da dinámica de TCC será máis complexo. Polo tanto, estudaremos en primeira instancia a estratexia PTCC na Sección 5.3; a continuación traballaremos con TCC na Sección 5.4. En ambos casos, combinamos resultados analíticos e numéricos para ofrecer unha ampla representación dos diferentes comportamentos dinámicos, que dependen da elección dos dous parámetros relevantes H e T.

Na Sección 5.3, levamos a cabo unha descrición analítica completa da dinámica e bifurcacións en modelos de poboación xerais con denso-dependencia compensatoria. No caso sobrecompensatorio, atopamos comportamentos dinámicos máis complexos e no caso xeral somos capaces de explicar a dinámica asintótica nalgunhas rexións do plano (H, T), pero consideramos o modelo de Ricker como caso particular para dar unha ilustración global da dinámica. Na Sección 5.4, a descontinuidade da aplicación asociada a TCC induce comportamentos dinámicos complexos en poboacións con denso-dependencia estritamente crecente (caso compensatorio). En consecuencia, restrinximos o noso estudo a este tipo de relacións, para as que consideramos o modelo de Beverton-Holt como caso particular. En relación á estratexia TCC, dedicamos unha subsección adicional para o estudo de dous obxectivos de xestión que se perseguen con frecuencia: o beneficio medio e a frecuencia de pesca.

Concluímos este capítulo cunha discusión das nosas achegas no contexto das ecuacións en diferenzas regulares a anacos e no ámbito das estratexias de pesca.

Capítulo 6: Modelo discreto de Lasota para a produción de glóbulos vermellos

Nun intento de explicar a evidencia experimental de comportamento caótico en poboacións de glóbulos vermellos, Andrzej Lasota propuxo en (Lasota, 1977) o seguinte modelo discreto unidimensional:

$$x_{n+1} = (1-\sigma)x_n + (cx_n)^\gamma e^{-x_n}, \quad n \in \mathbb{N} \cup \{0\}.$$

O modelo inclúe un parámetro $\sigma \in (0,1)$ representando a taxa de destrución de glóbulos vermellos e unha función de tipo gamma-Ricker determinando a cantidade de glóbulos vermellos que se producen na medula ósea. Esta función incorpora dous novos parámetros γ e $c > 0$.

Lasota quería explicar a influencia da taxa de destrución na dinámica, para o que fixou os parámetros $c = 0.47$, $\gamma = 8$ e seleccionou varios valores de σ. Esta selección permitiulle describir o comportamento dinámico para algúns casos clínicos relevantes: condicións normais ($\sigma = 0.1$: dependendo da condición inicial as solucións poden acercarse á extinción ou converxer a un equilibrio positivo), enfermidade leve ($\sigma = 0.4$: o equilibrio positivo é inestable, pero existe un 2-ciclo atractor), e enfermidade grave ($\sigma = 0.8$: para o que Lasota observou a presenza dun 3-ciclo e, como consecuencia, comportamento caótico).

Neste capítulo, estudaremos este modelo con detalle, facendo uso de métodos analíticos combinados con simulacións numéricas. En particular, revisare-

mos os resultados que aparecen no artigo orixinal, pero tamén descubriremos novos fenómenos de interese. Na parte analítica, atoparemos condicións suficientes para a extinción e a estabilidade (incluíndo unha condición óptima de estabilidade global para $\gamma \leqslant 1$) en función dos parámetros involucrados no modelo. A continuación, mostraremos algúns diagramas de bifurcación dun parámetro, utilizando tanto γ coma σ como parámetros de bifurcación, pero fixando $c = 0.47$ tal e como fixera Lasota (1977). Estes diagramas permiten descubrir a ampla variedade dos comportamentos dinámicos posibles para este modelo, tales como cambios de estabilidade (burbullas), ventás de extinción e colapsos, entre outros. Tamén incluímos un diagrama de bifurcación de dous parámetros que serve para resumir os comportamentos asintóticos máis importantes nunha única imaxe.

Finalmente, comparamos os nosos resultados cos previamente obtidos no traballo levado a cabo por Lasota e, adicionalmente, incluímos unha interpretación no contexto da dinámica de poboacións. Nese ámbito, a ecuación considerada resulta válida para modelar a dinámica de poboacións con períodos reprodutivos estacionais e discretos, supervivencia de adultos, denso-dependencia sobrecompensatoria e efecto Allee. Nese contexto, os nosos resultados mostran a ampla variedade de comportamentos dinámicos destes modelos e destacan a sutil relación entre a taxa de supervivencia de adultos e a intensidade da denso-dependencia (incluíndo efecto Allee).

AIMS AND OBJECTIVES

The main aim of the PhD thesis is to contribute to the development and application of mathematical analysis techniques to non-linear models in population dynamics. We work on two different research topics.

In the first part of this monograph, we continue the study on fixed point theory conducted by the PhD student and her supervisor during the master's degree (Lois-Prados and Rodríguez-López, 2020). Fixed point theory is a useful tool to deal with the existence and localization of solutions to initial or boundary value problems for differential equations. However, some classical results can just be applied to a particular type of problems, so we try to develop some generalizations which work for a wider range of them. Besides, the PhD student should also face the challenging task of finding the suitable result which applies to a particular class of initial or boundary value problems. Thus, we work to achieve the following specific goals:

G1 *Generalization of Krasnosel'skii fixed point theorem to* k*-set contractions and star-convex sets*: We first try to extend the recent results obtained during the master degree for the compressive case to general set contractions. Then we complement it with an analogous result for the expansive case, in which the conditions required to the mapping on the boundaries of the sets are interchanged. We also provide a suitable problem for a differential equation that allows us to show the relevance of the obtained generalizations for applications.

G2 *Applications of fixed-point theory to population models*: In the particular case of predator-prey type ordinary differential equations, the study made by Tsvetkov (1996) provides the existence of periodic solutions to the classical Lotka-Volterra system with periodic coefficients by means of topological results. To our knowledge, some well-known Krasnosel'skii type results have been applied to similar models (see Lv, Lu, and Yan, 2010; Precup, 2007); however, there is a gap in the literature concerning the application of fixed point results whose hypotheses are given directly in terms of the underlying mapping to these classical Lotka-Volterra population models, and we try to contribute to this research task.

In the second part of this document, we study discrete dynamical systems, particularly those modeling populations subject to protective intervention strategies. For long, the main objective in forestry and fishery was to apply a strategy that maximizes the yield, but it caused the collapse of several natural resources. Nowadays, there is a preference for rules that combine high yield with population protection. The supervisor Eduardo Liz and some other authors have recently carried out a theoretical study on the influence of different strategies

on the dynamics of discrete time population models (see Liz, 2010b). Here, we try to obtain similar results for intervention rules that consider a threshold value or minimum biomass level under which no harvesting is allowed. More precisely, we work in the following goals:

G3 *Dynamical study of one-dimensional piecewise-smooth population models applied to threshold harvesting*: We start by studying the dynamics of different sustainable intervention strategies applied to stricly increasing or unimodal maps with at most one positive fixed point, such as the classical Beverton-Holt and Ricker models. It is interesting to study the influence of the underlying harvesting parameters on the dynamics, for that purpose we look for regions of global stability, bistability, chaos, or parameter values where there is a change on the population asymptotic dynamics (bifurcations). Once we finish with the qualitative study, we find it significant to compare the results with those obtained for some related traditional strategies.

G4 *More flexible population models*: A similar but more ambitious objective is to describe the dynamics of the same intervention strategies applied to more general maps, not necessarily monotone nor unimodal and with 0, 1 or 2 positive fixed points (see, for example, Liz, 2018a). As the model flexibility usually increases the difficulty of the dynamical analysis, we can start studying the dynamics of these models without harvesting, which implies a reduction in the number of parameters.

METHODOLOGY

This chapter of the thesis is devoted to describe the methods or approaches used in the development of the goals G1-G4. In general, the research begins with a detailed review of some related classical and recent bibliographical references in order to acquire some necessary knowledge about relevant results and techniques in the related field. After that, we start to work on the underlying problem by following these approaches and, sometimes, we also need to look for or to develop other statements and methods.

In particular, in relation with the objective G1, we provide a generalization of the compression-expansion Krasnosel'skii fixed point theorem by using classical arguments of this theory, following the approach used by Krasnosel'skii and other authors. For the rest of the goals, unless we use distinct methods, somehow we follow a similar approach in which we formulate the model and then we look for the proper results and techniques that can be used for its analysis. In the following, we provide more details about the methodology that we use to attain each of the objectives. We use specific results and techniques for goals G1 and G2. In the case of goals G3 and G4, some methods are applied to both of them, so we explain the similarities and differences in M3.

M1 For the generalization of the compression-expansion Krasnosel'skii fixed point theorem to set contractions and star-convex sets, we first observe that, in the compressive case, the approach carried out by Potter (1974) for set contractions can be adapted to more general domains determined by star-convex sets instead of balls. Thus, we start by determining the properties we have to impose on the star-convex sets in order to reproduce the proof given by Potter in this more general framework and, then, we adapt his main results. After that, we observe that the approach due to Các and Gatica (1979), in the expansive case, cannot be properly adapted to our framework. So, we look for other methodologies and we finally use the idea in (Precup, 2006), that is, a change of variable to reduce the expansive case to the compressive one. It is worth mentioning that we do not use topological degree techniques.

M2 In the application of fixed point theory to periodic predator-prey models, we start by transforming the ordinary differential equation into its equivalent integral formulation, so we obtain an operator T whose fixed points are the solutions of the predator-prey model. Then, we look for a special set where we intend to localize a periodic solution, and for a proper fixed point theorem that could be applied to this type of problems. Finally, we also use some basic arguments in the analysis of ordinary differential equations to provide sufficient conditions that ensure the non-constancy and positiveness of the localized periodic solution.

M3 In order to realize a detailed study of the long-term dynamics of the one-dimensional difference equations that we consider in Chapters 5 and 6, we first determine the number of positive fixed points of the associated map depending on the parameter values, and we also study its local and global stability. By using this information, one can classify some of the bifurcations in which fixed points are involved. Then, we continue with the analytical study of other interesting phenomena, such as, the bifurcations of 2-cycles, the boundary-collision bifurcations, the regions of bistability or the sudden collapses. Once we conclude with the analytical study, we use 2-parameter BD to provide a global picture of the long term dynamics, and 1-parameter BD to illustrate the most relevant dynamical features. This is the general procedure that we follow to attain goals G3 and G4, however, we use different results and arguments to study the dynamics. On the one hand, the intervention strategies that we have mentioned in objective G3 produce a piecewise-smooth map whose long-term behavior presents some features that cannot occur for smooth models. On the other hand, the map in goal G4 is smooth but more flexible, which in some sense increases the difficulty of the dynamical study.

CONTENTS

Part I

RESEARCH LINE I

USC
UNIVERSIDADE
DE SANTIAGO
DE COMPOSTELA

1 BACKGROUND DEFINITIONS AND RESULTS I

For the sake of completeness, in this chapter we provide some notions and results on fixed point theory.

We begin introducing the type of problems we will deal with. In general, given an initial or boundary value problem for differential equations, we are interested in its integral characterization or, in obtaining a mapping T whose fixed points are in correspondence with solutions of the initial or boundary value problem. Once we get the associated mapping, fixed point results constitute a useful tool to prove the existence and to localize the fixed points of T. Throughout this part of the thesis, this procedure to find solutions of differential equations is referred to as *(classical) operator approach*. We illustrate the process with a simple initial value problem:

$$\begin{cases} x'(t) = f(t, x(t)), \ t \in [0,1]; \\ x(0) = 0; \end{cases} \tag{1}$$

where $f : [0,1] \times \mathbb{R} \longrightarrow \mathbb{R}$ is bounded and continuous. For some particular expressions of the map f, there exist techniques that allow to find the solutions of (1). In general, by using the continuity of f, we can assert that there exists at least a solution, but it may not be easy to find procedures to solve the problem explicitly. Thus, it is interesting to get the equivalent problem to which we can apply some existence and localization fixed point results. For that purpose, let us consider the non-linear operator $T : \mathcal{C}([0,1], \mathbb{R}) \longrightarrow \mathcal{C}([0,1], \mathbb{R})$ given by

$$T(x)(t) = \int_0^t f(s, x(s))ds, \ x \in \mathcal{C}([0,1], \mathbb{R}), \ t \in [0,1]. \tag{2}$$

Each solution of the initial value problem (1) in $\mathcal{C}([0,1], \mathbb{R})$ is in correspondence with a fixed point of the operator T given by (2), that is, an element $x \in \mathcal{C}^1([0,1], \mathbb{R})$ such that $x(t) = T(x)(t)$ for all $t \in [0,1]$. The simple expression of the map T, together with the regularity of f, allows us to use, for instance, the classical compression-expansion Theorem of Krasnosel'skii (see Krasnosel'skii, 1964, Chapter 4) to localize fixed points of T. However, the above-mentioned fixed point result cannot be applied directly to the map T in (2) without the establishment of additional structures and the imposition of certain restrictions on the mapping f, as we explain below.

We first should equip the set $\mathcal{C}([0,1], \mathbb{R})$ with a norm in order to obtain a Banach space. For instance, the pair $(\mathcal{C}([0,1], \mathbb{R}), \|x\|_\infty)$ is a Banach space, where $\|x\|_\infty := \max\{|x(t)|, \ t \in [0,1]\}$ and $|\cdot|$ denotes the absolute value in $\mathbb{R}$.

Secondly, the result does not work in the whole space $\mathcal{C}([0,1], \mathbb{R})$, so we have to consider a particular subset of the Banach space which is called a cone, for

example, $\mathcal{C}([0,1],\mathbb{R}_+)$. Thus, if we require that $f([0,1]\times\mathbb{R}_+)\subset\mathbb{R}_+$, then it is guaranteed that T maps $\mathcal{C}([0,1],\mathbb{R}_+)$ into itself.

Thirdly, the restriction of T to the cone $\mathcal{C}([0,1],\mathbb{R}_+)$ should be a compact mapping. This is indeed the case since f is bounded and continuous.

Finally, the compression or expansion conditions should be fulfilled. They depend on the mapping T and the elements of the cone with $\|x\|_\infty = r$ and $\|x\|_\infty = R$, where $r < R$ are two positive real numbers.

Once we have checked that all the hypotheses are fulfilled, the result provides the existence of a fixed point $x \in \mathcal{C}([0,1],\mathbb{R}_+)$ with $r \leqslant \|x\|_\infty \leqslant R$, and, therefore, a localization for this fixed point is given.

The mentioned classical results due to Krasnosel'skii can be applied to a huge amount of problems. However, if we relax or replace some of the required hypotheses, we can improve the localization of fixed points or even apply the results to a wider range of initial or boundary value problems.

The generalizations of Krasnosel'skii fixed point theorem can be stated by relaxing different hypotheses: the properties of the domain of T; the compactness of the mapping and the compression-expansion conditions. In Sections 1.1 and 1.2, we state some generalizations for two of these conditions, but for those regarding the domain of T we refer the reader to Chapter 2.

In Section 1.1, we start describing the concept of compact mapping and recalling the Arzelà-Ascoli characterization of relatively compact sets in the Banach space $(\mathcal{C}(I,\mathbb{R}^n),\|\cdot\|_\infty)$, where (I,d) is a compact metric space, that will be useful in applications. Then, we review some concepts that generalize the previous ones: the measure of noncompactness and α-Lipschitz maps. We also provide some results that state useful properties of both concepts.

Section 1.2 is devoted to recall some Krasnosel'skii type fixed point theorems that we use in this part of the monograph. We first review the concept of cone and the classical Krasnosel'skii compression-expansion result. Then, we organize the generalizations in two different subsections. In Subsection 1.2.1, we recall Krasnosel'skii type results for set contractions. These generalizations allow to localize solutions for implicit first order initial value problems of the form:

$$\begin{cases} x'(t) = f(t,x(t)) + g(t,x'(t)),\ t\in[0,1]; \\ x(0) = 0; \end{cases} \tag{3}$$

where $f,g:[0,1]\times\mathbb{R}\longrightarrow\mathbb{R}$ are continuous and g satisfies some Lipschitz type condition. It is worth mentioning that the non-linear operator T associated to this problem is not necessarily compact, but it can be a set contraction, see Chapter 2 for further details. In Subsection 1.2.2, we state three fixed point results preserving the compactness hypothesis of the mapping T, but considering different compression-expansion conditions. In Chapter 3, we study their applicability to a class of Lotka-Volterra type equations. The first result is a generalization due to Güo and Lakshmikantham (1998), with compression-expansion conditions of norm type, which localizes the solutions in more general domains

determined by a cone and two open sets. This generalization works for some particular Lotka-Volterra models with time-delays, but it cannot be applied to simpler formulations of these predator-prey systems. The second result is the vector version given in (Precup, 2007), which was applied to localize positive periodic solutions of a differential system with linear and non-linear terms. That system is quite similar to Lotka-Volterra type equations; however, it seems that the vector version presents some difficulties in its applicability to simple formulations of these population models, as it happens with the original result owed by Krasnosel'skii. Besides, the homotopy version of the original Theorem of Krasnosel'skii, stated at the end of Subsection 1.2.2, works for these type of predator-prey equations.

1.1 CONDITIONS FOR INTEGRAL MAPPINGS

In this section, we state some basic notions and results related with the regularity of the mapping. These concepts will appear in the hypothesis of our fixed point results.

We first recall the concepts of (relatively) compact set and compact mapping. We also provide the Arzèla-Ascoli theorem that gives a characterization of relatively compact sets in $(\mathcal{C}(I,\mathbb{R}^n),\|\cdot\|_\infty)$ where (I,d) is a compact metric space. This result will help to prove the compactness of mappings in applications, in particular, we will use Corollary 1.1.4. For further details, see (Precup, 2002, Chapter 1).

Definition 1.1.1. Let (X,d) be a metric space. We say that X is a *compact set* if, for each $\varepsilon>0$, X admits a finite covering by open balls of radius ε. More precisely, for each $\varepsilon>0$, there exist $N_\varepsilon\in\mathbb{N}$ and $x_i\in X$, $i=1,\dots,N_\varepsilon$, such that

$$X\subset\bigcup_{i=1}^{N_\varepsilon}B(x_i,\varepsilon),$$

where $B(x_i,\varepsilon)=\{y\in X: d(x_i,y)<\varepsilon\}$.
A subset D of X is *relatively compact* if its closure $\overline{D}$ is a compact set (as a metric subspace of X).

Definition 1.1.2. Let X,Y be metric spaces and $D\subset X$. The map $T:D\subset X\longrightarrow Y$ is *compact* if, for all $A\subset D$ bounded, $\overline{T(A)}$ is a compact set.

Theorem 1.1.3 (Arzelà-Ascoli)**.** *Let (I,d) be a compact metric space and consider the Banach space $(\mathcal{C}(I,\mathbb{R}^n),\|\cdot\|_\infty)$. A set $D\subset\mathcal{C}(I,\mathbb{R}^n)$ is relatively compact if and only if the following conditions are satisfied:*

1. *D is bounded, that is, there exists $M>0$ such that $\|x\|_\infty<M$ for all $x\in D$;*
2. *D is uniformly equicontinuous, that is, for all $\varepsilon>0$, there exists $\delta>0$ such that for every $x\in D$,*

$$|x(t)-x(s)|<\varepsilon,\ \textit{for all}\ t,s\in I,\ \textit{with}\ d(t,s)<\delta.$$

By using Theorem 1.1.3, Precup (2002) proved Corollary 1.1, which allows us to assert:

Corollary 1.1.4. *Let I be a bounded subset of the Banach space $\mathbb{R}^m$ and denote its closure by $\bar{I}$. The inclusion mapping $i : \mathcal{C}^1(\bar{I}, \mathbb{R}^n) \longrightarrow \mathcal{C}(\bar{I}, \mathbb{R}^n)$ is compact.*

In the following, we state the concepts which allow us to relax the compactness hypothesis assumed in the classical Krasnosel'skii compression-expansion result. We give their formal definitions and recall some of its principal properties, that can be found in (Potter, 1974). The first concept presented can be seen as a tool to determine how much a particular set differs from being (relatively) compact.

Definition 1.1.5. Let (X, d) be a metric space and $A \subset X$ be a bounded set. The *Kuratowski measure of noncompactness* of A is the nonnegative real number

$$\alpha(A) := \inf\left\{\varepsilon > 0 \,:\, A \subset \bigcup_{i=1}^{n} A_i,\ \operatorname{diam}(A_i) \leqslant \varepsilon,\ \forall i \in \{1, \ldots, n\}\right\},$$

where $\operatorname{diam}(A_i) := \sup\{d(x, y) : x, y \in A_i\}$, for all $i \in \{1, \ldots, n\}$, is the diameter of A_i.

Proposition 1.1.6. *Let A, B be subsets of a metric space (X, d). The Kuratowski measure of noncompactness satisfies the following properties:*

1. $A \subseteq B \Rightarrow \alpha(A) \leqslant \alpha(B)$.
2. $\alpha(A \cup B) = \max\{\alpha(A), \alpha(B)\}$.
3. $\alpha(A) = \alpha\left(\overline{A}\right)$.

Moreover, if $(X, \|\cdot\|)$ is a Banach space, then:

4. $\alpha(A + B) \leqslant \alpha(A) + \alpha(B)$.
5. $\alpha(\lambda A) = |\lambda|\alpha(A)$, $\forall \lambda \in \mathbb{R}$.
6. $\alpha(co(A)) = \alpha(A)$.
7. *$\overline{A}$ is a compact set if and only if $\alpha(A) = 0$.*

In property 6, the term $co(A)$ denotes the convex hull of A, that is,

$$co(A) := \left\{\sum_{i=1}^{n} \lambda_i x_i \,:\, n \in \mathbb{N},\ \sum_{i=1}^{n} \lambda_i = 1,\ x_i \in A,\ \lambda_i \in [0, 1],\ \forall i \in \{1, \ldots, n\}\right\}.$$

Now, we can define a concept close to the notion of compact mapping, which is known as set contraction. We use the notation in (Deimling, 1985, Subsection 9.1):

Definition 1.1.7. Let X, Y be metric spaces and $D \subset X$. Assume that the mapping $T : D \subset X \longrightarrow Y$ is continuous. We say that T is α-*Lipschitz* if there exists a constant $k \geqslant 0$ such that

$$\alpha(T(A)) \leqslant k\alpha(A), \text{ for all bounded } A \subset D.$$

When ir is important to mention the constant k, we say that T is a k-α-*Lipschitz* mapping, or an α-*Lipschitz mapping with constant* k. In case that $k \in [0, 1)$, we say that T is a *set contraction* or a k-*set contraction*.

It is worth mentioning that, by using properties 3 and 7 in Proposition 1.1.6, we have:

Example 1.1.8. If $(X, \|\cdot\|)$ is a Banach space, then the continuous and compact mappings are in correspondence with 0-set contractions.

Remark 1. If T is an α-Lipschitz mapping, it is implicitly required that $T(A)$ is bounded when $A \subset D$ is bounded, since it is a necessary condition to compute the measure of noncompactness of $T(A)$.

We conclude this section by recalling the following properties of α-Lipschitz mappings. We use them in Chapter 2 to extend the classical compression-expansion Theorem of Krasnosel'skii to set contractions and more general domains.

Proposition 1.1.9. *Let* (X_i, d_i) *be metric spaces for* $i \in \{1, 2, 3\}$, *and* $(X, \|\cdot\|)$ *be a Banach space. The following properties are satisfied:*

1. *If* $T_1 : X_1 \to X_2$ *is a* k_1-α-*Lipschitz map and* $T_2 : X_2 \to X_3$ *is a* k_2-α-*Lipschitz map, then* $T_2 \circ T_1 : X_1 \to X_3$ *is a* k_1k_2-α-*Lipschitz map.*

2. *If* $T_1 : X_1 \longrightarrow X$ *is a* k_1-α-*Lipschitz mapping,* $T_2 : X_1 \longrightarrow X$ *is a* k_2-α-*Lipschitz mapping, then* $T_1 + T_2 : X_1 \longrightarrow X$ *is a* $(k_1 + k_2)$-α-*Lipschitz mapping.*

3. *If* $T : D \subset X \to X$ *is a* k-α-*Lipschitz mapping and* $\lambda : D \to \mathbb{R}_+$ *is a continuous function such that* $\sup_{x\in D} \lambda(x) = l < \infty$, *then the mapping*

$$\widehat{T} : D \subset X \to X,\ \widehat{T}(x) = \lambda(x)\, T(x),\ x \in D,$$

is kl-α-*Lipschitz.*

Proposition 1.1.10. *Let* $D, \hat{D}$ *be closed subsets of a metric space* (X, d). *Suppose that* $T : D \longrightarrow X$ *is a* k-α-*Lipschitz mapping and* $\hat{T} : \hat{D} \longrightarrow X$ *is a* $\hat{k}$-α-*Lipschitz mapping such that* $T_{|D\cap\hat{D}} = \hat{T}_{|D\cap\hat{D}}$. *Define*

$$\tilde{T} : D \cup \hat{D} \longrightarrow X$$

$$x \longmapsto \tilde{T}(x) := \begin{cases} T(x), & x \in D; \\ \hat{T}(x), & x \in \hat{D}; \end{cases}$$

then $\tilde{T}$ *is a* $\tilde{k}$-α-*Lipschitz mapping with* $\tilde{k} = \max\{k, \hat{k}\}$.

1.2 KRASNOSEL'SKII TYPE FIXED POINT RESULTS

Here, we provide the Krasnosel'skii type theorems which we will use along this part of the thesis. We first recall the crucial definition of cone, and provide some examples which we use to illustrate the compression-expansion hypotheses or in applications. Before stating the compression-expansion result owed by Krasnosel'skii, we state some useful notations for specific subsets of the cone that appear in most of the fixed point results.

Definition 1.2.1. Let $(X, \|\cdot\|)$ be a Banach space. A subset C of X is a *cone* if:

- C is closed;
- for all $x, y \in C$, $a, b \in \mathbb{R}^+$, it is satisfied that $ax + by \in C$;
- $x \in C$, $-x \in C$ if and only if $x = 0$.

Example 1.2.2. Let us consider the Banach space $(\mathbb{R}^2, \|\cdot\|)$, where

$$\|\cdot\| : \mathbb{R}^2 \longrightarrow [0, +\infty), \quad (x, y) \longmapsto \|(x, y)\| := \sqrt{x^2 + y^2}.$$

The set $C := \{(x, y) \in \mathbb{R}^2 : x, y \geqslant 0\}$ is a cone in $\mathbb{R}^2$. We use this cone to illustrate the restrictions imposed in the statements of the main fixed point results studied.

Example 1.2.3. Let us consider the Banach space $(\mathcal{C}([0, 1], \mathbb{R}^n), \|\cdot\|_\infty)$, where the elements in $\mathcal{C}([0, 1], \mathbb{R}^n)$ are continuous functions on the interval $[0, 1]$ with values in $\mathbb{R}^n$ and

$$\|\cdot\|_\infty : \mathcal{C}([0, 1], \mathbb{R}^n) \longrightarrow [0, +\infty), \quad x \longmapsto \|x\|_\infty := \max_{i=1,\dots,n} \max_{t\in[0,1]} |x_i(t)|.$$

The set $C := \{x \in \mathcal{C}([0, 1], \mathbb{R}^n) : x_i \geqslant 0, \text{ for all } i = 1, \dots, n\}$ is a cone in $\mathcal{C}([0, 1], \mathbb{R}^n)$. We use it in the application of fixed point theory to the non-linear operator associated with the initial value problem (3).

Example 1.2.4. Let us consider $\omega > 0$ and the Banach space

$$\mathcal{C}_\omega\left(\mathbb{R}, \mathbb{R}^2\right) := \left\{(x, y) \in \mathcal{C}\left(\mathbb{R}, \mathbb{R}^2\right) : x(t) = x(t + \omega),\ y(t) = y(t + \omega)\ \forall\, t \in \mathbb{R}\right\}$$

endowed with the norm

$$\|(x, y)\|_\omega := \|x\|_\infty + \|y\|_\infty = \max_{t\in[0,\omega]} |x(t)| + \max_{t\in[0,\omega]} |y(t)|.$$

Given $q_1, q_2 > 0$, the set

$$C := \left\{(x, y) \in \mathcal{C}_\omega\left(\mathbb{R}, \mathbb{R}^2\right) :\ x(t) \geqslant q_1\|x\|_\infty,\ \ y(t) \geqslant q_2\|y\|_\infty,\ \forall\, t \in \mathbb{R}\right\}$$

is a cone in $\mathcal{C}_\omega\left(\mathbb{R}, \mathbb{R}^2\right)$. We use it in the application of fixed point results to Lotka-Volterra type systems. For the sake of completeness, we show that C is indeed a cone. Thus, we prove that it fulfills the three conditions given in Definition 1.2.1:

- We first show that C is closed. Let $\{(x_n, y_n)\}_{n\in\mathbb{N}} \subset C$ be an arbitrary sequence that converges to an element $(x, y) \in \mathcal{C}_\omega\left(\mathbb{R}, \mathbb{R}^2\right)$, we prove that $(x, y) \in C$. Since $\{(x_n, y_n)\} \to (x, y)$ as $n \to \infty$, then

  $$x_n(t) \to x(t),\ y_n(t) \to y(t),\ \text{as } n \to \infty,$$

  for all $t \in [0, \omega]$. Now, it follows easily that $(x, y) \in \mathcal{C}_\omega\left(\mathbb{R}, \mathbb{R}^2\right)$ and, by taking limits as $n \to \infty$ in the inequalities

  $$x_n(t) \geqslant q_1\|x_n\|_\infty,\ y_n(t) \geqslant q_2\|y_n\|_\infty,\ \text{for all } t \in [0, \omega],$$

  we conclude that $(x, y) \in C$.

- Next, given (x, y), $(\tilde{x}, \tilde{y}) \in C$ and $a, b \in \mathbb{R}_+$, we prove that the linear combination $a(x, y) + b(\tilde{x}, \tilde{y}) \in C$. It is clear that $a(x, y) + b(\tilde{x}, \tilde{y}) \in \mathcal{C}_\omega\left(\mathbb{R}, \mathbb{R}^2\right)$; so it remains to show that this element satisfies the corresponding inequalities. For each $t \in [0, \omega]$, we have

  $$\begin{aligned} ax(t) + b\tilde{x}(t) &\geqslant aq_1\|x\|_\infty + bq_1\|\tilde{x}\|_\infty \geqslant q_1\|ax + b\tilde{x}\|_\infty; \\ ay(t) + b\tilde{y}(t) &\geqslant aq_2\|y\|_\infty + bq_2\|\tilde{y}\|_\infty \geqslant q_2\|ay + b\tilde{y}\|_\infty. \end{aligned}$$

- Finally, if (x, y), $(-x, -y) \in C$, we prove that $(x, y) = (0, 0)$. We show that $x = 0$ and the proof of $y = 0$ is analogous. Since $x(t) \geqslant q_1\|x\|_\infty \geqslant 0$ and $-x(t) \geqslant q_1\|-x\|_\infty \geqslant 0$, then we conclude that x is the null function.

Notation 1. Let $(X, \|\cdot\|)$ be a Banach space and $C \subset X$ be a cone. For $r, R \in \mathbb{R}$, with $0 < r < R$, let

- $C_{r,R} = \{x \in C : r \leqslant \|x\| \leqslant R\}$;
- $B_r = \{x \in C : \|x\| \leqslant r\}$;
- $S_r = \{x \in C : \|x\| = r\}$.

We are now in a position to state the result due to Krasnosel'skii. We provide the version which appears in (Krasnosel'skii, 1964, Chapter 4), where the compression-expansion conditions are more general than those previously required in (Krasnosel'skii, 1960).

Theorem 1.2.5. *Let $(X, \|\cdot\|)$ be a Banach space, C a cone in X and $T : C \longrightarrow C$ a continuous and compact map such that $T(0) = 0$. If there exist $0 < r < R$ satisfying*

$$\begin{aligned} &x - Tx \notin C, \quad \forall\, x \in S_r; \\ &Tx - (1+\varepsilon)x \notin C, \quad \forall\, \varepsilon > 0 \ \text{and}\ x \in S_R; \end{aligned} \tag{4}$$

or

$$\begin{aligned} &Tx - (1+\varepsilon)x \notin C, \ \forall\, \varepsilon > 0 \ \text{and}\ x \in S_r; \\ &x - Tx \notin C, \ \forall\, x \in S_R; \end{aligned} \tag{5}$$

then T has a nontrivial fixed point in $C_{r,R}$.

We recall that the conditions in (4) are those of the *compressive case*, while the conditions in (5) correspond to the *expansive case.*

1.2.1 *Generalizations to set contractions*

This subsection includes the generalizations of Theorem 1.2.5 to set contractions obtained in (Potter, 1974) (compressive case) and (Các and Gatica, 1979) (expansive case). In Chapter 2, we provide some extensions of their results to more general sets. For the compressive case, we follow the ideas of Potter, so we state here some useful results he used in the proof. One tool is an extension of the Theorem of Schauder to set contractions (see Darbo, 1955), and the other is a lemma used by Potter (1974) to extend the domain of the set contractions preserving this property of the mapping.

Theorem 1.2.6 (Darbo)**.** *Let* $(X, \|\cdot\|)$ *be a Banach space and* $B \subset X$ *a closed, convex and bounded set. Assume that* $T : B \longrightarrow B$ *is a set contraction, then there exists* $x \in B$ *a fixed point of* T*.*

Lemma 1.2.1. *Assume that* $T : S_r \longrightarrow C$ *is an* α*-Lipschitz mapping with constant* k*. Let us consider*

$$\tilde{T} : B_r \longrightarrow C,\ x \longmapsto \tilde{T}(x) := \begin{cases} \frac{\|x\|}{r} T\left(\frac{r}{\|x\|}x\right), & x \neq 0; \\ 0, & x = 0; \end{cases}$$

then $\tilde{T}$ *is a* $\tilde{k}$*-*α*-Lipschitz mapping, with* $\tilde{k} > k$*,* $\tilde{k}$ *as near* k *as we please.*

Theorem 1.2.7 (Potter)**.** *Let* $(X, \|\cdot\|)$ *be a Banach space,* C *a cone in* X *and* $0 < r < R$ *real numbers. Suppose that* $T : C_{r,R} \longrightarrow C$ *is a set contraction and Condition* (4) *is satisfied, then* T *has at least one fixed point in* $C_{r,R} \subset C$*.*

Finally, we recall the expansive case result, where we can observe that the expansion conditions are more restrictive that those in Theorem 1.2.5. Thus, in Chapter 2, we use a different approach to prove the result under the expansion conditions (5), in this context and for more general sets.

Theorem 1.2.8 (Các-Gatica)**.** *Let* $(X, \|\cdot\|)$ *be a Banach space,* C *a cone in* X *and* $0 < r < R$ *real numbers. Assume that* $T : C \longrightarrow C$ *is a set contraction,* $T(0) = 0$ *and*

$$\begin{aligned} T(x) - (1+\varepsilon)x \notin C,\ \forall\ \varepsilon > 0 \ \text{ and } x \in B_r,\ x \neq 0; \\ x - T(x) \notin C,\ \forall\ x \in B_R; \end{aligned}$$

then T *has at least one nonzero fixed point in* C*.*

1.2.2 *Norm type, vector and homotopy versions*

In this subsection, we recall three Krasnosel'skii type fixed point results that differ from the original version given in Theorem 1.2.5 in the compression-expansion conditions. We use them in Chapter 3, where we localize a periodic solution of some particular Lotka-Volterra population models. Since the associated integral mapping will have two components, in this subsection, we use

the notation $N(u_1,u_2) = N(u) = (N_1(u),N_2(u))$, and in Chapter 3 we identify $u = (u_1,u_2)$ with the classical notation (x,y), where x refers to the prey population and y to that of predators.

We begin providing the norm type version, which also localizes the fixed points in more general domains.

Theorem 1.2.9. *Let $(X,\|\cdot\|)$ be a Banach space, C a cone in X and Ω_1, Ω_2 open and bounded sets with $0 \in \Omega_1 \subset \overline{\Omega_1} \subset \Omega_2$. Assume that $N : C \cap (\overline{\Omega_2}\backslash\Omega_1) \longrightarrow C$ is a continuous and compact mapping such that one of the following conditions holds:*

(NC) $\|N(u)\| \leqslant \|u\|$, *if* $u \in C \cap \partial\Omega_1$; $\|N(u)\| \geqslant \|u\|$, *if* $u \in C \cap \partial\Omega_2$;

(NE) $\|N(u)\| \geqslant \|u\|$, *if* $u \in C \cap \partial\Omega_1$; $\|N(u)\| \leqslant \|u\|$, *if* $u \in C \cap \partial\Omega_2$;

then N has a fixed point in $C \cap (\overline{\Omega_2}\backslash\Omega_1)$.

Now, we provide the vector version stated in (Precup, 2007, Theorem 2.1).

Theorem 1.2.10. *Let $(X,\|\cdot\|)$ be a Banach space, C_1, C_2 cones in X and $0 < r_1 < R_1$, $0 < r_2 < R_2$ real numbers. Assume that $N : (C_1)_{r_1,R_1} \times (C_2)_{r2,R2} \longrightarrow C_1 \times C_2$ is a continuous and compact map. If one of the following conditions is satisfied in $(C_1)_{r_1,R_1} \times (C_2)_{r2,R2}$ for each $i = 1,2$:*

(V1) $u_i - N_i(u) \notin C_i$, *if* $\|u_i\| = r_i$; $N_i(u) - u_i \notin C_i$, *if* $\|u_i\| = R_i$;

(V2) $N_i(u) - u_i \notin C_i$, *if* $\|u_i\| = r_i$; $u_i - N_i(u) \notin C_i$, *if* $\|u_i\| = R_i$;

then N has a fixed point $u = (u_1,u_2)$ in $(C_1)_{r_1,R_1} \times (C_2)_{r2,R2}$.

We observe that it improves the classical Theorem of Krasnosel'skii, letting the mapping N to satisfy different compression or expansion conditions in each component and variable, for example, one component could satisfy a compression type condition while the other fulfills the expansive one. Moreover, it localizes the solutions by components, so it could provide a better localization.

We conclude this section recalling the homotopy version provided in (O'Regan and Precup, 2001, Theorem 10.8) with expansive type conditions.

Theorem 1.2.11. *Let $(X,\|\cdot\|)$ be a Banach space, $C \subset X$ a cone, $0 < r < R$ and $N : B_R \longrightarrow C$ a continuous and compact mapping. Assume that:*

(H,E1) $N(u) \neq \lambda u$, *for every* $u \in C$, $\|u\| = r$ *and all* $\lambda > 1$;

(H,E2) *there exists* $v \in C \setminus \{0\}$ *such that* $u - N(u) \neq \lambda v$, *for every* $u \in C$, $\|u\| = R$ *and all* $\lambda > 0$;

then, N has a fixed point u in $C_{r,R}$.

USC
UNIVERSIDADE
DE SANTIAGO
DE COMPOSTELA

2 KRASNOSEL'SKII TYPE COMPRESSION-EXPANSION FIXED POINT THEOREM FOR SET CONTRACTIONS AND STAR CONVEX SETS

The contents of this chapter are comprised in the research articles (Lois-Prados and Rodríguez-López, 2020)[1] and (Lois-Prados, Precup, and Rodríguez-López, 2020)[2]. In both manuscripts, we deal with generalizations of Krasnosel'skii type compression-expansion results to set contractions and domains determined by a cone and two star convex sets; and we show the applicability of the results to initial or boundary value problems. We organize the contents of the chapter as follows.

We begin with the Introduction section, where we give a contextualization of our study in the framework of fixed point theory. In particular, we review some generalizations of the classical Theorem of Krasnosel'skii and we explain how we contribute to them. We also justify the use of a direct approach by means of classical fixed point arguments rather than topological degree techniques.

The theoretical results we have developed are contained in Sections 2.2-2.4. In Section 2.2 we describe the type of star convex sets we use to localize the

1 Cristina Lois-Prados (Instituto de Matemáticas, Universidade de Santiago de Compostela, Spain) & Rosana Rodríguez-López (Instituto de Matemáticas, Universidade de Santiago de Compostela, Spain), "A generalization of Krasnosel'skii compression fixed point theorem by using star convex sets", *Proceedings of the Royal Society of Edinburgh - A (ISSN: 14737124, 03082105)*, **150**, pp. 277-303, 2020. The final authenticated version is available online at: https://doi.org/10.1017/prm.2018.119.
JCR 2019 (category; impact factor; relative position; quartile): Mathematics; 1.009; Q2; 111/325.
SJR 2019 (category; impact factor; quartile; H index): Mathematics (miscellaneous); 1.08; Q1; 52.
PhD student contributions: The research idea was conceived by my supervisor R. Rodríguez-López, then C. Lois-Prados developed the majority of contents for her Master degree final dissertation. At the beginning of her PhD studies, she elaborated Section 3.1 within the published manuscript. My supervisor R. Rodríguez-López provided help, support and ideas through all the elaboration and publication process.

2 Cristina Lois-Prados & Radu Precup (Department of Mathematics, Babeş Bolyai University, Romania) & Rosana Rodríguez-López, "Krasnosel'skii type compression-expansion fixed point theorem for set-contractions and star convex sets", *Journal of Fixed Point Theory and Applications (ISSN: 16617738, 16617746)*, **22**, 2020. The final authenticated version is available online at: https://doi.org/10.1007/s11784-020-00799-0.
JCR 2019 (category; impact factor; relative position; quartile): Mathematics; 1.741; 29/325; Q1.
PhD student contributions: In this manuscript, we improved the two main results obtained in the Master degree final dissertation of C. Lois-Prados (supervised by R. Rodríguez-López). C. Lois-Prados developed almost all the contents of the submitted version of the article, following some suggestions from her supervisor (improvement of the compression result) and professor R. Precup (ideas for the expansion result and the application section). Asked by a reviewer, professor R. Precup enriched the application results, now working for systems rather than for a singular equation.

fixed points and we also derive some useful properties. Then, we are in a position to prove the main fixed point results in Section 2.3. Finally, in Section 2.4, we show that we can use functionals to describe the underlying star convex sets, and these functionals are more general than a norm.

In Section 2.5, we show the applicability of the compression type result to an initial value problem for a system of first order differential equations. The associated integral type mapping is noncompact but a set contraction; and the outer boundary of the localization domain is defined by several functionals more general than a norm.

We conclude with the Discussion section, where we summarize our main achievements and compare our research work with other related studies in the framework of fixed point theory.

2.1 INTRODUCTION

In this section, we introduce the research work developed within this chapter in the framework of fixed point theory. We present the contents divided in blocks.

Applicability of Krasnosel'skii type fixed point results

Krasnosel'skii type compression-expansion fixed point theorems are a powerful tool to prove the existence of positive solutions to several classes of problems and also to obtain multiple solutions. Erbe and Wang (1994), Torres (2003), and Zima (2004) have applied a generalization of Theorem 1.2.5 written in terms of the norm to different second order boundary value problems. For instance, Torres (2003) considers a second order equation with periodic boundary conditions and a Caratheodory non-linear term. He also shows several applications, such as one to equations with jumping nonlinearities. O'Regan and Precup (2005) have applied to Hammerstein integral equations a generalization of Theorem 1.2.5 with compression-expansion conditions given in terms of two norms. Other authors have applied this type of results to first order differential systems. In (Wang, 2011), it is proved the existence and multiplicity of ω-periodic solutions for a non-autonomous singular system; while Bolojan and Precup (2014) have studied an implicit system with nonlocal conditions.

Generalizations of the Krasnosel'skii compression-expansion fixed point theorem

We already mentioned, in the introductory paragraphs of Chapter 1, that the classical Krasnosel'skii compression-expansion fixed point theorem can be generalized by relaxing different hypothesis. In Subsection 1.2.1, we recall some extensions of the Theorem of Krasnosel'skii working for more general mappings, more precisely, for set contractions. In Subsection 1.2.2, we consider the norm type, vector and homotopy versions in which the compression-expansion condi-

tions differ from the original ones. Moreover, one of these extensions considers more general domains. This is the result due to Güo and Lakshmikantham (1998) which localizes the fixed point in the more general region $C \cap (\overline{\Omega_2} \setminus \Omega_1)$, where C is a cone in a Banach space $(X, \|\cdot\|)$ and Ω_1, Ω_2 are bounded open sets. Another generalization in this direction can be found in (Precup, 2006), where the fixed point is located in the region $\{x \in C : r < \|x\|_1, \ \|x\|_2 < R\}$, which is determined by the cone and two norms. These two generalizations work for continuous and compact mappings, but change the compression-expansion conditions and consider more general domains. This is also the case of Theorem 4.1 in (Anderson, Avery, and Henderson, 2010), which considers continuous concave/convex functionals that are involved in the Legget-Williams type conditions and the localization domains. In the work by Kwong (2008), we find several extensions of Theorem 1.2.5.

In this chapter, we deal with a generalization that preserves the compression-expansion type conditions of the Krasnosel'skii original result, but works for set contractions and more general domains, which are determined by a cone and two star convex sets. The motivation for working with star convex sets comes from the necessity to distinguish between two solutions in case that they have the same norm, see Figure 1. It is worth mentioning that the results owed by Precup (2006) could also overcome this problem. However, our results work for more general mappings and we claim that the star convex sets can provide a better localization than the sets determined by two norms. Moreover, in Section 2.4, the statements of Corollary 2.4.4 is given in terms of two norms and it is similar to Theorem 3 in (Precup, 2006), with the difference that our result works for more general mappings, but the other does not require the completeness of the space.

Direct approach vs degree theory

Krasnosel'skii proved his theorem directly, using only classical arguments of fixed point theory, particularly Schauder's fixed point theorem (Krasnosel'skii, 1960, 1964). However, it is well-known that this result can also be deduced as a consequence of the topological degree theory (see Granas and Dugundji, 2013). Moreover, many of the generalizations of the classical results due to Krasnosel'skii have been proved using topological degree theory, such as those in (Anderson, Avery, and Henderson, 2010; Güo and Lakshmikantham, 1998).

Nevertheless, from a theoretical perspective, a direct approach without using degree arguments could be useful when trying to extend the results from compact mappings to more general ones. Such a possibility is shown in (O'Regan and Precup, 2001, Chapter 10), where some compression-expansion results are established for a family of mappings for which the topological degree has not been developed. Also, for applications, it seems more convenient to use the Theorem of Krasnosel'skii rather than the degree theory, because the fixed

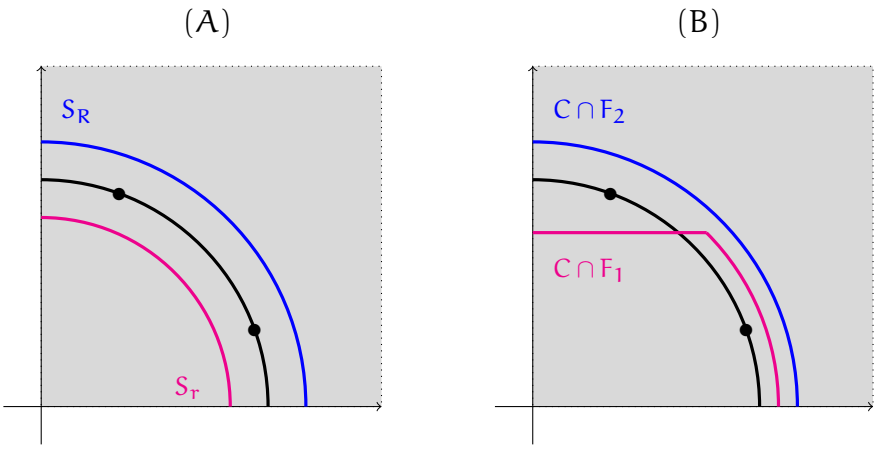

Figure 1: Illustration of the regions where the Krasnosel'skii compression-expansion fixed point theorem (A) and our main results (B) locate the fixed points. The cone $C = \{(x, y) \in \mathbb{R}^2 : x, y \geqslant 0\}$ is represented in gray color; the black dots are the fixed points and the black arc represents the points with the same norm as the fixed points. The magenta and blue curves are the sets where the compression or expansion conditions are satisfied. The regions in between these curves correspond to those where the results localize the fixed points. In (A) both fixed points are inside this region, while in (B) the region isolates one of them.

point result offers directly the compression-expansion conditions that have to be fulfilled.

The direct approach owed by Krasnosel'skii was also followed by Potter (1974) and Các and Gatica (1979), who respectively extended the compression and expansion result from continuous and compact mappings to set contractions (see Theorems 1.2.7, 1.2.8). Notice that both Krasnosel'skii and Potter obtained a solution localized in conical annular sets determined by the norm, but the result obtained by Các and Gatica provides a less refined localization, since they can only assert that there exists a positive fixed point in the cone.

Our main results can be seen as generalizations of the results due to Potter (1974) and Các and Gatica (1979) to more general domains; and our proofs also follow a direct approach without using topological degree techniques.

Overview of the research development

Our study is focused on the generalization of the compression-expansion results for set contractions to conical domains determined by two star convex sets. In this regard, we first require some additional conditions to these non necessarily convex sets. An essential property is the following one: each ray traveling from zero and passing through any other point in the star convex set meets a unique element in its boundary. We notice that, for the theoretical arguments, we use an equivalent condition given in terms of a continuous functional. Once we have determined the framework where we will develop

our research, to prove the compression result we adapt Potter's ideas to star convex sets. Nevertheless, for the expansive case we do not follow the proof given by Các and Gatica, but we use the idea of reducing the expansive case to the compressive one, as shown in (Precup, 2006) for compact mappings. In this way, we improve the localization of fixed points provided by the existing theorem for balls and state a new result for star convex sets. The possibility to use star convex sets instead of balls allows to determine the conical domain by functionals more general than a norm. The use of such functionals seems to be very useful for applications, so we derive some sufficient conditions that they shall satisfy. Finally, it is important to show the applicability of the new results. For that purpose, we consider an initial value problem for a system of first order implicit differential equations, we apply the compression result to the associated noncompact integral mapping, and we use functionals to define a star convex set.

2.2 GENERAL FRAMEWORK

We have already mentioned that our results improve the localization of fixed points in Theorem 1.2.5 by using star convex sets. Thus, we begin this section by recalling this concept and by stating some additional conditions we will require to the sets considered. We provide two characterizations of the underlying star convex sets, one easier for visualization and the other more useful for the theoretical aspects. Then we prove the equivalence between these characterizations and we deduce some helpful properties of these sets.

We notice that most of the section contents were developed for the Master degree dissertation of Cristina Lois Prados. However, it was during the PhD period when the equivalence between the characterizations in Condition 1 was completed with Proposition 2.2.2.

Definition 2.2.1. Let $(X, \|\cdot\|)$ be a Banach space, $E \subset X$ and $x_0 \in E$. We say that E is an x_0-star convex set if

$$\lambda x_0 + (1-\lambda)x \in E, \text{ for all } \lambda \in [0,1] \text{ and } x \in E.$$

In case that $x_0 = 0$, E is simply called a star convex set.

Condition 1. In the following, we consider a Banach space $(X, \|\cdot\|)$, C a cone in X and $E \subset X$ a star convex set (which trivially satisfy $E \cap C \neq \emptyset$). In addition, the star convex set shall fulfill:

1. E is bounded and closed;
2. If F is the boundary of E in X, then $0 \notin F$;

and one of the following equivalent hypotheses:

3. for every $x \in E\backslash\{0\}$, there exists a unique $\beta_x > 0$ with $\beta_x x \in F$;

4. there exists a continuous mapping $\partial : E\backslash\{0\} \longrightarrow F$, $x \longmapsto \partial(x)$, such that

$$\begin{cases} \partial(x) = \partial(\lambda x), & \forall\, x \in E,\ \forall\, \lambda \in (0,1]; \\ \partial(x) = x, & \forall\, x \in F. \end{cases}$$

The following result proves that hypothesis 3 in Condition 1 implies statement 4, but in the general context of an x_0-star convex set.

Proposition 2.2.2. *Let $(X, \|\cdot\|)$ be a Banach space, $x_0 \in X$ and $E \subset X$ be a bounded closed x_0-star convex set such that its boundary F does not contain x_0, and*

$$\text{for all } x \in E \setminus \{x_0\}, \text{ there is a unique } \lambda_x > 0 \text{ with } \lambda_x x + (1-\lambda_x)x_0 \in F. \tag{6}$$

Then there exists a continuous mapping $\partial : E \setminus \{x_0\} \to F$ such that

$$\begin{aligned} &\partial(x) = \partial(\lambda x + (1-\lambda)x_0), \ \textit{for all} \ \ x \in E \setminus \{x_0\},\ \lambda \in (0,1]; \\ &\partial(x) = x, \ \textit{for all} \ \ x \in F. \end{aligned} \tag{7}$$

Proof. As $x_0 \in E \setminus F$, there exists $\gamma > 0$ such that $B := B(x_0, \gamma) \subset E \setminus F$. Let S be the boundary of B, i.e., $S := \{x \in X : \ \|x - x_0\| = \gamma\}$. We define the mapping ∂ as the composition $\eta \circ \eta_0$, where η_0 is the radial projection

$$\eta_0 : E \setminus \{x_0\} \to S, \quad \eta_0(x) = \frac{\gamma}{\|x - x_0\|}(x - x_0),$$

and

$$\eta : S \to F, \quad \eta(x) = \lambda_x x + (1-\lambda_x)x_0.$$

From (6), the mapping η is well-defined. Also, it is easy to see that condition (7) is satisfied. Clearly, η_0 is continuous, so it remains to prove the continuity of η. To this aim, it suffices to prove the continuity of the function

$$\lambda : S \longrightarrow \mathbb{R}^+, \ \ \lambda(x) = \lambda_x.$$

For that purpose, let $\{y_n\}_{n\in\mathbb{N}}$ be any sequence in S converging to some $y \in S$. Since E is bounded and $\lambda(S) \subset [0, +\infty)$, then there exists $m \in \mathbb{R}^+$ such that $\lambda(S) \subset [0, m]$. Therefore, the sequence $\{\lambda(y_n)\}_{n\in\mathbb{N}}$ is included in the compact interval $[0, m]$, so any of its limit points is finite. Let l be any limit point of $\{\lambda(y_n)\}_{n\in\mathbb{N}}$. From

$$\eta(y_n) = \lambda(y_n)y_n + (1-\lambda(y_n))x_0 \in F,$$

we find that

$$ly + (1-l)x_0 \in F.$$

This, in view of (6), gives $l = \lambda(y)$. Hence $\lambda(y_n) \to \lambda(y)$ as $n \to +\infty$. Therefore, λ is continuous as wished. □

The next result proves the remaining implication.

Proposition 2.2.3. *Let* C *be a cone a Banach space* $(X, \|\cdot\|)$ *and* E *be a star convex set satisfying Condition 1 with hypothesis 4. Then,* E *also satisfies hypothesis 3, that is, for all* $x \in E\backslash\{0\}$*, there exists a unique real number* $\beta_x > 0$ *such that* $\beta_x x \in F$*. In particular, if* $x \in C \cap (E\backslash\{0\})$*, then* $\beta_x x \in C \cap F$*.*

Proof. The existence of such a number is clear since C is a cone and E is closed, bounded, with non-empty interior, and a star convex set. Suppose that there exist β_x^1, $\beta_x^2 \in \mathbb{R}^+$ such that $\beta_x^1 \neq \beta_x^2$ and $\beta_x^1 x$, $\beta_x^2 x \in F$. Without loss of generality, we assume that $\beta_x^2 > \beta_x^1$, then $0 < \frac{\beta_x^1}{\beta_x^2} < 1$ and, therefore,

$$\partial(\beta_x^1 x) = \partial\left(\frac{\beta_x^1}{\beta_x^2}\beta_x^2 x\right) = \partial(\beta_x^2 x) = \beta_x^2 x \in F. \tag{8}$$

Moreover, since $\beta_x^1 x \in F$, we have $\partial(\beta_x^1 x) = \beta_x^1 x \in F$. By using (8), we obtain $\beta_x^1 x = \beta_x^2 x$. Taking the norm, we get $\beta_x^1\|x\| = \beta_x^2\|x\|$, and, since $x \neq 0$, we conclude that $\beta_x^1 = \beta_x^2$, i.e., the element β_x in the statement is unique.

Besides, if $x \in C$ and $\beta_x > 0$, then it is clear that $\beta_x x \in C$ by using the definition of cone. □

Apart from the continuous map ∂ given by hypothesis 4 in Condition 1, the map defined by the scalar number referred to in the equivalent hypothesis 3 also plays an important role in the theoretical development. Thus, it is interesting to deduce some of its properties.

Proposition 2.2.4. *Let* C *be a cone and* E *be a star convex set satisfying Condition 1. Then the mapping*

$$\begin{aligned} \beta : C \cap (E\backslash\{0\}) &\longrightarrow [1, +\infty) \\ x &\longmapsto \beta(x) := \beta_x; \end{aligned}$$

where β_x *is the unique positive real number such that* $\beta_x x \in F \cap C$*, is continuous and* $\beta(x) \to +\infty$ *as* $x \to 0$*.*

Proof. First of all, we prove that the image of β is a subset of $[1, +\infty)$. Let $x \in C \cap (E\backslash\{0\})$, then it is satisfied that $\beta_x x = \partial(x) \in C \cap F$. Thus, by using that E is a star convex set satisfying Condition 1, we get

$$\beta_x = \frac{\|\partial(x)\|}{\|x\|} \geqslant 1.$$

The continuity of β follows easily since it can be expressed as a composition of continuous functions:

$$\begin{aligned} \beta : C \cap (E\backslash\{0\}) &\longrightarrow [1, +\infty) \\ x &\longmapsto \beta(x) = \frac{d(0, \partial(x))}{d(0, x)} = \frac{(d_0 \circ \partial)(x)}{d_0(x)}; \end{aligned}$$

where ∂ is continuous by hypothesis and $d_0(x) := d(0,x) = \|x\|$, $x \in X$, is continuous because of the distance properties.

Finally, it remains to prove that $\beta(x)$ tends to infinity as x goes to 0. Thus, for all $M \in \mathbb{R}^+$, we look for $\delta \in \mathbb{R}^+$ such that

$$\beta(x) > M, \text{ for all } x \in C \cap (E\backslash\{0\}) \text{ with } \|x\| < \delta.$$

If $M \in (0,1)$, then $\beta(x) > M$ is trivially satisfied for all $x \in C \cap (E\backslash\{0\})$, since $\beta \in [1, +\infty)$.
If $M \geqslant 1$, we take $0 < \delta := d(0,F)/M < +\infty$, with $d(0,F) := \inf\{d(0,y) : y \in F\}$. Let $x \in C \cap (E\backslash\{0\})$ with $\|x\| < \delta$, then we prove that $\beta(x) > M$:

$$\beta(x) = \frac{d(0,\partial(x))}{d(0,x)} \geqslant \frac{d(0,F)}{d(0,x)} = \frac{d(0,F)}{\|x\|} > \frac{d(0,F)}{\delta} = M.$$

□

We conclude this section by showing another useful property of both mappings ∂ and β, the fact that they can be continuously extended to $C\backslash\{0\}$.

Remark 2. Let C be a cone and E be a star convex set satisfying Condition 1. As E is closed, a star convex set and $0 \in \mathring{E}$, then the restriction of the mapping ∂ to $C \cap (E\backslash\{0\})$ can be continuously extended to $C\backslash\{0\}$ as follows

$$\partial^C : C\backslash\{0\} \longrightarrow F$$

$$x \longmapsto \partial^C(x) := \begin{cases} \partial(x), & x \in E\backslash\{0\}; \\ \partial\left(\frac{d(0,F)}{\|x\|}x\right), & x \in C\backslash(C \cap \mathring{E}). \end{cases}$$

Figure 2 illustrates the behavior of ∂^C in a particular case.

By using ∂^C, we can also continuously extend β to $C\backslash\{0\}$ as:

$$\beta^C(x) = \frac{d(0,\partial^C(x))}{d(0,x)}, \text{ for all } x \in C\backslash\{0\}.$$

2.3 MAIN RESULTS

In this section, we extend the Krasnosel'skii compression-expansion fixed point theorem to set contractions and star convex sets. For that purpose, the first step will be to reformulate the compression-expansion conditions in (4)-(5) to star convex sets satisfying Condition 1. After that, we are in a position to prove the more general results. Since we use different approaches to prove the compressive and expansive cases, we devote one subsection to each one.

Let us consider C a cone and E_i, $i = 1, 2$, star convex sets satisfying Condition 1. We establish the following notations for $i = 1, 2$:

- $\mathring{E}_i$ and F_i are the interior and the boundary of E_i, respectively.

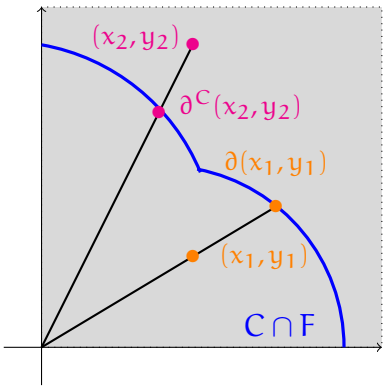

Figure 2: Illustration of mappings ∂ and ∂^C for the cone $C = \{(x, y) \in \mathbb{R}^2 : x, y \geqslant 0\}$. The blue curve represents the intersection of the cone with the boundary of the star convex set. The black segment lines are rays traveling from $(0, 0)$ to the points $(x_i, y_i) \in C \setminus \{0\}$, for $i = 1, 2$.

- $\partial_i : E_i \setminus \{0\} \longrightarrow F_i$ is the continuous mapping given in Condition 1 and ∂_i^C the continuous extension to $C \setminus \{0\}$ provided in Remark 2.
- $\beta_i : C \cap (E_i \setminus \{0\}) \longrightarrow [1, +\infty)$ is the continuous map defined in Proposition 2.2.4 and β_i^C is the corresponding continuous extension to $C \setminus \{0\}$ provided in Remark 2.

Next, we assume that $E_1 \subset E_2$, $F_1 \cap F_2 = \emptyset$, and consider a mapping

$$T : C \cap \left(E_2 \setminus \mathring{E}_1\right) \to C.$$

We say that T is a *compression* of the set $C \cap \left(E_2 \setminus \mathring{E}_1\right)$ (see Figure 3 (A)) if:

(C1) $x - T(x) \notin C$, for all $x \in C \cap F_1$;

(C2) $T(x) - (1 + \varepsilon)x \notin C$, for all $\varepsilon > 0$ and $x \in C \cap F_2$.

We say that T is an *expansion* of the set $C \cap \left(E_2 \setminus \mathring{E}_1\right)$ (see Figure 3 (B)) if:

(E1) $T(x) - (1 + \varepsilon)x \notin C$, for all $\varepsilon > 0$ and $x \in C \cap F_1$;

(E2) $x - T(x) \notin C$, for all $x \in C \cap F_2$.

Before going through the details of the proof of the generalized results, we provide some arguments to justify that, unless there exists a bounded homeomophism h that transforms a star convex set E_i ($i = 1, 2$) satisfying Condition 1 in a bounded closed ball B_i, we cannot adapt Theorems 1.2.7 and 1.2.8 to these star convex sets by simply using the classical idea of composing the mapping T with the mentioned homeomorphic transformation. The main reasons are:

- T is a k-set contraction: while if we first apply a continuous and compact mapping (0-set contraction) and then a continuous and bounded map, the composition inherits the compactness property, if $k \in (0, 1)$, then the corresponding condition is not generally preserved.

- The domain of T is $C \cap (E_2 \backslash \mathring{E}_1)$: the homeomorphic transformations depend on the star convex sets E_i $(i = 1, 2)$, then we cannot ensure the existence of a homeomorphism transforming $C \cap (E_2 \backslash \mathring{E}_1)$ in $C \cap (B_2 \backslash \mathring{B}_1)$.
- The range of T is C: in order to use the idea of composing with h and h^{-1}, we would have to require that T maps the domain $C \cap (E_2 \backslash \mathring{E}_1)$ into itself.
- The compression-expansion conditions: even if the previous requirements are fulfilled, conditions **(C1)-(C2)** or **(E1)-(E2)** will not be generally inherited by the composition $h \circ T \circ h^{-1}$.

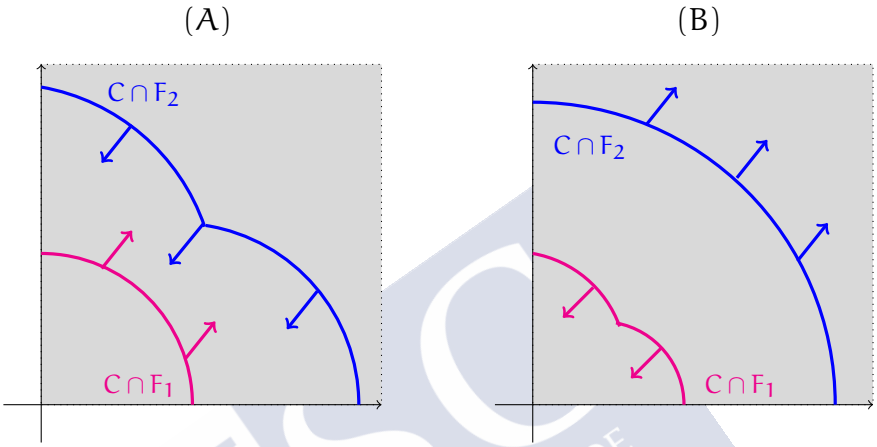

Figure 3: Behavior of the mapping in the inner and outer boundaries for a compression (A) and an expansion (B) of the set $C \cap (E_2 \backslash \mathring{E}_1)$, where $C = \{(x, y) \in \mathbb{R}^2 : x, y \geqslant 0\}$ and E_1, E_2 are star convex sets. The magenta and blue curves, are referred as inner and outer boundaries and, represent the intersection of the cone C with the boundary of E_1 and E_2, respectively. The arrows illustrate the compression-expansion conditions satisfied by the points lying in the boundaries.

2.3.1 *Compressive case*

In this section, we give an extension of the Potter compression result to the more general domains of the type $C \cap (E_2 \backslash \mathring{E}_1)$. For that purpose, we adapt the proof of Lemma 1.2.1 and Theorem 1.2.7 to this more general framework.

It is worth mentioning that most of this research was developed during the Master degree studies of Cristina Lois Prados, but with some restrictive assumptions over the constant k. The extension of the results to any constant $k \in [0, 1)$ corresponds to the PhD period. This improvement was achieved by changing the definition of the sets A_m^n in the proof of Lemma 2.3.1. The proof of Theorem 2.3.1 remained the same, but we included it in this document for the sake of completeness.

Lemma 2.3.1. *Assume that* $(X, \|\cdot\|)$ *is a Banach space,* C *a cone in* X *and* E *a set satisfying Condition 1. Let* $T : C \cap F \longrightarrow C$ *be* α*-Lipschitz with constant* k *and consider the mapping*

$$\tilde{T} : C \cap E \longrightarrow C$$
$$x \longmapsto \tilde{T}(x) := \begin{cases} \frac{1}{\beta(x)} T(\beta(x)x), & x \neq 0; \\ 0, & x = 0. \end{cases}$$

Then $\tilde{T}$ *is* α*-Lipschitz with constant* $\tilde{k}$ *for every* $\tilde{k} > k$ *as close to* k *as we wish.*

Proof. We first show that $\tilde{T}$ is continuous by distinguishing the cases $x_0 \neq 0$ and $x_0 = 0$. Then we prove the existence of $\tilde{k}$ as close to k as we wish such that

$$\alpha\left(\tilde{T}(A)\right) \leqslant \tilde{k}\alpha(A), \text{ for all } A \subset C \cap E \tag{9}$$

and we also consider two cases: $\alpha(A) = 0$ and $\alpha(A) \neq 0$.

Continuity of $\tilde{T}$

Let $x_0 \in C \cap (E \backslash \{0\})$ and $\varepsilon > 0$ be arbitrarily fixed. As $x_0 \neq 0$, then $d(0, x_0) > 0$, therefore we can choose $\delta \in \mathbb{R}$ with $0 < \delta < d(0, x_0)$. As a consequence,

$$\tilde{T}_{|_{B(x_0,\delta)}} : B(x_0, \delta) \cap (C \cap E) \longrightarrow C$$
$$x \longmapsto \tilde{T}_{|_{B(x_0,\delta)}}(x) = \frac{1}{\beta(x)} T(\beta(x)x)$$

is continuous, because T, β and $\frac{1}{\beta}$ are continuous too.

Now, let $x_0 = 0$. Since X is a Banach space, in particular a metric space, we can characterize the continuity property of $\tilde{T}$ at 0 working with convergent sequences. Assume that $\{x_n\}_{n\in\mathbb{N}} \subset C \cap E$ converges to 0. We can consider that $x_n \neq 0$ for all $n \in \mathbb{N}$, so

$$\|\tilde{T}(x_n)\| = \left\| \frac{1}{\beta(x_n)} T(\beta(x_n)x_n) \right\| = \frac{1}{\beta_{x_n}} \|T(\beta_{x_n} x_n)\| .$$

For all $n \in \mathbb{N}$, $\beta_{x_n} x_n \in C \cap F$. Besides, as $C \cap F$ is bounded and T is a k-set contraction, then $T(C \cap F)$ is necessarily a bounded set in order to consider its measure of non compactness. Therefore, there exists $K \in \mathbb{R}^+$ such that $\sup\{T(\beta_{x_n} x_n) : n \in \mathbb{N}\} < K$, so

$$\|\tilde{T}(x_n)\| \leqslant \frac{1}{\beta_{x_n}} K, \text{ for all } n \in \mathbb{N}.$$

By Proposition 2.2.4, we can assert that $\left\{\frac{1}{\beta_{x_n}}\right\}_{n\in\mathbb{N}}$ converges to 0, and consequently $\{\|\tilde{T}(x_n)\|\}_{n\in\mathbb{N}}$ also converges to 0. As $\tilde{T}(0) = 0$, the continuity of $\tilde{T}$ at $x_0 = 0$ is proved.

Existence of $\tilde{k}$.

Let us consider an arbitrary set $A \subset C \cap E$. If $\alpha(A) = 0$, the proof follows easily. Indeed, the set $\overline{A}$ is a compact set and $\tilde{T}$ is continuous, so $\tilde{T}\left(\overline{A}\right)$ is also

a compact set. Using that the measure of non compactness of a compact set is null and $\tilde{T}(A) \subseteq \tilde{T}\left(\overline{A}\right)$, we have

$$\alpha(\tilde{T}(A)) \leqslant \alpha(\tilde{T}\left(\overline{A}\right)) = 0 = k\alpha(A),\ \forall k \in \mathbb{R},\ k \geqslant 0.$$

Now, let $A \subset C \cap E$ be such that $\alpha(A) \neq 0$ and $k > 0$ (if this is not true, we can consider $\hat{k} > 0$ as close to k as we wish). As k, $\alpha(A) > 0$, there exists $d > 0$ such that $k\,\alpha(A)/2 > d > 0$. We fix d satisfying these conditions.

To accomplish the aim of proving that (9) is satisfied, we proceed as follows.

Step 1: Cover any set A by a finite number of subsets with the property that the restriction of $\tilde{T}$ to each of them is α-Lipschitz for some suitable constant.

To this aim, we start by using the continuity of $\tilde{T}$ that ensures the existence of $\delta_d > 0$ such that

$$\tilde{T}((C \cap E) \cap B(0, \delta_d)) \subset B(0, d).$$

Then, we have

$$\tilde{T}(A \cap B(0, \delta_d)) \subset B(0, d). \tag{10}$$

On the other hand, for each natural number $n \geqslant 1$, take $\varepsilon_n = \delta_d/n$ and, for all natural number $m \geqslant 1$, define

$$A_m^n := \{x \in A\ :\ \beta(x) \in [1 + (m-1)\varepsilon_n,\ 1 + m\varepsilon_n]\}.$$

For any natural number $n \geqslant 1$, there exists $N_n \in \mathbb{N}$, $N_n > 1$, such that, if $\beta(x) > 1 + N_n\varepsilon_n$, then $x \in A \cap B(0, \delta_d)$. Therefore,

$$A \subset (A \cap B(0, \delta_d)) \cup \left(\bigcup_{m=1}^{N_n} A_m^n\right). \tag{11}$$

Step 2: Fix $n \in \mathbb{N}$, $n > 1$, arbitrarily and, for each $m \in \{1, \ldots, N_n\}$, we show that $\tilde{T}_{|A_m^n}$ is α-Lipschitz with constant $k\,(1 + m\varepsilon_n)/(1 + (m-1)\varepsilon_n)$.

For each $m \in \{1, \ldots, N_n\}$, we have $0 \notin A_m^n$, so $\tilde{T}_{|A_m^n}$ is given by

$$\tilde{T}_{|A_m^n}(x) = \frac{1}{\beta(x)} T(\beta(x)x).$$

Let $m \in \{1, \ldots, N_n\}$ and define the following auxiliary mappings:

$$\frac{1}{\beta_{|A_m^n}} : A_m^n \longrightarrow C,\ x \longmapsto \frac{1}{\beta_{|A_m^n}}(x) := \frac{1}{\beta(x)};$$
$$S_m^n : A_m^n \longrightarrow C,\ x \longmapsto S_m^n(x) := \beta(x)x.$$

Since β is continuous and its image is a subset of $[1, \infty)$, we deduce that $1/\beta_{|A_m^n}$ is a continuous function. Besides, for all $x \in A_m^n$, it is satisfied that

$$\beta(x) \in [1 + (m-1)\,\varepsilon_n, 1 + m\,\varepsilon_n] \Leftrightarrow \frac{1}{\beta(x)} \in \left[\frac{1}{1 + m\,\varepsilon_n}, \frac{1}{1 + (m-1)\,\varepsilon_n}\right],$$

hence

$$\sup\left\{\frac{1}{\beta(x)} \,:\, x\in A_m^n\right\}\leqslant \frac{1}{1+(m-1)\,\varepsilon_n}.$$

As T is a k-set contraction, in view of statement 3 in Proposition 1.1.9, it remains to prove that S_m^n is α-Lipschitz with constant $(1+m\varepsilon_n)$. Let $B\subset A_m^n$, then B is bounded and, using the definition of A_m^n, we have

$$\begin{aligned}S_m^n(B)&=\Big\{\beta(x)x \,:\, x\in B\Big\}\\&\subset\Big\{[\lambda(1+(m-1)\varepsilon_n)+(1-\lambda)(1+m\varepsilon_n)]x \,:\, \lambda\in[0,1],\, x\in B\Big\}\\&=\mathrm{co}\Big(\big\{[1+(m-1)\varepsilon_n]B\big\}\cup\big\{[1+m\varepsilon_n]B\big\}\Big).\end{aligned}$$

Now, by using the properties of the measure of noncompactness, we obtain

$$\alpha(S_m^n(B))\leqslant\max\Big\{\alpha\big([1+(m-1)\varepsilon_n]B\big),\,\alpha\big([1+m\varepsilon_n]B\big)\Big\}=(1+m\varepsilon_n)\alpha(B).$$

Also, as β is continuous, then S_m^n is continuous. Therefore, S_m^n is α-Lipschitz with constant $(1+m\varepsilon_n)$.

As a consequence, by using properties 1,3 of α-Lipschitz mappings in Proposition 1.1.9, we can assert that $\tilde{T}_{|A_m^n}$ is an α-Lipschitz mapping with constant $k\,(1+m\varepsilon_n)/(1+(m-1)\varepsilon_n)$.

Step 3: Taking into account the two previous steps, we can conclude that $\tilde{T}$ is α-Lipschitz with constant $\tilde{k}$ as close to k as we wish.

It follows from (10), (11) and the properties of the measure of noncompactness, that:

$$\begin{aligned}\alpha\left(\tilde{T}(A)\right)&\leqslant\alpha\left(\tilde{T}(A\cap B(0,\delta_d))\cup\bigcup_{m=1}^{N_n}\tilde{T}(A_m^n)\right)\\&=\alpha\left(\tilde{T}(A\cap B(0,\delta_d))\cup\tilde{T}(A_1^n)\cup\cdots\cup\tilde{T}(A_{N_n}^n)\right)\\&=\max\left\{\alpha\left(\tilde{T}(A\cap B(0,\delta_d))\right),\,\alpha\left(\tilde{T}(A_1^n)\right),\ldots,\,\alpha\left(\tilde{T}(A_{N_n}^n)\right)\right\}\\&\leqslant\max\left\{\alpha\left(B(0,d)\right),\,\alpha\left(\tilde{T}(A_1^n)\right),\ldots,\,\alpha\left(\tilde{T}(A_{N_n}^n)\right)\right\}\\&\leqslant\max\left\{2d,\frac{1+\varepsilon_n}{1}k\alpha(A_1^n),\ldots,\frac{1+N_n\varepsilon_n}{1+(N_n-1)\varepsilon_n}k\alpha(A_{N_n}^n)\right\}\\&\leqslant\max\left\{2d,\frac{1+\varepsilon_n}{1}k\alpha(A),\ldots,\frac{1+N_n\varepsilon_n}{1+(N_n-1)\varepsilon_n}k\alpha(A)\right\}\\&\leqslant(1+\varepsilon_n)k\alpha(A),\end{aligned}$$

where the last inequality holds since $2d<k\alpha(A)$ and

$$\frac{1+m\varepsilon_n}{1+(m-1)\varepsilon_n}\leqslant 1+\varepsilon_n \text{ for all } m\in\{1,\ldots,N_n\}.$$

Since $\varepsilon_n\to 0$ as $n\to\infty$, if n is large enough, the number $\tilde{k}:=(1+\varepsilon_n)k$ can be as close to k as we wish. □

Theorem 2.3.1. *Let* $(X, \|\cdot\|)$ *be a Banach space,* C *be a cone in* X*, and* E_1*,* E_2 *be sets fulfilling Condition 1. Assume that* $T : C \cap (E_2 \backslash \mathring{E}_1) \longrightarrow C$ *is a* k*-set contraction and a compression of the set* $C \cap (E_2 \backslash \mathring{E}_1)$*. Then* T *has at least one fixed point in* $C \cap (E_2 \backslash \mathring{E}_1)$*.*

Proof. We will use Theorem 1.2.6 to prove the existence of a fixed point for T. But this result cannot be directly applied to this mapping, so we first extend T from $C \cap (E_2 \backslash \mathring{E}_1)$ to C in a proper way. Next, we look for a bounded, closed and convex set B that is mapped into itself by the new mapping $\overline{T}$. Then, we shall prove that $\overline{T}_{|B}$ is a $\overline{k}$-set contraction. Finally, we have to show that the fixed point $\overline{x} \in B$ belongs to the conical domain $C \cap (E_2 \backslash \mathring{E}_1)$.

Extension of the mapping T *to the cone* C

We define the mapping $\overline{T}$ that is the extension of $T : C \cap (E_2 \backslash \mathring{E}_1) \longrightarrow C$ to the cone C. To that purpose, we should take into account that, since $0 \in E_1 \backslash F_1$, then $d(0, F_1) > 0$. Hence, it is possible to choose $\delta \in \mathbb{R}$ such that $0 < \delta < d(0, F_1)$. We fix arbitrarily some $\delta \in \mathbb{R}$ satisfying such condition and we define the set

$$E_1^{\delta} := \{x \in E_1 \,:\, d(x, F_1) \geqslant \delta\}.$$

Now, we consider $\overline{T}$ defined by (see Figure 4)

$$x \longmapsto \overline{T}(x) := \begin{cases} \delta h, & \|x\| = 0; \\ \frac{1}{\beta_1(x)} T(\beta_1(x)x) + \delta h, & x \in C \cap \left(E_1^{\delta} \backslash \{0\}\right); \\ \frac{1}{\beta_1(x)} T(\beta_1(x)x) + d(x, F_1)h, & x \in C \cap \left(E_1 \backslash \mathring{E}_1^{\delta}\right); \\ T(x), & x \in C \cap \left(E_2 \backslash \mathring{E}_1\right); \\ T\left(\partial_2^C(x)\right), & x \in C \backslash \left(C \cap \mathring{E}_2\right); \end{cases}$$

where $h \in C$ and

$$\|h\| > \frac{1}{\delta}\left[\sup\{d(0, x) \,:\, x \in C \cap E_1\} + \sup\{\|T(\beta_1(x)x)\| \,:\, x \in C \cap E_1\}\right].$$

We show that there exists such an h. Indeed:

- Since $C \cap E_1$ is a bounded set, there exists $\sup\{d(0, x) \,:\, x \in C \cap E_1\} < +\infty$.
- For each $x \in C \cap E_1$, $\beta_1(x)x \in C \cap F_1$ and, as T is a k-set contraction, then the image of the bounded set $C \cap F_1$ is also bounded, hence there exists

  $$\sup\{\|T(\beta_1(x)x)\| \,:\, x \in C \cap E_1\} < +\infty.$$

Hence, as C is a cone in X, it is possible to choose such an h.

It is worth mentioning that $\overline{T}$ is well defined, since the different expressions of $\overline{T}$ coincide at the respective intersections between the sets $C \cap (E_1^{\delta} \backslash \{0\})$, $C \cap \left(E_1 \backslash \mathring{E}_1^{\delta}\right)$, $C \cap (E_2 \backslash \mathring{E}_1)$ and $C \backslash \left(C \cap \mathring{E}_2\right)$.

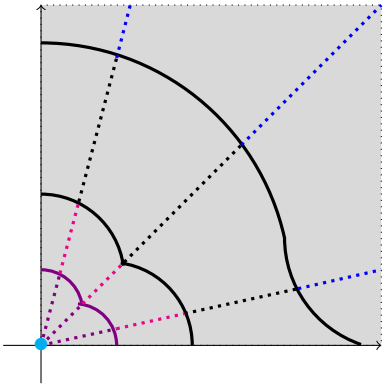

Figure 4: Illustration of the sets used in the extension of the mapping T from the conical domain $C \cap (E_2 \backslash \mathring{E}_1)$ to the cone $C = \{(x, y) \in \mathbb{R}^2 : x, y \geqslant 0\}$. The region with black dashed lines represents the set $C \cap (E_2 \backslash \mathring{E}_1)$ where $\overline{T} \equiv T$. The rest of the regions are divided as follows: the origin is the light blue point, the set $C \cap (E_1^{\delta} \setminus \{0\})$ is represented in purple, $C \cap (E_1 \setminus \mathring{E}_1^{\delta})$ in magenta and $C \setminus (C \cap \mathring{E}_2)$ in dark blue.

Application of Theorem 1.2.6 to $\overline{T}_{|B}$

We look for a bounded, closed and convex set B such that the restriction of $\overline{T}$ to this set is a $\overline{k}$-set contraction. To accomplish this aim, we proceed as follows.

Step 1: We define the set B that will be mapped into itself by $\overline{T}$.

We first prove that there exists $R_1 \in \mathbb{R}^+$, $R_1 = \sup\left\{\left\|\overline{T}(x)\right\| : x \in C \cap E_2\right\}$. We distinguish four cases, since the definition of $\overline{T}$ depends on the subset of $C \cap E_2$ under consideration:

- If $x = 0$, then $\|\overline{T}(x)\| = \delta\|h\|$.
- If $x \in C \cap \left(E_1^{\delta} \backslash \{0\}\right)$, then $\left\|\overline{T}(x)\right\| = \left\|\frac{1}{\beta_1(x)} T(\beta_1(x)x) + \delta h\right\|$. Taking into account that $\beta_1(x) \in [1, +\infty)$ implies $\frac{1}{\beta_1(x)} \in (0, 1]$, and using the triangular inequality, we obtain $\|\overline{T}(x)\| \leqslant \|T(\beta_1(x)x)\| + \delta\|h\|$. As the set $C \cap F_1 \subset C \cap \left(E_2 \backslash \mathring{E}_1\right)$ is bounded and $T : C \cap \left(E_2 \backslash \mathring{E}_1\right) \longrightarrow C$ is a k-set contraction, then $T(C \cap F_1)$ is also bounded, therefore there exists $M_1 \in \mathbb{R}^+$ such that $\|T(x)\| \leqslant M_1$ for all $x \in C \cap F_1$. Besides, for all $x \in C \cap (E_1^{\delta} \backslash \{0\})$, we have $\beta_1(x)x \in C \cap F_1$, so we conclude

$$\left\|\overline{T}(x)\right\| \leqslant M_1 + \delta\|h\|, \quad \forall x \in C \cap (E_1^{\delta} \backslash \{0\}).$$

- If $x \in C \cap \left(E_1 \backslash \mathring{E}_1^{\delta}\right)$, then

$$\left\|\overline{T}(x)\right\| \leqslant M_1 + \delta\|h\|,$$

where we use the existence of M_1 proved before.

- If $x \in C \cap (E_2 \backslash \mathring{E}_1)$, as it is a bounded set and T is a k-set contraction, there exists $M_2 \in \mathbb{R}^+$ such that $\left\|\overline{T}(x)\right\| = \|T(x)\| \leqslant M_2$, for all $x \in C \cap (E_2 \backslash \mathring{E}_1)$.

Therefore, we conclude that there exists $R_1 \in \mathbb{R}^+$ with the above property.

In addition, there exists $R_2 \in \mathbb{R}^+$ such that $R_2 = \sup\{d(0,x) \,:\, x \in C \cap E_2\}$, since $C \cap E_2$ is a bounded set.

Thus, we consider $R = \max\{R_1, R_2\} \in \mathbb{R}^+$ and $B \equiv B_R = \{x \in C \,:\, d(0,x) \leqslant R\}$. We have chosen $R \in \mathbb{R}^+$ such that $\overline{T}(B_R) \subseteq B_R$. Besides, the set B_R is bounded, closed and convex, because it is the intersection of the closed and convex set C with the bounded, closed and convex set $\overline{B}(0,R) = \{x \in X \,:\, d(0,x) \leqslant R\}$.

Step 2: We prove that $\overline{T}_{|B_R}$ is a $\overline{k}$-set contraction.

We first show that $\overline{T}$ is continuous. It is clearly continuous on $C\backslash\{0\}$ and the continuity at $x = 0$ follows from similar arguments to those in Lemma 2.3.1.

Then, we shall prove that there exists $\overline{k} < 1$ such that

$$\alpha(\overline{T}(A)) \leqslant \overline{k}\alpha(A), \text{ for all } A \subset B_R.$$

In order to prove it, we define some helpful auxiliary mappings:

$T_1 : B_R \cap E_1 \longrightarrow B_R$ is given by

$$T_1(x) := \begin{cases} \delta h, & x = 0; \\ \frac{1}{\beta_1(x)} T(\beta_1(x)x) + \delta h, & x \in B_R \cap \left(E_1^{\delta} \backslash \{0\}\right); \\ \frac{1}{\beta_1(x)} T(\beta_1(x)x) + d(x, F_1)h, & x \in B_R \cap \left(E_1 \backslash \mathring{E}_1^{\delta}\right). \end{cases}$$

$T_2 : B_R \backslash \left(B_R \cap \mathring{E}_1\right) \longrightarrow B_R$ is given by

$$T_2(x) := \begin{cases} T(x), & x \in B_R \cap \left(E_2 \backslash \mathring{E}_1\right); \\ T\left(\partial_2^C(x)\right), & x \in B_R \backslash \left(B_R \cap \mathring{E}_2\right). \end{cases}$$

We first deal with T_1, which can be expressed as the sum of two mappings T_1^1 and T_1^2. The mapping

$$T_1^1 : B_R \cap E_1 \longrightarrow B_R$$

$$x \longmapsto T_1^1(x) := \begin{cases} \delta h, & x \in B_R \cap E_1^{\delta}; \\ d(x, F_1)h, & x \in B_R \cap \left(E_1 \backslash \mathring{E}_1^{\delta}\right) \end{cases}$$

is a 0-set contraction. Indeed, let $A \subset B_R \cap E_1$, then A is bounded and

$$T_1^1(A) = T_1^1\left(A \cap \left(B_R \cap E_1^{\delta}\right)\right) \cup T_1^1\left(A \cap \left(B_R \cap \left(E_1 \backslash \mathring{E}_1^{\delta}\right)\right)\right).$$

By using that $T_1^1\left(A \cap \left(B_R \cap \left(E_1 \backslash \mathring{E}_1^{\delta}\right)\right)\right) \subset \overline{co}(\{0\} \cup \{\delta h\})$, and the properties 1, 2, 3, 6, 7 of Proposition 1.1.6, we can conclude

$$\alpha(T_1^1(A)) \leqslant \max\{\alpha(\{\delta h\}), \alpha(co(\{0\} \cup \{\delta h\}))\} = 0.$$

Furthermore, the mapping

$$T_1^2 : B_R \cap E_1 \longrightarrow B_R$$
$$x \longmapsto T_1^2(x) := \begin{cases} 0, & x = 0; \\ \frac{1}{\beta_1(x)} T(\beta_1(x)x), & x \neq 0 \end{cases}$$

is a k_1^2-set contraction with $k_1^2 < 1$, because it is the restriction to $B_R \cap E_1$ of $\tilde{T}$ in Lemma 2.3.1 with $E = E_1$ and $F = F_1$.

Finally, by using statement 2 of Proposition 1.1.9, we can assert that T_1 is a $k_1 = 0 + k_1^2$-set contraction with $k_1 < 1$.

Now, we show that T_2 is a k_2-set contraction with $k_2 = k$, because it can be written as the composition $T \circ S$, where $S : B_R \backslash \left(B_R \cap \overset{\circ}{E_1}\right) \longrightarrow B_R \cap \left(E_2 \backslash \overset{\circ}{E_1}\right)$, which is given by

$$S(x) := \begin{cases} x, & x \in B_R \cap \left(E_2 \backslash \overset{\circ}{E_1}\right); \\ \partial_2^C(x) = \beta_2\left(\frac{d(0,F_2)}{\|x\|}x\right)\frac{d(0,F_2)}{\|x\|}x, & x \in B_R \backslash \left(B_R \cap \overset{\circ}{E_2}\right); \end{cases}$$

is a 1-set contraction. Therefore, statement 1 of Proposition 1.1.9 is satisfied and, as a consequence, T_2 is a k-set contraction. We now prove that S is a 1-set contraction. For this, let us consider $\lambda : B_R \backslash \left(B_R \cap \overset{\circ}{E_1}\right) \longrightarrow \mathbb{R}^+$ given by

$$\lambda(x) := \begin{cases} 1, & x \in B_R \cap \left(E_2 \backslash \overset{\circ}{E_1}\right); \\ \beta_2\left(\frac{d(0,F_2)}{\|x\|}x\right)\frac{d(0,F_2)}{\|x\|}, & x \in B_R \backslash \left(B_R \cap \overset{\circ}{E_2}\right); \end{cases}$$

which is a continuous function and satisfies

$$\sup\left\{\lambda(x) \,:\, x \in B_R \cap \left(B_R \backslash \overset{\circ}{E_1}\right)\right\} \leqslant 1.$$

Hence, by using statement 3 in Proposition 1.1.9, we can conclude that S is a 1-set contraction, since the identity map also fulfills this property.

Finally, applying Corollary 1.1.10 to T_1 and T_2, we get that $\overline{T}_{|B_R}$ is a $\overline{k}$-set contraction with $\overline{k} = \max\{k_1, k\} < 1$.

Therefore, the hypotheses of Theorem 1.2.6 are satisfied and $\overline{T}_{|B_R}$ has at least one fixed point $\overline{x} \in B_R$.

The fixed point is in the conical domain $C \cap (E_2 \backslash \overset{\circ}{E_1})$

We finish the proof by showing that $\overline{x} \in C \cap (E_2 \backslash \overset{\circ}{E_1})$. To that purpose, we assume that the fixed point belongs to one of the other four sets involved in the definition of $\overline{T}$:

- Suppose that $\overline{x} = 0$.
  Since $\overline{T}(0) = 0$, then $\delta\|h\| = 0$ and this is not possible because $\delta, \|h\| > 0$.

- Assume that $\overline{x} \in B_R \cap (E_1^{\delta} \backslash \{0\})$.
  Consequently, $\overline{T}(\overline{x}) = \frac{1}{\beta_1(\overline{x})} T(\beta_1(\overline{x})\overline{x}) + \delta h = \overline{x}$, so

  $$\|h\| \leqslant \frac{1}{\delta}\|\overline{x}\| + \frac{1}{\delta\beta_1(\overline{x})}\|T(\beta_1(\overline{x})\overline{x})\|$$

  and it is a contradiction with the selection of h in the definition of the mapping $\overline{T} : C \longrightarrow C$.

- Let $\overline{x} \in B_R \cap \left(E_1 \backslash E_1^{\delta}\right)$.
  Since $\overline{x}$ is a fixed point, then $\overline{T}(\overline{x}) = \frac{1}{\beta_1(\overline{x})} T(\beta_1(\overline{x})\overline{x}) + d(\overline{x}, F_1)h = \overline{x}$, so

  $$\overline{x} - \frac{1}{\beta_1(\overline{x})} T(\beta_1(\overline{x})\overline{x}) = d(\overline{x}, F_1)h \in C,$$

  due to $d(\overline{x}, F_1) \geqslant 0$ and $h \in C$. Moreover, $\beta_1(\overline{x}) \in [1, +\infty)$, thus

  $$\beta_1(\overline{x})\overline{x} - T(\beta_1(\overline{x})\overline{x}) \in C, \quad \text{where} \quad \beta_1(\overline{x})\overline{x} \in C \cap F_1,$$

  which contradicts the hypothesis **(C1)** for T being a compression of the cone C.

- Suppose that $\overline{x} \in B_R \backslash (B_R \cap E_2)$.
  Let us define $y_{\overline{x}} = \frac{d(0,F_2)}{\|\overline{x}\|}\overline{x}$, then

  $$\begin{aligned}\overline{T}(\overline{x}) &= T\left(\partial_2^C(\overline{x})\right) = T\left(\partial_2\left(y_{\overline{x}}\right)\right) \\ &= T\left(\beta_2\left(y_{\overline{x}}\right) y_{\overline{x}}\right) = T\left(\frac{d(0, \partial_2(y_{\overline{x}}))}{\|y_{\overline{x}}\|}\frac{d(0,F_2)}{\|\overline{x}\|}\overline{x}\right).\end{aligned}$$

  As $\|y_{\overline{x}}\| = d(0, F_2)$, then $\overline{T}(\overline{x}) = T\left(\frac{d(0,\partial_2(y_{\overline{x}}))}{\|\overline{x}\|}\overline{x}\right)$. Take $\varepsilon = \frac{\|\overline{x}\|}{d(0,\partial_2(y_{\overline{x}}))} - 1$, we have that $\varepsilon > 0$ since $\frac{\|\overline{x}\|}{d(0,\partial_2(y_{\overline{x}}))} > 1$. Moreover, we can express $\overline{x}$ as $(1+\varepsilon)\frac{d(0,\partial_2(y_{\overline{x}}))}{\|\overline{x}\|}\overline{x}$ and

  $$\overline{T}(\overline{x}) = T\left(\frac{d(0, \partial_2(y_{\overline{x}}))}{\|\overline{x}\|}\overline{x}\right) = (1+\varepsilon)\frac{d(0, \partial_2(y_{\overline{x}}))}{\|\overline{x}\|}\overline{x}.$$

  By using that $\frac{d(0,\partial_2(y_{\overline{x}}))}{\|\overline{x}\|}\overline{x} \in C \cap F_2$ and

  $$T\left(\frac{d(0, \partial_2(y_{\overline{x}}))}{\|\overline{x}\|}\overline{x}\right) - (1+\varepsilon)\frac{d(0, \partial_2(y_{\overline{x}}))}{\|\overline{x}\|}\overline{x} = 0 \in C,$$

  we arrive to a contradiction with the hypothesis **(C2)** of T being a compression of the cone C.

Thus, we have shown that the fixed point of $\overline{T}$ belongs to $C \cap \left(E_2 \backslash \mathring{E}_1\right)$. Since $\overline{T}$ and T coincide on this set, then we conclude that T has a fixed point in the mentioned set. □

2.3.2 *Expansive case*

We begin this section by improving the expansion type result in Theorem 1.2.8. The proof developed by Các and Gatica (1979) followed the ideas used by Krasnosel'skii. Nevertheless, by using the idea in (Precup, 2006) to reduce the expansive case to the compressive one, we can provide a better localization of the fixed point in a conical annular set. Finally, the same idea is used to extend the result to star convex sets.

Theorem 2.3.2. *Let* $(X, \|\cdot\|)$ *be a Banach space,* C *be a cone in* X, $r, R \in \mathbb{R}$, $0 < r < R$, *and* $T : C_{r,R} \longrightarrow C$ *be a* k*-set contraction satisfying the expansion condition* (5)*. Then,* T *has a fixed point in* $C_{r,R}$.

Proof. We consider an auxiliary mapping $\tilde{T} : C_{r,R} \longrightarrow C$ given by

$$\tilde{T}(x) := \frac{1}{\theta(x)} T(\theta(x)x),$$

where $\theta(x) = (r+R)/\|x\| - 1$, for every $x \in C_{r,R}$. Then, we show that it satisfies the hypotheses of Theorem 1.2.7 due to Potter, that is, we prove separately that the mapping $\tilde{T}$ is well-defined, it satisfies the compression conditions given in (4) and it is a set contraction.

$\tilde{T}$ is well-defined

We need to show that $\theta(x)x \in C_{r,R}$ for every $x \in C_{r,R}$. Since $\theta(x) > 0$ and $x \in C$, we can assert that $\theta(x)x \in C$. Therefore, it remains to prove that $r \leqslant \|\theta(x)x\| \leqslant R$. If $x \in C_{r,R}$, then $r \leqslant \|x\| \leqslant R$, whence $r \leqslant r + R - \|x\| \leqslant R$, that is, $r \leqslant \theta(x)\|x\| \leqslant R$. Due to this, we can assert that $\theta(x)x \in C_{r,R}$ and, finally, $\tilde{T}$ is well-defined.

$\tilde{T}$ satisfies the compression condition (4)

If $\|x\| = r$, then $\|\theta(x)x\| = R$ and, if $\|x\| = R$, then $\|\theta(x)x\| = r$. As a consequence, T satisfying (5) satisfies that $\tilde{T}$ verifies (4).

$\tilde{T}$ is a set contraction

It is clear that $\tilde{T}$ is continuous since T, θ are continuous and $\theta > 0$. Therefore, it remains to prove that, for every $A \subset C_{r,R}$ (A is bounded), we have

$$\alpha(\tilde{T}(A)) \leqslant \tilde{k}\alpha(A), \tag{12}$$

for some constant $0 \leqslant \tilde{k} < 1$, independent of A. For that purpose, we proceed similarly the proof of Lemma 2.3.1 or (Potter, 1974, Lemma 3.1). We begin by distinguishing two cases.

If $\alpha(A) = 0$, then $\overline{A}$ is compact. As $\tilde{T}$ is continuous, then $\tilde{T}(\overline{A})$ is compact and, therefore,

$$\alpha(\tilde{T}(A)) \leqslant \alpha(\tilde{T}(\overline{A})) = 0 = \tilde{k}\,\alpha(A), \quad \text{for any } \tilde{k} \geqslant 0.$$

If $\alpha(A) \neq 0$, let us assume that $k \neq 0$, but, if it is not the case, we consider $0 < \hat{k} < 1$ as close to k as we wish. We proceed as follows:

Step 1: We cover A by a finite number of subsets such that the restrictions of $\tilde{T}$ to each of them are α-Lipschitz with a suitable constant.

As $0 < r < R$, then $\delta_{r,R} = \frac{R}{r} - \frac{r}{R} > 0$ and, for each $n \in \mathbb{N}$, we can consider $\varepsilon^n_{r,R} := \delta_{r,R}/n$.

Let $n \in \mathbb{N}$, $n \geqslant 1$, be arbitrarily fixed, for each integer number $m \geqslant 0$, we define the following sets:

$$A^n_m := \left\{ x \in A \,:\, \theta(x) \in \left[\frac{r}{R} + m\,\varepsilon^n_{r,R}, \frac{r}{R} + (m+1)\,\varepsilon^n_{r,R} \right] \right\}.$$

Since $A \subset C_{r,R}$, we can assert that $\frac{r}{R} \leqslant \theta(x) \leqslant \frac{R}{r}$. Moreover, noticing that $\frac{r}{R} + 0\,\varepsilon^n_{r,R} = \frac{r}{R}$ and $\frac{r}{R} + [(n-1)+1]\,\varepsilon^n_{r,R} = \frac{R}{r}$, we get

$$A \subset \bigcup_{m=0}^{n-1} A^n_m.$$

From this, by using some properties of the measure of noncompactness in Proposition 1.1.6, it follows that

$$\alpha\left(\tilde{T}(A)\right) \leqslant \alpha\left(\bigcup_{m=0}^{n-1} \tilde{T}(A^n_m) \right) = \max_{m \in \{0,\ldots,n-1\}} \left\{ \alpha\left(\tilde{T}(A^n_m)\right) \right\}.$$

Step 2: For each $m \in \{0,\ldots,n-1\}$, we show that $\tilde{T}_{|A^n_m}$ is α-Lipschitz with constant $k\left(\frac{r}{R} + (m+1)\,\varepsilon^n_{r,R}\right) / \left(\frac{r}{R} + m\,\varepsilon^n_{r,R}\right)$.

We study some properties of the following auxiliary mappings:

$$\frac{1}{\theta_{|A^n_m}} : A^n_m \longrightarrow C,\ x \longmapsto \frac{1}{\theta(x)};$$
$$S^n_m : A^n_m \longrightarrow C,\ x \longmapsto S^n_m(x) := \theta(x)x.$$

On the one hand, for each $x \in A^n_m$, it is satisfied that $1/\theta(x) \leqslant 1/(\frac{r}{R} + m\,\varepsilon^n_{r,R})$, then

$$\sup\left\{ \frac{1}{\theta(x)} \,:\, x \in A^n_m \right\} \leqslant \frac{1}{\frac{r}{R} + m\,\varepsilon^n_{r,R}}.$$

On the other hand, for every $B \subset A^n_m$, we have

$$\begin{aligned} S^n_m(B) &= \{\theta(x)x \,:\, x \in B\} \\ &\subset \left\{ \left[\lambda\left(\frac{r}{R} + m\,\varepsilon^n_{r,R}\right) + (1-\lambda)\left(\frac{r}{R} + (m+1)\,\varepsilon^n_{r,R}\right) \right] x \,:\, \lambda \in [0,1],\, x \in B \right\} \\ &= \operatorname{co}\left(\left\{ \left[\frac{r}{R} + m\,\varepsilon^n_{r,R} \right] B \right\} \cup \left\{ \left[\frac{r}{R} + (m+1)\,\varepsilon^n_{r,R} \right] B \right\} \right). \end{aligned}$$

Now, by using the properties of the measure of noncompactness, we can assert

$$\begin{aligned}\alpha\left(S_m^n(B)\right) &\leqslant \alpha\left(\left\{\left[\frac{r}{R}+m\,\varepsilon_{r,R}^n\right]B\right\}\cup\left\{\left[\frac{r}{R}+(m+1)\,\varepsilon_{r,R}^n\right]B\right\}\right)\\ &= \left(\frac{r}{R}+(m+1)\,\varepsilon_{r,R}^n\right)\alpha(B).\end{aligned}$$

Consequently, S_m^n is α-Lipschitz with constant $r/R+(m+1)\,\varepsilon_{r,R}^n$.

As T is a k-set contraction and $\tilde{T}_{|A_m^n}=(T\circ S_m^n)/\theta_{|A_m^n}$, we finally get that $\tilde{T}_{|A_m^n}$ is α-Lipschitz with constant $k\left(\frac{r}{R}+(m+1)\,\varepsilon_{r,R}^n\right)/\left(\frac{r}{R}+m\,\varepsilon_{r,R}^n\right)$.

Step 3: $\tilde{T}$ is a set contraction.

Indeed, for each $m\in\{1,\dots,n-1\}$, it follows that

$$\frac{\frac{r}{R}+(m+1)\,\varepsilon_{r,R}^n}{\frac{r}{R}+m\,\varepsilon_{r,R}^n}<\frac{\frac{r}{R}+\varepsilon_{r,R}^n}{\frac{r}{R}}.$$

Thus, taking into account the different statements which have been proved, we have

$$\begin{aligned}\alpha\left(\tilde{T}(A)\right) &\leqslant \max_{m\in\{0,\dots,n-1\}}\left\{\alpha\left(\tilde{T}(A_m^n)\right)\right\}\\ &\leqslant \max_{m\in\{0,\dots,n-1\}}\left\{\frac{\frac{r}{R}+(m+1)\,\varepsilon_{r,R}^n}{\frac{r}{R}+m\,\varepsilon_{r,R}^n}\,\alpha(A_m^n)\right\}\\ &\leqslant \frac{\frac{r}{R}+\varepsilon_{r,R}^n}{\frac{r}{R}}k\,\alpha(A).\end{aligned}$$

Since $\varepsilon_{r,R}^n\to 0$ as $n\to\infty$, one has that, for n large enough, the number

$$\tilde{k}:=\frac{\frac{r}{R}+\varepsilon_{r,R}^n}{\frac{r}{R}}k$$

is as close to k as we wish. Therefore, we can guarantee that $\tilde{k}\in(0,1)$.

Existence of a fixed point of T *in* $C_{r,R}$

To finish the proof, we apply Theorem 1.2.7 to the mapping $\tilde{T}$. Hence, $\tilde{T}$ has a fixed point $\tilde{x}\in C_{r,R}$, that is,

$$\tilde{x}=\tilde{T}(\tilde{x})=\frac{1}{\theta(\tilde{x})}T(\theta(\tilde{x})\tilde{x}),$$

or, equivalently,

$$\theta(\tilde{x})\tilde{x}=T(\theta(\tilde{x})\tilde{x}).$$

This shows that the point $\hat{x}:=\theta(\tilde{x})\tilde{x}$ is a fixed point of T in $C_{r,R}$. □

The next result extends Theorem 2.3.2 to star convex sets. We notice that the proof is quite similar, the main difference appears in the definition of the map θ, which transforms the expansion conditions in compressive ones.

Theorem 2.3.3. *Let $(X, \|\cdot\|)$ be a Banach space, C be a cone in X, and E_1, E_2 be star convex sets fulfilling Condition 1. If $T : C \cap (E_2 \backslash \overset{\circ}{E_1}) \longrightarrow C$ is a k-set contraction and an expansion of the set $C \cap (E_2 \backslash \overset{\circ}{E_1})$, then T has a fixed point in $C \cap (E_2 \backslash \overset{\circ}{E_1})$.*

Proof. We consider the auxiliary mapping $\tilde{T} : C \cap (E_2 \backslash \overset{\circ}{E_1}) \longrightarrow C$ given by

$$\tilde{T}(x) := \frac{1}{\theta(x)} T(\theta(x)x),$$

where $\theta(x) = \beta_1^C(x) + \beta_2(x) - 1$, for $x \in C \cap (E_2 \backslash \overset{\circ}{E_1})$. Then, we show that it satisfies the hypotheses of Theorem 2.3.1, that is, we prove separately that $\tilde{T}$ is well-defined, it is a compression of the set $C \cap (E_2 \backslash \overset{\circ}{E_1})$ and it is a set contraction.

$\tilde{T}$ is well-defined

We need to show that $\theta(x)x \in C \cap (E_2 \backslash \overset{\circ}{E_1})$, for every $x \in C \cap (E_2 \backslash \overset{\circ}{E_1})$. Since $\theta(x) > 0$ and $x \in C$, we clearly have $\theta(x)x \in C$. To prove that $\theta(x)x \in E_2 \backslash \overset{\circ}{E_1}$, we note the equivalence between $\lambda x \in E_2 \backslash \overset{\circ}{E_1}$ and the inequality $\beta_1^C(x) \leqslant \lambda \leqslant \beta_2(x)$. Now, let us consider $x \in E_2 \backslash \overset{\circ}{E_1}$, then $\beta_1^C(x) \leqslant 1 \leqslant \beta_2(x)$, and we can assert that $\beta_1^C(x) \leqslant \beta_1^C(x) + \beta_2(x) - 1 \leqslant \beta_2(x)$, that is, $\beta_1^C(x) \leqslant \theta(x) \leqslant \beta_2(x)$, which shows that $\theta(x)x \in E_2 \backslash \overset{\circ}{E_1}$. Therefore, we conclude that $\tilde{T}$ is well-defined.

$\tilde{T}$ is a compression of the set $C \cap (E_2 \backslash \overset{\circ}{E_1})$

For that purpose, we prove that, if $x \in F_1$, then $\theta(x)x \in F_2$, and, if $x \in F_2$, then $\theta(x)x \in F_1$. Consequently, if T fulfills **(E1)** then $\tilde{T}$ fulfills **(C2)**; and if T fulfills **(E2)** then $\tilde{T}$ fulfills **(C1)**. This way, $\tilde{T}$ is a compression of the set $C \cap (E_2 \backslash \overset{\circ}{E_1})$.

Indeed, if $x \in F_1$, then $\beta_1^C(x) = 1$ and so $\theta(x) = \beta_2(x)$. Hence, according to Proposition 2.2.4, $\theta(x)x \in F_2$. Similarly, if $x \in F_2$, then $\beta_2(x) = 1$ and so $\theta(x) = \beta_1^C(x)$. Thus, by using the definition of β_1^C, $\theta(x)x \in F_1$.

$\tilde{T}$ is a set contraction

On the one hand, as β_1^C, β_2 and T are continuous and $\theta(x) \neq 0$, for all $x \in C \cap (E_2 \backslash \overset{\circ}{E_1})$, one has that $\tilde{T}$ is continuous.

On the other hand, for every $A \subset C \cap (E_2 \backslash \overset{\circ}{E_1})$, we have to prove that

$$\alpha\left(\tilde{T}(A)\right) \leqslant \tilde{k}\alpha(A), \tag{13}$$

for some constant $0 \leqslant \tilde{k} < 1$, independent of A.

The proof of (13) is identical to that of formula (12) in the proof of Theorem 2.3.2, once we have shown the existence of two positive numbers r and R with $r < R$ such that

$$\frac{r}{R} \leqslant \theta(x) \leqslant \frac{R}{r}, \text{ for all } x \in C \cap \left(E_2 \backslash \overset{\circ}{E_1}\right). \tag{14}$$

Indeed, as $0 \in E_1 \backslash F_1$, there exists $r > 0$ such that $\overline{B}(0, r) \subset \overset{\circ}{E_1}$. Since $E_1 \subset E_2$ and E_2 is bounded, then there exists $R > r$ such that $E_2 \subset \overline{B}(0, R)$. Therefore, we

have that $C \cap \left(E_2 \backslash \mathring{E}_1\right) \subset C \cap (\overline{B}(0,R) \backslash B(0,r))$. Hence, for any $x \in C \cap \left(E_2 \backslash \mathring{E}_1\right)$, we obtain

$$x,\ \theta(x)x \in C \cap (\overline{B}(0,R) \backslash B(0,r)),$$

implying

$$r \leqslant \|x\|,\ \theta(x)\|x\| \leqslant R,$$

which immediately yield (14).

Existence of a fixed point of T *in* $C \cap \left(E_2 \backslash \mathring{E}_1\right)$

To finish the proof, we apply Theorem 2.3.1 to the mapping $\tilde{T}$. Thus, $\tilde{T}$ has a fixed point $\tilde{x} \in C \cap \left(E_2 \backslash \mathring{E}_1\right)$. Then

$$\tilde{x} = \tilde{T}(\tilde{x}) = \frac{1}{\theta(\tilde{x})} T(\theta(\tilde{x})\tilde{x}),$$

or, equivalently,

$$\theta(\tilde{x})\tilde{x} = T(\theta(\tilde{x})\tilde{x}).$$

This shows that the point $\hat{x} := \theta(\tilde{x})\tilde{x}$ is a fixed point of T in $C \cap \left(E_2 \backslash \mathring{E}_1\right)$. □

2.4 ADMISSIBLE SETS DEFINED BY FUNCTIONALS

The fixed point theorems due to Krasnosel'skii, Potter, or Các and Gatica provide the existence of fixed points for a mapping T in certain subsets of a Banach space $(X, \|\cdot\|)$. An interesting characteristic of the sets involved in these results, either in the compression-expansion conditions required to the mapping T or in the set where the fixed points are located, is that they are determined by a norm. These sets can be expressed in terms of:

$$B_r = C \cap \{x \in X : \|x\| \leqslant r\},\quad S_r = C \cap \{x \in X : \|x\| = r\},$$

where r is a positive real number.

In Section 2.3, we generalized the mentioned results to star convex sets, which in general cannot be expressed by using a norm. Thus, for applications, it is interesting to determine some conditions over a functional $\varphi : X \longrightarrow [0, +\infty)$ such that, for a real number $r > 0$, the sets

$$E_r := \{x \in X : \varphi(x) \leqslant r\},\quad F_r := \{x \in X : \varphi(x) = r\},$$

satisfy Condition 1. Thus, in this subsection, we first determine some suitable conditions to be imposed the functional φ. Then, we derive some corollaries of Theorems 2.3.1 and 2.3.3.

We notice that, if $\varphi = \|\cdot\|$, then $C \cap E_r \equiv B_r$ and $C \cap F_r \equiv S_r$. However, this approach allows to consider functionals with weaker properties in comparison

with the norm. In order to see that we work with weaker hypotheses, once we know how to choose a suitable functional φ, we provide an example of a functional satisfying the new restrictions that is not a norm. Moreover, we will show that we cannot relax the continuity hypothesis, at least by considering an upper/lower semicontinuous functional φ.

Proposition 2.4.1. *Let* $(X, \|\cdot\|)$ *be a Banach space,* $x \in X$, $r \in \mathbb{R}$, $r > 0$, *and* $\varphi : X \longrightarrow [0, +\infty)$ *be a functional satisfying:*

(F1) *if* $\varphi(x) \leqslant r$, *then* $\varphi(\lambda x) \leqslant r$ *for all* $\lambda \in [0, 1]$;

(F2) φ *is continuous;*

(F3) *for all* $x \in E_r$, $\varphi(x) = 0$ *if and only if* $x = 0$;

(F4) $\varphi(\lambda x) = \lambda\varphi(x)$ *for all* $\lambda \in (0, +\infty)$ *and* $x \in E_r$;

(F5) *there exists* $m \in \mathbb{R}, m > 0$ *such that*

$$m\|x\| \leqslant \varphi(x) \text{ for all } x \in X \text{ with } \|x\| > \varphi(x),$$

or $\liminf_{\|x\|\to+\infty} \varphi(x) > r$.

Under these assumptions, E_r *and* F_r *satisfy Condition 1.*

Proof. We proceed step by step, i.e., we prove each of the properties required to E_r and F_r by using the appropriate hypothesis over φ. Indeed:

- **(F1)** is equivalent to E_r being a star convex set.
- **(F2)** implies that E_r is closed and $\varphi^{-1}([0, r))$ is open in X. Indeed, we can write $E_r = \varphi^{-1}([0, r])$. As $[0, r]$ is a closed subset of $([0, +\infty), |\cdot|)$, where $|\cdot|$ is the absolute value for real numbers, then E_r is closed since it is the preimage of a closed set by a continuous function. Besides, we can assert that $\varphi^{-1}([0, r))$ is open in X since $[0, r)$ is an open subset of $[0, +\infty)$.
- **(F3)** implies that $0 \notin F_r$, because $\varphi(x) = r > 0$ for all $x \in F_r$.
- By hypothesis **(F4)**, we prove two conditions over the sets E_r and F_r. First, we show that F_r is the boundary of E_r. We have just proved that E_r is closed and $E_r \backslash F_r = \varphi^{-1}([0, r))$ is open, so the boundary of E_r is a subset of F_r. Let us consider $y \in F_r$ arbitrarily fixed, we want to prove that y is a boundary point of E_r. As $y \in F_r \subset E_r$, we must prove that, for all $\varepsilon > 0$, $B(y, \varepsilon) \cap (X \backslash E_r) \neq \emptyset$. We take $z = \left(1 + \frac{\varepsilon}{2\|y\|}\right) y \in B(y, \varepsilon)$, then it is satisfied that $\varphi(z) = \left(1 + \frac{\varepsilon}{2\|y\|}\right) \varphi(y)$, and, as $\left(1 + \frac{\varepsilon}{2\|y\|}\right) > 1$, we can conclude that $\varphi(z) > \varphi(y) = r$. Therefore, $z \in X \backslash E_r$ and y is a point in

the boundary of E_r.
Secondly, we prove that the mapping

$$\partial : E_r\backslash\{0\} \longrightarrow F_r,\ x \longmapsto \partial(x) := \frac{r}{\varphi(x)}x$$

satisfies the desired conditions. By using hypotheses **(F3)** and **(F4)**, we can assert that ∂ is well-defined. Let $x \in E_r\backslash\{0\}$, $\varphi(\partial(x)) = \varphi\left(\frac{r}{\varphi(x)}x\right) = r$, so $\partial(x) \in F_r$. Then, **(F2)** implies that ∂ is continuous. Now, if $x \in F_r$, then $\varphi(x) = r$ and, therefore, $\partial(x) = x$. By using again the hypothesis **(F4)**, we can assert that $\partial(\lambda x) = \partial(x)$ for all $x \in E_r$ and $\lambda \in (0, 1]$.

- Finally, **(F5)** implies that E_r is a bounded set.

□

Example 2.4.2. Let $(\mathcal{C}([0,1],\mathbb{R}), \|\cdot\|_\infty)$ be the Banach space in Example 1.2.3 for $n = 1$. We consider the functional $\varphi : \mathcal{C}([0,1],\mathbb{R}) \longrightarrow [0,\infty)$ given by

$$\varphi(x) := a \min_{t\in[0,1]} |x(t)| + b\|x\|_\infty,\ \text{for all } x \in \mathcal{C}([0,1],\mathbb{R}), \tag{15}$$

where a, b are positive real numbers. It is easy to see that φ satisfies the hypotheses **(F1)-(F5)** in Proposition 2.4.1. However, this functional does not fulfill the triangular inequality, then it is not a norm. Indeed, let us consider the functions $x(t) = t$ for all $t \in [0,2]$; $y(t) = 1 - t$ if $t \in [0,1]$, $y(t) = t - 1$ if $t \in [1,2]$, then we have

$$\varphi(x + y) = a + 3b > \varphi(x) + \varphi(y) = 3b.$$

Next, we make the following question: is it possible to extend this study to upper or lower semicontinuous functionals? In the following, we prove that the answer is negative, since this assumption is not enough.

Assume that φ is upper semicontinuous. We show that $E_r\backslash F_r$ is open, but E_r is not necessarily closed. Indeed:

- Let $r \in \mathbb{R}$, $r > 0$, then $\varphi^{-1}([0,r))$ is open. We take $y \in \varphi^{-1}([0,r))$ arbitrarily fixed and show that it is an interior point, i.e., there exists $\delta \in \mathbb{R}$, $\delta > 0$ such that

$$B(y,\delta) \subset \varphi^{-1}([0,r)). \tag{16}$$

As $\varphi(y) < r$, we can take $\varepsilon > 0$ such that $\varphi(y) + \varepsilon < r$. Besides, by using that φ is upper semicontinuous, there exists δ_ε^y such that, for all $x \in B(y,\delta_\varepsilon^y)$, $0 \leqslant \varphi(x) < \varphi(y) + \varepsilon < r$. Thus, $B(y,\delta_\varepsilon^y) \subset \varphi^{-1}([0,r))$, and it proves that $\varphi^{-1}([0,r))$ is an open set.

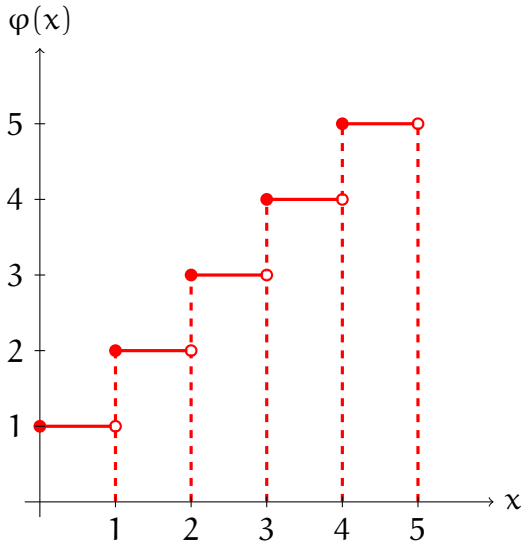

Figure 5: Graph of the upper semicontinuos function $\varphi(x) = \lfloor x \rfloor + 1$, $x \in [0, \infty)$.

- However, $\varphi^{-1}([0, r])$ is not always closed. As an example, we work with the function

$$\begin{aligned} \varphi : [0, +\infty) &\longrightarrow [0, +\infty) \\ x &\longmapsto \varphi(x) = \lfloor x \rfloor + 1, \end{aligned}$$

  where $\lfloor \cdot \rfloor$ denotes the floor function (see Figure 5).

  First of all, we prove that φ is upper semicontinuous. Let us consider a real number $\varepsilon > 0$ and $y \in [0, +\infty)$. For $\delta_y = d(y, \varphi(y))/2 > 0$, we have

$$\varphi\left(B_{[0,+\infty)}(y, \delta_y)\right) \subset [0, \varphi(y + \delta_y)) \subset [0, \varphi(y)) \subset [0, \varphi(y) + \varepsilon).$$

  Then, φ is upper semicontinuous.

  Secondly, for each $r \in \mathbb{R}$, $r > 0$, it is satisfied that: if $r \in (0, 1)$, then $\varphi^{-1}([0, r]) = \emptyset$; if $r \in [1, +\infty)$, then $\varphi^{-1}([0, r]) = [0, \lfloor r \rfloor]$, which is an open set in $([0, +\infty), |\cdot|)$.

On the other hand, assume that φ is lower semicontinuous. We show that E_r is closed, but $E_r \backslash F_r$ is not necessarily open. Indeed:

- Let $r \in \mathbb{R}$, $r > 0$, then $\varphi^{-1}([0, r])$ is closed. As $\varphi^{-1}([0, r]) = X \backslash \varphi^{-1}((r, +\infty))$, we prove that $\varphi^{-1}((r, +\infty))$ is an open subset of $[0, +\infty)$. We consider an element $y \in \varphi^{-1}(r, +\infty)$ arbitrarily fixed and prove that it is an interior point, i.e., there exists $\delta \in \mathbb{R}$, $\delta > 0$ such that

$$B(y, \delta) \subset \varphi^{-1}((r, +\infty)). \tag{17}$$

  Now, as $\varphi(y) > r$, we can take $\varepsilon > 0$ such that $\varphi(y) - \varepsilon > r$. Besides, by using that φ is lower semicontinuous, there exists $\delta_\varepsilon^y > 0$ such that, $r < \varphi(y) - \varepsilon < \varphi(x) < +\infty$, for all $x \in B\left(y, \delta_\varepsilon^y\right)$. As a consequence, $B\left(y, \delta_\varepsilon^y\right) \subset \varphi^{-1}\left((r, +\infty)\right)$, and we can conclude that $\varphi^{-1}((r, +\infty))$ is open, or, equivalently, $\varphi^{-1}([0, r])$ is closed.

- Nevertheless, $\varphi^{-1}([0,r))$ is not always open. For example, we consider the function

$$\varphi : [0,+\infty) \longrightarrow [0,+\infty)$$
$$x \longmapsto \varphi(x) := \begin{cases} \lfloor x \rfloor, & x \notin \mathbb{N}; \\ x-1, & x \in \mathbb{N}; \end{cases}$$

where $\lfloor \cdot \rfloor$ denotes the floor function (see Figure 6).

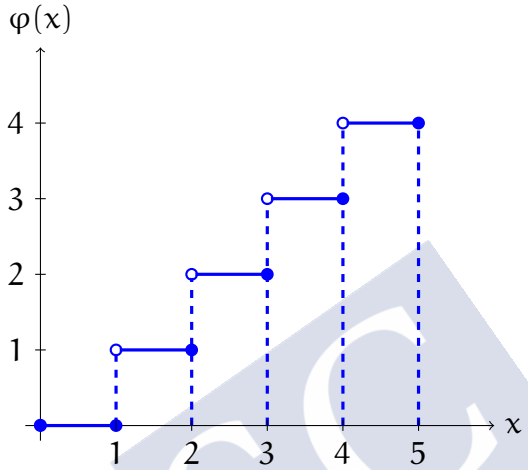

Figure 6: Graph of the lower semicontinuous function $\varphi(x) = \lfloor x \rfloor$, $x \in [0,\infty)\backslash\mathbb{N}$; $\varphi(x) = x-1$, $x \in \mathbb{N}$.

First, we show that φ is lower semicontinuous. Let $y = 0$ and $\varepsilon \in \mathbb{R}$, $\varepsilon > 0$, since

$$\varphi([0,\delta)) \subset [0,+\infty) = [\varphi(0),+\infty) \subset (\varphi(0)-\varepsilon,+\infty), \ \forall \delta \in \mathbb{R},\ \delta > 0,$$

then φ is clearly lower semicontinuous at 0. Let $y \in (0,+\infty)$ and $\varepsilon \in \mathbb{R}$, $\varepsilon > 0$ be arbitrarily fixed. We take $\delta_y = d(y,\varphi(y))/2 > 0$, then it is easy to prove that

$$\varphi\left(B_{[0,+\infty)}(y,\delta_y)\right) \subset (\varphi(y)-\varepsilon,+\infty).$$

As a consequence, we can assert that φ is lower semicontinuous.

Next, let $r \in \mathbb{R}$, $r > 0$, it is satisfied that: if $r \in \mathbb{N}$, then $\varphi^{-1}([0,r)) = [0,r]$, which is a closed subset of $[0,+\infty)$; if $r \notin \mathbb{N}$, then $\varphi^{-1}([0,r)) = [0,\lfloor r \rfloor + 1]$, which is a closed subset of $[0,+\infty)$.

To conclude this section, we provide two corollaries of Theorems 2.3.1 and 2.3.3. First, in Theorem 2.4.3, we write the fixed point results in terms of functionals satisfying the hypotheses **(F1)-(F5)**. Then, since a norm also fulfills these properties, we derive a corollary where the functionals are replaced by two norms, it is similar to (Precup, 2006, Theorem 3).

Theorem 2.4.3. *Let $(X, \|\cdot\|)$ be a Banach space, C be a cone in X and r, R be two positive real numbers with $r < R$. Assume that $\varphi, \psi : X \longrightarrow [0, +\infty)$ are functionals satisfying the hypotheses **(F1)-(F5)** in Proposition 2.4.1, for r, R respectively; and that the following condition holds:*

$$\psi(x) < \frac{R}{r}\varphi(x) \text{ for all } x \in X \text{ such that } \varphi(x) \leqslant r. \tag{18}$$

We consider $E_1 := \{x \in X : \varphi(x) \leqslant r\}$ and $E_2 := \{x \in X : \psi(x) \leqslant R\}$. Then E_1 and E_2 satisfy Condition 1, $0 \in E_1 \subset E_2$ and $F_1 \cap F_2 = \emptyset$. Moreover, assume that the mapping $T : C \cap \left(E_2 \backslash \mathring{E_1}\right) \longrightarrow C$ is a set contraction and a compression or an expansion of the set $C \cap \left(E_2 \backslash \mathring{E_1}\right)$. Then T has at least one fixed point in the conical domain $C \cap \left(E_2 \backslash \mathring{E_1}\right)$.

Proof. First of all, by Proposition 2.4.1, since φ, ψ satisfy hypotheses **(F1)-(F5)**, the sets E_i, F_i fulfill Condition 1, for $i = 1, 2$.

Secondly, we check that $0 \in E_1 \subset E_2$ and $F_1 \cap F_2 = \emptyset$ in order to deal with the concept of a compression or an expansion. Since $\psi(x) < \frac{R}{r}\varphi(x)$ for all $x \in E_1$, we have:

- For all $y \in E_1$, $\psi(y) < \frac{R}{r}\varphi(y) \leqslant R$, then $y \in E_2$.
- Let $y \in F_1$, $\psi(y) < \frac{R}{r}\varphi(y) = R$, then $y \notin F_2$.

Therefore, the hypotheses of Theorem 2.3.1 or Theorem 2.3.3 are satisfied and, as a consequence, T has at least a fixed point in $C \cap (E_2 \backslash \mathring{E_1})$. □

Remark 3. The hypothesis (18) in Theorem 2.4.3 can be replaced by:

$$\psi(x) \leqslant \frac{R}{r}\varphi(x), \text{ for all } x \in X \text{ such that } \varphi(x) < r;$$
$$\psi(x) < \frac{R}{r}\varphi(x), \text{ for all } x \in X \text{ such that } \varphi(x) = r.$$

Corollary 2.4.4. *Let $(X, \|\cdot\|_1)$ be a Banach space, C be a cone in X and r, R be two positive real numbers with $r < R$. Assume that $\|\cdot\|_2$ is a norm in X satisfying the following conditions:*

$$\begin{aligned} &\|x\|_2 \leqslant \frac{R}{r}\|x\|_1, \text{ for all } x \in X \text{ such that } \|x\|_1 < r; \\ &\|x\|_2 < \frac{R}{r}\|x\|_1, \text{ for all } x \in X \text{ such that } \|x\|_1 = r. \end{aligned} \tag{19}$$

We consider $E_1 := \{x \in C : \|x\|_1 \leqslant r\}$ and $E_2 := \{x \in C : \|x\|_2 \leqslant R\}$. Assume that the mapping $T : C \cap \left(E_2 \backslash \mathring{E_1}\right) \longrightarrow C$ is a set contraction and a compression or an expansion of the set $C \cap \left(E_2 \backslash \mathring{E_1}\right)$. Then T has at least one fixed point in the conical domain

$$C \cap \left(E_2 \backslash \mathring{E_1}\right) := \{x \in C : \|x\|_1 \geqslant r, \|x\|_2 \leqslant R\}.$$

2.5 APPLICATION TO A FIRST ORDER IMPLICIT DIFFERENTIAL SYSTEM

Let us consider the following initial value problem for a first order implicit differential system,

$$\begin{cases} x'(t) = f(t, x(t)) + g(t, x'(t)), \quad t \in [0,1]; \\ x(0) = 0; \end{cases} \tag{20}$$

where $f, g : [0,1] \times \mathbb{R}^n \longrightarrow \mathbb{R}^n$. We look for solutions $x \in \mathcal{C}^1([0,1], \mathbb{R}^n)$.

For that purpose, we first transform the initial value problem (20) in an equivalent integral equation and obtain the associated non-linear operator T. Then, we require some conditions on the mappings f and g to guarantee that T is under the hypothesis of Theorem 2.3.1. In the reminder of the section, we consider the particular case $n = 1$, for which we provide two examples of initial value problems, one as a test for the required conditions on f and g, and the other one to show the applicability to implicit equations that cannot be explicitly solved. We conclude this section showing that the expansion result does not work for this type of problems, at least by using the approach we have developed.

Deduction of sufficient conditions to apply Theorem 2.3.1

Let us define $y := x'$, then the initial value problem (20) becomes

$$y(t) = f\left(t, \int_0^t y(s)ds\right) + g(t, y(t)), \quad t \in [0,1], \tag{21}$$

where $\int_0^t y(s)ds := \left(\int_0^t y_1(s)ds, \ldots, \int_0^t y_n(s)ds\right)$. Denote by T the mapping associated to the right-hand side of (21), namely, $T : \mathcal{C}([0,1], \mathbb{R}^n) \to \mathcal{C}([0,1], \mathbb{R}^n)$,

$$T(y)(t) = f\left(t, \int_0^t y(s)ds\right) + g(t, y(t)).$$

Thus, the solutions to (20) are the fixed points in $\mathcal{C}([0,1], \mathbb{R}^n)$ of the mapping T.

To localize the fixed points of T, we use Theorem 2.3.1 and the Banach space considered in Example 1.2.3, that is, the pair $(\mathcal{C}([0,1], \mathbb{R}^n), \|\cdot\|_\infty)$, with

$$\|y\|_\infty := \max\left\{\max_{t\in[0,1]} |y_1(t)|, \ldots, \max_{t\in[0,1]} |y_n(t)|\right\}, \text{ for } y = (y_1, \ldots, y_n).$$

We begin by stating some conditions on the mappings f and g to guarantee that the mapping $T : \mathcal{C}([0,1], \mathbb{R}^n) \longrightarrow \mathcal{C}([0,1], \mathbb{R}^n)$ is well-defined and a set contraction:

(H1) $f, g : [0,1] \times \mathbb{R}^n \to \mathbb{R}^n$ are continuous.

(H2) For each $t \in [0,1]$, there exists $L(t) \in \mathbb{R}_+$ such that

$$|g_i(t,u) - g_i(t,v)| \leqslant L(t) \max\{|u_j - v_j|,\ j = 1,\dots,n\},$$

for all $u, v \in \mathbb{R}^n$, $i \in \{1,\dots,n\}$, and

$$\sup_{t\in[0,1]} L(t) =: k < 1. \tag{22}$$

Under conditions **(H1)** and **(H2)**, the non-linear operator T is a sum of a continuous and compact mapping (0-set contraction) and a k-set contraction. Indeed, $T = A + B$, where the mappings $A, B : \mathcal{C}([0,1],\mathbb{R}^n) \to \mathcal{C}([0,1],\mathbb{R}^n)$ are given by

$$A(y)(t) = f\left(t, \int_0^t y(s)ds\right), \quad B(y)(t) = g(t, y(t)).$$

The mapping A is continuous and compact as a composition of three continuous bounded mappings J, i and N_f, such that one of them is compact. In fact, $A = N_f \circ i \circ J$, where

$$\begin{aligned} J &: \mathcal{C}([0,1],\mathbb{R}^n) \to \mathcal{C}^1([0,1],\mathbb{R}^n), \quad J(y)(t) = \int_0^t y(s)\,ds; \\ i &: \mathcal{C}^1([0,1],\mathbb{R}^n) \to \mathcal{C}([0,1],\mathbb{R}^n), \quad i(y) = y; \\ N_f &: \mathcal{C}([0,1],\mathbb{R}^n) \to \mathcal{C}([0,1],\mathbb{R}^n), \quad N_f(y)(t) = f(t, y(t)). \end{aligned}$$

All these maps are continuous and bounded (they map bounded sets into bounded sets), while i is compact as a consequence of Theorem 1.1.3.

The mapping B is a set contraction with the Lipschitz constant k given by (22). Indeed, for any y, $\overline{y} \in \mathcal{C}([0,1],\mathbb{R}^n)$, and every $t \in [0,1]$, one has

$$\begin{aligned} |B_i(y)(t) - B_i(\overline{y})(t)| &= |g_i(t, y(t)) - g_i(t, \overline{y}(t))| \\ &\leqslant L(t) \max\{|y_j(t) - \overline{y}_j(t)|,\ j = 1,\dots,n\} \\ &\leqslant k \|y - \overline{y}\|_\infty, \end{aligned}$$

for each $i \in \{1,\dots,n\}$, whence

$$\|B(y) - B(\overline{y})\|_\infty \leqslant k \|y - \overline{y}\|_\infty.$$

Consequently, B is continuous and $\alpha(B(D)) \leqslant k\alpha(D)$ for all $D \subset \mathcal{C}([0,1],\mathbb{R}^n)$.

Next, we consider the cone of non-negative functions $C := \mathcal{C}([0,1],\mathbb{R}^n_+)$ in Example 1.2.3, and we add the following positivity condition in order to guarantee the invariance condition $T(C) \subset C$:

(H3) $f([0,1] \times \mathbb{R}^n_+) \subset \mathbb{R}^n_+$ and $g([0,1] \times \mathbb{R}^n_+) \subset \mathbb{R}^n_+$.

Now, we define two star convex sets E_1, $E_2 \subset \mathcal{C}([0,1],\mathbb{R}^n)$ satisfying Condition 1. For their definition, we use the norm $\|\cdot\|_\infty$ and the functionals

$$\varphi_i : \mathcal{C}([0,1],\mathbb{R}) \to \mathbb{R}_+, \quad \varphi_i(z) = a_i \min_{t\in[0,1]} |z(t)| + b_i \|z\|_\infty,$$

where $a_i, b_i \in \mathbb{R}_+$ and $b_i \neq 0$, for all $i \in \{1, \dots, n\}$. We notice the following relationship between the functional φ_i and the norm:

$$b_i \|z\|_\infty \leqslant \varphi_i(z) \leqslant (a_i + b_i) \|z\|_\infty,$$

or, equivalently,

$$\frac{\varphi_i(z)}{a_i + b_i} \leqslant \|z\|_\infty \leqslant \frac{\varphi_i(z)}{b_i}. \tag{23}$$

Given $r, R \in (0, \infty)^n$ two vectors with $(a_i + b_i) r_i < R_i$, for $i = 1, \dots, n$, we define

$$E_1 := \{y \in \mathcal{C}([0,1], \mathbb{R}^n) : \ \|y_i\|_\infty \leqslant r_i, \ i = 1, \dots, n\};$$
$$E_2 := \{y \in \mathcal{C}([0,1], \mathbb{R}^n) : \ \varphi_i(y_i) \leqslant R_i, \ i = 1, \dots, n\}.$$

Clearly, E_1 and E_2 are star convex sets satisfying Condition 1. It is worth mentioning that, if $n = 1$, then E_2 is the star convex set E_R ($R = R_1$) defined by the functional φ in Example 2.4.2 with $a = a_1$, $b = b_1$. However, if $n \geqslant 2$, then E_2 cannot be expressed by using a unique functional.

Finally, we require some additional conditions to f and g in order to guarantee that $T : C \cap (E_2 \backslash \overset{\circ}{E_1}) \longrightarrow C$ is a compression of the set $C \cap (E_2 \backslash \overset{\circ}{E_1})$. We begin by stating the following notation, for each $i \in \{1, \dots, n\}$:

$$\underline{f_i} := \min\left\{f_i(t,y) : \ t \in [0,1], \ y_j \in [0, r_j], \ j = 1, \dots, n\right\};$$
$$\underline{g_i} := \min\left\{g_i(t,y) : \ t \in [0,1], \ y_j \in \left[0, r_j\right], \ j = 1, \dots, n, \ j \neq i, \ y_i = r_i\right\};$$
$$\overline{f_i} := \max\left\{f_i(t,y) : \ t \in [0,1], \ y_j \in \left[0, \frac{R_j}{b_j}\right], \ j = 1, \dots, n\right\};$$
$$\overline{g_i} := \max\left\{g_i(t,y) : \ t \in [0,1], \ y_j \in \left[0, \frac{R_j}{b_j}\right], \ j = 1, \dots, n, \ j \neq i, \right.$$
$$\left. y_i \in \left[\frac{R_i}{a_i + b_i}, \frac{R_i}{b_i}\right]\right\}.$$

Next, we assume that the following conditions are satisfied for each $i \in \{1, \dots, n\}$:

(H4,c1) $\underline{f_i} + \underline{g_i} > r_i$;

(H4,c2) $\overline{f_i} + \overline{g_i} \leqslant \frac{R_i}{a_i + b_i}$.

Let us prove that, under these conditions, $E_1 \subset \overset{\circ}{E_2}$, and **(C1)-(C2)** hold.

First, using the inequalities $(a_i + b_i) r_i < R_i$, we have $E_1 \subset \overset{\circ}{E_2}$. Indeed, if $y \in E_1$, then, for every $i \in \{1, \dots, n\}$, one has

$$\varphi_i(y_i) = a_i \min_{t \in [0,1]} |y_i(t)| + b_i \|y_i\|_\infty \leqslant (a_i + b_i) \|y_i\|_\infty \leqslant (a_i + b_i) r_i < R_i,$$

which gives $y \in \overset{\circ}{E_2}$.

Next, we show that **(H4,c1)** guarantees that condition **(C1)** is fulfilled. Indeed, if we assume the contrary, then there exists $y \in C$ with $\|y_j\|_\infty \leqslant r_j$, for all $j \in \{1,\dots,n\}$, and $\|y_k\|_\infty = r_k$ for some $k \in \{1,\dots,n\}$, such that

$$y(t) \geqslant T(y)(t), \text{ for all } t \in [0,1].$$

Let $t_0 \in [0,1]$ be such that $y_k(t_0) = \|y_k\|_\infty = r_k$. From the previous inequality, by using the definition of T, we obtain

$$r_k = y_k(t_0) \geqslant T_k(y)(t_0) = f_k\left(t_0, \int_0^{t_0} y(s)ds\right) + g_k(t_0, y(t_0)) \geqslant \underline{f}_k + \underline{g}_k,$$

which contradicts **(H4,c1)**. Hence, **(C1)** holds.

We conclude by proving that **(C2)** is also satisfied as a consequence of hypothesis **(H4,c2)**. If we assume the contrary, then there exist $\varepsilon > 0$ and $y \in C$ with $\varphi_j(y_j) \leqslant R_j$ for all $j \in \{1,\dots,n\}$, and $\varphi_k(y_k) = R_k$ for some $k \in \{1,\dots,n\}$, such that

$$T(y)(t) \geqslant (1+\varepsilon)y(t), \text{ for all } t \in [0,1].$$

Let $t_0 \in [0,1]$ be such that $y_k(t_0) = \|y_k\|_\infty$. Then, using the last inequality, the expression of T, and (23), we obtain

$$\overline{f}_k + \overline{g}_k \geqslant f_k\left(t_0, \int_0^{t_0} y(s)ds\right) + g_k\left(t_0, y(t_0)\right) > y_k(t_0) \geqslant \frac{R_k}{a_k + b_k},$$

which contradicts **(H4,c2)**. Hence, **(C2)** holds.

Therefore, since all the assumptions of Theorem 2.3.1 are fulfilled, we have the following existence and localization result.

Theorem 2.5.1. *Under conditions* ***(H1)-(H3)*** *and* ***(H4,c1)-(H4,c2)****, problem* (20) *has a non-negative and increasing solution* $x \in C^1([0,1],\mathbb{R}^n)$ *such that*

$$\begin{aligned} &r_k \leqslant \|x_k'\|_\infty, \text{ for at least one } k \in \{1,\dots,n\}, \text{ and} \\ &\varphi_i(x_i') \leqslant R_i, \text{ for all } i \in \{1,\dots,n\}. \end{aligned} \tag{24}$$

Particular case $n = 1$

In particular, if we assume that $n = 1$, and the following monotonicity condition on f and g:

(H5) For each $t \in [0,1]$, the functions $f(t,\cdot)$ and $g(t,\cdot)$ are increasing in $\mathbb{R}_+$;

then conditions **(H4,c1)** and **(H4,c2)**, with r_1, R_1, a_1, b_1 simply denoted by r, R, a, b, turn into

(H5,c1) $f(t,0) + g(t,r) > r$, for all $t \in [0,1]$;

(H5,c2) $f\left(t, \frac{R}{b}\right) + g\left(t, \frac{R}{b}\right) \leqslant \frac{R}{a+b}$, for all $t \in [0,1]$.

Let us present two examples. The first one, which is in fact an explicitly solvable equation, is given to test the conditions **(H1)-(H3)**, **(H5,c1)-(H5,c2)**.

Example 2.5.2. Let us consider the equation

$$x'(t) = \lambda x(t) + \alpha x'(t) + \beta,\ t \in [0,1].$$

In this case

$$f(t,s) = \lambda s \text{ and } g(t,s) = \alpha s + \beta, \text{ for all } s \in \mathbb{R},\ t \in [0,1],$$

where we assume that $\lambda, \alpha \geqslant 0$, $\beta > 0$ and $\lambda + \alpha < \frac{b}{a+b}$. If

$$r < \frac{\beta}{1-\alpha} \quad \text{and} \quad R\left(\frac{1}{a+b} - \frac{\lambda+\alpha}{b}\right) \geqslant \beta, \tag{25}$$

then the assumptions of Theorem 2.5.1 are fulfilled.

One we have determined some sufficient conditions on the parameters, we deal with some particular values and show that the particular solution of problem (20) satisfies condition (24) in Theorem 2.5.1. First, we have that condition (25) is satisfied for $a = b = 1$, $r = 1$, $R = 6$, $\beta = 1$ and $\lambda = \alpha = 1/6$. In this case, the exact solution of the problem with $x(0) = 0$ is $x(t) = 6\left(e^{\frac{t}{5}} - 1\right)$, $t \in [0,1]$, whose derivative is $x'(t) = \frac{6}{5}e^{\frac{t}{5}}$, $t \in [0,1]$. Then

$$\|x'\|_\infty = \frac{6}{5}e^{\frac{1}{5}} \text{ and } \varphi(x') = \frac{6}{5}\left(1 + e^{\frac{1}{5}}\right),$$

and it is easy to see that condition (24) holds.

The second example deals with an equation that cannot be explicitly solved. However, for some particular parameter values, this equation reduces to the solvable implicit problem given in Example 2.5.2. Thus, in this particular case, we can see that the sufficient conditions required to the parameters correspond to those in Example 2.5.2.

Example 2.5.3. Consider the equation

$$x'(t) = \lambda x(t) + \alpha x'(t) + \beta + \gamma \sin(x'(t)),\ t \in [0,1]. \tag{26}$$

In this case,

$$f(s) = \lambda s \text{ and } g(s) = \alpha s + \beta + \gamma \sin s\ (s \in \mathbb{R}),$$

where we assume that α, β, γ and λ are non-negative.

Now, we explain how to fulfill the conditions **(H1)-(H3)**, **(H5,c1)-(H5,c2)** in Theorem 2.5.1.

Clearly, condition **(H1)** holds.

Next, if $\alpha < 1 - \gamma$, then $|g'(s)| = |\alpha + \gamma \cos s| \leqslant \alpha + \gamma < 1$. Therefore, **(H2)** is satisfied for $k = \alpha + \gamma < 1$.

To guarantee condition **(H3)**, we need $g(\mathbb{R}_+) \subset \mathbb{R}_+$, which takes place if $\beta \geqslant \gamma$.

Furthermore, condition **(H5)** is fulfilled if g is increasing in $\mathbb{R}_+$, and this happens if $\alpha \geqslant \gamma$. This condition, together with $\alpha < 1-\gamma$, gives $\gamma \leqslant \alpha < 1-\gamma$. Then, obviously, γ has to satisfy $0 \leqslant \gamma < \frac{1}{2}$.

Finally, we have to check conditions **(H5,c1)** and **(H5,c2)**. For the first, we need $r > 0$ such that $g(r) > r$, that is, $\alpha r + \beta + \gamma \sin r > r$. This clearly happens if $\alpha r + \beta - \gamma > r$, or, equivalently, $r < \frac{\beta-\gamma}{1-\alpha}$, which requires $\beta > \gamma$ since r has to be positive. Condition **(H5,c2)** reads as

$$\lambda \frac{R}{b} + \alpha \frac{R}{b} + \beta + \gamma \sin \frac{R}{b} \leqslant \frac{R}{a+b}. \tag{27}$$

We show that there exists R large enough that satisfies this inequality. Indeed, if we divide by $\frac{R}{b}$, we obtain

$$\lambda + \alpha + \frac{\beta b}{R} + \gamma \frac{\sin \frac{R}{b}}{\frac{R}{b}} \leqslant \frac{b}{a+b}.$$

The limit of the left hand side, when R tends to ∞, being $\lambda + \alpha$ guarantees the existence of R provided that $\lambda + \alpha < \frac{b}{a+b}$ or, equivalently, $\lambda < \frac{b}{a+b} - \alpha$. In view of $\lambda \geqslant 0$, it requires that $\alpha < \frac{b}{a+b}$.

Therefore, the conditions of Theorem 2.5.1 are fulfilled if the non-negative parameters α, β, γ and λ satisfy:

$$\gamma \leqslant \alpha < 1-\gamma, \ \lambda + \alpha < \frac{b}{a+b}, \text{ and } \gamma < \min\left\{\frac{1}{2}, \beta\right\}.$$

Under these conditions, for every

$$r < \frac{\beta-\gamma}{1-\alpha},$$

there exists a solution $x \in \mathcal{C}^1([0,1],\mathbb{R})$ of equation (26) with $x(0) = 0$ that is non-negative, increasing and with $\|x'\|_\infty \geqslant r$.

If, in addition, a number R is chosen such that inequality (27) holds, then the solution x also satisfies

$$a \min_{t\in[0,1]} x'(t) + b \max_{t\in[0,1]} x'(t) \leqslant R.$$

We finally show that a similar approach does not work for expansion type conditions, that is, Theorem 2.3.3 does not apply for the initial value problem (20), at least if we use arguments like those developed for the compressive case. Indeed, if we take

$$E_1 = \{y \in \mathcal{C}([0,1],\mathbb{R}) : \ \varphi(y) \leqslant r\}, \quad E_2 = \{y \in \mathcal{C}([0,1],\mathbb{R}) : \ \|y\|_\infty \leqslant R\},$$

where φ is the functional defined in Example 2.4.2 and r, R are positive numbers with $r < bR$; and we proceed similarly to the compression case, we arrive to the following sufficient expansion type conditions:

(H4,E1) $\max_{t\in[0,1],\, y\in[0,\frac{r}{b}]} f(t,y) + \max_{t\in[0,1],\, y\in[\frac{r}{a+b},\frac{r}{b}]} g(t,y) \leqslant \dfrac{r}{a+b}$;

(H4,E2) $\min_{t\in[0,1],\, y\in[0,R]} f(t,y) + \min_{t\in[0,1]} g(t,R) > R.$

These conditions ensure that E_1 and E_2 are star convex sets satisfying Condition 1, $0 \in E_1 \subset \mathring{E}_2$ and **(E1)-(E2)** hold; but, unfortunately, they are not compatible with hypothesis **(H2)**, and thus Theorem 2.3.3 can not be applied. We prove this incompatibility in the autonomous case, that is, when f and g do not depend on t, and conditions **(H4,E1)-(H4,E2)** read as

$$\max_{y\in[0,\frac{r}{b}]} f(y) + \max_{y\in[\frac{r}{a+b},\frac{r}{b}]} g(y) \leqslant \frac{r}{a+b};$$

$$\min_{y\in[0,R]} f(y) + g(R) > R.$$

Subtracting the two inequalities yields

$$g(R) - \max_{y\in[\frac{r}{a+b},\frac{r}{b}]} g(y) > R - \frac{r}{a+b} + \max_{y\in[0,\frac{r}{b}]} f(y) - \min_{y\in[0,R]} f(y). \tag{28}$$

From $r < bR$, we have $[0, r/b] \subset [0, R]$, whence

$$\min_{y\in[0,R]} f(y) \leqslant \min_{y\in[0,\,\frac{r}{b}]} f(y) \leqslant \max_{y\in[0,\,\frac{r}{b}]} f(y).$$

Hence, the right-hand side in (28) is greater than or equal to $R - r/(a+b)$, so

$$g(R) - \max_{y\in[\frac{r}{a+b},\frac{r}{b}]} g(y) > R - \frac{r}{a+b}. \tag{29}$$

On the other hand, if $\hat{y} \in [r/(a+b), r/b]$ is such that $g(\hat{y}) = \max_{y\in[r/(a+b),\, r/b]} g(y)$, then, by using **(H2)**, we have

$$\begin{aligned} g(R) - \max_{y\in[\frac{r}{a+b},\frac{r}{b}]} g(y) &= g(R) - g(\hat{y}) \leqslant k(R-\hat{y}) \\ &\leqslant k\left(R - \frac{r}{a+b}\right) < R - \frac{r}{a+b}. \end{aligned}$$

This together with condition (29) clearly yields a contradiction.

Thus, we did not succeed in applying the expansion type result to (20). However, we claim that it may work for other types of initial or boundary value problems, since the expansion conditions are compatible with many other problems involving compact operators, as illustrated extensively in the literature.

2.6 DISCUSSION

In this section, we summarize and discuss the research work we have developed throughout the chapter. We present the contents classified in blocks for a better distribution.

Interest of the new extensions of Krasnosel'skii fixed point theorem

In Section 2.1, we consider some of the several generalizations of Krasnosel'skii compression-expansion fixed point theorem. Then, in Sections 2.2 and 2.3, we extend the results for set contractions to star convex sets. In the following, we justify the usefulness of the obtained results.

The initial motivation to work in this particular generalization was the possibility to localize different solutions with the same norm. We notice that there exist other results with this potential, like those owed by Güo and Lakshmikantham (1998) and Precup (2006). Our results generalize the ones in (Precup, 2006) (see Section 2.4 for details), but do not work for the general domains determined by two open sets in (Güo and Lakshmikantham, 1998). However, the key point of our results is that they consider set contractions instead of continuous and compact maps, and it allows us to deal with more general problems, such as the system of implicit first order differential equations in Section 2.5.

The results in (Precup, 2006) extend the applicability of Krasnosel'skii type fixed point theorems to boundary value problems for partial differential equations, such as semi-linear elliptic problems. The key ingredient of these results is the possibility to work in more general domains determined by two norms. Since our fixed point theorems can consider funtionals more general than a norm, we claim that they can be also useful to deal with this type of problems.

It is worth mentioning that, apart from the generalization of the results to conical domains determined by two star convex sets, we also improve the expansion type fixed point theorem for balls owed by Các and Gatica (1979). In the work (Potter, 1974), it is said that Theorem 2.3.2 follows from similar arguments to those developed for the compressive case, but the proof is not given. Besides, Các and Gatica (1979) follow Krasnosel'ski ideas in the proof of the expansive case in Theorem 1.2.5, but they needed to impose more restrictive expansion conditions and the balls did not play a role in the localization of fixed points. Thus, we realized that a change of variable which transforms the expansive case in the compressive one helps to relax the expansion hypotheses and to localize the fixed points in a conical shell determined by two balls.

Complexity of the hypotheses in our main results

At the beginning of Section 2.3, we show that the generalization of the existing results for balls to star convex sets cannot be simply adapted by using the classical idea of composing with a homeomorphic transformation. We provided

different reasons related with the set contraction property, the domain and range of the mapping and the compression-expansion conditions.

Besides, in Subsection 2.3.1, where we adapt Potter's results to star convex sets, we observe that the difficulty when working with k-set contractions comes from the fact that the geometric transformations can change uncontrollably the constant k. Moreover, the use of star convex sets introduces much more complicated geometric transformations connected to their retro-activity property, which have to be put into accordance with the constant k, as Lemma 2.3.1 shows.

Relevance of defining the star convex sets by using functionals

We already mentioned that Erbe and Wang (1994), Torres (2003), and Zima (2004) apply generalizations of Theorem 1.2.5 in terms of the norm to different second order boundary value problems. These fixed point results enable to localize solutions in the general domain $C \cap (\overline{\Omega_2} \backslash \Omega_1)$, where C is a cone and Ω_1, Ω_2 are open sets. However, for applications, they choose the simplest possibility and determine the open sets by using the norm. In this way, they are missing the good localization qualities of this type of results. In our case, the compression-expansion results work for star convex sets more general than balls, so to take advantage of this general framework in applications, we determine conditions over a functional in order to define admissible star convex sets while being more general than a norm.

To conclude, we recall that there exist other research studies dealing with generalizations of Krasnosel'skii fixed point theorem in terms of functionals. We mentioned in the Introduction the work by Anderson, Avery, and Henderson (2010), where the conditions required do not meet hypotheses **(F1)-(F5)**, since they consider convex/concave functionals.

USC
UNIVERSIDADE
DE SANTIAGO
DE COMPOSTELA

3 APPLICATIONS OF FIXED POINT THEORY TO PERIODIC PREDATOR-PREY DIFFERENTIAL EQUATIONS

This chapter includes the contents of the research article (Lois-Prados and Precup, 2020)[1], in which we contribute to the application of fixed point results to Lotka-Volterra type models. The chapter is organized as follows:

We start with an introductory section, where we first revisit different formulations of predator-prey systems, we provide the formulation of the model into consideration and we also describe our initial motivation to develop the present research. Next, we explain the interest of our study in the framework of fixed point theory, where we contribute to the application of Krasnosel'skii type fixed point theorems. Finally, we briefly review the research developed throughout this chapter.

Then, in Section 3.2, we prepare the underlying model for the application of fixed point techniques, so we obtain its integral version and we state some useful notations.

The central part of the research is comprised in Section 3.3, which is divided into three subsections. In the first one, we state and prove the main result about the existence and localization of periodic solutions as a consequence of the homotopy version of Krasnosel'skii fixed point theorem; and we discuss the possibility of localization for some particular expressions of the model. In Subsection 3.3.2, we study two interesting properties of the localized solutions. In the last subsection, the existence results are improved for the particular case in which the predator functional response does not depend on time.

Finally, we include a Discussion section, where we summarize our main contributions to the study of Lotka-Volterra type systems, by means of fixed point theory techniques, and we compare our approach with other similar research works. We also devote some lines to talk about the qualitative properties of the localized solutions.

1 Cristina Lois-Prados (Instituto de Matemáticas, Universidade de Santiago de Compostela, Spain) & Radu Precup (Department of Mathematics, Babeş Bolyai University, Romania), "Positive periodic solutions for Lotka–Volterra systems with a general attack rate", *Nonlinear Analysis: Real World Applications (ISSN: 14681218)*, **52**, 2020. The final authenticated version is available online at: https://doi.org/10.1016/j.nonrwa.2019.103024.
JCR 2019 (category; impact factor; relative position; quartile): Applied Mathematics; 2.072; 37/261; Q1.
PhD student contributions: The authors have equally contributed to the development of the article contents, they were continuously collaborating during the research stay of C. Lois-Prados at Babeş Bolyai University. The initial idea of studying the involved Lotka-Volterra type model was conceived by C. Lois-Prados.

3.1 INTRODUCTION AND MODEL DESCRIPTION

In this section, we include the formulation of the non-autonomous predator-prey population model studied in this chapter, as well as some motivations and interests of our research work. We organize the contents by dividing them in blocks with their corresponding descriptive headline.

Review of different Lotka-Volterra type systems and research motivation

Lotka-Volterra type systems are commonly used to describe interactions between two species, prey and predator. In the autonomous case, these models have a Kolmogorov structure, being of the form

$$\begin{cases} x' = x\,F(x,y); \\ y' = y\,G(x,y); \end{cases}$$

and most of them satisfy the following conditions:

$$F_y(x,y) < 0,\ G_x(x,y) > 0 \text{ and } G_y(x,y) \leqslant 0$$

(see, e.g., Brauer and Castillo Chávez, 2001, Section 5.4). For non-autonomous Kolmogorov type systems, we refer the reader to the paper by Zanolin (1992).

The original model proposed by Lotka (1925) and Volterra (1926) is given by

$$\begin{cases} x' = ax - \lambda xy; \\ y' = -by + c\lambda xy. \end{cases} \tag{30}$$

For a historical note on this classical model see (Bacaër, 2011). As suggested by Volterra himself, a more realistic prey growth is the logistic one, which was considered by several authors. For instance, Rosenzweig and MacArthur (1963) proposed the following model:

$$\begin{cases} x' = ax\left(1 - \frac{x}{K}\right) - \phi(x)y; \\ y' = -by + c\phi(x)y. \end{cases}$$

Some generalizations of the Rosenzweig-MacArthur model are given in (Van der Hoff and Fay, 2016), where, in particular, it is considered the logistic growth for both prey and predator populations (see also Buffoni, Groppi, and Soresina, 2011).

In this paper, we look for periodic solutions for the following periodic Lotka-Volterra type systems with a general prey growth g and a general functional response of predators φ:

$$\begin{cases} x' = a(t)xg(x) - \varphi(t,x,y)xy; \\ y' = -b(t)y + c(t)\varphi(t,x,y)xy; \end{cases} \tag{31}$$

where $a, b, c \in \mathcal{C}(\mathbb{R}, \mathbb{R}_+)$ are ω-periodic with the same period $\omega > 0$, $a, b \not\equiv 0$, $\min_{s\in[0,\omega]} c(s) > 0$; $\varphi \in \mathcal{C}(\mathbb{R} \times \mathbb{R}_+ \times \mathbb{R}_+, \mathbb{R}_+)$ is such that $\varphi(\cdot, x, y)$ is ω-periodic for every $(x, y) \in \mathbb{R}_+ \times \mathbb{R}_+$; and $g \in \mathcal{C}(\mathbb{R}_+, \mathbb{R})$ is decreasing, with $g(0) \leqslant 1$. We notice that x, y represent the prey and predator populations, respectively.

In particular, we use

$$\begin{aligned} g(x) &\equiv 1 \qquad \text{(linear growth of the prey), or} \\ g(x) &\equiv 1 - \tfrac{x}{K} \quad \text{(logistic growth of the prey)} \end{aligned}$$

and one of the following expressions for the functional response φ,

$$\begin{aligned} \varphi_I(t, x, y) &\equiv \lambda(t) + \alpha(t)\, y; \\ \varphi_{II}(t, x, y) &\equiv \frac{\lambda(t) + \alpha(t)\, y}{1 + \beta(t)(\lambda(t) + \alpha(t)\, y)\, x}. \end{aligned}$$

Here, we assume that α, β, $\lambda \in \mathcal{C}(\mathbb{R}, \mathbb{R}_+)$ are ω-periodic functions and λ, $\beta \not\equiv 0$.

The particular expressions for both φ_I and φ_{II} involving constant coefficients (λ, $\beta > 0$ and $\alpha \geqslant 0$) are used in the literature to simulate the effects of hunting cooperation between predators (see Berec, 2010; Teixeira Alves and Hilker, 2017).

The motivation to study the existence of ω-periodic solutions of system (31) comes from the research carried out by Teixeira Alves and Hilker (2017). They consider constant coefficients and the functional response $\varphi(x, y) = \lambda + \alpha y$, where λ is the attack rate and α represents the cooperation term. This model does not sustain predator-prey oscillations in the absence of hunting cooperation ($\alpha = 0$), so they can assert that the observed oscillations are clearly generated by the cooperative behavior.

Fixed point theory and predator-prey models

The existence of ω-periodic solutions for Lotka-Volterra type models has been studied by means of different fixed point theory approaches. For instance, Tsvetkov (1996) and Zanolin (1992) use topological arguments, such as index theory or Mawhin's coincidence degree. However, Lv, Lu, and Yan (2010) and Tang and Zou (2006) consider more complex predator-prey models including periodic time-delays, but they apply directly the norm type generalization of Krasnosel'skii fixed point theorem given in Theorem 1.2.9.

To our knowledge, there are not research works available in which Krasnosel'skii type compression or expansion results are applied to simpler models such as the one in Tsvetkov (1996). One possible reason is that the most common versions of Krasnosel'skii fixed point theorem do not apply for this class of Lotka-Volterra equations.

In this chapter, we contribute to fill this gap in the application of Krasnosel'skii type results for Lotka-Volterra population models. For the non-autonomous predator-prey system (31), which is a generalization of the model

considered by Tsvetkov (1996), we find that the homotopy version in Theorem 1.2.11 is an appropriate result, while the classical fixed point theorem, the norm type version used in models with time-delays or the vector version are not applicable or present some obstacles in their application.

Overview of the research study

Here, we consider the periodic non-autonomous predator-prey type system (31), which includes general expressions for the prey growth and the functional response of predators. Our main contribution is the localization of periodic solutions by means of a classical operator approach with the application of fixed point results whose hypotheses are given directly in terms of the associated mapping, as it is explained in the previous paragraphs. In addition, we show that our procedure is not useful to prove the existence of multiple solutions. We also take into account the possibility to localize steady states instead of non-constant periodic solutions. Thus, for the general formulation of the model, we provide sufficient conditions for the localization of non-constant solutions; but these results do not apply for the autonomous case, where we show that the steady states may belong to the localization region. In the general framework, under uniqueness conditions, we also prove that the prey and predator populations corresponding to a localized non-constant periodic solution cannot end in extinction.

3.2 INTEGRAL VERSION OF THE SYSTEM AND RELATED NOTATIONS

We are interested in ω-periodic solutions of system (31), so for this purpose we adapt the operator approach used in (Precup, 2007) (see also Tsvetkov, 1996). Thus, given two ω-periodic functions $f_1, f_2 \in \mathcal{C}(\mathbb{R}, \mathbb{R})$ and $a, b \in \mathcal{C}(\mathbb{R}, \mathbb{R}_+)$, $a, b \not\equiv 0$, there is a unique ω-periodic solution (x, y) of the system

$$\begin{cases} x' = a(t)x - f_1(t); \\ y' = -b(t)y + f_2(t); \end{cases} \tag{32}$$

given by

$$\begin{cases} x(t) = \int_t^{t+\omega} H_1(t,s)\, f_1(s)\, ds; \\ y(t) = \int_t^{t+\omega} H_2(t,s)\, f_2(s)\, ds; \end{cases}$$

where

$$H_1(t,s) = \frac{e^{-\int_t^s a(\tau)d\tau}}{1 - e^{-\int_0^\omega a(\tau)d\tau}},\ H_2(t,s) = \frac{e^{\int_t^s b(\tau)d\tau}}{e^{\int_0^\omega b(\tau)d\tau} - 1},\ (t,s) \in \mathbb{R} \times \mathbb{R}.$$

Now, if, instead of the linear system (32), we consider the non-linear system

$$\begin{cases} x' = a(t)x - f_1(t,x,y); \\ y' = -b(t)y + f_2(t,x,y); \end{cases}$$

then its ω-periodic solutions are exactly the ω-periodic solutions of the non-linear integral system

$$\begin{cases} x(t) = \int_t^{t+\omega} H_1(t,s)\, f_1(s,x(s),y(s))\, ds; \\ y(t) = \int_t^{t+\omega} H_2(t,s)\, f_2(s,x(s),y(s))\, ds; \end{cases}$$

which can be studied as a fixed point problem. Therefore, if we express the model (31) as

$$\begin{cases} x' = a(t)x - [a(t)x(1-g(x)) + \varphi(t,x,y)xy]; \\ y' = -b(t)y + c(t)\varphi(t,x,y)xy; \end{cases}$$

their ω-periodic solutions are the fixed points of the mapping $N = (N_1, N_2)$, where:

$$N_1(x,y)(t) := \int_t^{t+\omega} H_1(t,s)[a(s)x(s)(1-g(x(s))) + \varphi(s,x(s),y(s))x(s)y(s)]ds;$$
$$N_2(x,y)(t) := \int_t^{t+\omega} H_2(t,s)c(s)\varphi(s,x(s),y(s))x(s)y(s)ds.$$

To conclude this section, we provide a list of useful notations that simplify the computations related to the application of Theorem 1.2.11 to the previously defined integral mapping N:

$$\underline{a} := \min_{s\in[0,\omega]} a(s),\ \underline{b} := \min_{s\in[0,\omega]} b(s),\ \underline{c} := \min_{s\in[0,\omega]} c(s);$$
$$\overline{a} := \max_{s\in[0,\omega]} a(s),\ \overline{b} := \max_{s\in[0,\omega]} b(s),\ \overline{c} := \max_{s\in[0,\omega]} c(s);$$

$$m_1 := \min_{(t,s)\in[0,\omega]\times[t,t+\omega]} H_1(t,s) = \frac{1}{e^{\int_0^\omega a(\tau)d\tau} - 1};$$
$$\underline{m}_1 := \min_{t\in[0,\omega]} \int_t^{t+\omega} H_1(t,s)\, ds;$$
$$m_2 := \min_{(t,s)\in[0,\omega]\times[t,t+\omega]} H_2(t,s) = \frac{1}{e^{\int_0^\omega b(\tau)d\tau} - 1};$$
$$\underline{m}_2 := \min_{t\in[0,\omega]} \int_t^{t+\omega} H_2(t,s)\, ds;$$

$$M_1 := \max_{(t,s)\in[0,\omega]\times[t,t+\omega]} H_1(t,s) = \frac{1}{1-e^{-\int_0^\omega a(\tau)\,d\tau}};$$
$$\overline{M}_1 := \max_{t\in[0,\omega]} \int_t^{t+\omega} H_1(t,s)\,ds;$$
$$M_2 := \max_{(t,s)\in[0,\omega]\times[t,t+\omega]} H_2(t,s) = \frac{1}{1-e^{-\int_0^\omega b(\tau)\,d\tau}};$$
$$\overline{M}_2 := \max_{t\in[0,\omega]} \int_t^{t+\omega} H_2(t,s)\,ds;$$
$$q_1 := \frac{m_1}{M_1},\ q_2 := \frac{m_2}{M_2};$$
$$m_3 := q_1\,q_2\,\min\{m_1, \underline{c}\,m_2\},\ M_3 := \max\{M_1, \overline{c}\,M_2\};$$
$$\underline{m}_3 := q_1\,q_2\,\min\{\underline{m}_1, \underline{c}\,\underline{m}_2\},\ \overline{M}_3 := \max\{\overline{M}_1, \overline{c}\,\overline{M}_2\}.$$

3.3 EXISTENCE, LOCALIZATION AND OTHER PROPERTIES OF SOLUTIONS

This section includes the main research contributions of this chapter. In Subsections 3.3.1, 3.3.2, we work with the general formulation of system (31); while in Subsection 3.3.3, we assume that the predators functional response does not depend on time. The first and latter subsections deal with existence and localization results; since the particular conditions in Subsection 3.3.3 allow us to provide a better localization of periodic solutions. The central subsection analyses some other interesting properties of solutions: the non-constancy and the positiveness of both prey and predator populations.

3.3.1 *Existence and localization*

In this subsection, we state and prove our main result about the existence and localization of ω-periodic solutions for system (31). The required hypotheses contain some conditions in which the prey growth g and the functional response φ are involved. Thus, in Subsection 3.3.1.2, we study the viability of these conditions, in particular, for linear and logistic prey growth. Moreover, in each situation, the possibility to localize the periodic solutions is discussed separately for $\varphi = \varphi_I$ and $\varphi = \varphi_{II}$. Before that, in Subsection 3.3.1.1, we discuss the applicability problems found when working with some different versions of Krasnosel'skii fixed point theorem.

Throughout this subsection, we assume that the following conditions are satisfied by the functional response φ:

(G1) There exists $\eta \in \mathcal{C}(\mathbb{R}\times\mathbb{R}_+\times\mathbb{R}_+, \mathbb{R}_+)$ such that

- $\eta(\cdot, x, y)$ is ω-periodic for every $(x,y) \in \mathbb{R}_+\times\mathbb{R}_+$;
- $\eta(t,\cdot,y)$, $\eta(t,x,\cdot)$ are increasing functions for every (t,y), $(t,x) \in \mathbb{R}\times\mathbb{R}_+$;
- $\varphi(t,x,y) \leqslant \eta(t,x,y)$ for every $(t,x,y) \in \mathbb{R}\times\mathbb{R}_+\times\mathbb{R}_+$.

(G2) There exists $\psi \in \mathcal{C}(\mathbb{R} \times \mathbb{R}_+, \mathbb{R}_+)$ such that

- $\psi(\cdot, z)$ is ω-periodic for every $z \in \mathbb{R}_+$;
- $\psi(t, \cdot)$ is decreasing for every $t \in \mathbb{R}$;
- $\varphi(t, x, y) \geqslant \psi(t, x + y)$ for every $(t, x, y) \in \mathbb{R} \times \mathbb{R}_+ \times \mathbb{R}_+$.

Now, we can prove the main result of this chapter by using the homotopy version of Krasnosel'skii fixed point theorem stated in Theorem 1.2.11.

Theorem 3.3.1. *Let us consider the Banach space* $\left(\mathcal{C}_\omega\left(\mathbb{R}, \mathbb{R}^2\right), \|\cdot\|_\omega\right)$ *and the cone* C *in Example 1.2.4, with* $q_1 = m1/M1$ *and* $q2 = m2/M2$. *If conditions* ***(G1)*** *and* ***(G2)*** *hold and there exist* r, $R \in \mathbb{R}$, $0 < r < R$, *such that*

$$1 \geqslant \overline{a}\,\overline{M}_1\,(1 - g(r))\,, \tag{33}$$

$$\overline{M}_1\,\overline{a}\,(1 - g(r)) + M_3\,r \int_0^\omega \eta(s, r, r)ds \leqslant 2, \tag{34}$$

$$R \int_0^\omega \psi(s, R)ds \geqslant \frac{2}{m_3}, \tag{35}$$

then the system (31) *has an* ω*-periodic solution* $(x, y) \in C$ *such that*

$$r \leqslant \|(x, y)\|_\omega = \|x\|_\infty + \|y\|_\infty \leqslant R.$$

Proof. From the arguments given in Section 3.2, we can assert that the continuous ω-periodic solutions of system (31) are the fixed points in $\mathcal{C}_\omega\left(\mathbb{R}, \mathbb{R}^2\right)$ of the non-linear operator $N = (N_1, N_2)$, where

$$N_1(x, y)(t) := \int_t^{t+\omega} H_1(t, s) f_1(s, x(s), y(s))ds;$$
$$N_2(x, y)(t) := \int_t^{t+\omega} H_2(t, s) f_2(s, x(s), y(s))ds;$$

and $f_1(s, x, y) := a(s)x(1 - g(x)) + \varphi(s, x, y)xy$, $f_2(s, x, y) := c(s)\varphi(s, x, y)xy$.

In the following, we show that the Banach space $\left(\mathcal{C}_\omega\left(\mathbb{R}, \mathbb{R}^2\right), \|\cdot\|_\omega\right)$, the cone C, the positive real numbers $r < R$, and the mapping $N_{|C_R}$ fulfill the hypotheses of Theorem 1.2.11.

N *maps* C_R *into the cone* C

We prove a more general statement, that is, $N(C) \subset C$. Thus, we consider a pair $(x, y) \in C$, and we show that $N(x, y) = (N_1(x, y), N_2(x, y)) \in C$. For that purpose, for each $i \in \{1, 2\}$, we prove that $N_i(x, y)(t) = N_i(x, y)(t + \omega)$ and

$N_i(x,y)(t) \geqslant q_i \|N_i(x,y)\|_\infty$, for all $t \in \mathbb{R}$. On the one hand, the ω-periodicity of $N_i(x,y)$ follows easily by means of the change of variable $s \to s+\omega$ and the periodicity hypothesis on the involved functions. On the other hand, by using the definitions of q_i, m_i and M_i, we obtain

$$\begin{aligned} q_i \|N_i(x,y)\|_\infty &= \frac{m_i}{M_i} \max_{t\in[0,\omega]} \int_t^{t+\omega} H_i(t,s) f_i(s,x(s),y(s))\,ds \\ &\leqslant \max_{t\in[0,\omega]} \int_t^{t+\omega} m_i f_i(s,x(s),y(s))\,ds \leqslant N_i(x,y)(t); \end{aligned}$$

for all $t \in \mathbb{R}$.

$N_{|C_R}$ is continuous and compact

It follows from the continuity property required to the involved functions and the Arzelà-Ascoli result provided in Theorem 1.1.3.

$N_{|C_R}$ satisfies conditions ***(H,E1)-(H,E2)***

We start by proving condition **(H,E1)**, which in our case reads as follows

$$(N_1(x,y), N_2(x,y)) \neq \lambda(x,y), \text{ for all } (x,y) \in C,\ \|(x,y)\|_\omega = r \text{ and } \lambda > 1. \quad (36)$$

To this aim, we consider three cases:

Case 1: Assume $x \equiv 0$ and $y \not\equiv 0$. Then condition (36) trivially holds since

$$N_1(x,y), N_2(x,y) \equiv 0.$$

Case 2: If $x \not\equiv 0$ and $y \equiv 0$, then $N_2(x,y) \equiv 0$ and (36) reduces to

$$N_1(x,0) \neq \lambda x, \text{ for all } (x,0) \in C,\ \|x\|_\infty = r \text{ and } \lambda > 1. \quad (37)$$

To prove this, assume the contrary, namely that there exist $(x,0) \in C$, $\|x\|_\infty = r$, and $\lambda > 1$ such that

$$N_1(x,0)(t) = \lambda x(t), \text{ for all } t \in [0,\omega].$$

Let $t_0 \in [0,\omega]$ be such that $x(t_0) = \|x\|_\infty = r > 0$, then also using that $-g$ is increasing, one has

$$\begin{aligned} r = x(t_0) < \lambda x(t_0) &= \int_{t_0}^{t_0+\omega} H_1(t_0,s) a(s) x(s) \left(1 - g(x(s))\right) ds \\ &\leqslant \overline{a}\, r \left(1 - g(r)\right) \int_{t_0}^{t_0+\omega} H_1(t_0,s)\, ds \leqslant \overline{a}\, r \left(1 - g(r)\right) \overline{M}_1. \end{aligned}$$

Dividing by $r > 0$, it yields $1 < \overline{a}\,(1 - g(r))\,\overline{M}_1$, which contradicts our hypothesis (33). Thus, condition (37) holds.

Case 3: Finally, we prove that condition (36) holds for $x, y \not\equiv 0$. If it does not hold, then there exist a pair $(x,y) \in C$, $\|(x,y)\|_\omega = r$, and $\lambda > 1$ such that

$$N_1(x,y)(t) = \lambda x(t),\ N_2(x,y)(t) = \lambda y(t), \text{ for all } t \in [0,\omega].$$

Let $t_0 \in [0, \omega]$ be such that $\|x\|_\infty = x(t_0)$. Then, by using condition **(G1)** over φ, one has

$$\begin{aligned}\|x\|_\infty = x(t_0) < \lambda x(t_0) = N_1(x,y)(t_0) \\ = \int_{t_0}^{t_0+\omega} H_1(t_0,s)[a(s)x(s)(1-g(x(s))) + \varphi(s,x(s),y(s))x(s)y(s)]ds \\ \leqslant \|x\|_\infty \left(\overline{a}(1-g(\|x\|_\infty))\overline{M}_1 + \|y\|_\infty M_1 \int_{t_0}^{t_0+\omega} \eta(s,\|x\|_\infty,\|y\|_\infty)ds\right).\end{aligned} \tag{38}$$

After dividing by $\|x\|_\infty$ and using the fact that $\|x\|_\infty, \|y\|_\infty < \|(x,y)\|_\omega = r$ together with the increasing properties of η and $-g$, it gives

$$1 < \overline{a}(1-g(r))\overline{M}_1 + \|y\|_\infty M_1 \int_0^\omega \eta(s,r,r)ds. \tag{39}$$

Similarly, from $N_2(x,y) = \lambda y$, we obtain

$$1 < \|x\|_\infty \overline{c} M_2 \int_0^\omega \eta(s,r,r)ds. \tag{40}$$

Now, adding (39) and (40) yields

$$2 < \overline{a}(1-g(r))\overline{M}_1 + M_3(\|x\|_\infty + \|y\|_\infty)\int_0^\omega \eta(s,r,r)ds,$$

which, by virtue of $\|x\|_\infty + \|y\|_\infty = r$, contradicts our assumption (34). Therefore, condition (36) is satisfied.

Now, to prove condition **(H,E2)**, we choose the element $v \in C\backslash\{0\}$ as any pair (x_0, y_0) with $x_0, y_0 > 0$. Then, **(H,E2)** reads as follows: for all $(x,y) \in C$, with $\|(x,y)\|_\omega = R$, and all $\lambda > 0$

$$(x,y) - (N_1(x,y), N_2(x,y)) \neq \lambda(x_0,y_0). \tag{41}$$

To this aim, we distinguish again three cases:

Case I: If $x \equiv 0$ and $y \not\equiv 0$, then $N_1(x,y)$, $N_2(x,y) \equiv 0$, so condition (41) trivially holds.

Case II: If $x \not\equiv 0$ and $y \equiv 0$, then $N_2(x,y) \equiv 0$. Therefore condition (41) is satisfied since $0 < \lambda y_0$.

Case III: Finally, we consider the case $x, y \not\equiv 0$. If condition (41) does not hold, then there exists a pair $(x,y) \in C$ with $\|(x,y)\|_\omega = R$ such that

$$x(t) > N_1(x,y)(t),\ y(t) > N_2(x,y)(t),\ \text{for all } t \in [0,\omega],$$

where we have used that $\lambda, x_0, y_0 > 0$.
On the one hand, for each $t \in [0, \omega]$, using condition **(G2)** over φ, one has

$$\begin{aligned}
\|x\|_\infty \geqslant x(t) &> N_1(x,y)(t) \\
&= \int_t^{t+\omega} H_1(t,s)[a(s)x(s)(1-g(x(s))) + \varphi(s,x(s),y(s))x(s)y(s)]ds \\
&\geqslant \int_t^{t+\omega} H_1(t,s)\varphi(s,x(s),y(s))\, x(s)\, y(s)ds \\
&\geqslant m_1 q_1 q_2 \|x\|_\infty \|y\|_\infty \int_0^\omega \psi(s, x(s)+y(s))ds \\
&\geqslant m_1 q_1 q_2 \|x\|_\infty \|y\|_\infty \int_0^\omega \psi(s, \|(x,y)\|_\omega)ds,
\end{aligned}$$

which, after dividing by $\|x\|_\infty$, yields

$$1 > m_1 q_1 q_2 \|y\|_\infty \int_0^\omega \psi(s,R)ds. \tag{42}$$

On the other hand, in a similar way, from $y(t) > N_2(x,y)(t)$, for all $t \in [0,\omega]$, we deduce that

$$1 > m_2 \underline{c}\, q_1 q_2 \|x\|_\infty \int_0^\omega \psi(s,R)ds. \tag{43}$$

Now, by adding inequalities (42), (43) and using $\|x\|_\infty + \|y\|_\infty = \|(x,y)\|_\omega = R$, we obtain

$$2 > m_3 R \int_0^\omega \psi(s,R)ds,$$

which contradicts our assumption (35). Thus, condition (41) is fulfilled.

Application of Theorem 1.2.11

We have proved that all the conditions of Theorem 1.2.11 are satisfied, therefore the non-linear operator N has a fixed point $(x,y) \in C$ with $r \leqslant \|(x,y)\| \leqslant R$. This fixed point (x,y) is a continuous ω-periodic solution of the Lotka-Volterra type system (31). □

3.3.1.1 *Applicability problems of Theorems 1.2.5, 1.2.9 and 1.2.10*

In this subsection, we show the appropriateness of the homotopy version of the Theorem of Krasnosel'skii for Lotka-Volterra type systems, as compared to the other more popular versions.

We first show that the classical Krasnosel'skii compression-expansion fixed point result considered in Theorem 1.2.5 is not applicable for the Banach space $\left(C_\omega(\mathbb{R},\mathbb{R}^2), \|\cdot\|_\omega\right)$, the cone C in Example 1.2.4 and the integral mapping N associated to the Lotka-Volterra type system (31).

One of the compression or expansion hypotheses of the Theorem of Krasnosel'skii requires that, for some real number $\tau > 0$,

$$(x, y) - N(x, y) \notin C, \text{ for all } (x, y) \in C \text{ with } \|(x, y)\|_\omega = \tau. \tag{44}$$

However, if we choose pairs of the form $(0, y) \in C$, with $\|(0, y)\|_\omega = \|y\|_\infty = \tau$, then, since $N(0, y) = (0, 0)$, one has

$$(0, y) - N(0, y) = (0, y) \in C.$$

Consequently, condition (44) does not hold.

Next, we use similar arguments to show that the norm type version provided in Theorem 1.2.9 can neither be applied to systems of the form (31). We follow the approach in (Lv, Lu, and Yan, 2010; Tang and Zou, 2006), where they also use the Banach space $\left(C_\omega(\mathbb{R}, \mathbb{R}^2), \|\cdot\|_\omega\right)$ and the cone C in Example 1.2.4. Moreover, for some positive real numbers $r_1 < R_1$, $r_2 < R_2$, they consider the open and bounded sets

$$\Omega_1 := \left\{(x, y) \in \left(C_\omega(\mathbb{R}, \mathbb{R}^2), \|\cdot\|_\omega\right) : \|x\|_\infty < r_1, \|y\|_\infty < r_2\right\};$$
$$\Omega_2 := \left\{(x, y) \in \left(C_\omega(\mathbb{R}, \mathbb{R}^2), \|\cdot\|_\omega\right) : \|x\|_\infty < R_1, \|y\|_\infty < R_2\right\}.$$

One of the hypotheses in conditions **(NC)**, **(NE)** requires that, for some $i \in \{1, 2\}$,

$$\|N(x, y)\|_\omega \geqslant \|(x, y)\|_\omega, \text{ for all } (x, y) \in C \cap \partial\Omega_i, \tag{45}$$

where for $\tau_j = r_j$ or $\tau_j = R_j$ (for both $j \in \{1, 2\}$) the elements of $\partial\Omega_i$ satisfy

$$\|x\|_\infty \leqslant \tau_1, \|y\|_\infty = \tau_2 \text{ or } \|x\|_\infty = \tau_1, \|y\|_\infty \leqslant \tau_2.$$

Thus, if we choose pairs of the form $(0, y) \in C \cap \partial\Omega_i$, with $\|y\|_\infty = \tau_2$, since $N(0, y) = (0, 0)$, one has

$$0 = \|N(0, y)\|_\omega < \|(0, y)\|_\omega := \|y\|_\infty = \tau_2.$$

Consequently, condition (45) does not hold.

Finally, we consider the classical Lotka-Volterra system with continuous and ω-periodic coefficients and we show that the vector version in Theorem 1.2.10 still cannot be applied, at least by following the proof of Theorem 3.3.1. It is worth mentioning that the result could work for this type of problems if we used a distinct reasoning, but the difficulty intrinsic to the computations obscures the visualization of this possible application.

Let us consider the real numbers $0 < r_1 < R_1$, $0 < r_2 < R_2$, the following cones in the Banach space $(\mathcal{C}(\mathbb{R}, \mathbb{R}), \|\cdot\|_\infty)$

$$C_1 := \{x \in \mathcal{C}(\mathbb{R}, \mathbb{R}) : x(t) = x(t + \omega), \ x(t) \geqslant q_1\|x\|_\infty, \text{ for all } t \in [0, \omega]\};$$
$$C_2 := \{y \in \mathcal{C}(\mathbb{R}, \mathbb{R}) : y(t) = y(t + \omega), \ y(t) \geqslant q_2\|y\|_\infty, \text{ for all } t \in [0, \omega]\};$$

and the mapping $N = (N_1, N_2) : (C_1)_{r_1,R_1} \times (C_2)_{r_2,R_2} \longrightarrow C_1 \times C_2$ given by

$$N_1(x,y)(t) := \int_t^{t+\omega} H_1(t,s)\lambda(s)x(s)y(s)ds;$$
$$N_2(x,y)(t) := \int_t^{t+\omega} H_2(t,s)c(s)\lambda(s)x(s)y(s)ds.$$

The non-applicability of the result is deduced once we show that both conditions **(V1)** and **(V2)** cannot be satisfied for one of the index values $i \in \{1,2\}$. Let us see, for instance, what happens for $i = 1$ and condition **(V1)**. If we proceed like in the proof of Theorem 3.3.1, this condition is satisfied provided that the following inequalities hold

$$M_1\overline{\lambda}R_2\omega < 1 < m_1\underline{\lambda}r_2q_1q_2\omega,$$

but this is not possible since $m_1 \leqslant M_1$, $\underline{\lambda} \leqslant \overline{\lambda}$, $r_2 < R_2$ and $q_1q_2 \in (0,1)$.

3.3.1.2 *Viability of conditions* (33)-(35)

In this subsection, we study the existence of real numbers $0 < r < R$ satisfying the required hypotheses in Theorem 3.3.1. For general expressions of the prey growth g and the predators functional response φ, we prove the existence of small enough $r > 0$ fulfilling conditions (33) and (34). However, we study condition (35) in the particular cases of linear and logistic growth, where we also specify how to choose suitable values of r and R. Under the simplest expressions for g and φ, we also discuss whether it is possible or not to localize multiple solutions and compare our results with those in (Tsvetkov, 1996).

Remark 4. Let us consider the Lotka-Volterra model (31) with a functional response φ satisfying conditions **(G1)-(G2)**. If

$$g(0) > 1 - \frac{1}{\overline{M}_1\overline{a}}, \tag{46}$$

then there exists a number $r > 0$ such that conditions (33) and (34) hold.

Indeed, by using the continuity of g at 0, if (46) is satisfied, then there exists $r_0 > 0$ such that $g(r) \geqslant 1 - 1/\left(\overline{M}_1\overline{a}\right)$, or, equivalently, condition (33) holds for every $r \in (0, r_0)$.

From (46), we also have $g(0) > 1 - 2/\left(\overline{M}_1\overline{a}\right)$, or, equivalently,

$$(1 - g(0))\overline{M}_1\overline{a} < 2,$$

which, together with the increasing character of η required in condition **(G1)**, guarantees (34) for any small enough $r > 0$.

Notice that condition (46) is trivially satisfied when $g(0) = 1$, which is the case of both linear and logistic growth of the prey population.

We consider now the particular expression of g which corresponds to the linear or logistic growth for the prey population, and we show how the conditions over $r, R > 0$ in Theorem 3.3.1 look like. Moreover, we study the existence of such numbers r and R, when $\varphi \equiv \varphi_I$ or $\varphi \equiv \varphi_{II}$.

For that purpose, let us start by proving that φ_I and φ_{II} satisfy all the conditions previously required to a general φ. It is clear that both functions belong to $\mathcal{C}(\mathbb{R} \times \mathbb{R}_+ \times \mathbb{R}_+, \mathbb{R}_+)$ and are ω-periodic in the first variable. Concerning conditions **(G1)** and **(G2)**, for function φ_I, we can take

$$\eta = \varphi_I \text{ and } \psi \equiv \lambda,$$

while for function φ_{II}, we can set

$$\eta = \varphi_I \text{ and } \psi(t,z) = \frac{\lambda(t)}{1+\beta(t)(\lambda(t)+\alpha(t)\,z)z}.$$

Additionally, we fix the following notations

$$\underline{\lambda} := \min_{s\in[0,\omega]} \lambda(s),\ \overline{\lambda} := \max_{s\in[0,\omega]} \lambda(s),\ \overline{\alpha} := \max_{s\in[0,\omega]} \alpha(s) \text{ and } \overline{\beta} := \max_{s\in[0,\omega]} \beta(s).$$

Linear growth

In this case, the localization result provided in Theorem 3.3.1 reads as follows.

Corollary 3.3.2. *Assume that $g \equiv 1$ and conditions **(G1)**, **(G2)** over φ are satisfied. If there exist $r, R \in \mathbb{R}$, $0 < r < R$, such that*

$$r \int_0^\omega \eta(s,r,r)\,ds \leqslant \frac{2}{M_3}, \tag{47}$$

and (35) hold, then the system

$$\begin{cases} x' = a(t)x - \varphi(t,x,y)xy; \\ y' = -b(t)y + c(t)\varphi(t,x,y)xy \end{cases} \tag{48}$$

has an ω-periodic solution $(x,y) \in C$, being C the cone in Example 1.2.4, such that

$$r \leqslant \|(x,y)\|_\omega = \|x\|_\infty + \|y\|_\infty \leqslant R.$$

Next, for each particular expression of φ, we give sufficient conditions for (47) and (35) to hold.

Case I: When $\varphi = \varphi_I$, conditions (47), (35) read as

$$r \int_0^\omega \lambda(s) + \alpha(s)\,r\,ds \leqslant \frac{2}{M_3},\ R \geqslant \frac{2}{m_3 \int_0^\omega \lambda(s)\,ds} \tag{49}$$

and are respectively satisfied provided that

$$r\left(\overline{\lambda} + \overline{\alpha} r\right) \leqslant \frac{2}{M_3\,\omega},\ R \geqslant \frac{2}{m_3\,\omega\,\underline{\lambda}},$$

or, equivalently,

$$r \leqslant \frac{-\overline{\lambda} + \sqrt{\overline{\lambda}^2 + 4\,\overline{\alpha}\,2/(M_3\omega)}}{2\overline{\alpha}},\ R \geqslant \frac{2}{m_3\,\omega\,\underline{\lambda}}. \tag{50}$$

Therefore, under condition (50), which is satisfied for small enough r and sufficiently large R, Corollary 3.3.2 applies. We notice that the existence of small enough $r > 0$ was already proved in Remark 4. However, the expressions in (50) tell us how to choose suitable values of r and R.

The simplicity of the conditions over r, R given in (50) allows us to easily discuss the possibility to localize multiple solutions, reaching a negative conclusion, as we will justify.

Remark 5. Since ω-periodic functions are also $n\omega$-periodic, for every natural number $n \geqslant 2$, it makes sense to ask to what extent the numbers r and R depend on the period. For each natural number $n \geqslant 1$, we denote by r_n and R_n the numbers r and R satisfying the conditions (50), when ω is replaced by $n\omega$.

Making some computations, it can be shown that

$$r_{n+1} < r_n < R_n < R_{n+1},\ \text{for all } n \in \mathbb{N},\ n \geqslant 1;$$
$$\lim_{n\to\infty} r_n = 0,\ \lim_{n\to\infty} R_n = \infty.$$

Therefore, by taking a multiple of the period ω, it may happen to localize the same ω-periodic solution for every $n \geqslant 1$, so that the best localization region is that for $n = 1$. It is worth mentioning that one should take into account that the terms M_3 and m_3 involved in the inequalities depend on the period.

Remark 6. In the particular case of $\varphi = \varphi_I$ and $\alpha = 0$, system (48) reduces to the model

$$\begin{cases} x' = a(t)x - \lambda(t)xy; \\ y' = -b(t)y + c(t)\lambda(t)xy; \end{cases} \tag{51}$$

which was studied in (Tsvetkov, 1996) by means of index theory. Even in this particular case, our result based on Theorem 1.2.11 gives a better localization of ω-periodic solutions, namely in the annular conical set

$$C_{r,R} := \{(x,y) \in C :\ r \leqslant \|x\|_\infty + \|y\|_\infty \leqslant R\},$$

where

$$r = \frac{2}{M_3 \int_0^\omega \lambda(s)\,ds},\ R = \frac{2}{m_3 \int_0^\omega \lambda(s)\,ds}.$$

Case II: When $\varphi = \varphi_{II}$, conditions (47), (35) become

$$r\int_0^\omega \lambda(s) + \alpha(s)r\,ds \leqslant \frac{2}{M_3},\ R\int_0^\omega \frac{\lambda(s)}{1+\beta(s)(\lambda(s)+\alpha(s)R)R}ds \geqslant \frac{2}{m_3} \tag{52}$$

and are respectively satisfied provided that

$$r(\overline{\lambda}+\overline{\alpha}\,r)\leqslant\frac{2}{M_3\,\omega},\ R\frac{\underline{\lambda}}{1+\overline{\beta}(\overline{\lambda}+\overline{\alpha}\,R)R}\geqslant\frac{2}{m_3\,\omega}. \tag{53}$$

The first inequality in (53) is satisfied for $r\leqslant\left(-\overline{\lambda}+\sqrt{\overline{\lambda}^2+4\,\overline{\alpha}\,2/(M_3\omega)}\right)/(2\overline{\alpha})$ as it happens in *Case I*. Next, we study the existence of R as required by the second inequality in (53). To this aim, we consider the auxiliary function

$$f(z):=\frac{Az}{1+Bz+Cz^2},\ z\in\mathbb{R}_+\setminus\{0\},$$

where $A:=m_3\,\omega\,\underline{\lambda}$, $B:=\overline{\beta}\,\overline{\lambda}$ and $C:=\overline{\beta}\,\overline{\alpha}$. Let us show that there exists $R>0$ fulfilling the last inequality in (53) if, and only if,

$$A\geqslant 2\,(2\sqrt{C}+B). \tag{54}$$

One can easily prove that $\lim_{z\to 0}f(z)=\lim_{z\to+\infty}f(z)=0$ and $f(z)>0$, for all $z>0$. Additionally, f has a unique critical point at $1/\sqrt{C}>0$ and the previous properties ensure that f attains a maximum at $z_{\max}:=1/\sqrt{C}$. Therefore, if

$$f(z_{\max})\geqslant 2,$$

or, equivalently, $A\geqslant 2\,(2\sqrt{C}+B)$, then it is possible to choose R close enough or equal to $z_{\max}$, such that the required inequality holds. Moreover, under assumption (54), we can precise the interval where we can choose R. It is $[z_1,z_2]$, where z_1,z_2 are the solutions of the equation $f(z)=2$, namely

$$z_1=\frac{A-2B-\sqrt{(A-2B)^2-4^2C}}{4C},\ z_2=\frac{A-2B+\sqrt{(A-2B)^2-4^2C}}{4C}. \tag{55}$$

3.3.1.3 *Logistic growth*

In this particular case, we can rewrite Theorem 3.3.1 as follows.

Corollary 3.3.3. *Assume that* $g(x)\equiv 1-x/K$ *and conditions* ***(G1)***, ***(G2)*** *over* φ *are satisfied. If there exist* $r,R\in\mathbb{R}$, $0<r<R$, *such that*

$$r\leqslant\frac{K}{\overline{a}\,\overline{M}_1}, \tag{56}$$

$$\frac{\overline{a}\,\overline{M}_1}{K}\,r+M_3\,r\int_0^\omega\eta(s,r,r)\,ds\leqslant 2, \tag{57}$$

and (35) *hold, then the system*

$$\begin{cases}x'=a(t)x\left(1-\frac{x}{K}\right)-\varphi(t,x,y)xy;\\ y'=-b(t)y+c(t)\varphi(t,x,y)xy\end{cases} \tag{58}$$

has an ω*-periodic solution* $(x,y)\in C$, *being* C *the cone in Example 1.2.4, such that*

$$r\leqslant\|(x,y)\|_\omega=\|x\|_\infty+\|y\|_\infty\leqslant R.$$

It is clear how condition (56) can be satisfied. In addition, it is not necessary to study again the existence of $R > 0$ fulfilling condition (35), since it does not depend on the expression of g, and therefore we can follow the arguments of Subsection 3.3.1.2. Thus, let us state some sufficient conditions on $r > 0$, such that (57) holds when $\varphi \equiv \varphi_I$ or $\varphi \equiv \varphi_{II}$. We have already mentioned that we can consider $\eta = \varphi_I$ for both expressions of φ. Then, for both cases, condition (57) reads as

$$\frac{\overline{M}_1 \overline{a}}{K} r + M_3 r \int_0^\omega (\lambda(s) + \alpha(s) r)\, ds \leqslant 2,$$

being trivially satisfied provided that

$$\frac{\overline{M}_1 \overline{a}}{K} r + M_3\, \omega\, r \left(\overline{\lambda} + \overline{\alpha}\, r\right) \leqslant 2. \tag{59}$$

We know, from Remark 4, that there exists a small enough $r > 0$ fulfilling condition (57). However, condition (59) tells us how to obtain suitable values of $r > 0$.

3.3.2 *Properties of solutions*

We devote this subsection to study some interesting properties of the ω-periodic solutions of the Lotka-Volterra system (31). First, in Subsection 3.3.2.1, we determine the steady states or constant solutions of the model. Then, we use this information and the localization results in Subsection 3.3.1 to find sufficient conditions that ensure the nonconstancy of the solutions. Finally, under uniqueness hypotheses, we show that, if the localized solution is nonconstant, then the prey and predator populations do not get extinct.

3.3.2.1 *Steady states*

The steady states of system (31) are points $(x_0, y_0) \in \mathbb{R}_+ \times \mathbb{R}_+$ such that

$$\begin{aligned} x_0\,(a(t)g(x_0) - \varphi(t, x_0, y_0)y_0) &= 0; \\ y_0(c(t)\varphi(t, x_0, y_0)x_0 - b(t)) &= 0; \end{aligned} \tag{60}$$

for all $t \in \mathbb{R}$. It is clear that $(0, 0)$ is a solution of (60). To determine other possible solutions, we distinguish three cases:

Case 1: $x_0 = 0$, $y_0 > 0$. Under these conditions, the first equation in (60) is obviously satisfied, while from the second one we have $y_0 b(t) = 0$, for all $t \in [0, \omega]$, which is not possible for $y_0 > 0$ and $b \not\equiv 0$. Therefore, there are no steady states of the form $(0, y_0)$, with $y_0 > 0$.

Case 2: $x_0 > 0$, $y_0 = 0$. Now the second equation in (60) trivially holds, while the first one gives $a(t)g(x_0) = 0$, for all $t \in [0, \omega]$. As $a \not\equiv 0$, one must have

$g(x_0) = 0$. Therefore, a point of the form $(x_0, 0)$, $x_0 > 0$, is a steady state if and only if $g(x_0) = 0$.

Case 3: $x_0 > 0$, $y_0 > 0$. Under these conditions, system (60) is equivalent to

$$\varphi(t, x_0, y_0) = \frac{a(t)g(x_0)}{y_0} = \frac{b(t)}{c(t)x_0}, \text{ for all } t \in [0, \omega].$$

We collect these results about the existence of steady states for system (31) in the following proposition.

Proposition 3.3.4. *A point $(x_0, y_0) \in \mathbb{R}_+ \times \mathbb{R}_+$ is a steady state of system (31) if, and only if, one of the following conditions holds:*

1. $x_0 = 0$ *and* $y_0 = 0$;
2. $x_0 > 0$, $g(x_0) = 0$ *and* $y_0 = 0$;
3. $x_0 > 0$, $y_0 > 0$ *and*

$$\varphi(t, x_0, y_0) = \frac{a(t)g(x_0)}{y_0} = \frac{b(t)}{c(t)x_0}, \textit{ for all } t \in [0, \omega]. \tag{61}$$

Linear growth

According to this proposition, in case of considering the linear growth of the prey population, statement 2 is not possible, and steady states of the form (x_0, y_0) with x_0, $y_0 > 0$ exist if and only if

$$\varphi(t, x_0, y_0) = \frac{a(t)}{y_0} = \frac{b(t)}{c(t)x_0}, \text{ for all } t \in [0, \omega]. \tag{62}$$

Logistic growth

If one considers the logistic growth of the prey population, then from statement 2 in Proposition 3.3.4 we obtain the steady state $(K, 0)$, and steady states of the form (x_0, y_0) with x_0, $y_0 > 0$ exist if and only if

$$\varphi(t, x_0, y_0) = \frac{a(t)\left(1 - \frac{x_0}{K}\right)}{y_0} = \frac{b(t)}{c(t)x_0}, \text{ for all } t \in [0, \omega]. \tag{63}$$

General prey growth

Coming back to the general system (31), let us note that, if there is not any constant $k > 0$ such that

$$a(t) = k\,\frac{b(t)}{c(t)}, \text{ for all } t \in [0, \omega], \tag{64}$$

then the system has no steady states (x_0, y_0) with $x_0, y_0 > 0$. Therefore, under condition (64), the orbits of all ω-periodic solutions (x, y), with $x(t)$, $y(t) > 0$ for all $t \in [0, \omega]$, do not reduce to points.

3.3.2.2 *Nonconstant solutions*

Here, we deduce sufficient conditions to ensure that the periodic solution obtained in Theorem 3.3.1 does not reduce to a steady state, letting it the possibility to be a limit cycle. We state a general result which is useful for the particular case of linear prey growth, but cannot be applied to prey populations with logistic growth. Therefore, we study the latter case separately, and we provide an example to illustrate the theoretical arguments.

Theorem 3.3.5. *Assume that condition* (61) *does not hold and*

$$g(x) \neq 0, \text{ for all } x > 0. \tag{65}$$

Then any ω*-periodic solution* (x, y) *of system* (31) *with* $\|(x, y)\|_\omega > 0$ *does not reduce to a steady state.*

Proof. In view of the inequality $\|(x, y)\|_\omega > 0$, the result follows once we have proved that the unique steady state is $(0, 0)$.

From Proposition 3.3.4, we know that there are no steady states of the form $(0, y_0)$ with $y_0 > 0$; moreover, if $g(x) \neq 0$, for all $x > 0$, then there are no steady states of the type $(x_0, 0)$ with $x_0 > 0$; and, if condition (61) does not hold, then there are no positive (with both positive components) steady states. Therefore, the unique steady state of the system is $(0, 0)$, as wished. □

Linear growth

In case of linear growth of the prey population, condition (65) in Theorem 3.3.5 trivially holds. Consequently, given two real numbers $0 < r < R$ satisfying the required hypotheses in Corollary 3.3.2, if condition (62) is not fulfilled, then, applying Theorem 3.3.5, we can assert that there exists a nonconstant ω-periodic solution $(x, y) \in C$ with $r \leqslant \|(x, y)\|_\omega \leqslant R$.

In particular, when $\varphi = \varphi_I$, the hypotheses in Corollary 3.3.2 read as (49), which can always be satisfied for small enough r and sufficiently large R. Therefore, if we ensure that condition (62) does not hold, then there is an ω -periodic solution which is nonconstant. For instance, if a, b, c, λ are constants, but the cooperation coefficient α is nonconstant, then condition (62) is not fulfilled.

Logistic growth

However, for the logistic growth of the prey population, Theorem 3.3.5 does not apply since $g(K) = 0$. Nevertheless, if condition (63) does not hold, then the steady states of system (58) are $(0, 0)$ and $(K, 0)$. Recall that we can always consider small enough $r > 0$ such that conditions (56)-(57) in Corollary 3.3.3 are fulfilled. Therefore, if the exists a number $R > 0$ such that $K > R > r > 0$ and condition (35) holds, then the orbit of the ω-periodic solution given by Corollary 3.3.3 does not reduce to a point.

For the particular cases of $\varphi = \varphi_I$ and $\varphi = \varphi_{II}$, it is possible to choose a real number $0 < R < K$ provided that

$$K > \frac{2}{m_3 \int_0^\omega \lambda(s)\,ds} \quad \text{or} \quad z_1 < K,$$

respectively, where z_1 is given in (55).

In particular, when $\varphi = \varphi_I$, if a, b, c, λ are constants and α is nonconstant, then condition (63) does not hold. Therefore, for every

$$K > \frac{2}{m_3 \omega \lambda},$$

the ω-periodic solution of system (58), given by Corollary 3.3.3, is nonconstant.

We conclude this subsection with an example where all the coefficients, except c, are nonconstant.

Example 3.3.6. Let the coefficients of system (58), with $\varphi = \varphi_I$, be

$$a(t) := \sin^2 \pi t, \ b(t) := \cos^2 \pi t, \ c(t) := c \in (0,1);$$

$$\lambda(t) := \theta a(t) + (1-\theta) b(t) \ (\theta \in (0,1)), \ \alpha(t) := (1 - b(t)) b(t).$$

We start with a brief interpretation of this particular system, which could be suitable to model the interplay between prey and predator populations in which we take into account the following factors: ecological seasonal effects; the prey growth rate a attains its maximum value when the predator mortality rate b reaches its minimum and vice versa; the attack rate of predators λ is a convex combination of the prey growth and the predator mortality rates; and the hunting cooperation coefficient α vanishes when the mortality rate of predators attains its maximum or minimum.

For this particular system, condition (63) does not hold. Indeed, we can show that there are no constants $k > 0$ satisfying condition (64). For $t = 0$ and any $k > 0$, we obtain

$$a(0) = \sin^2 0 = 0 \neq \frac{k}{c} = k \frac{\cos^2 0}{c} = k \frac{b(0)}{c}.$$

So, condition (64) does not hold for $t = 0$ and, consequently, condition (63) is not fulfilled. Therefore, if

$$K > \frac{2}{m_3 \int_0^1 \lambda(s) ds} = \frac{4e(\sqrt{e}-1)}{c},$$

then the 1-periodic solution given by Corollary 3.3.3 is nonconstant.

3.3.2.3 *Positive nonconstant solutions*

Theorem 3.3.1 yields the existence of a continuous ω-periodic solution (x, y) such that

$$x(t) \geqslant q_1 \|x\|_\infty, \; y(t) \geqslant q_2 \|y\|_\infty, \text{ for all } t \in [0, \omega], \tag{66}$$

and $r \leqslant \|x\|_\infty + \|y\|_\infty \leqslant R$. In general, these conditions do not guarantee that x and y do not vanish. The following result shows that this is the case when (x, y) is not a steady state and system (31) is under uniqueness hypotheses.

Theorem 3.3.7. *Let us consider the Banach space* $\left(\mathcal{C}_\omega\left(\mathbb{R}, \mathbb{R}^2\right), \|\cdot\|_\omega\right)$ *and the cone* C *in Example 1.2.4, with* $q_1 = m1/M1$, $q2 = m2/M2$. *Assume that the functions* $\varphi(t, \cdot, \cdot) : \mathbb{R}_+ \times \mathbb{R}_+ \longrightarrow \mathbb{R}_+$ $(t \in \mathbb{R})$ *and* $g : \mathbb{R}_+ \longrightarrow \mathbb{R}$ *are locally Lipschitz. Then, for every nonconstant* ω*-periodic solution* $(x, y) \in C$ *of system* (31) *such that*

$$\|(x, y)\|_\omega = \|x\|_\infty + \|y\|_\infty > 0, \tag{67}$$

one has

$$x(t) > 0 \text{ and } y(t) > 0, \text{ for all } t \in [0, \omega].$$

Proof. First, note that the Lipschitz property over φ and g guarantees the uniqueness of the solution to any Cauchy problem associated to system (31).

Let $(x, y) \in C$ be a nonconstant ω-periodic solution of system (31) satisfying condition (67). As $(x, y) \in C$, it satisfies condition (66), therefore we just have to prove that $\|x\|_\infty > 0$ and $\|y\|_\infty > 0$.

Assume that $\|x\|_\infty = 0$. Then, from (67), one has $\|y\|_\infty > 0$, so there exists $t_0 \in [0, \omega]$ such that $y(t_0) > 0$. Also, since $\|x\|_\infty = 0$, i.e., $x \equiv 0$, the second equation in system (31) becomes

$$y'(t) = -b(t)y(t), \; t \in \mathbb{R},$$

and gives the following expression for y:

$$y(t) = y(t_0)e^{-\int_{t_0}^{t} b(s)ds}, \text{ for all } t \in \mathbb{R}.$$

Since y is periodic and for $y(t_0) \neq 0$ the function in the right-hand side is not periodic, the above equality yields a contradiction. Thus, $\|x\|_\infty > 0$.

Assume next that $\|y\|_\infty = 0$. Then the first equation in (31) reads as

$$x'(t) = a(t)x(t)g(x(t)), \; t \in \mathbb{R}. \tag{68}$$

We claim that

$$x(t)g(x(t)) \neq 0, \text{ for all } t \in \mathbb{R}. \tag{69}$$

To prove this, we start by showing that

$$x(t) > 0, \text{ for all } t \in \mathbb{R}.$$

Indeed, if there exists $t_0 \in \mathbb{R}$ such that $x(t_0) = 0$, then $(x, 0)$ is a solution of the Cauchy problem with the initial conditions $x(t_0) = y(t_0) = 0$. But $(0, 0)$ is also a solution of this Cauchy problem, and, by the uniqueness of solution, we must have $x \equiv 0$, which is excluded by our assumption (67). Hence $x(t) > 0$, for all $t \in \mathbb{R}$, as wished. Next, we prove that

$$g(x(t)) \neq 0, \text{ for all } t \in \mathbb{R}.$$

Indeed, assuming the contrary, there exists $t_1 \in \mathbb{R}$ such that $g(x(t_1)) = 0$. Then, as shown by statement 2 in Proposition 3.3.4, $(x(t_1), 0)$ is a steady state of system (31). Therefore, the steady state $(x(t_1), 0)$ and $(x, 0)$ solve the same Cauchy problem with the initial conditions $x(t_1) = x(t_1)$ and $y(t_1) = 0$. Again by the uniqueness of solution, one has $(x, 0) \equiv (x(t_1), 0)$, i.e., $(x, 0)$ is a constant solution of the system, which is excluded from the hypotheses. Thus, $g(x(t)) \neq 0$, for all $t \in \mathbb{R}$ and our claim is proved.

Now using (69), we can write equation (68) under the equivalent form

$$\frac{x'(t)}{x(t)g(x(t))} = a(t), \ t \in \mathbb{R},$$

which, by integration, gives

$$\int_0^t \frac{x'(s)}{x(s)g(x(s))} ds = \int_0^t a(s) ds, \ t \in \mathbb{R}. \tag{70}$$

Let $D := \{\tau \in \mathbb{R}_+ \setminus \{0\} : \ g(\tau) \neq 0\}$ and $G : D \longrightarrow \mathbb{R}$ be such that

$$G'(\tau) = \frac{1}{\tau\, g(\tau)}.$$

Then, from (70), we have

$$G(x(t)) = G(x(0)) + \int_0^t a(s) ds, \ t \in \mathbb{R}.$$

As x is periodic, $G(x)$ is also periodic, while the function at the right-hand side is not periodic, since $a \not\equiv 0$. This contradiction shows that $\|y\|_\infty > 0$, and the proof is finished. □

3.3.3 *Time independent predators functional response* φ

If we consider that the functional response does not depend on time, we can repeat the proof of Theorem 3.3.1 and improve the localization of periodic solutions. As a particular case, we can consider Lotka-Volterra autonomous systems, such as the classical model with linear or logistic prey growth, for which we show that the localized solution could be an steady state.

3.3.3.1 *Periodic coefficients*

In case that φ does not depend on t, then η and ψ do not depend on t either and we can obtain a better localization result.

Theorem 3.3.8. *Let us consider the Banach space* $\left(\mathcal{C}_\omega\left(\mathbb{R},\mathbb{R}^2\right),\|\cdot\|_\omega\right)$ *and the cone* C *in Example 1.2.4. Assume that* φ, η *and* ψ *in conditions* ***(G1)*** *and* ***(G2)*** *do not depend on* t. *If there exist* r, $R\in\mathbb{R}$, $0<r<R$, *such that condition* (33) *is satisfied and*

$$\overline{M}_1\,\overline{a}\,(1-g(r))+\overline{M}_3\,r\,\eta(r,r)\leqslant 2, \tag{71}$$

$$R\,\psi(R)\geqslant\frac{2}{\underline{m}_3}, \tag{72}$$

then system (31) *has an* ω*-periodic solution* $(x,y)\in C$ *such that*

$$r\leqslant\|(x,y)\|_\omega=\|x\|_\infty+\|y\|_\infty\leqslant R.$$

Proof. The proof is similar to that of Theorem 3.3.1, except *Case 3* and *Case III* in the proof of conditions (36) and (41), respectively. For instance, in the proof of hypothesis (36), we can replace the estimations in (38) by:

$$\begin{aligned}\|x\|_\infty&=x(t_0)<\lambda x(t_0)=N_1(x,y)(t_0)\\&=\int_{t_0}^{t_0+\omega}H_1(t_0,s)[a(s)\,x(s)(1-g(x(s)))+\varphi(x(s),y(s))\,x(s)\,y(s)]ds\\&\leqslant\overline{a}\|x\|_\infty(1-g(\|x\|_\infty))\overline{M}_1+\|x\|_\infty\|y\|_\infty\eta(\|x\|_\infty,\|y\|_\infty)\int_{t_0}^{t_0+\omega}H_1(t_0,s)ds\\&\leqslant\overline{a}\|x\|_\infty(1-g(\|x\|_\infty))\overline{M}_1+\|x\|_\infty\|y\|_\infty\eta(\|x\|_\infty,\|y\|_\infty)\overline{M}_1,\end{aligned}$$

which gives

$$1<\overline{a}\,(1-g(r))\,\overline{M}_1+\|y\|_\infty\,\eta(r,r)\,\overline{M}_1.$$

Similarly, instead of (40), we obtain

$$1<\|x\|_\infty\,\overline{c}\,\overline{M}_2\,\eta(r,r).$$

So, adding the two last inequalities, we find that

$$2<\overline{M}_1\,\overline{a}\,(1-g(r))+r\,\eta(r,r)\,\overline{M}_3,$$

which now contradicts our assumption (71).

The sufficiency of condition (72) to prove condition (41) can be shown in a similar way. □

Linear growth

For the linear growth of the prey population, when φ does not depend on t, we have the following result that improves Corollary 3.3.2.

Corollary 3.3.9. *Assume that* $g \equiv 1$ *and* φ, η, ψ *fulfill conditions* ***(G1)***, ***(G2)*** *without depending on* $t \in \mathbb{R}$. *If there exist* $r, R \in \mathbb{R}$, $0 < r < R$, *such that*

$$r\,\eta(r,r) \leqslant \frac{2}{\overline{M}_3},\ R\,\psi(R) \geqslant \frac{2}{\underline{m}_3},$$

then system (48) *has an* ω*-periodic solution* $(x,y) \in C$ *such that*

$$r \leqslant \|(x,y)\|_\omega = \|x\|_\infty + \|y\|_\infty \leqslant R.$$

Logistic growth

For the logistic growth of the prey population, when φ does not depend on t, we improve Corollary 3.3.3 as follows.

Corollary 3.3.10. *Assume that* $g(x) = 1 - x/K$ *and* φ, η, ψ *fulfill conditions* ***(G1)***, ***(G2)*** *and do not depend on* $t \in \mathbb{R}$. *If there exist* $r, R \in \mathbb{R}$, $0 < r < R$, *such that*

$$r \leqslant \frac{K}{\overline{a}\,\overline{M}_1},\ \frac{\overline{M}_1\,\overline{a}}{K}\,r + \overline{M}_3\,r\,\eta(r,r) \leqslant 2,$$

$$R\,\psi(R) \geqslant \frac{2}{\underline{m}_3},$$

then system (58) *has an* ω*-periodic solution* $(x,y) \in C$ *such that*

$$r \leqslant \|(x,y)\|_\omega = \|x\|_\infty + \|y\|_\infty \leqslant R.$$

3.3.3.2 *Constant coefficients: autonomous case*

Under the conditions required to φ in Subsection 3.3.3.1, we now assume that a, b and c are constant. Then

$$H_1(t,s) = \frac{e^{-a(s-t)}}{1-e^{-a\,\omega}},\ H_2(t,s) = \frac{e^{b(s-t)}}{e^{b\,\omega}-1}.$$

Moreover, for every $t \in \mathbb{R}$, one can compute

$$\overline{M}_1 = \underline{m}_1 = \int_t^{t+\omega} H_1(t,s)\,ds = \frac{1}{a},\ \overline{M}_2 = \underline{m}_2 = \int_t^{t+\omega} H_2(t,s)\,ds = \frac{1}{b};$$
$$M_1 = \frac{1}{1-e^{-a\omega}},\ m_1 = \frac{1}{e^{a\omega}-1},\ M_2 = \frac{1}{1-e^{-b\omega}},\ m_2 = \frac{1}{e^{b\omega}-1};$$
$$\underline{m}_3 = q_1 q_2 \min\left\{\frac{1}{a},\frac{c}{b}\right\} = \frac{1}{e^{a\omega}e^{b\omega}}\min\left\{\frac{1}{a},\frac{c}{b}\right\},\ \overline{M}_3 = \max\left\{\frac{1}{a},\frac{c}{b}\right\}.$$

As a direct consequence of Theorem 3.3.8, we have the following result, where the conditions over r, R look much simpler.

Corollary 3.3.11. *Let* a, b, c *be constant and* φ, η, ψ *in conditions* ***(G1)***, ***(G2)*** *do not depend on time. If there exist* r, $R \in \mathbb{R}$, $0 < r < R$, *such that*

$$g(r) \geqslant 0,\ r\eta(r,r) \max\left\{\frac{1}{a}, \frac{c}{b}\right\} - g(r) \leqslant 1, \tag{73}$$

$$R\psi(R) \geqslant \frac{2}{q_1 q_2 \min\left\{\frac{1}{a}, \frac{c}{b}\right\}},$$

then the system

$$\begin{cases} x' = axg(x) - \varphi(x,y)xy; \\ y' = -by + c\varphi(x,y)xy \end{cases} \tag{74}$$

has an ω*-periodic solution* $(x,y) \in C$ *such that*

$$r \leqslant \|(x,y)\|_\omega = \|x\|_\infty + \|y\|_\infty \leqslant R.$$

Linear growth

Notice that, in particular if $g \equiv 1$, condition (73) becomes

$$r\eta(r,r) \leqslant \frac{2}{\max\left\{\frac{1}{a}, \frac{c}{b}\right\}}$$

and we have the following remark about the classical predator-prey system.

Remark 7. For the particular expressions of $g \equiv 1$ and $\varphi \equiv \lambda > 0$, system (74) reduces to the classical Lotka-Volterra model (30). Then, one can consider η, $\psi = \varphi = \lambda$, and the conditions over r and R reduce to

$$r \leqslant \frac{2}{\max\left\{\frac{1}{a}, \frac{c}{b}\right\}\lambda} = 2\min\left\{a, \frac{b}{c}\right\}\frac{1}{\lambda};$$
$$R \geqslant \frac{2}{q_1 q_2 \min\left\{\frac{1}{a}, \frac{c}{b}\right\}\lambda} = 2\max\left\{a, \frac{b}{c}\right\}\frac{e^{a\omega}e^{b\omega}}{\lambda}.$$

It is easy to see that the non-trivial steady state $(x_*, y_*) := (b/(c\lambda), a/\lambda)$ satisfies

$$r \leqslant 2\min\left\{a, \frac{b}{c}\right\}\frac{1}{\lambda} \leqslant \|(x_*, y_*)\| = \left(\frac{b}{c} + a\right)\frac{1}{\lambda} \leqslant 2\max\left\{a, \frac{b}{c}\right\}\frac{1}{\lambda}$$
$$\leqslant 2\max\left\{a, \frac{b}{c}\right\}\frac{1}{q_1 q_2 \lambda} \leqslant R.$$

Therefore, it may happen that the localized solution given by Corollary 3.3.11 is in fact the steady state (x_*, y_*). Besides, in this particular case, we also observe the unfeasibility to localize multiple solutions.

Logistic growth

In case that $g(x) = 1 - x/K$, condition (73) becomes

$$r \leqslant K,\ \max\left\{\frac{1}{a}, \frac{c}{b}\right\} r\eta(r,r) + \frac{r}{K} \leqslant 2,$$

and we can make the following remark about the classical Lotka-Volterra model with logistic growth on the prey population.

Remark 8. For the particular expressions of $g(x) = 1 - x/K$ and $\varphi(x,y) = \lambda > 0$, system (74) reduces to the classical Lotka-Volterra model with logistic growth on prey

$$\begin{cases} x' = ax\left(1 - \frac{x}{K}\right) - \lambda xy; \\ y' = -by + c\lambda xy. \end{cases}$$

Then, one can consider η, $\psi = \varphi = \lambda$, and the conditions over r and R become

$$r \leqslant K,\ r \leqslant \frac{2}{\frac{1}{K} + \max\left\{\frac{1}{a}, \frac{c}{b}\right\}\lambda},$$

$$R \geqslant 2\max\left\{a, \frac{b}{c}\right\}\frac{1}{q_1 q_2 \lambda}. \tag{75}$$

If one has

$$K > 2\max\left\{a, \frac{b}{c}\right\}\frac{1}{q_1 q_2 \lambda},$$

then (75) holds for $R = 2\max\{a, b/c\}/\lambda < K$. Therefore, we are not localizing the steady state $(K, 0)$, but it may also happen that the localized solution given by Corollary 3.3.11 is in fact the steady state

$$(x^*, y^*) = \left(\frac{b}{c\lambda},\ \frac{a}{\lambda}\left(1 - \frac{b}{c\lambda K}\right)\right),$$

where x^*, $y^* > 0$.

3.4 DISCUSSION

In this section, we review the research work we have included in this chapter and compare it with that in some related studies. As usual, we use headlines to identify the different topics considered.

Contributions to the direct application of fixed point theorems to Lotka-Volterra models

In Section 3.1, we observe that the existence of periodic solutions to simple generalizations of Lotka-Volterra type systems has been studied by means of fixed point theory based on topological arguments. In our view, for applications, the use of topological techniques may complexify the details of the research development in comparison with the use of some classical restrictions in fixed point theory, i.e., those given directly in terms of the underlying mapping. Thus, we study the applicability of different versions of Krasnosel'skii fixed point theorem, whose hypotheses are directly expressed in terms of the non-linear operator, to the periodic predator-prey system (31).

In Subsection 3.3.1, we use the homotopy version to prove the existence of periodic solutions to this class of models. We follow a similar approach to that in (Lv, Lu, and Yan, 2010; Tang and Zou, 2006), where they show the applicability of the norm-type version to more complex predator-prey models including time-delays. However, we prove that both classical and norm-type versions do not apply for system (31). Moreover, for the particular case of the classical Lotka-Volterra system with periodic coefficients, we also show some problems with the applicability of the vector version, which had been used to deal with similar periodic systems (see Precup, 2007).

On the other hand, we improve the localization results in (Tsvetkov, 1996), where system (51) was studied by means of index theory. Besides, our approach holds for a more general formulation of Lotka-Volterra type systems.

First steps on the qualitative study of system (31)

Our main result allows to localize continuous and periodic solutions to the general system (31), which describes a periodic interplay between prey and predator populations. However, these periodic solutions could be in fact steady states, i.e, solutions that do not vary with time, as we showed for the autonomous case (see Subsection 3.3.3). Moreover, the localization domain does exclude the possibility of extinction for some of the species. Therefore, it is interesting to determine sufficient conditions that ensure the nonconstancy of the periodic solution and the positiveness of both populations. We develop this study in Subsection 3.3.2, where we can observe that the sufficient conditions depend on the expressions of the prey growth g and the predators functional response φ. Thus, we analyzed their viability for the linear and logistic prey growth and the expressions of φ_I, φ_{II}, which consider hunting cooperation between predators.

This is a preliminary study of the solutions properties, which lets the possibility to localize a limit cycle. A further step on the qualitative study of this class of models would be to determine the stability properties of the steady states and the localized periodic solution.

CONCLUSIONS AND FUTURE PROSPECTS I

In this research line, we have contributed to both the generalization and application of Krasnosel'skii type compression-expansion fixed point results. In our view, one of the most relevant aspects of our research are the approaches we used, since one of them allows to continue with the extension of the localization region provided by our fixed point results and the other fills a gap in the application of Krasnosel'skii type fixed point theorems to Lotka-Volterra population models. We devote the following lines to describe the research skills we have gained working on the objectives of this part of the thesis. Then, we give details about some ideas to continue with the investigation, which could potentially increase the interest of our work.

A. Conclusions

In Chapters 2 and 3 within Research Line I, we include the research we have developed in the framework of fixed point theory. The most relevant results we have obtained are summarized and compared with other present in the related literature at the end of each chapter. In this section, we complement this discussion by reviewing the learning process in which I got involved when I was working in goals G1 and G2.

I begin with Chapter 2, where we achieve objective G1. As we already mentioned, an important part of the research carried out to generalize Krasnosel'skii compression-expansion fixed point theorem to set contractions and star convex sets has been developed during my Master degree studies. For instance, it was during that period when my supervisor Rosana Rodríguez López proposed me the idea to adapt the results for balls owed by Các and Gatica (1979) and Potter (1974) to more general sets, which contain the rays connecting the points on its boundary to the origin. Thus, before the beginning of my PhD studies, I had developed this more general setting and proved the compression type result. In this way, I had acquired the capacity to analyze the proof of a result and to adapt it to a more general framework. We had also proved the expansion type result as a generalization of the work in (Các and Gatica, 1979), but the localization domain was not so precise. Moreover, the boundary value problem we had considered to illustrate the applicability of our results satisfied the hypotheses of some classical results, so we had not justified properly the necessity of our generalizations. It was during the PhD studies when we proved both compression and expansion results under the general hypotheses considered in this document. For the expansive case, professor Radu Precup suggested us to use a change of variable to reduce it to the compressive one. For both proofs, I needed to become familiar with the par-

ticular behavior of set contractions. Besides, regarding the applications of the obtained results, I worked for the first time with a noncompact mapping and perceived the relevance of defining the star convex sets by means of functionals.

The contents of Chapter 3 contribute to reach the goal G2 and were completely developed during the PhD studies. In this case, I reviewed some existing literature and decided to study predator-prey models including cooperation between predators by means of fixed point theory. Our main aim was to apply directly some Krasnosel'skii type results, since, in our view, this methodology is clearer and easier to reproduce than topological approaches that have been used to localize solutions of similar models. The main difficulties were to overcome the problems in the application of some popular versions of Krasnosel'skii fixed point theorem and also to find the appropriate result for our problem of interest. Moreover, I also learned how to discuss the possibility to localize multiple solutions. Finally, it is also interesting to comment that, to obtain some basic qualitative properties of periodic solutions, we combined the localization results with some knowledge acquired during my degree studies about ordinary differential equations.

B. Future prospects

In this section, we provide some ideas that we would like to develop as a continuation of the research carried out in this part of the thesis. It is worth mentioning that we have already started the research on the future prospect I, which is part of a joint work with my supervisor Rosana Rodríguez López.

i. generalization of krasnosel'skii compression-expansion fixed point theorem for set contractions to more general domains

Along this part of the thesis, we provided different reasons to consider new generalizations of Krasnosel'skii compression-expansion fixed point theorem, such as the higher applicability and the better localization they can provide. Moreover, in the Introductory section of Chapter 2, we also commented the advantages of using classical fixed point arguments rather than topological techniques, both in applications and to obtain theoretical extensions. In the latter case, we also consider that the classical approach exhibits the key points of the proofs in a clearer way, allowing to easily identify the generalization potential of the results.

We recall that we have obtained a generalization of the classical compression-expansion Theorem of Krasnosel'skii for set contractions which localizes the solutions in conical domains determined by star convex sets. A deeper analysis of the proofs reveals that their key points are the properties of set contractions and the shape of the localization domain. Moreover, we also observe that we are not taking advantage of all the possibilities offered by the set contractions,

and we claim that the obstacle to obtain better localization results comes from the peculiarities of the cone.

Therefore, to continue with the extension of these results, we decided to preserve the ideas in the proof for both compression and expansion cases, as well as the regularity of the mapping, but to construct a more general framework for the localization domains. We notice that, for applications, we must take care of the extension of the cone, since its characteristics are relevant to determine the properties of the localized solution.

Apart from the theoretical interest of this research idea, it would also be interesting to justify its potential in applications.

II. QUALITATIVE STUDY OF THE PERIODIC LOTKA-VOLTERRA SYSTEM WITH GENERAL PREY GROWTH AND PREDATORS FUNCTIONAL RESPONSE

In Section 3.1, we mentioned that the motivation to study the predator-prey system (31) came from the research developed in (Teixeira Alves and Hilker, 2017). However, we do not follow their methodology and, inspired by the work in (Tsvetkov, 1996), we decided to use an operator approach to localize periodic solutions.

Once we have proved the existence of periodic solutions, we also started to study some of their properties. We first determined sufficient conditions to ensure that the localized solutions do not reduce to steady states. Then, under uniqueness hypotheses, we also proved that the nonconstant periodic solutions are positive, so none of the species ends in extinction. In this way, we slightly contributed to the qualitative study of the nonautonomous system (31). However, there are still many interesting aspects of the dynamical behavior of the model which deserve to be studied. For instance, in Section 3.4, we proposed to study the stability of steady states and the localized periodic solution, which is interesting to understand the long-term behavior of the populations. To that purpose, as a beginner in this field, the first step would be a careful revision of the existing literature on the topic. Moreover, it can also be useful to consider the approach in (Faria and Oliveira, 2019), where they prove the global attraction of a periodic orbit for a nonautonomous model of hematopoiesis.

In the research developed in (Teixeira Alves and Hilker, 2017) for an autonomous model, after the stability study, they continue with an analysis of bifurcations, that is, they observe how the stability behavior of the system changes as a parameter is varied. It would also be interesting to develop a similar study for the more general nonautonomous Lotka-Volterra systems (31). There are plenty of research works devoted to the study of bifurcations in autonomous systems; however, the analogous research for nonautonomous differential equations seems to be under construction and it does not exist a whole theoretical framework in which we can base our research. In spite of that, we can start looking at the works in (Langa, Robinson, and Suárez, 2002;

Rasmussen, 2007), where two different generalizations of some bifurcation notions are developed for the nonautonomous case.

REFERENCES I

Anderson, D. R., R. I. Avery, and J. Henderson (2010). "Functional expansion-compression fixed point theorem of Leggett-Williams type." In: *Electronic Journal of Differential Equations* 2010:63, pp. 1–9.

Bacaër, N. (2011). "Lotka, Volterra and the predator-prey system (1920-1926)." In: *A short history of mathematical population dynamics*. Springer, pp. 71–76.

Berec, L. (2010). "Impacts of foraging facilitation among predators on predator-prey dynamics." In: *Bulletin of Mathematical Biology* 72:1, pp. 94–121.

Bolojan, O. and R. Precup (2014). "Implicit first order differential systems with nonlocal conditions." In: *Electronic Journal of Qualitative Theory of Differential Equations* 69, pp. 1–13.

Brauer, F. and C. Castillo Chávez (2001). *Mathematical models in population biology and epidemiology*. Texts in Applied Mathematics. New York: Springer.

Buffoni, G., M. Groppi, and C. Soresina (2011). "Effects of prey over-under-crowding in predator-prey systems with prey-dependent trophic functions." In: *Nonlinear Analysis: Real World Applications* 12:5, pp. 2871–2887.

Các, N. P. and J. A. Gatica (1979). "Fixed point theorems for mappings in ordered Banach spaces." In: *Journal of Mathematical Analysis and Applications* 71:2, pp. 547–557.

Darbo, G. (1955). "Punti uniti transformazioni a condominio non-compactto." In: *Rendiconti del Seminario Matematico della Università di Padova* 24, pp. 84–92.

Deimling, K. (1985). *Nonlinear functional analysis*. Berlin: Springer-Verlag.

Erbe, L. H. and H. Wang (1994). "On the existence of positive solutions of ordinary differential equations." In: *Proceedings of the American Mathematical Society* 120:3, pp. 743–748.

Faria, T. and J. J. Oliveira (2019). "A note on global attractivity of the periodic solution for a model of hematopoiesis." In: *Applied Mathematics Letters* 94, doi: 10.1016/j.aml.2019.02.009.

Granas, A. and J. Dugundji (2013). *Fixed Point Theory*. Springer Monographs in Mathematics. New York: Springer-Verlag.

Güo, D. and V. Lakshmikantham (1998). *Nonlinear problems in abstract cones*. Vol. 5. Notes and Reports in Mathematics in Science and Engineering. California: Academic Press.

Krasnosel'skii, M. A. (1960). "Fixed points of cone-compressing and cone-expanding operators." In: *Soviet Mathematics Doklady* 1, pp. 1285–1288.

— (1964). *Positive solutions of operator equations*. Netherlands: P. Noordhoff Ltd.

Kwong, M. K. (2008). "On Krasnoselskii's cone fixed point theorem." In: *Fixed Point Theory and Applications* 2008, doi: 10.1155/2008/164537.

Langa, J. A., J. C. Robinson, and A. Suárez (2002). "Stability, instability, and bifurcation phenomena in non-autonomous differential equations." In: *Nonlinearity* 15:3, pp. 1–7.

Lois-Prados, C. and R. Precup (2020). "Positive periodic solutions for Lotka-Volterra systems with a general attack rate." In: *Nonlinear Analysis: Real World Applications* 52, doi: 10.1016/j.nonrwa.2019.103024.

Lois-Prados, C., R. Precup, and R. Rodríguez-López (2020). "Krasnosel'skii type compression-expansion fixed point theorem for set contractions and star convex sets." In: *Journal of Fixed Point Theory and Applications* 22:3, doi: 10.1007/s11784–020–00799–0.

Lois-Prados, C. and R. Rodríguez-López (2020). "A generalization of Krasnosel'skii compression fixed point theorem by using star convex sets." In: *Proceedings of the Royal Society of Edinburgh , Section A: Mathematics* 150:1, pp. 277–303.

Lotka, A. J. (1925). *Elements of Physical Biology*. Baltimore: Williams and Wilkins.

Lv, X., S. Lu, and P. Yan (2010). "Existence and global attractivity of positive periodic solutions of Lotka-Volterra predator-prey systems with deviating arguments." In: *Nonlinear Analysis: Real World Applications* 11:1, pp. 574–583.

O'Regan, D. and R. Precup (2001). *Theorem of Leray-Schauder type and its applications*. Singapore: Gordon and Breach.

— (2005). "Compression-expansion fixed point theorem in two norms and applications." In: *Journal of Mathematical Analysis and Applications* 309:2, pp. 383–391.

Potter, A. J. B. (1974). "A fixed point theorem for positive k-set contractions." In: *Proceedings of the Edinburgh Mathematical Society* 19:1, pp. 93–102.

Precup, R. (2002). *Methods in nonlinear integral equations*. Netherlands: Springer.

— (2006). "Positive solutions of semi-linear elliptic problems via Krasnosel'skii type theorems in cones and Harnack's inequalities." In: *AIP Conference Proceedings* 835, pp. 125–132.

— (2007). "A vector version of Krasnosel'skii fixed point theorem in cones and positive periodic solutions of nonlinear systems." In: *Journal of Fixed Point Theory and Applications* 2, pp. 141–151.

Rasmussen, M. (2007). "Nonautonomous bifurcation patterns for one-dimensional differential equations." In: *Journal of Differential Equations* 234:1, pp. 267–288.

Rosenzweig, M. L. and R. H. MacArthur (1963). "Graphical representation and stability conditions of predator-prey interactions." In: *The American Naturalist* 97:895, pp. 209–223.

Tang, X. and X. Zou (2006). "On positive periodic solutions of Lotka-Volterra competition systems with deviating arguments." In: *Proceedings of the American Mathematical Society* 134:10, pp. 2967–2974.

Teixeira Alves, M. and F. M. Hilker (2017). "Hunting cooperation and Allee effects in predators." In: *Journal of Theoretical Biology* 419, pp. 13–22.

Torres, P. J. (2003). "Existence of one-signed periodic solutions of second-order differential equations via a Krasnosel'skii fixed point theorem." In: *Journal of Differential Equations* 190:2, pp. 643–662.
Tsvetkov, D. (1996). "A periodic Lotka-Volterra system." In: *Serdica Mathematical Journal* 22:2, pp. 109–116.
Van der Hoff, Q. and T. H. Fay (2016). "A predator-prey model with predator population saturation." In: *Mathematics and Statistics* 4:4, pp. 101–107.
Volterra, V. (1926). "Variazioni e fluttazioni del numero d'individui in specie animali conviventi." In: *Memoria della Reale Accademia Nazionale dei Lincei* 2, pp. 31–113.
Wang, H. (2011). "Positive periodic solutions of singular systems of first order ordinary differential equations." In: *Applied Mathematics and Computation* 218:5, pp. 1605–1610.
Zanolin, F. (1992). "Permanence and positive periodic solutions for Kolmogorov competing species systems." In: *Results in Mathematics* 21, pp. 224–250.
Zima, M. (2004). "Fixed point theorem of Legget-Williams type and its applications." In: *Journal of Mathematical Analysis and Applications* 299:1, pp. 254–260.

USC
UNIVERSIDADE
DE SANTIAGO
DE COMPOSTELA

Part II

RESEARCH LINE II

USC
UNIVERSIDADE
DE SANTIAGO
DE COMPOSTELA

4 BACKGROUND DEFINITIONS AND RESULTS II

For the sake of completeness, we devote this chapter to fix some notions on single-species population models and the qualitative theory of one-dimensional difference equations used throughout this part of the monograph.

In Section 4.1, we start describing different prototypes of population models and the conditions they satisfy. These models are given by discrete-time one-dimensional dynamical systems, so we devote the remainder sections to state some useful notions and results in this framework. For that purpose, we consider an interval $J \subseteq \mathbb{R}$, a general map $h : J \longrightarrow J$ and the related one-dimensional difference equation

$$x_{n+1} = h(x_n), \quad n \in \mathbb{N} \cup \{0\}, \, x_0 \in J. \tag{76}$$

If $h \in \mathcal{C}^r$ with $r \geqslant 1$, we say that h is a *smooth map* and equation (76) is a *smooth dynamical system*. Some classical references on the qualitative theory of this type of one-dimensional difference equations are (Devaney, 1989) and (Wiggins, 1990).

If $h \notin \mathcal{C}^1$ but there exist a finite number $m \in \mathbb{N}$ of points $d_j \in J$ for all $j \in \{1, \ldots, m\}$, such that $h|_{(d_j, d_{j+1})} \in \mathcal{C}^1$ for all $j \in \{0, \ldots, m\}$ ($d_0 = -\infty$ or $d_0 = \inf\{x : x \in J\}$, $d_{m+1} = \infty$ or $d_{m+1} = \sup\{x : x \in J\}$), then we say that h is a *piecewise-smooth map* and equation (76) is a *piecewise-smooth dynamical system*. In particular, if h is continuous, then the dynamical system is *piecewise-smooth continuous*, otherwise it is *piecewise-smooth discontinuous*. Some recent books on the qualitative theory of this type of systems are (Bernardo et al., 2008) for piecewise-smooth continuous models and (Avrutin et al., 2019) for the discontinuous ones.

Our main aim is to describe the asymptotic dynamics of system (76), so given an initial condition $x_0 \in J$, we are interested in determining the long-term behavior of the sequence $\{x_n\}_{n\in\mathbb{N}} = \{h(x_{n-1})\}_{n\in\mathbb{N}} = \{h^n(x_0)\}_{n\in\mathbb{N}}$, where $h^0 \equiv id$ and $h^n \equiv h \circ h^{n-1}$ for all $n \in \mathbb{N}$. In Sections 4.2-4.4 we state some notions and results useful for carrying out a qualitative study of its asymptotic dynamics. In Section 4.2, we review some stability concepts (see (Avrutin et al., 2019, Chapter 1) and (Liz and Lois-Prados, 2020b, Subsection III C), for further reference): critical point and absorbing interval; repelling set, attracting set, attractor and basin of attraction; unstable, stable, locally or globally asymptotically stable, semi-stable fixed point and essential (global) attractor. A discussion of essential asymptotic stability (Melbourne, 1991) can be found in (Podvigina and Ashwin, 2011). After that, we state some results useful to ensure the convergence of all initial conditions to the same point, that is, global stability. In Section 4.3, we describe the bifurcations and related terminology. We will consider map

definitions which depend on one or several parameters, and the notion of *bifurcation* is associated with a qualitative change on the asymptotic dynamics of the related systems under infinitesimal variation of those parameters. Finally, Section 4.4 is devoted to interesting features which appear in 1-parameter bifurcation diagrams, such as long-transients and hysteresis; bubbles and hydra effect; extinction windows and sudden collapses; periodic windows, star-like intersections and effectively chaotic behavior. *Bifurcation diagrams* (BDs) are representations of long-term dynamics and bifurcations of a system with respect to variation of parameters. We use two types of BD:

- 2-*parameter BD*, where we plot the different bifurcation curves as functions of two parameters of the system and we identify regions in which qualitative dynamics do not vary. Bifurcation curves are obtained from analytic expressions (often implicit) and are represented using the software Mathematica.

- 1-*parameter BD*, where we plot long-term population sizes with respect to a unique parameter. They are numerically obtained in the usual way: for a given function h, we fix all parameter values but one; then for each value of that parameter a random initial condition x_0 from a suitable interval is selected, and a number $M \in \mathbb{N}$ of iterations by h are computed. To capture the asymptotic dynamics, we remove the first $M^* < M$ iterations and plot the rest of the data. We use blue points/curves to represent asymptotic population sizes.

It is worth mentioning that the notions related to fixed points in Sections 4.2 and 4.3 can be extended to any m-cycle ($m \in \mathbb{N}$, $m \geqslant 2$), since it is a fixed point of the map h^m.

4.1 TYPICAL CONDITIONS FOR SINGLE-SPECIES POPULATION MODELS

In population dynamics, particularly in the context of fisheries, the mathematical modeling of the regenerative process of a population is of fundamental importance. In (Quinn and Deriso, 1999, Chapter 3), there is a list of processes described by a *spawner-recruit* or *stock-recruit* relation $R = f(S)$ which establishes the recruits R that are produced by the spawning stock S in each time cycle (Liz, 2018a). Thus, these type of regenerative processes are described by a one-dimensional difference equation

$$x_{n+1} = f(x_n), \tag{77}$$

where x_n denotes the population size at the n-th generation ($n = 0, 1, 2, \ldots$) and the function $f : [0, \infty) \longrightarrow [0, \infty)$ is the *production* or *stock-recruitment curve*. In (Liz, 2010a), it is mentioned that these models are usually applied to *semelparous populations* in which the adult population x_n dies during spawning and is replaced by the subsequent cohort of recruits $x_{n+1} = f(x_n)$. If a fraction of the

adult population survives the reproductive season, they refer to it as *iteroparous population* and consider the equation

$$x_{n+1} = (1-\sigma)x_n + f(x_n), \tag{78}$$

where $\sigma \in [0,1]$. They notice that the case $\sigma = 1$ corresponds to equation (77) and they interpret the term $1-\sigma$ as the adult's probability of surviving one generation including the reproductive season.

To carry out our theoretical study, we assume some typical conditions for the stock-recruitment map f:

(A1) $f : [0,\infty) \to [0,\infty)$ is continuous, has a unique positive fixed point K, $f(x) > x$ for $x \in (0,K)$, and $0 < f(x) < x$ for $x > K$. Moreover, $f(0) = 0$ and there exists $\lim_{x\to\infty} f(x) < \infty$.

Most of the results will require additional conditions, which are summarized in the next hypothesis:

(A2) f is a $\mathcal{C}^2$ map with at most one critical point $x_c \in (0,\infty)$ such that $f'(x) > 0$ for all $x \in (0,x_c)$, and $f'(x) < 0$ for all $x > x_c$. Moreover, $f''(x) < 0$ on $(0,x_c)$. If f has no critical points, then we consider $x_c = \infty$ and f strictly increasing and concave. If f has one critical point, we assume that $\lim_{x\to\infty} f(x) = 0$.

We understand that a model defined by (77) or (78) is *compensatory* if f satisfies **(A1)-(A2)** with $x_c \geqslant K$ (that is, f is nondecreasing at the positive equilibrium), and *overcompensatory* otherwise.

It is worth mentioning that a direct consequence of conditions **(A1)-(A2)** is the existence of a unique $\tilde{x} \in (0,x_c) \cap (0,K)$ such that $f'(\tilde{x}) = 1$. This property is derived from the Mean Value Theorem and the concavity of f in $(0,x_c)$.

Sometimes, we will also assume that f is a $\mathcal{C}^3$ map with negative Schwarzian derivative. We recall that the *Schwarzian derivative* is defined by the expression

$$(Sf)(x) = \left(\frac{f'''(x)}{f'(x)}\right) - \frac{3}{2}\left(\frac{f''(x)}{f'(x)}\right)^2, \tag{79}$$

whenever $f'(x) \neq 0$. When **(A2)** holds with finite x_c, the map f is *unimodal*; if, in addition, $(Sf)(x) < 0$ for all $x \neq x_c$, then f is an *S-unimodal map* (Thunberg, 2001). The concavity condition on $(0,x_c)$ is not usually assumed, but it is not very restrictive and for S-unimodal maps $f''(0^+) < 0$ implies $f''(x) < 0$ for all $x \in (0,x_c)$ (Liz and Franco, 2010).

Some prominent models in the context of fisheries satisfy these conditions (see Figure 7). We next provide a few examples which appear throughout this part of the thesis.

Example 4.1.1. We first consider the *Beverton-Holt model* (Beverton and Holt, 1957)

$$z_{n+1} = \frac{r\,z_n}{1+a\,z_n},$$

where $r,\ a \in (0,\infty)$ and z_n denotes the population size at time step n, for all $n = 0,1,2,\ldots$ Applying the change of variable $x_n = az_n$, we get the difference equation:

$$x_{n+1} = \frac{r\,x_n}{1+x_n}. \tag{80}$$

Thus, we consider the Beverton-Holt model defined by $f(x) = r\,x/(1+x)$, which fulfills conditions **(A1)-(A2)** if, and only if $r > 1$, with $K = r-1$, $x_c = \infty$ and $\lim_{x\to\infty} f(x) = r$, that is, f is strictly increasing and the model is compensatory.

Example 4.1.2. Another typical stock-recruitment process is the *Ricker model* (Ricker, 1954)

$$x_{n+1} = x_n\, e^{r\,(1-x_n)}, \tag{81}$$

where $r > 0$. The associated production map $f(x) = x\, e^{r\,(1-x)}$ satisfies conditions **(A1)-(A2)** with $K = 1$ and $x_c = 1/r$. Thus, it is compensatory if $0 < r \leqslant 1$ and overcompensatory if $r > 1$. Moreover, the Ricker map is S-unimodal.

Following a convention set by Ricker in (Ricker, 1975), by substituting e^r by $\beta > 0$, we get other frequently used form of the spawner-recruitment Ricker model (81), that is,

$$x_{n+1} = \beta\, x_n\, e^{-r\,x_n}. \tag{82}$$

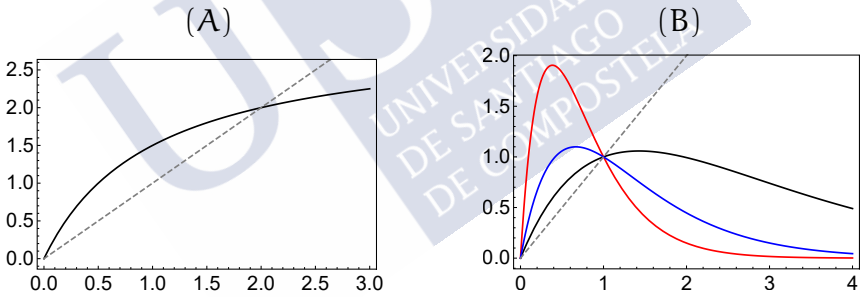

Figure 7: Illustration of the graph of the stock-recruitment map f. We also plot the line $y = x$ (gray, dashed). (A): Beverton-Holt map $f(x) = 3x/(1+x)$. (B): Ricker map $f(x) = xe^{r(1-x)}$; in black $r = 0.7$ (compensatory); in blue $r = 1.5$ (overcompensatory), in red $r = 2.6$ (overcompensatory).

The stock-recruitment function of both Beverton-Holt and Ricker models involve a number of parameters that usually have a biological meaning (Quinn and Deriso, 1999). The parameters offer some flexibility to find a suitable model that fits well the available population data, but it has been argued that models with two parameters are relatively inflexible (Liz, 2018a). In (Quinn and Deriso, 1999), we find some three-parameter generalizations of (80) and (82). In the case of the Ricker model, the generalized stock-recruitment difference equation, to which we will refer as *gamma-Ricker model*, has the form

$$x_{n+1} = \beta\, x_n{}^{\gamma}\, e^{-r\,x_n}, \tag{83}$$

where $\gamma > 0$. Notice that for $\gamma = 1$, $\beta > 0$ we get the Ricker model given by (82). Some properties of the associated map $f(x) = \beta\, x^{\gamma}\, e^{-r\,x}$ have been recently studied in (Liz, 2018a). By using Propositions 1 and 2 therein we can assert that, for $\gamma \in (0, 1)$, the gamma-Ricker map satisfies conditions **(A1)-(A2)** with $x_c = \gamma/r$ and $Sf(x) < 0$ for all $x > x_c$, but the map is not necessarily S-unimodal. We can also justify the larger flexibility of the model with respect to the Ricker map, since for $\gamma = 1, \beta \leqslant 1$ the gamma-Ricker map has no positive fixed points ($f(x) < x$ for all $x > 0$); and for $\gamma > 1$ the map can have two, one or no positive fixed points. We illustrate some configurations of the model in Figure 8, which is a reproduction of (Liz, 2018a, Figure 1).

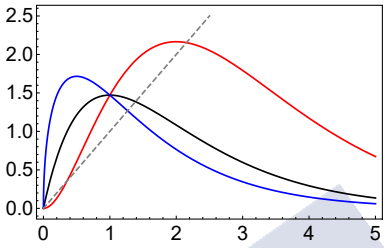

Figure 8: Illustration of the graph of the gamma-Ricker map (83) for $r = 1$, $\beta = 4$ and different values of γ: in black $\gamma = 1$ (f is the S-unimodal Ricker model (82)); in blue $\gamma = 0.5 < 1$ (f is not S-unimodal but satisfies **(A1)-(A2)**); in red $\gamma = 2 > 1$ (f has 3 fixed points). We also plot $y = x$ (gray, dashed).

4.2 STABILITY CONCEPTS AND RESULTS

We begin this section by stating some basic concepts of points and sets which play a crucial role in the study of asymptotic dynamics of the one-dimensional difference-equation (76). Then we state some results which allow to prove the most desirable long-term behavior of the population, that is, the convergence of (almost) all initial population sizes $x_0 \in J$ to an equilibrium of the map h. To illustrate their applicability, we use the model prototypes described in Examples 4.1.1 and 4.1.2.

Definition 4.2.1. A *critical point* c is a local extremum associated with the continuous branches of h or a limiting value of the function h at the discontinuity points.

An interval $E \subset J$ is *absorbing* if $h(E) \subseteq E$ (either E is invariant, $h(E) = E$; or it is strictly mapped into itself, $h(E) \subsetneq E$); there exists a neighborhood $\mathcal{U}$ of E such that any point in $\mathcal{U}$ is mapped inside E in a finite number of iterations; and E is bounded by two different critical points, or a critical point and its image.

From the definition of absorbing interval, we see that the critical points are relevant in the investigation of the asymptotic behavior, since the study of bounded orbits dynamics can be restricted to absorbing intervals confined by critical points and their images.

Definition 4.2.2. A closed invariant set R is called *repelling* if there exists a neighborhood $\mathcal{U}$ of R such that every point in $\mathcal{U}\backslash R$ is mapped outside $\mathcal{U}$ in a finite number of iterations.

An *attracting set* $A \subset J$ is a closed invariant set for which there exists a neighborhood $\mathcal{U}$ of A such that $h(\mathcal{U}) \subset \mathcal{U}$ and $\cap_{i=0}^{\infty} h^i(\mathcal{U}) = A$. An *attractor* $\mathcal{A}$ is an attracting set with a dense orbit.

The *basin of attraction* of an attractor $\mathcal{A}$ is the set of all points converging to $\mathcal{A}$, that is, the points $x \in J$ such that $\lim_{n\to\infty} h^n(x) \in \mathcal{A}$.

According to (Avrutin et al., 2019, Section 1.4), discontinuous one-dimensional maps can have four types of attractors: k-cycles and k-band chaotic attractors, $k \geqslant 1$; and two other types of attractors associated with quasi-periodic orbits. In general, we use the notation *oscillatory attractor* for those attractors which are not fixed points of the map h.

For a *fixed point* $x^* \in J$, defined by $h(x^*) = x^*$, we use some additional notions.

Definition 4.2.3. A repelling fixed point is also called *unstable*.

The fixed point x^* is *stable* if for every neighborhood $\mathcal{V}$ of x^*, there exists another neighborhood $\mathcal{U}$ of x^* such that $h^n(x) \in \mathcal{V}$ for all $x \in \mathcal{U}$, $n \geqslant 1$. We say x^* is *locally asymptotically stable* (LAS) if it is stable and an attractor. If x^* is an attractor with $\mathcal{U} = J$, we say that x^* is a *global attractor*. If a global attractor is stable, then we refer to it as *globally asymptotically stable* (GAS).

We use the term *stabilizing* when an unstable fixed point becomes LAS under variation of a parameter; and *destabilizing* when a stable equilibrium loses its stability as a parameter is changed.

If x^* is not an attractor, but $\lim_{n\to\infty} h^n(x) = x^*$ for all $x \in [x^*, x^* + \varepsilon)$ or $x \in (x^* - \varepsilon, x^*]$ and some $\varepsilon > 0$, then we say x^* is *semi-stable*.

If x^* is not an attractor but $\lim_{n\to\infty} h^n(x) = x^*$ for Lebesgue almost every x in a neighborhood $\mathcal{U}$ of x^*, we say that x^* is an *essential attractor*. If $\mathcal{U} = J$, then we call x^* an *essential global attractor*. In the context of population dynamics, when the fixed point is $x^* = 0$, then we refer to this phenomena as *essential extinction*.

Throughout this monograph, the first step on the study of asymptotic dynamics is to find parameter restrictions which ensure the existence of positive fixed points x^* of the one-dimensional map h, which is usually an easy task. Then, we study the stability of the equilibrium points which are located at the smooth branches of the map h by means of the value $h'(x^*)$. It is also straightforward, specially in the hyperbolic case, that is, when $|h'(x^*)| \neq 1$. For fixed points which are locally asymptotically stable, it is natural to study their global stability. Although the statement "LAS implies GAS" is not generally true, it holds when the map h satisfies some additional conditions. In the work by Coppel (1955), we find a simple condition which ensures the global stability of an equilibrium for continuous maps defined on bounded intervals. If the interval is bounded or unbounded, we have to require some additional conditions (Franco, Perán, and Segura, 2020):

Lemma 4.2.1. *If the map h related to the difference equation (76) is continuous in J, then a fixed point x^* is GAS if and only if $h^2(x) \neq x$ for all $x \in J\backslash\{x^*\}$ and x^* is stable for the dynamical system associated to h^n, for some $n \in \mathbb{N}$.*

In general, it is difficult to ensure analytically the absence of 2-cycles, but based on numerical simulations we can use the result to conjecture GAS. In the literature we can find several papers devoted to find conditions on the map h that are easier to check, an example is the following simple result which works for continuous maps and is a generalization of (Braverman and Liz, 2012) stated in (Liz and Lois-Prados, 2020a):

Lemma 4.2.2. *If the map h related to the one-dimensional discrete-time difference equation (76) is continuous on $J = (a, b)$ $(-\infty \leqslant a < b \leqslant \infty)$ and has a unique fixed point x^* such that*

1. *$x < h(x) < x^*$ for all $x \in (a, x^*)$;*
2. *$a < h(x) < x$ for all $x \in (x^*, b)$;*

then x^* is GAS on J.

This result ensures the global asymptotic stability of the unique positive fixed point for compensatory models, in particular, we obtain the following result.

Corollary 4.2.4. *Let us consider the Beverton-Holt model given by (80) and the Ricker model given by (81) with $0 < r \leqslant 1$, then the positive fixed point K ($K \leqslant x_c$) is GAS.*

Other results in this line make use of Lemma 4.2.1 in their proof, this is the case of the following result by Cull and Chaffee (2000) (see also (Cull, 2007)).

Lemma 4.2.3. *Let $\phi : [0, \infty) \longrightarrow [0, \infty)$ be a decreasing function which is positive on $(0, 1)$ and so that $\phi^2(x) = x$ for all $x \in [0, \infty)$. If the map h related to the difference equation (76) is continuous on $J = [0, \infty)$, has a positive fixed point x^* and*

1. *$\phi(x) > h(x)$ on $(0, x^*)$;*
2. *$\phi(x) < h(x)$ on $(x^*, 1)$;*
3. *$h(x) > x$ on $(0, x^*)$;*
4. *$h(x) < x$ on (x^*, ∞);*
5. *$h(x) > 0$ on $(0, \infty)$;*

then x^* is GAS on $(0, \infty)$.

This result applies for compensatory and overcompensatory models, in particular for those with $f'(x) \geqslant -1$ for all $x \in [0, \infty)$ and at most one point in $[0, \infty)$ such that $f'(x) = -1$. We illustrate it with the Ricker model given by (81).

Corollary 4.2.5. *Let us consider the Ricker model given by (81). If $0 < r \leqslant 2$, then $f'(x) \geqslant -1$ for all $x > 0$. Moreover, $f'(x) = -1$ if and only if $r = 2$ and $x = K = 1$. In particular, if $0 < r \leqslant 2$, then the positive equilibrium $K = 1$ is GAS in $(0, \infty)$. While, if $r > 2$, then $K = 1$ is unstable.*

Proof. Let us consider $r > 0$ and $x > 0$, since

$$f'(x) = (1 - rx)e^{r(1-x)} \text{ and } f''(x) = -r(2 - rx)e^{r(1-x)},$$

it follows that $f''(x) < 0$ for all $x \in (0, 2/r)$, $f''(2/r) = 0$ and $f''(x) > 0$ for all $x > 2/r$. Hence, f' attains its global minimum at $2/r$ with $f'(2/r) = -e^{r-2}$. Therefore, $f'(x) < -1$ if and only if $r > 2$ and $f'(x) = -1$ if and only if $r = 2$, $x = 1$.

Now, we assume $0 < r \leqslant 2$. The global attraction of the positive fixed point $K = 1$ follows from Lemma 4.2.3 with $\phi(x) = 2K - x = 2 - x$ and $h(x) = f(x)$ for all $x \in (0, \infty)$; $l = 2$ and $x^* = K = 1$. Let us prove that the required conditions are fulfilled (see Figure 9).

First we have $\phi^2(x) = 2 - (2 - x) = x$ and it is well-known that the Ricker map f satisfies conditions 3-5.

It remains to prove that ϕ and f fulfill conditions 1,2. On the one hand, since $\phi(0) = 2 > f(0) = 0$, $\phi(1) = f(1) = 1$, $\phi'(x) = -1$ for all $x > 0$ and $f'(x) < -1$ for all $x > 0$, $x \neq 1$; then $f(x) < \phi(x)$ for all $x \in (0, K) = (0, 1)$. On the other hand, since $\phi(1) = f(1) = 1$, $\phi'(x) = -1$ and $f'(x) \geqslant -1$ for all $x > 0$ ($f'(x) = -1$ if and only if $r = 2$, $x = 1$), then $f(x) > \phi(x)$ for all $x > K = 1$.

Finally, if $r > 2$, then we have $f'(K) = f'(1) = (1 - r) < -1$, so the equilibrium is unstable. □

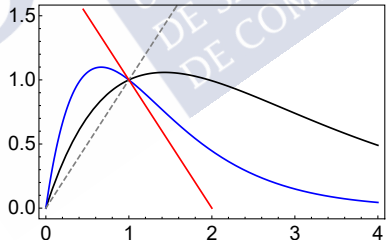

Figure 9: Diagram showing the Ricker map $f(x) = xe^{r(1-x)}$, $r \leqslant 2$ (compensatory, $r = 0.7 \in (0, 1]$ in black; overcompensatory, $r = 1.5 \in (1, 2]$ in blue) enveloped by $\phi(x) = 2 - x$ (red line). We also plot $y = x$ (gray, dashed).

Notice that we have obtained *sharp global stability* for the Ricker map, that is, we proved that the positive equilibrium is GAS for all the values of the parameter $r > 0$ for which the fixed point is LAS.

The next result provides a simple criterion to compare global stability of two continuous maps (see (El-Morshedy and Jiménez López, 2008, Theorem B)).

Lemma 4.2.4. *Assume that the continuous map h related to the difference equation (76) has a GAS equilibrium x^* in $J = (0, \infty)$, and let $H : (0, \infty) \longrightarrow (0, \infty)$ be a continuous map satisfying*

1. $x < H(x) \leqslant \max\{h(x), x^*\}$, *for all* $x \in (0, x^*)$;
2. $x > H(x) \geqslant \min\{h(x), x^*\}$, *for all* $x \in (x^*, \infty)$;

then x^* *is a GAS fixed point of* $x_{n+1} = H(x_n)$.

For smooth maps $h \in \mathcal{C}^3$, a typical condition required in the global stability results is the negative sign of the Schwarzian derivative. This term was first formulated in 1869 by Hermann A. Schwarz in his work on conformal mappings, but it was not until the work by Singer (1978) that it was introduced in the study of one-dimensional dynamical systems. The following result follows from Theorem 2.7 and *Addendum* in (Singer, 1978).

Lemma 4.2.5. *Let the map* $h : [0, \infty) \longrightarrow [0, \infty)$ *related to the one-dimensional difference equation* (76) *be S-unimodal, then the positive fixed point* $x^* = K$ *is GAS in* $(0, \infty)$ *if and only if* $h'(K) \geqslant -1$.

By using that the Ricker map is S-unimodal and the conditions proved in Corollary 4.2.5 for its derivative when $0 < r \leqslant 2$, we can also apply Lemma 4.2.5 to prove the sharp global stability of the Ricker model.

A generalization of Lemma 4.2.5 is given in (El-Morshedy and Jiménez López, 2008), where the condition on the negative Schwarzian derivative is restricted to a suitable subinterval of J.

Lemma 4.2.6. *Let the map* h *related to the one-dimensional discrete-time difference equation* (76) *be continuous in a closed interval* J *and have a unique fixed point* $x^* \in J$, *such that* $h(x) > x$ *for all* $x \in J$, $x < x^*$ *and* $h(x) < x$ *for all* $x \in J$, $x > x^*$. *Assume that there exist* $c, d \in J$, $c < x^* < d$ *such that:*

1. $h|_{(c,d)}$ *has at most one critical point;*
2. $h(x) \leqslant h(c)$ *for all* $x \in J$, $x \leqslant c$;
3. $h(x) \geqslant h(d)$ *for all* $x \in J$, $x \geqslant d$.

If h *is decreasing at* x^*, $-1 \leqslant h'(x^*) < 0$ *and* $(Sh)(x) < 0$ *for all* $x \in (c, d)$ *except for at most one critical point of* h; *then* x^* *is GAS in* J.

For the remainder of this section, assume that $0 < \sigma < 1$ and let the map h related to the one-dimensional discrete-time difference equation (76) be a $\mathcal{C}^3$ function on $J = [0, \infty)$ given by $h(x) = (1 - \sigma)x + f(x)$. For general S-unimodal maps f, the corresponding map h does not necessarily inherit all the properties of f, this is the case of the condition on the Schwarzian derivative (see (Liz and Franco, 2010) for details). Thus, the previous results cannot be directly applied to the system (78). This gap on the literature was filled by Liz and Franco (2010, Theorem 1) and the next result from (Liz and Lois-Prados, 2020a) is a generalization.

Lemma 4.2.7. *Assume that* $0 < \sigma < 1$ *and* $f : [0, \infty) \longrightarrow [0, \infty)$ *satisfy the following conditions:*

1. $f_\sigma(x) = (1/\sigma)f(x)$ *has a unique positive fixed point* $x^* > 0$, $f_\sigma(0) = 0$ *and* $\lim_{x\to 0^+} f'_\sigma(x) > 1$ *(it can be* ∞*);*
2. f *has a unique critical point* x_c*; moreover,* $f'(x) > 0$ *for all* $x \in (0, x_c)$ *and* $f'(x) < 0$ *for all* $x > x_c$*;*
3. $f''(x) < 0$ *for all* $x \in (0, x_c)$*;*
4. $(Sf)(x) < 0$ *for all* $x > x_c$*.*

Then the unique positive equilibrium x^* *of equation* (78) *is GAS in* $(0, \infty)$ *if and only if*

$$h'(x^*) = (1-\sigma) + f'(x^*) \geqslant -1. \tag{84}$$

Moreover, if condition (84) *does not hold, then* x^* *is unstable.*

Proof. Equation (78) can be written in the form of equation (4) in (Liz and Franco, 2010), that is:

$$x_{n+1} = \alpha x_n + (1-\alpha) f_\sigma(x_n),$$

with $\alpha = 1 - \sigma$ and $f_\sigma(x) = (1/\sigma)f(x)$.

It is clear that conditions 2-4 hold for f_σ because

$$f'_\sigma(x) = (1/\sigma)f'(x),\ f''_\sigma(x) = (1/\sigma)f''_\sigma(x), \text{ and } (Sf_\sigma)(x) = (Sf)(x).$$

There are two relevant differences with respect to Theorem 1 in (Liz and Franco, 2010). On the one hand, condition 4 there required $(Sf)(x) < 0$ for all $x \neq x_c$. However, a simple inspection of the proof shows that the less restrictive condition $(Sf)(x) < 0$ for all $x > x_c$ is enough to get the result. On the other hand, the restriction $x_c < x^*$ is required in (Liz and Franco, 2010, Theorem 1). In case $x_c \geqslant x^*$, the map $h(x) = (1-\sigma)x + f(x)$ defining the right-hand side of (78) satisfies the hypothesis of Lemma 4.2.2. First, the fixed points of h are exactly those of f_σ, therefore h has a unique positive fixed point. Second, since $h(x) = x$ if and only if $x \in \{0, x^*\}$, $\lim_{x\to 0^+} h'(x) = \lim_{x\to 0^+} (1-\sigma) + \sigma f'_\sigma(x) > 1$ and $h'(x) > 0$ for all $x \in (0, x^*)$, then $x < h(x) < x^*$ for all $x \in (0, x^*)$. Third, as h satisfies $h(x^*) = x^*$, $h'(x) = (1-\sigma) + f(x) > 0$ and $h''(x) = f''(x) < 0$ for all $x \in (x^*, x_c)$ and $h'(x) = (1-\sigma) + f(x) < (1-\sigma) < 1$ for all $x > x_c$, then $0 < h(x) < x$ for all $x > x^*$. Thus, we can conclude that x^* is GAS in $(0, \infty)$. □

4.3 BIFURCATION TYPES

We distinguish between two categories of bifurcations: local and global. We use the term *local* for those occurring in a neighborhood of a fixed point and the term *global* for all the rest. In Chapters 5 and 6, once we have determined the stability of fixed points, we use that information to study first local and then global bifurcations.

In the category of local bifurcations, there exists a well developed classification theory when, at the bifurcation point, the equilibrium lies in a smooth or continuous branch of the map h. We begin reviewing these types of bifurcations and then we continue with the ones which take place when a fixed point collides with a discontinuity point.

We use the term *smooth bifurcations* (SBs) for those bifurcations that are typical of smooth dynamical systems, which are associated with the multiplier $h'(x^*)$ of a fixed point x^* passing through the values ± 1. We recall that, when $|h'(x^*)| \neq 1$ we say that x^* is hyperbolic. We can find the following classification with illustrations in (Wiggins, 1990, Chapter 3):

- A *saddle-node* or *fold SB* occurs when two coexisting LAS and unstable fixed points become a unique equilibrium with multiplier 1 and then disappear.
- A *transcritical SB* occurs when two coexisting LAS and unstable curves of fixed points become a unique equilibrium with multiplier 1, and then the curves of fixed points interchange their stability.
- A *pitchfork SB* occurs when three branches of fixed points collide and then only one remains. In the supercritical case, two LAS fixed points collide with an unstable fixed point and the remaining fixed point is LAS. In the subcritical case, two unstable fixed points collide with a LAS fixed point, and the remaining fixed point is unstable. At the bifurcation point, there is a unique equilibrium with multiplier 1.
- A *flip* or *period-doubling SB* occurs when a fixed point x^* becomes hyperbolic with multiplier -1 and then the fixed point changes its stability and a 2-cycle $\{p_1, p_2\}$ appears, where $p_1 < x^* < p_2$. In the supercritical case, the LAS fixed point becomes unstable and the 2-cycle is LAS. In the subcritical case, the unstable fixed point becomes LAS and the 2-cycle is unstable. We use the term *period-halving SB* when the bifurcation takes place in the opposite direction.

For smooth maps $h \in \mathcal{C}^r$ ($r \geqslant 2$ for fold and transcritical; $r \geqslant 3$ for pitchfork and flip), the book by Wiggins (1990) states a list of sufficient conditions for the map h under which each of these types of SBs takes place. Similar bifurcations related to the multiplier of a fixed point passing through ± 1, but occurring under some degeneracy conditions, are referred as *degenerate SBs* (see (Avrutin et al., 2019, Section 2.2) for details).

Before describing local bifurcations of fixed points for piecewise-smooth (continuous or discontinuous) maps, we need to adopt some special notations introduced in (Bernardo et al., 2008). For that purpose, we consider h_l and h_r

two smooth maps on J, a point $d_1 \in \mathrm{Int}(J)$ such that $h_l'(d_1) \neq h_r'(d_1)$, and we assume that the map h associated to the difference equation (76) is defined by

$$h(x) = \begin{cases} h_l(x), & x < d_1; \\ h_l(x) \text{ or } h_r(x), & x = d_1; \\ h_r(x), & x > d_1; \end{cases} \tag{85}$$

which is not differentiable at d_1. The point d_1 where h is not differentiable is called a *break point*. If a break point is a fixed point of h, then we say it is a *boundary fixed point*. We recall that the map h in (85) is defined by two smooth maps h_l and h_r, so there may are fixed points of h_l and h_r that are not fixed points of h, we refer to them as *virtual fixed points*; while the fixed points of h are called *admissible fixed points*.

The local bifurcations at a boundary fixed point where introduced by Nusse and Yorke (1992) and occur when, under infinitesimal parameter variation, a fixed point collides with a break point and the collision leads to a qualitative change on the dynamics, with the fixed point transitioning from being admissible to being virtual or viceversa. We refer to these types of bifurcations as *border-collision bifurcations* (BCBs).

A classification of BCBs in piecewise-smooth continuous discrete-time difference equations is given in (Bernardo et al., 2008, Chapter 3). In Section 3.4, there is a classification for one-dimensional systems, which is given in terms of the derivatives of h_l, h_r at the boundary fixed point. We pay special attention to the contents in Subsection 3.1.2, where they describe and illustrate the four basic dynamical scenarios which take place at a BCB:

- A *fold BCB* occurs when two coexisting admissible fixed points collide at a break point and become two virtual fixed points.
- A *persistence BCB* occurs when an admissible and a virtual fixed point collide at a break point and interchange their roles. No other periodic points are created or destroyed at the bifurcation point.
- A *flip* or *period-doubling BCB* occurs when an admissible fixed point x^* collides with a break point and a 2-cycle $\{p_1, p_2\}$, with $p_1 < x^* < p_2$, appears.
- A *period-multiplying BCB* occurs when an admissible fixed point collides with a break point and an m-cycle appears, with $m > 2$.

We observe that new dynamic transitions at the bifurcation points occur due to the lack of differentiability of the map h, such as the persistence or period-multiplying BCBs. Moreover, there exist more complex bifurcations, where after the border collision of an admissible fixed point, the asymptotic dynamics become chaotic. It is well-known that such a transition in general does not occur in smooth systems.

The previously mentioned bifurcations can also be observed in the long-term dynamics of a piecewise-smooth discontinuous dynamical system, but the discontinuity character increases again the variety of fixed point local bifurcations. We devote the next lines to describe some additional BCBs taking place at discontinuity points of systems that we will consider in Chapter 5 (see (Avrutin et al., 2019, Chapters 2 and 3) for details):

- An *existence BCB* occurs when a virtual fixed point of h becomes admissible after a collision with a break point. No other orbits are created or destroyed at the bifurcation point.

- A *period-adding BCB* occurs when a LAS admissible fixed point collides with a break point; at the collision point, there is a homoclinic orbit (we recall the definition at the end of this subsection); after the collision the fixed point becomes virtual, and an attracting m-cycle becomes admissible, giving rise to a period-adding scenario. The *period-adding scenario* refers to the order of periodicity regions in the parameter space where between two cycles of periods n and l there is an $(n+l)$-cycle (see Granados, Alsedà, and Krupa, 2017, for details).

In the category of global bifurcations, we consider two different groups:

- *Boundary-collision bifurcations*, which are caused by the collision of an attractor with an unstable fixed point or m-cycle ($m \in \mathbb{N}$, $m \geqslant 2$). These bifurcations where introduced as *crises* by Grebogi, Ott, and Yorke (1982) for the case of a chaotic attractor. They use the term *boundary crisis* when the unstable orbit is on the boundary of the chaotic attractor and the collision causes termination of the attractor; and *interior crisis* when the collision occurs within the basin of attraction. They mention that the interior crisis often results in a sudden expansion of the basin.

- *Basin boundary metamorphoses*, which are those related with transformations of the basins of attraction. We will find transitions from a simply-connected to a multiply-connected basin. The transitions can be more complex, as those in (Grebogi, Ott, and Yorke, 1983) from a regular basin to a fractal one.

We have already mentioned that a homoclinic orbit appears at the period-adding BCBs, and we will also observe the presence of this type of orbits in boundary-collision bifurcations and basin boundary metamorphoses. We recall that a homoclinic orbit is formed by a homoclinic point, its preimages and its (finite) forward orbit . A point x is homoclinic to an n-cycle $p = \{p_1, \dots, p_n\}$ if $(f^n)^m(x) = p_k$ for some $m \in \mathbb{N}$ and $k \in \{1, \dots, n\}$, and x belongs to the unstable manifold of p_k. For further details, see (Devaney, 1989, Section 1.16) or (Liz, 2010a, Appendix C).

Finally, it is worth mentioning that, in general, we study bifurcations of attractors, but bifurcations of other invariant sets also deserve to be investigated since they can influence the asymptotic dynamics as well.

4.4 1-PARAMETER BIFURCATION DIAGRAMS FEATURES

The last step in the analysis of asymptotic dynamics is to illustrate the influence of parameters. For that purpose, we first reflect the information we have on stability of fixed points and bifurcations in a 2-parameter BD. Then we plot several 1-parameter BDs to get more insight and complete the global picture of the dynamics.

In this section we review some relevant features or phenomena that have been observed in 1-parameter BDs of a wide range of discrete one-dimensional dynamical systems.

Long-transients and hysteresis

Let us first discuss some consequences of focusing on asymptotic dynamics in ecology. In (Hastings et al., 2018), there is a review summary on the *long transient* phenomena, defined as a dynamical regime that persists for more than a few and as many of ten generations, but which is not the stable long-term dynamics that would eventually occur. In the particular framework of mathematical analysis of the dynamical systems given by (76), the study of non-asymptotic dynamics has not much interest, since long-transients are just iterations of an initial condition by the map h. However, the presence of long-transients can obscure the decisions on the management of ecological systems, so it becomes interesting to categorize different ways in which transients can arise.

With this possibility in mind, we start defining the long-term dynamics phenomenon of *hysteresis*, which can also have unexpected consequences for the management in biological systems. In (Blackwood, Hastings, and Mumby, 2012), for a system with multiple stable states, the authors say that this feature occurs when the previous history of the system influences the convergence of an initial condition to one of the stable states or the others. They also describe the phenomenon in other words, saying that the critical parameter conditions under which some points converging to one stable state switch and converge to another one are different from the conditions that will allow the convergence of such points to the original state. See Figure 22 (A).

Bubbles, bistability and hydra effect

We now deal with three features that have been observed in bifurcation diagrams of both semelparous and iteroparous population models.

We begin with a phenomenon related to the period-doubling sequence of bifurcations as a universal route to chaos, which can be broken and reversed as shown in (Bier and Bountis, 1984) for simple non-linear discrete dynamical systems involving the variation of two or more parameters. As a consequence, the bifurcation diagrams form closed loop-like structures similar to bubbles

and the effect is usually referred to as *bubbling*. Definition 3 in (Liz and Ruiz-Herrera, 2012) gives a formal definition of the concept of *bubble*. The complexity of the bubble structure depends on the point at which the period-doubling sequence is reversed. The simplest bubble occurs when an equilibrium loses its asymptotic stability through a period-doubling bifurcation and, at the next bifurcation point, a period-halving bifurcation occurs, so that the local asymptotic stability of the fixed point is regained, we refer to it as *primary bubble*. If the period-doubling sequence of bifurcations is reversed after a region of chaotic dynamics, we use the term *chaotic bubble*.

The *bistability* feature refers to the coexistence of two attractors, and it occurs due to fold bifurcations (either smooth or border-collisions). Bistability has important consequences in population dynamics because, in this case, the long-term behavior of the solutions strongly depends on the initial condition.

Another formal definition stated in (Liz and Ruiz-Herrera, 2012) is the *hydra effect*. This term was used by Abrams (2009) and the references therein for the phenomenon of a population increase in response to an increase in its mortality rate. This feature has been first recognized by Ricker (1954) for the well-know Ricker model which assumes that mortality precedes reproduction. That is one of the three mechanisms underlying hydra effect which are developed in (Abrams, 2009) for non-overlapping populations models. Liz and Ruiz-Herrera (2012) studied the hydra effect for iteroparous population models, in which a percentage of the adult population survives the reproductive season.

Extinction windows and sudden collapses

The following features are typical of models with *Allee effect*, where populations cannot survive in the long-term if its abundance is below a critical size, they are called extinction windows and sudden collapses.

The term *extinction window* refers to the survival-extinction dynamics described by Sinha and Parthasarathy (1996) as an unusual structure with alternating regions of survivals and extinction under variation of parameters, so that the population can persist under very low and fairly high values of the parameter, though it is not able to survive at intermediate parameter values.

The *sudden collapse* phenomenon appears also in (Sinha and Parthasarathy, 1996), but a description of the feature is given in (Schreiber, 2001) where it is said that there exists a critical parameter value above which populations are driven to extinction for all initial densities and below which persistence is possible. By *persistence* we mean that population remains at densities bounded away from zero.

Periodic-windows, star-like intersections and effectively chaotic behaviour

We finally describe some typical features of bifurcation diagrams for piecewise-smooth maps with flat branches (see (Sinha, 1994) for further details).

If long-term dynamics are governed by an m-cycle ($m \in \mathbb{N}$, $m \geqslant 2$) in a non-empty interval of the parameter space, we say that there is a *periodic-window*.

If, given a parameter value, a LAS m-cycle $\{x_0, h(x_0), \ldots, h^{m-1}(x_0)\}$ ($m \in \mathbb{N}$, $m \geqslant 2$) collides with an unstable fixed point x^*, we assume that $h^{m-1}(x_0) = x^*$, then all the subsequent iterates of x_0 must necessarily collide with x^*. If for small variations of the parameter the equilibrium remains unstable, then the iterates of x_0 diverge from x^* giving rise to many long-period cycles. Thus, in a neighborhood of x^*, the LAS m-cycle forms a *star-like intersection* and the presence of many attracting long-period cycles is called *effectively chaotic behavior*.

5 COMBINATIONS OF CONSTANT QUOTA AND THRESHOLD BASED HARVESTING STRATEGIES

This chapter comprises the contents of the research articles: (Liz and Lois-Prados, 2020b)[1] and (Lois-Prados and Hilker, submitted)[2]. In both cases, we consider single-species population models subject to a protective and yield stabilizing harvesting rule, and we study the influence of harvesting parameters in the dynamics. The chapter is divided into five distinct sections.

We begin with the Introduction section, where we give a contextualization of our study in the field of fisheries management and we summarize our contributions to the qualitative theory of piecewise-smooth dynamical systems.

In Section 5.2, we provide the mathematical expression for the harvesting strategies that appear through the research study in this chapter. For the classical control rules, we recall some well-known results on long-term dynamics and we show that they can be obtained as particular or limit cases of the threshold based strategies. We additionally explain the main differences between precautionary threshold constant catch (PTCC) and threshold constant catch (TCC), and relate TCC with a similar strategy.

The analytical results and numerical simulations we use to determine the long-term population dynamics of PTCC and TCC appear in Sections 5.3 and 5.4, respectively. For the TCC rule, we additionally study the influence of harvesting parameters in two management objectives: long-term average yield

1 Eduardo Liz (Departamento de Matemática Aplicada II, Universidade de Vigo, Spain) & Cristina Lois-Prados (Instituto de Matemáticas, Universidade de Santiago de Compostela, Spain), "Dynamics and bifurcations of a family of piecewise-smooth maps arising in population models with threshold harvesting", *Chaos (ISSN:* 10541500, 10897682*)*, **30**, pp. 1-16, 2020. The final authenticated version is available online at: https://doi.org/10.1063/5.0010144
JCR 2019 (category; impact factor; relative position; quartile): Applied Mathematics; 2.832; 16/261; Q1.
PhD student contribution: The authors have equally contributed to the development of the article contents, except that the initial idea was conceived by my supervisor E. Liz.

2 Cristina Lois-Prados & Frank M. Hilker (Institute of Environmental Systems Research and Institute of Mathematics and School of Mathematics/Computer Science, Osnabrück University, Germany), "Bifurcation sequences in a discontinuous piecewise-smooth map combining constant-catch and threshold-based harvesting strategies", *SIAM Journal on Applied Dynamical Systems (ISSN:* 1536 − 0040*)*, **submitted**.
JCR 2019 (category; impact factor; relative position; quartile): Applied Mathematics; 1.956; 49/261; Q1.
PhD student contribution: The initial idea was conceived by professor F. M. Hilker, then C. Lois-Prados carried out the qualitative study of the dynamics and wrote down an almost complete first draft of the manuscript, following some suggestions of F. M. Hilker. He revised, improved and enriched many parts of the manuscript, in particular from an ecology-oriented point of view.

and harvest frequency. We give a detailed description of the contents at the beginning of each section.

Finally, in Section 5.5, we discuss the obtained results in the framework of piecewise-smooth dynamical systems (with special attention to the asymptotic behavior typical of maps containing flat branches for PTCC and to those features induced by discontinuity points for TCC), population dynamics and harvesting management.

5.1 INTRODUCTION

This section aims to put in context the research study that we have included in this chapter. We organize the contents in different paragraphs and each of them corresponds to a distinct topic.

General contextualization in the field of fisheries management

Rational fisheries management requires to determine harvest or yield levels that are consistent with management objectives. To prevent historical management consequences, such as fish stock declines and even collapses, the rules or guidelines on how to set harvest levels should be more explicit. These guidelines are referred to as harvest policies and aim to determine the best control rule to meet specific fishery objectives. Control rules or harvest strategies are specifications of the amount of catch, fishing effort or mortality as a function of the current estimate of the system state (e.g., the stock or spawning biomass). Several methods are used to evaluate control rules for meeting given management objectives. In this PhD thesis, we use an analytical approach, this type of methods can be used to determine the optimal control rule between several candidates. While they provide quite general results, they present some drawbacks as they are feasible only for simple models and are mainly deterministic. Another method for selecting an optimal strategy is stochastic dynamic programming. This method allows to consider more flexible policies than a simple control rule, but computational cost of searching between a wide range of strategies has also generally limited the study to some relatively simple models. When considering too complex models, many harvest policy works use Monte Carlo simulations to evaluate the performance and trade-offs of a specific control rule with fixed policy parameters. This approach permits to include random error terms often related to model assessment or implementation errors. The results work for the chosen policy parameters and cannot prove that a particular control rule is optimal. For extra details, see (Deroba and Bence, 2008), where one can find a detailed review of the relevant literature that compares the ability of control rules to meet some widely used fishery objectives. They comment that the determination of harvest policies based on a combination of results obtained by these complementary approaches seems to be very useful. It is worth noticing that "a harvest strategy is not of much value unless a mech-

anism or set of tactics can be devised to implement in the field" (Hilborn and Walters, 1992). In (Hilborn, 2012) we find a review on the changes in qualitative marine fisheries management during the period 1985-2010. They comment that, in 1985, the majority of fisheries were open-access or relied on technical measures such as vessel size, closed areas or season lengths. However, the inefficiency of these tactics resulted in a dramatic change during the interviewing 25 years between 1985 and 2010, with most fisheries using total allowable catch (TAC) levels and open-access almost disappeared. In the following, we pay special attention to the evolution of control rules and management objectives.

Description of traditional control rules and common management objectives

Harvest policies are based on relatively simple control rules; Deroba and Bence (2008) argue that complex harvesting strategies can lack appeal for managers since the intuitive basis of the rule or changes in year's allowable catch may not be apparent. Punt (2010) categorizes the traditional harvest control rules into: constant catch (CC), which removes a constant amount of yield or quota $H > 0$ from the population per unit time; constant fishing mortality or proportional harvesting (PH), which removes a constant fraction $q \in (0, 1)$ of biomass per unit time; and constant escapement or threshold harvesting (TH), which reset the population to a threshold level $T > 0$ if the population is larger than T, and takes no harvest if the biomass is below T. Figure 10 shows an illustration of catch and escapement as functions of the population biomass for these three harvesting strategies. Several authors have studied the performance of CC, PH and TH by means of different analytical or statistical approaches. In the following, we provide a list of benefits and drawbacks for the three rules. They were compiled from different studies, which were developed under distinct assumptions on the stock-recruitment relationship. First of all, let us introduce some common management objectives: "A frequently used fishery objective is cumulative harvest over the time horizon, which is considered a risky approach, because performance is measured only by the total catch over the time horizon, with the frequency of low and high annual values playing no role" (Deroba and Bence, 2008). A related concept is the *maximum sustainable yield* (MSY), which is defined in the book by Ricker (1975) as the largest average catch or yield that can be continuously taken from a stock under existing environmental conditions. In (Quinn and Deriso, 1999), it is mentioned that MSY corresponds with the point where the unharvested population increases the most. Several risk-averse alternatives to cumulative yield or MSY are mentioned in (Deroba and Bence, 2008), an example is how frequently the biomass or harvest have been at or below a reference value.

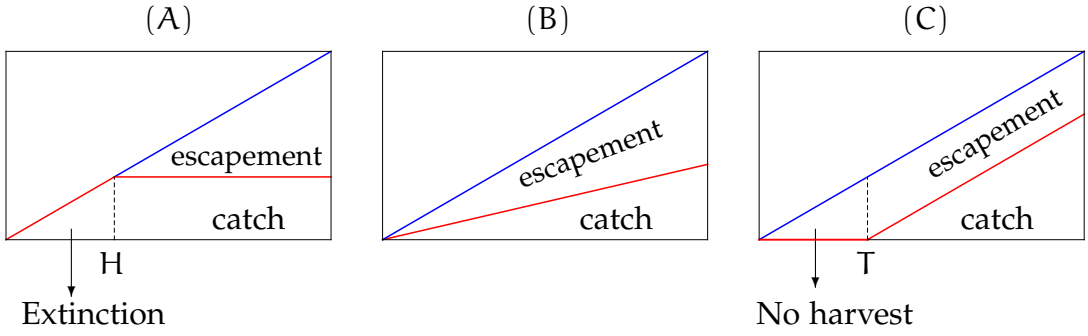

Figure 10: Classical control rules illustrated by sketching catch (red solid lines) as a function of population density or biomass. The blue line represents the identity map, T is the threshold and H the maximum allowed quota. (A): constant quota harvesting; (B): proportional harvesting; (C): threshold harvesting.

Comparison of the performance of traditional harvesting strategies

In the work by Ludwig (1998), there is a comparison between CC, PH and TH control rules when maximum yield and low probability of extinction are the criteria for success. They consider a modification of the Ricker model that includes random catastrophic years and Allee effect and conclude that TH is the optimal strategy, as it was previously demonstrated by other authors under different assumptions for the population. In addition, TH is considered to be the safest rule, but Sinclair, Fryxell, and Caughley (2006) argue that fixed escapement becomes unsafe when there is uncertainty on stock recruitment abundance; moreover it produces high variable yields, which make TH less attractive for managers than CC. In (Punt, 2010), they comment that the time-invariant catch-limit of CC should theoretically provide industry with a level of stability that can be applied for the future, but contrary to TH, the constant catch control rule is considered to increase the risk of population collapse and to produce lower yields. Indeed, Sinclair, Fryxell, and Caughley (2006) show that the marten population cannot sustain a constant quota at MSY for any appreciable length of time. Their simulations show that PH is much more sustainable than CC. However, the uncertainty in current stock abundance considerably increases the risk of unintentionally overharvesting for the constant fishing mortality strategy. This drawback was also found out by Deriso (1985), who considers that TH is in that case less precise than PH. They carry out a comparison between the performance of TH and PH. While TH is a risk adverse control rule that maximizes average catch, they highlight two reasons why PH is a better option than TH. On the one hand, they comment that the type of sustainable optimal policy depends on the stock-recruitment relationship, and some numerical simulations show that PH produces high and stable catches. On the other hand, they found that the parameter identification may be easier in PH than TH. The research articles cited through this paragraph are based on statistical and numerical results. Some other authors obtained similar results

by using an analytical approach: CC (Schreiber, 2001; Sinha and Parthasarathy, 1996), PH (Liz, 2010b; Liz and Ruiz-Herrera, 2012), TH (Hilker and Liz, 2020).

Description of current control rules based on thresholds

In order to minimize the drawbacks of these simple harvesting strategies and take advantage of their different benefits, many authors have recently considered several combinations of CC, PH and TH. Besides, in order to prevent overexplotation, most fisheries management agencies have adopted control rules based on thresholds or population abundance levels below which harvesting is suspended (Hilborn, 2012). Above the threshold, several options are possible, e.g., harvesting a proportion of the excess (PTH) (Enberg, 2005; Engen, Lande, and Sæther, 1997; Hilker and Liz, 2019; Quinn and Deriso, 1999), a proportion of the population (Bischi, Lamantia, and Tramontana, 2014), or a constant quota (AlSharawi and Rhouma, 2009; Butterworth, 1987; Deroba and Bence, 2008; Hjerne and Hansson, 2001; Liz and Lois-Prados, 2020b; Lois-Prados and Hilker, submitted; Steiner, Criddle, and Adkinson, 2011). It is worth mentioning that the research in (Enberg, 2005; Hjerne and Hansson, 2001) supports the use of threshold based strategies and introduces precautionary strategies that include two different threshold levels to prevent harvesting moratoria. Their control rules use either fixed mortality (Enberg, 2005) or constant catch (Hjerne and Hansson, 2001) strategies if population biomass is above a high population abundance level, harvesting is forbidden when biomass falls below a lower threshold and, for intermediate values, harvesting is curtailed by taking a smaller proportion of the excess or a reduced quota, respectively. The "40-10" control rule used to manage the U.S. west coast ground-fish is an example of the precautionary combination of TH and PH described in (Enberg, 2005), see (Deroba and Bence, 2008).

Reasons to consider combinations of constant quota and threshold based control rules

In the following, we focus our attention on combinations of TH and CC. Constant catch strategies above the threshold are referred to as *conditional constant catch* strategies by Deroba and Bence (2008).[3] Analytical and simulation models of such strategies are relatively rare and scattered in the literature. We consider two different control rules, the simplest one consists in allowing to harvest a constant quota $H > 0$ if the population size after reproduction is above a threshold $T > 0$; and prohibiting harvesting when the biomass is below T. We refer to this strategy as threshold constant catch (TCC). If, in addition, we require that a minimum biomass level must remain after harvesting, the strategy becomes more protective, and we refer to it as precautionary threshold constant catch (PTCC). Figure 11 shows an illustration of catch and escapement for both

3 But it should be noted that this term was used by Clark and Hare (2004) for a specific harvest strategy for Pacific Halibut with CC harvesting above the threshold and PH below it.

harvesting strategies. The consideration of constant quotas instead of fixed mortality rates can reduce the risk of overcapacity when the stock decreases, since PH stimulates investment when stock size is large. The results in (Hjerne and Hansson, 2001) show that long-term yield for the precautionary combination of TH and CC (referred to as quasi constant catch, QCC for short) is 10% less than that of PH at MSY. They consider that it is a small difference and emphasize that the much lower inter annual variability of QCC gives the opportunity of better fishery capacity utilization. We notice that they first considered the TCC control rule, and then QCC as a precautionary modification to reduce fishery closures. To our knowledge, the TCC strategy has been considered so far only by Hjerne and Hansson (2001) and in a slightly different form by AlSharawi and Rhouma (2009). We also notice that Punt (2010) cites the article (Butterworth, 1987) to talk about threshold management strategies in which catch becomes constant when the stock size is greater than a target level. We finally provide a different reason to consider this type of control rules. Steiner, Criddle, and Adkinson (2011) looked for a solution to the revenue decline of Bristol Bay sockeye salmon managed with a fixed escapement control rule. In contrast to other fisheries, the landings had remained high, but the prices fell as a consequence of competition resulting from the increased production of trout and salmon farmed species in Chile. They provide several reasons to consider implementing the PTCC strategy rather than TH or PTH: the fact that PTCC induces lower harvests allows to improve the quality of the fish delivered, thus producing a high exvessel price per pound; the lower variability in harvest provides more efficiency of the management operations because the harvest levels will be known at the beginning of the season.

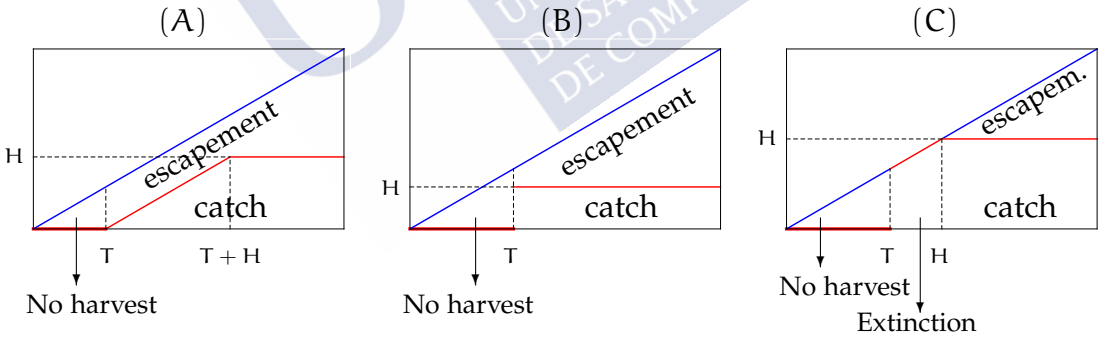

Figure 11: Different harvesting strategies that combine constant catches with threshold reference points. We represent the catch (red solid line) as a function of the population biomass. The blue line represents the identity map, T is the threshold and H the maximum allowed quota. (A): Precautionary threshold constant catch harvesting. The other panels show threshold constant catch harvesting with (B): $H < T$ and (C): $H > T$.

Contextualization in the framework of piecewise-smooth one-dimensional difference equations

As far as we know, we formulate and study the PTCC and TCC rules in the framework of one-dimensional discrete-time dynamical systems by means of an analytical approach for the first time. As these harvesting strategies are based on threshold population sizes, the associated map will be composed of different branches (corresponding to high or low/no harvesting) defined on intervals which are separated at the biomass reference points (also called break points in the mathematical literature). As the maps are not differentiable at the threshold points, they give rise to piecewise-smooth dynamical systems (Avrutin et al., 2019; Bernardo et al., 2008). They can exhibit so-called non-smooth bifurcations that differ substantially from those that occur in smooth dynamical systems, e.g., border-collision bifurcations (Nusse and Yorke, 1992). Non-smooth bifurcations are related to invariant sets colliding with a break point, which is given by the harvesting threshold. In recent years, a lot of progress has been made in understanding the dynamics of piecewise-smooth maps, e.g., (Banerjee et al., 2000; Radi and Gardini, 2018; Sushko, Gardini, and Matsuyama, 2014). However, even though they emerge quite naturally in the context of threshold-based harvesting, their mathematical analysis in the context of fisheries models is just at the beginning (Bischi, Lamantia, and Tramontana, 2014; Franco and Hilker, 2013, 2014; Hilker and Liz, 2019, 2020; Liz and Lois-Prados, 2020b; Lois-Prados and Hilker, submitted; Segura, Hilker, and Franco, 2016, 2020).

Overview of the research development

Our study is focused on stability and bifurcations; in this regard, we consider the two relevant harvest parameters H and T and obtain 1-parameter and 2-parameter bifurcation diagrams that help to understand how a continuous variation of any of them influences the dynamics, and the interplay between both parameters. We identify regions where global attraction, periodic attractors, multi-stability and complex behavior are likely to occur, paying special attention to non-smooth bifurcations. We first study the long-term behavior of the continuous map associated with PTCC, which will serve as a baseline against which we can compare the effects induced by the discontinuity in TCC. For the PTCC rule, we completely determine the asymptotic dynamics and bifurcations for general compensatory population models; we also understand the long-term behavior in some regions of the parameter plane (H, T) for general overcompensatory maps, for which we consider the Ricker map as a case study to give a global picture of the dynamics. For the TCC rule, we just deal with strictly increasing stock-recruitment maps, while in this case all initial conditions would converge to an equilibrium for the PTCC rule, the discontinuity point of TCC gives rise to highly complex dynamics, including multiple attrac-

tors, different periodic cycles, homoclinic orbits and even chaotic oscillations. The bifurcations in which these dynamical patterns emerge and disappear involve border- and boundary-collision bifurcations as well as basin boundary metamorphoses. Hence, the discontinuity in the harvest control rule produces rich dynamics that, to our knowledge, have not been observed in continuous harvesting models applied to population maps that are strictly increasing in the absence of harvesting. The research on PTCC totally focuses on dynamical systems theoretical aspects, we notice that for some particular parameter values the long-term behavior is influenced by the dynamics of constant-catch or threshold harvesting. Nevertheless, some characteristic dynamics of CC or TH are not completely preserved, e.g., the extinction attractor of CC or the convergence of almost all solutions to a periodic orbit containing T of TH. For the TCC rule, we thoroughly combine the qualitative study of population dynamics with management-oriented interpretations; additionally we study the influence of harvesting parameters in long-term average yield and harvest frequency. We pay special attention to the influence of the threshold point (that is, the effect that TCC has in comparison to CC) in population, average yield and harvest frequency behavior.

5.2 MODELS DESCRIPTION

In this section, for the sake of completeness, we first state the mathematical formulation and recall some results on asymptotic dynamics for the classical control rules that can be considered as particular cases of TCC or PTCC, that is, constant quota (subsection 5.2.1) and threshold harvesting (subsection 5.2.2). In subsections 5.2.3 and 5.2.4, we provide the mathematical expression for PTCC and TCC, respectively. We compare the TCC control rule with the precautionary version given by PTCC and the similar strategy considered by Avrutin et al. (2019).

5.2.1 *Constant catch rule*

For later reference, we state some well-known results for the CC harvesting rule. For a general map $f : [0,\infty) \longrightarrow [0,\infty)$ and the constant quota $H > 0$, the model reads

$$x_{n+1} = F_{CC}(x_n) = \max\{0, f(x_n) - H\}. \tag{86}$$

Let us consider the map $g(x) = f(x) - H$, $x \in [0,\infty)$, then we can rewrite F_{CC} in the form: $F_{CC}(x) = \max\{0, g(x)\}$.

The following result establishes a critical value H_{20} for the harvesting quota. Harvesting above this level ($H > H_{20}$) will drive the population to extinction. Below this level, several long-term dynamics can occur. The simplest dynamics take place for a map f satisfying conditions **(A1)-(A2)** (defined in Section 4.1) with $x_c = \infty$, for which the population will survive provided the initial con-

dition is large enough. By contrast, the most complex dynamics occur when $x_c < K$ and there is bistability between the LAS fixed point 0 and other attractor. The proposition uses that there exists a unique $\tilde{x} > 0$ such that $f'(\tilde{x}) = 1$. This follows from assumptions **(A1)-(A2)** and the Mean Value Theorem. Moreover, $\tilde{x} \in (0, K)$.

Proposition 5.2.1. *Assume that $H > 0$ and f satisfies **(A1)-(A2)**. Denote by $\tilde{x}$ the unique solution of $f'(x) = 1$.*

1. *If $H < H_{20} := f(\tilde{x}) - \tilde{x}$, then g has two positive equilibria x_-^* and x_+^* with $0 < x_-^* < \tilde{x} < x_+^* < K$. While x_-^* is always unstable and 0 is locally asymptotically stable, the fixed point x_+^* can be either stable or unstable:*
   a) *If $x_c = \infty$, then x_+^* is LAS with basin of attraction (x_-^*, ∞) and $[0, x_-^*)$ is the basin of attraction of 0.*
   b) *If $K < x_c < \infty$, then x_+^* is LAS with basin of attraction $(x_-^*, g^{-1}(x_-^*))$ and $[0, x_-^*) \cup (g^{-1}(x_-^*), \infty)$ is the basin of attraction of 0.*
   c) *If $x_c < K$, then x_+^* can be LAS with basin of attraction $(x_-^*, g^{-1}(x_-^*))$ or unstable. If x_+^* is unstable, the dynamics depend on the position of $g^2(x_c)$ with respect to x_-^*:*
   If $g^2(x_c) > x_-^*$, then $I = [g^2(x_c), g(x_c)]$ is absorbing and the initial conditions in $(x_-^*, g^{-1}(x_-^*))$ enter I in finite time; besides, $[0, x_-^*) \cup (g^{-1}(x_-^*), \infty)$ is the basin of attraction of 0.
   If $g^2(x_c) < x_-^*$, then 0 is an essential global attractor.
2. *If $H = H_{20}$, then $\tilde{x}$ is the unique positive fixed point of g. The equilibrium $\tilde{x}$ is semi-stable and 0 is locally asymptotically stable. If $x_c = \infty$, $[\tilde{x}, \infty)$ and $[0, \tilde{x})$ are their respective basins of attraction; while if $x_c < \infty$ they are $[\tilde{x}, g^{-1}(\tilde{x})]$ and $[0, \tilde{x}) \cup (g^{-1}(\tilde{x}), \infty)$, respectively.*
3. *If $H > H_{20}$, then g has no positive fixed points and 0 is GAS.*

We refer the reader to (Schreiber, 2001) for a rigorous proof and analysis of the results in Proposition 5.2.1.

5.2.2 *Threshold harvesting rule*

We consider now the TH rule, which can be seen as the antipode to the CC harvesting strategy. For a general map $f : [0, \infty) \longrightarrow [0, \infty)$ and a threshold level $T > 0$, the dynamics of TH are governed by the difference equation:

$$x_{n+1} = F_{TH}(x_n) = \min\{f(x_n), T\} = \begin{cases} f(x_n), & f(x_n) \leqslant T; \\ T, & f(x_n) > T. \end{cases} \tag{87}$$

In the recent work by Hilker and Liz (2019), we find a rigorous theoretical study on the influence of the threshold T on the dynamics of (87). Under some

general conditions for the map f, they show that threshold harvesting can never have a destabilizing effect on the managed population. The following result summarizes the findings in (Hilker and Liz, 2019, Section 2.1).

Proposition 5.2.2. *Assume that* $T > 0$ *and* f *satisfies* ***(A1)****.*

1. *If* $T \leqslant K$*, then* T *is the unique positive equilibrium of* (87) *and it is GAS.*
2. *If* $T > K$*, the dynamics of the managed system* (87) *depend on the dynamics of the unmanaged system* $x_{n+1} = f(x_n)$*:*
   a) *If* K *is GAS for the unmanaged system, then* K *is the unique positive equilibrium of* (87) *and it is GAS.*
   b) *If* K *is unstable but the unmanaged system has a finite number of periodic orbits, then decreasing threshold induces a sequence of period-halving bifurcations until the equillibrium becomes stable.*
   c) *If* K *is unstable and the unmanaged system is chaotic, for S-unimodal maps there is a unique periodic orbit that is an essential global attractor of the managed system* (87)*. Decreasing* T *from* $f(x_c)$ *to* K*, there is Li-Yorke chaos (see Definition* 3.1*, Aulbach and Kieninger, 2001) as long as the period of the attracting cycle is not a power of* 2*. Once the dynamics become simpler due to smaller threshold values, we have the situation considered in the previous case.*

5.2.3 *Precautionary threshold constant catch rule*

Applying the PTCC harvesting rule to a semelparous population model given by (77), we obtain the difference equation

$$x_{n+1} = F_{PTCC}(x_n) = \begin{cases} f(x_n), & f(x_n) \leqslant T; \\ T, & T < f(x_n) \leqslant T + H; \\ f(x_n) - H, & f(x_n) > T + H. \end{cases} \tag{88}$$

The map $g(x) = f(x) - H$ allows to write F_{PTCC} in the form

$$F_{PTCC}(x) = \begin{cases} f(x), & f(x) \leqslant T; \\ T, & g(x) \leqslant T < f(x); \\ g(x), & g(x) > T. \end{cases}$$

The piecewise smooth continuous map F_{PTCC} can also be written in a line as

$$F_{PTCC}(x) = \min\{f(x), f(x) - \min\{H, f(x) - T\}\} = \min\{f(x), \max\{g(x), T\}\};$$

and depends on the two harvesting parameters H and T. Throughout the analysis of the PTCC harvesting strategy (88), we will assume that $H > 0$ and $T > 0$. It is worth noticing that we get the unmanaged map f or the CC and TH rules as particular or limit cases:

- If $H = 0$ or $T \geqslant \sup\{f(x),\, x \geqslant 0\}$, then $F_{PTCC} \equiv f$.
- In the limit case $T = 0$, (88) becomes the usual constant catch policy, defined by (86).
- If $T < \sup\{f(x),\, x \geqslant 0\} \leqslant H + T$, then the PTCC harvesting strategy becomes the pure threshold harvesting rule (87).

The typical shape of F_{PTCC} can be seen in Figure 12. Roughly speaking, the graphs of f and g are joined by flat segments defined by T, which typically results in five intervals of smoothness for F_{PTCC} if f is unimodal, and three if f is strictly increasing.

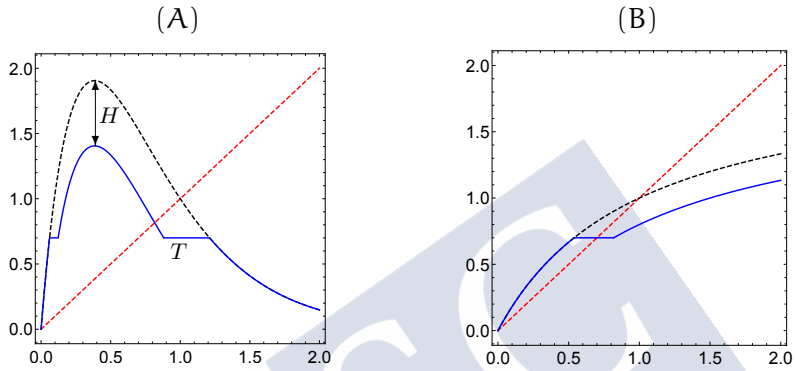

Figure 12: Illustration of the graph of the piecewise smooth map F_{PTCC} (blue solid line). We also plot the line $y = x$ (red, dashed) and the graph of f (black, dashed). (A): Unimodal Ricker map $f(x) = x\,e^{2.6(1-x)}$, with $H = 0.5$ and $T = 0.7$. (B): Strictly increasing Beverton-Holt map $f(x) = 2x/(1+x)$, with $H = 0.2$ and $T = 0.7$.

5.2.4 *Threshold constant catch rule*

When harvesting a population that is growing according to (77) with the TCC rule, we obtain

$$x_{n+1} = F_{TCC}(x_n) := \begin{cases} f(x_n), & f(x_n) < T; \\ \max\{0, f(x_n) - H\}, & f(x_n) \geqslant T. \end{cases} \tag{89}$$

Let us consider the map $g(x) = f(x) - H$, then we can rewrite the map F_{TCC} in the form

$$F_{TCC}(x) = \begin{cases} f(x), & f(x) < T; \\ 0, & T \leqslant f(x) < H; \\ g(x), & f(x) \geqslant \max\{T, H\}. \end{cases} \tag{90}$$

The piecewise-smooth map F_{TCC} depends on the two harvesting parameters T and H. For the study of TCC harvesting rule (89), we assume $H > 0$ and $T > 0$. As particular or limit cases, we obtain the unmanaged map f and the CC rule, asking the same conditions to the harvesting parameters as in PTCC. By contrast, we cannot get the TH harvesting strategy as a particular case of TCC.

The typical shape of F_{TCC} applied to strictly increasing maps is shown in Figure 13. The main differences with respect to F_{PTCC} are the existence of a point of discontinuity at $x_T = f^{-1}(T)$ and the absence of a flat segment defined by T.

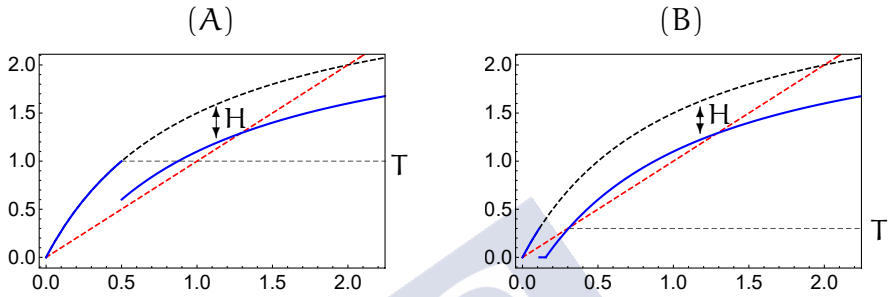

Figure 13: Illustration of the graph of the piecewise-smooth discontinuous map F_{TCC} (blue solid line). We also plot the line $y = x$ (red, dashed) and the graph of the Beverton-Holt map $f(x) = 3x/(1+x)$. $(A) : T = 1$, $H = 0.4$. $(B) : T = 0.3$, $H = 0.4$.

Related harvesting strategy

We point out that AlSharawi and Rhouma (2009, Section 4) proposed a harvesting strategy very similar to TCC. It reads

$$x_{n+1} = \begin{cases} f(x_n), & x_n < x_{th}; \\ f(x_n) - h, & x_n \geqslant x_{th}; \end{cases} \tag{91}$$

where they considered specifically the Beverton-Holt map for f, $x_{th} \in (0, K)$ is a threshold population size and $h \in (0, f(x_{th}))$ is the constant quota. The difference with (89) is that TCC compares the threshold with the population size $f(x_n)$ *after* reproduction, whereas (91) compares the threshold with the population size x_n *before* reproduction. However, for the strictly increasing population maps considered in this paper, there is a correspondence between (89) and (91). To see this, we note that f is bijective and that we just have to establish the following relation: $T := f(x_{th})$, $H := h$ or, equivalently, $x_{th} := f^{-1}(T)$, $h := H$ for $T \in (0, K)$, $H \in (0, T)$. The correspondence allows us to use some results obtained by AlSharawi and Rhouma (2009) on the existence of (stable or unstable) 2-cycles and to describe the bifurcations of F^2_{TCC}. For non-monotone population maps like the Ricker map, there can be two break points in the harvest rule (89), and there is no correspondence between (89) and (91). That is,

the two harvest strategies could differ qualitatively in their dynamics. As the harvest rule in (91) refers to a measurement of population size that is further in the past, this introduces a time lag that, for overcompensatory population maps, could lead to delayed density-dependent effects which are known to change dynamics quantitatively and qualitatively (Franco and Hilker, 2014).

5.3 PRECAUTIONARY THRESHOLD CONSTANT CATCH (PTCC)

We organize the section as follows: Subsection 5.3.1 is devoted to the study of fixed points. We start giving the location of positive equilibria depending on the relevant parameters. Then we provide stability results for the positive fixed points: while for compensatory models all solutions converge to an equilibrium, in the overcompensatory case there are stability switches and the global picture is more complicated; we give some general results for global stability and study in more detail the Ricker map, which is a prototype for discrete population models, especially in the context of fisheries (Quinn and Deriso, 1999; Ricker, 1954). Finally, we describe all posible bifurcations of fixed points (smooth and border-collision bifurcations). In Subsection 5.3.2, we focus on a particular region of the parameter plane for which chaos and essential attraction can occur. We recall that the latter means that an equilibrium is not globally attracting, but solutions converge to it with probability one. The obtained results allow us to determine some boundary-collision bifurcations. In Subsection 5.3.3, we address two case studies: a simple compensatory model, where only bifurcations of fixed points appear, and an overcompensatory model that exhibits richer dynamics; in both cases numerical bifurcation diagrams help to understand the influence of the parameters. In the overcompensatory case we pay special attention to bifurcations of 2-cycles, bistability regions and the influence of flat branches on the dynamics.

5.3.1 *Fixed points: location, stability and local bifurcations*

In this subection, we study the fixed points of F_{PTCC} depending on the parameter values H and T. We first focus on the number of positive fixed points and their location; secondly we study their stability properties; and thirdly we describe the local bifurcations of fixed points, that is, we determine the critical values of the parameters for which fixed points are created or destroyed, or stability switches can occur. We notice that existence and localization results hold for both compensatory and overcompensatory models, while the stability ones depend on the type of stock-recruitment relationship.

We recall that a consequence of conditions **(A1)-(A2)**, the Mean Value Theorem and the concavity of f in $(0, x_c)$ is the existence of a unique point $\tilde{x}$ in $(0, \min\{K, x_c\})$ such that $f'(\tilde{x}) = 1$. The point $\tilde{x}$ plays an important role in the study of fixed points.

5.3.1.1 *Existence and localization of positive fixed points*

The following result provides the number of positive fixed points of the map F_{PTCC} defined in (88). We assume that $0 < T < \sup\{f(x) : x > 0\}$ and $H > 0$.

Proposition 5.3.1. *Assume that* ***(A1)-(A2)*** *hold. Denote by* $\tilde{x}$ *the unique solution of* $f'(x) = 1$ *and by* x_-^*, x_+^* $(0 < x_-^* \leqslant \tilde{x} \leqslant x_+^* < K)$ *the positive fixed points of* $g(x) = f(x) - H$, *when they exist. The following assertions hold:*

1. *If* $T \geqslant K$, *then* K *is the unique positive equilibrium of* (88).
2. *If* $\tilde{x} \leqslant T < K$, *then* F_{PTCC} *has a unique positive fixed point, which is* T *if* $H \geqslant f(T) - T$; *or* $x_+^* \in (T, K)$ *if* $H < f(T) - T$.
3. *If* $0 < T < \tilde{x}$, *then:*
   a) F_{PTCC} *has a unique positive fixed point* $x_+^* \in (\tilde{x}, K)$ *if* $H < f(T) - T$.
   b) F_{PTCC} *has three positive fixed points (*T *and the two fixed points of* g*) if*
   $$f(T) - T < H < f(\tilde{x}) - \tilde{x}.$$
   c) T *is the unique positive fixed point of* F_{PTCC} *if* $H > f(\tilde{x}) - \tilde{x}$.
   d) F_{PTCC} *has two positive fixed points if either* $H = f(T) - T$ *(*T *and* x_+^**) or* $H = f(\tilde{x}) - \tilde{x}$ *(*T *and* $\tilde{x}$*).*

Proof. In view of (88), K is a fixed point of F_{PTCC} if and only if $K = f(K) \leqslant T$. Moreover, if $K \leqslant T$, then K is the only positive fixed point of F_{PTCC} because $F_{PTCC}(x) \geqslant \min\{f(x), T\} > x$ if $x < K$, and $F_{PTCC}(x) \leqslant f(x) < x$ if $x > K$.

If $T < K$, then there are two possibilities for the positive fixed points of F_{PTCC}: the threshold T and the positive equilibria of g.

It is obvious from the definition of F_{PTCC} that T is a fixed point if and only if $f(T) \leqslant T + H$, that is, $H \geqslant f(T) - T$. The condition $T < f(T)$ holds since $T < K$.

Since $g'(x) = f'(x)$ and $g''(x) = f''(x)$, g can have at most two positive fixed points $x_-^* \leqslant x_+^*$. Then, by the Mean Value Theorem, $x_-^* \leqslant \tilde{x} \leqslant x_+^*$, where $\tilde{x}$ is the only point for which $f'(\tilde{x}) = 1$. It also follows that $T < x_-^* \leqslant x_+^* < K$, because $x_-^* = F_{PTCC}(x_-^*) = g(x_-^*) = f(x_-^*) - H > T$, and $g(x) = f(x) - H \leqslant x - H < x$ for all $x \geqslant K$.

Now, statements 2 and 3 follow easily. We include the proof of 2 and omit the details of the other assertion since it is analogous, so assume that $\tilde{x} \leqslant T < K$.

If $H \geqslant f(T) - T$, then the threshold T is the unique equilibrium of F_{PTCC} because $g(T) = f(T) - H \leqslant T$ and, for $T \geqslant x_c$, it follows from $g'(x) < 1$ for all $x > T$; while for $T < x_c$, it follows from $g'(x) > 0$, $x < x_c$ and $g'(x) < 0$, $x > x_c$. See Figure 14 as an illustration of the proof.

If $H < f(T) - T$, then F_{PTCC} has a positive fixed point $x_+^* \in (T, K)$ because $g(T) = f(T) - H > T$ and $g(K) = f(K) - H = K - H < K$. This fixed point is unique because, if there were two fixed points $x_-^* < x_+^*$, then $T < x_-^*$ and $g(x) < x$ for all $x < x_-^*$ would imply that $g(T) < T$, a contradiction. □

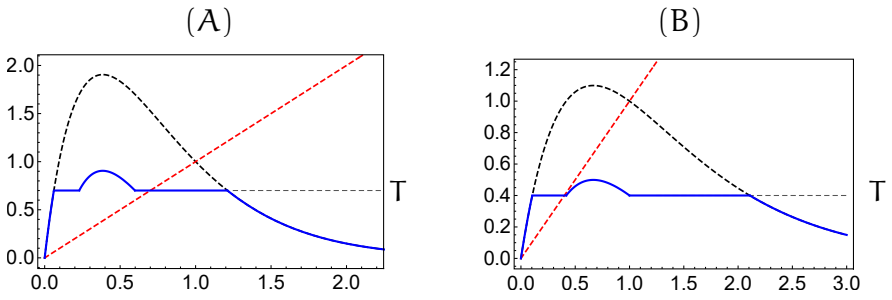

Figure 14: Illustration of the piecewise-smooth continuous map F_{PTCC} (blue solid line). We also plot the line $y = x$ (red, dashed) and the Ricker map $f(x) = rx/(1+x)$ (black, dashed). (A) : $r = 2.6$, $T = 0.7 \in (x_c, K) \approx (0.3846, 1)$, $H = 1 > f(T) - T \approx 0.827$. (B) : $r = 1.5$, $T = 0.4 \in (\tilde{x}, x_c) \approx (0.3969, 0.6667)$, $H = 0.6 > f(T) - T \approx 0.5838$.

Figure 15 illustrates the number of fixed points in the parameter plane (H, T).

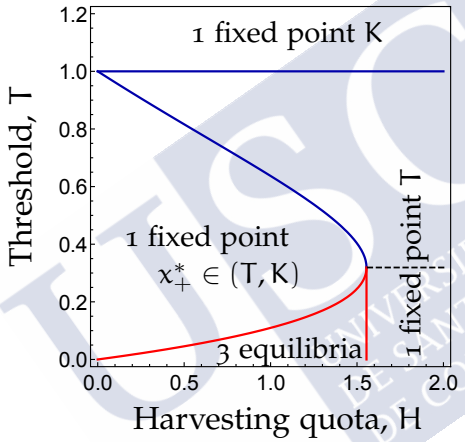

Figure 15: Number of positive equilibria of F_{PTCC} with $f(x) = xe^{2.6(1-x)}$. There are two positive fixed points for the parameter values in the boundaries colored in red: $H = f(T) - T$, $0 < T < \tilde{x}$; and $H = f(\tilde{x}) - \tilde{x}$, $0 < T < \tilde{x}$. There is only one positive fixed point for parameters at the boundaries colored in blue: $H = f(T) - T$, $\tilde{x} < T < 1$; and $T = 1$.

5.3.1.2 *Stability of positive fixed points*

This section is devoted to study the stability properties of the positive fixed points of F_{PTCC}. It is worth mentioning that, for a map f satisfying conditions **(A1)-(A2)**, 0 is a fixed point of F_{PTCC}, and it is always unstable.

We first consider the case $T \geqslant K$, for which we obtain a global stability result if f is a general map satisfying condition **(A1)**. The proof follows the one of the analogous result for proportional threshold harvesting (Hilker and Liz, 2019, Proposition A.3).

Theorem 5.3.2. *Assume that* f *satisfies* ***(A1)*** *and* K *is GAS for the difference equation* $x_{n+1} = f(x_n)$. *If* $T \geqslant K$, *then* K *is GAS for the model given by* F_{PTCC}.

Proof. To prove the theorem, let us show that the conditions of Lemma 4.2.4 are fulfilled with $h = f$ and $H = F_{PTCC}$.

First, by Proposition 5.3.1, K is the unique positive equilibrium of (88). In particular, $x < F_{PTCC}(x)$ for all $x < K$; and $x > F_{PTCC}(x)$ for all $x > K$.

Hence, the result is trivial for $x < K$, because $F_{PTCC}(x) \leqslant f(x) \leqslant \max\{f(x), K\}$ for all $x \geqslant 0$.

Now, it is clear by (88) that $F_{PTCC}(x) \geqslant \min\{f(x), T\}$, and therefore, since we are assuming that $T \geqslant K$, it follows that $x > F_{PTCC}(x) \geqslant \min\{f(x), T\} \geqslant \min\{f(x), K\}$ for all $x > K$. □

The case $0 < T < K$ deserves more attention, so that we divide the study into three parts: we first deal with the simplest case, that is, compensatory models; then we give some global stability results for general overcompensatory models; finally, we focus on the overcompensatory Ricker model to get a more comprehensive description of the stability properties of positive equilibria.

Compensatory models

Recall that the model (77) defined by $x_{n+1} = f(x_n)$ is compensatory if f satisfies **(A1)** and **(A2)** with $K \leqslant x_c$. This framework includes strictly increasing maps like the Beverton-Holt model and unimodal maps as the Ricker function $f(x) = xe^{r(1-x)}$, $0 < r \leqslant 1$.

Theorem 5.3.3. *Assume that* f *satisfies* ***(A1)*** *and* ***(A2)*** *with* $K \leqslant x_c$ *and let* $0 < T < K$ *and* $H > 0$. *Denote by* $x_-^* \leqslant x_+^*$ *the positive fixed points of* $g(x) = f(x) - H$ *when they exist. Then, every solution of* (88) *converges to an equilibrium. More specifically:*

1. *If* $H < f(T) - T$, *then there is a unique positive equilibrium* $x_+^* \in (T, K)$ *of* F_{PTCC} *and it is globally attracting.*

2. *If* $H \geqslant f(T) - T$ *and* $T \geqslant \tilde{x}$ *or* $H > f(\tilde{x}) - \tilde{x}$ *and* $T < \tilde{x}$; *then* T *is the unique positive equilibrium of* F_{PTCC} *and it is globally attracting.*

3. *If* $f(T) - T \leqslant H \leqslant f(\tilde{x}) - \tilde{x}$, *then there is bistability between two positive equilibria:* T *and* $x_+^* \in (T, K)$. *If* $H < f(\tilde{x}) - \tilde{x}$, *denote by* x_-^* *the largest fixed point of* F_{PTCC} *smaller than* x_+^*, *and* $(x_-^*)^{-1} = \min\{x \in F_{PTCC}^{-1}(x_-^*) : x > x_-^*\}$ *(*$(x_-^*)^{-1} = \infty$ *if there are no* $x > x_-^*$ *such that* $F_{PTCC}(x) = x_-^*$*).*

   - *If* $f(T) - T < H < f(\tilde{x}) - \tilde{x}$, *then the basin of attraction of the threshold* T *is* $(0, x_-^*) \cup ((x_-^*)^{-1}, \infty)$ *and the basin of attraction of* x_+^* *is* $(x_-^*, (x_-^*)^{-1})$.
   - *If* $H = f(\tilde{x}) - \tilde{x}$, *then* $x_+^* = x_-^* = \tilde{x}$ *is semistable and its basin of attraction is* $[x_-^*, (x_-^*)^{-1}]$.
   - *If* $H = f(T) - T$, *then* $T = x_-^*$ *and the basin of attraction of the threshold* T *is* $(0, x_-^*] \cup [(x_-^*)^{-1}, \infty)$.

Proof. The existence of positive fixed points follows directly from Proposition 5.3.1. The proofs of 1 and 2 follow from Lemma 4.2.2.

Then, we prove statement 3 when $f(T) - T < H < f(\tilde{x}) - \tilde{x}$ and the limit cases $H = f(\tilde{x}) - \tilde{x}$ and $H = f(T) - T$ are not described in detail. On the one hand, F_{PTCC} maps the interval $I = (x_-^*, (x_-^*)^{-1})$ into itself, and Lemma 4.2.2 ensures that x_+^* attracts I. On the other hand, F_{PTCC} maps the interval $L = (0, x_-^*)$ into itself, and Lemma 4.2.2 also applies to prove that T attracts L. Finally, it is clear that F_{PTCC} maps $((x_-^*)^{-1}, \infty)$ into L. □

Overcompensatory models: global stability results

In this subsection, we provide some sufficient conditions under which the positive equilibrium is unique and globally asymptotically stable. Since the compensatory case was previously studied, we deal with the overcompensatory case, thus we assume that conditions **(A1)-(A2)** hold with $x_c < K$. This framework includes unimodal maps as the Ricker function $f(x) = xe^{r(1-x)}$, for $r > 1$.

Our next result deals with sufficient conditions for the global stability of T ($T < K$).

Theorem 5.3.4. *Assume that* $T < K$ *and* $H \geqslant f(T) - T$. *If any of the following conditions holds, then* T *is the unique positive fixed point of* F_{PTCC} *and it is globally asymptotically stable:*

1. $T < \tilde{x}$ *and* $H > f(\tilde{x}) - \tilde{x}$;
2. $\tilde{x} \leqslant T \leqslant x_c$;
3. $f(x_c) - H \leqslant T < K$;
4. $f(g(x_c)) \geqslant T$ *and* $T > x_c$.

Proof. In all cases, it follows from Proposition 5.3.1 that T is the unique positive fixed point of F_{PTCC}.

In statements 1 and 2, it is easy to check that $x < F_{PTCC}(x) \leqslant T$ for $x < T$ and $0 < F_{PTCC}(x) < x$ for $x > T$. Hence, the result follows from Lemma 4.2.2.

Since the scheme (88) becomes TH when $H + T \geqslant f(x_c)$, in case 3 the result follows from Proposition 5.2.2.

Finally, condition $f(g(x_c)) \geqslant T$ in 4 implies that the long-term behavior of the solutions of (88) and equation $x_{n+1} = G(x_n)$, $n \geqslant 0$, is the same (see Figure 16), where

$$G(x) = \begin{cases} T, & g(x) \leqslant T; \\ g(x), & g(x) > T. \end{cases} \tag{92}$$

Since $T > x_c$ and $H \geqslant f(T) - T$, T is stable for G. By Lemma 4.2.1, to prove the global stability, it is enough to exclude periodic orbits of G with prime period 2. However, the conditions $T < x_c$ and $H \geqslant f(T) - T$ imply that $G(x) = T$ for all $x \geqslant T$, then G cannot have 2-periodic orbits. □

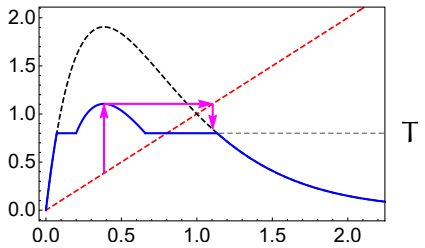

Figure 16: Illustration of the correspondence between asymptotic dynamics of the model given by the map G (92) and PTCC if $x_c < T < K$, $H \geqslant f(T) - T$ and $f(g(x_c)) \geqslant T$. We plot the Ricker map with $r = 2.6$ (black, dashed), the graph of F_{PTCC} for $T = 0.8$ and $H = 0.6 > f(T) - T \approx 0.5456$ (blue). The magenta arrows show that $f(g(x_c)) \geqslant T$. We also plot the line $y = x$ (red, dashed).

In the line of case 4 in the previous theorem, we can prove a global stability result for the fixed point x_+^* of F_{PTCC}, in case f is S-unimodal.

Theorem 5.3.5. *Assume that* $T < K$, $H < f(T) - T$ *and* f *is an S-unimodal map. If* $f(g(x_c)) \geqslant T$ *and* $g'(x_+^*) \geqslant -1$, *then the fixed point* x_+^* *of* F_{PTCC} *is GAS.*

Proof. Condition $H < f(T) - T$ implies that x_+^* is the unique positive fixed point of F_{PTCC}.

Since $f(g(x_c)) \geqslant T$, F_{PTCC} can be replaced by the map G defined in (92) for the analysis of convergence of solutions, as in the proof of Theorem 5.3.4 (see Figure 16). Now, the proof follows from Lemma 4.2.6, with $c = \min g^{-1}(T)$ and $d = \max g^{-1}(T)$. □

We illustrate the results of Theorems 5.3.4 and 5.3.5 in Figure 17.

Specific results for the Ricker map

In this subsection, we focus our attention on the PTCC scheme (88) with the Ricker map $f(x) = xe^{r(1-x)}$, $r > 1$, in order to give a more comprehensive description of the stability properties of the positive equilibria. Recall that the compensatory case $r \leqslant 1$ has been previously addressed.

We begin considering the case when the Ricker map has a stable equilibrium, that is, $f(x) = xe^{r(1-x)}$, $1 < r \leqslant 2$ (see Corollary 4.2.5). The following results prove that the asymptotic dynamics correspond to those of compensatory models, where every solution of the PTCC model (88) with $x_0 > 0$ converge to a positive equilibrium. We first deal with the case when F_{PTCC} has a unique positive fixed point. The global asymptotic stability of T when $0 < T \leqslant x_c$ was already proved in Theorem 5.3.4, so we work with the case $T > x_c$. Then, we consider parameter conditions under which F_{PTCC} has at least two positive fixed points.

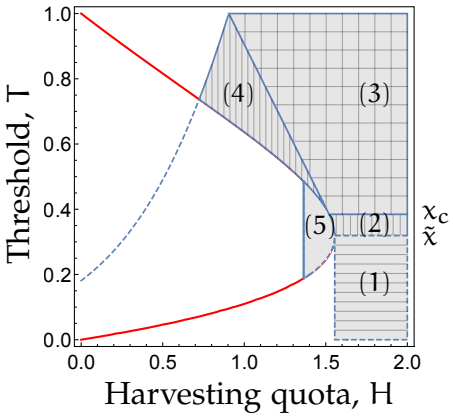

Figure 17: Regions of global stability for PTCC with the Ricker map $f(x) = xe^{2.6(1-x)}$, based on Theorems 5.3.4 and 5.3.5. The red solid curve is the graph of $H = f(T) - T$. T is GAS in the regions defined by $H \geqslant f(T) - T$ and $(1) : T < \tilde{x}$ and $H > f(\tilde{x}) - \tilde{x}$; (2): $\tilde{x} \leqslant T \leqslant x_c$; (3): $f(x_c) - H \leqslant T < K$; and $(4) : f(g(x_c)) \geqslant T$, $T > x_c$. Notice that, when $H < f(T) - T$, condition $f(g(x_c)) \geqslant T$ holds to the right of the dashed line, so x_+^* is GAS in region (5), determined by condition $g'(x_+^*) \geqslant -1$.

Theorem 5.3.6. *Assume that* $1 < r \leqslant 2$ *and denote by* $x_-^* \leqslant x_+^*$ *the positive fixed points of* g, *when they exist. The following assertions hold:*

1. *If* $H < f(T) - T$, *then* x_+^* *is the unique positive fixed point of* F_{PTCC} *and it is GAS.*

2. *If* $x_c < T < 1$ *and* $H \geqslant f(T) - T$ *then* T *is the unique positive fixed point of* F_{PTCC} *and it is GAS.*

Proof. The existence of a unique positive fixed point follows from Proposition 5.3.1. We provide a detailed proof for case 1 and illustrate the one for case 2 since it follows from analogous arguments (see Figure 18(B)). An application of the enveloping method by Cull in Lemma 4.2.3 for $h = F_{PTCC}$ proves both statements. The same approach was previously used in (Hilker and Liz, 2019, Proposition A.4) for proportional threshold harvesting.

Let us consider $T \in (0, 1)$, $H \in (0, f(T) - T)$ arbitrarily fixed and the linear map $\phi(x) = 2x_+^* - x$. Let us prove that F_{PTCC} fulfills the following inequalities: $x < F_{PTCC}(x) < \phi(x)$ for all $x \in (0, x_+^*)$, and $x > F_{PTCC}(x) > \phi(x)$ for all $x > x_+^*$ (see Figure 18(A)).

We know by Proposition 5.3.1 that x_+^* is the unique fixed point of F_{PTCC} in $(0, \infty)$. Moreover, $x < F_{PTCC}(x)$ for all $x \in (0, x_+^*)$ and $x > F_{PTCC}(x)$ for all $x > x_+^*$.

Hence, it remains to prove that $F_{PTCC}(x) < 2x_+^* - x$ for all $x \in (0, x_+^*)$ and $F_{PTCC}(x) > 2x_+^* - x$ for all $x > x_+^*$. Let us consider p_1 and p_2 the points such that

$$0 < p_1 < T < x_+^* < p_2, \quad g(p_1) = T = g(p_2).$$

Note that, for all $x \in (p_1, p_2)$, we have $F_{PTCC}(x) = g(x)$, so F_{PTCC} is differentiable on (p_1, p_2). We distinguish three cases:

- If $x \in (0, p_1]$, then $F_{PTCC}(x) = \min\{f(x), T\} \leqslant T < 2T - x < 2x_+^* - x$.
- If $x \in (p_1, p_2)$, then $F_{PTCC}(x) = g(x)$. By Corollary 4.2.5, $g'(x) \geqslant -1$ for all $x > 0$; moreover, $g'(x) > -1$ for all $x \neq 1$. Hence, the Mean Value Theorem guarantees that $g(x) \neq 2x_+^* - x$ for all $x \neq x_+^*$. Therefore, $g(x) < 2x_+^* - x$ for all $x \in (p_1, x_+^*)$ and $g(x) > 2x_+^* - x$ for all $x \in (x_+^*, \infty)$.
- If $x > p_2$, then we have $F_{PTCC}(x) > g(x) > 2x_+^* - x$.

An application of Cull's theorem proves that x_+^* is globally asymptotically stable. □

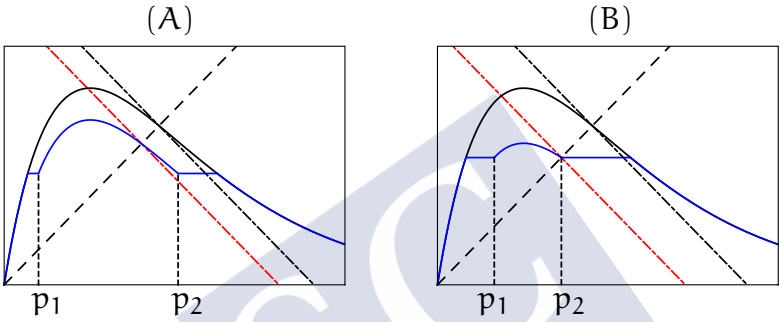

Figure 18: Diagrams showing the map F_{PTCC} (blue solid curve) enveloped by ϕ (red dot-dashed line). The original Ricker map $f(x) = xe^{1.8(1-x)}$ is represented by the solid black curve, which is enveloped by the black dot-dashed line $y = 2 - x$. The black dashed line is $y = x$. (A): $\phi(x) = 2x_+^* - x$. The equilibrium x_+^* is GAS for $T \in (0, 1)$ and $H \in (0, f(T) - T)$. (B): $\phi(x) = 2T - x$. The fixed point T is GAS for $T \in (x_c, 1)$ and $H \geqslant f(T) - T$.

Theorem 5.3.7. *Assume* $1 < r \leqslant 2$, $T < \tilde{x}$, *and* F_{PTCC} *has at least one positive fixed point different from* T. *Denote by* $x_-^* \leqslant x_+^*$ *the positive fixed points of* g. *If* $H \geqslant f(T) - T$, *then* T *is a fixed point of* F_{PTCC} *and we distinguish three cases:*

- *If* $f(T) - T < H < f(\tilde{x}) - \tilde{x}$, *then* x_+^* *attracts* $(x_-^*, (x_-^*)^{-1})$ *and* T *attracts* $(0, x_-^*) \cup ((x_-^*)^{-1}, \infty)$, *where* $(x_-^*)^{-1} = \max g^{-1}(x_-^*)$.
- *If* $H = f(\tilde{x}) - \tilde{x}$, *then there are two fixed points* $T < x_-^* = x_+^*$, x_+^* *attracts* $[x_-^*, (x_-^*)^{-1}]$, *while* T *attracts* $(0, x_-^*) \cup ((x_-^*)^{-1}, \infty)$.
- *If* $H = f(T) - T$, *then there are two fixed points* $T = x_-^* < x_+^*$, x_+^* *attracts* $(x_-^*, (x_-^*)^{-1})$, *while* T *attracts* $(0, x_-^*] \cup [(x_-^*)^{-1}, \infty)$.

Proof. The proof of this result partially follows the one of case 3 in Theorem 5.3.3, that is, the analogous result for compensatory models. The main difference appears when determining the basin of attraction of the positive equilibrium x_+^*. We give a detailed proof when $f(T) - T \leqslant H < f(\tilde{x}) - \tilde{x}$ and we skip the case $H = f(\tilde{x}) - \tilde{x}$ because it is very similar.

First, recall that, by using Lemma 4.2.2, we can prove that the threshold T attracts $(0, x_-^*] \cup [(x_-^*)^{-1}, \infty)$ if $H = f(T) - T$; or the set $(0, x_-^*) \cup ((x_-^*)^{-1}, \infty)$ if $f(T) - T < H < f(\tilde{x}) - \tilde{x}$.

Now, let as prove that $(x_-^*, (x_-^*)^{-1})$ is the basin of attraction of x_+^*. Notice that $F_{PTCC} = g$ in $(x_-^*, (x_-^*)^{-1})$, so we can use the properties of the map g. As $\tilde{x} < x_+^* < K$, by Corollary 4.2.5, $g'(x_+^*) \in (-1, 1)$. In addition, g is S-unimodal and has a unique critical point $x_c \in (x_-^*, (x_-^*)^{-1})$. Thus, if we shift the origin of coordinates from $(0, 0)$ to (x_-^*, x_-^*), the results follows from the application of Theorem 2.7 and *Addendum* in (Singer, 1978) to $g_{|[x_-^*, (x_-^*)^{-1}]}$. □

Now, we state and proof the main result in this subsection, which includes the stability results already proved and new statements for the case when $r > 2$, for which the equilibrium of the Ricker map is unstable. From the properties of the Ricker map in Corollary 4.2.5 and its proof; if $r > 2$, then there exists a unique $\bar{x} \in (x_c, 2/r)$ such that $f'(x) \in (-1, 0)$ for all $x \in (x_c, \bar{x})$; $f'(\bar{x}) = -1$; and $f'(x) < -1$ for all $x \in (\bar{x}, 1)$. The value of $\bar{x}$ can be numerically computed as the smallest root of the equation $f'(x) = -1$, that is, the unique solution of $(rx - 1)\, e^{r(1-x)} = 1$ in $(0, 1)$.

Theorem 5.3.8. *Consider the map F_{PTCC} defined by (88) with $f(x) = xe^{r(1-x)}$, $r > 1$. Denote by x_-^*, x_+^* the positive fixed points of $g(x) = f(x) - H$, when they exist, with $T \leqslant x_-^* \leqslant x_+^*$.*

1. *If $T \geqslant K = 1$, then the positive fixed point $K = 1$ of f is the unique positive equilibrium of F_{PTCC}. It is GAS if $1 < r \leqslant 2$, and unstable if $r > 2$.*

2. *If $T < K = 1$ and $1 < r \leqslant 2$, then the conclusions 1, 2 and 3 of Theorem 5.3.3 hold. In particular, every solution of (88) with initial condition $x_0 > 0$ converges to a positive equilibrium.*

3. *If $T < K = 1$ and $r > 2$, then:*
   - *If $H \geqslant f(T) - T$, then T is a fixed point of F_{PTCC}. Moreover, T is semi-stable if $0 < T < \tilde{x}$ and $H = f(T) - T$, and it is asymptotically stable otherwise. The threshold T is a GAS in the cases stated in Theorem 5.3.4 (see Figure 17).*
   - *The fixed point x_-^* is unstable if $x_-^* < x_+^*$, and semi-stable if $x_-^* = x_+^*$.*
   - *The fixed point $x_+^* \in (\tilde{x}, 1)$ is unstable if $H < f(\bar{x}) - \bar{x}$, and asymptotically stable if $H \geqslant f(\bar{x}) - \bar{x}$. In the latter case, x_+^* is GAS if $H < f(T) - T$ and $f(g(x_c)) \geqslant T$.*

Proof. The existence of the different fixed points of F_{PTCC} is given in Proposition 5.3.1. The proof of statement 1 follows from Theorem 5.3.2 and Corollary 4.2.5. The proof of statement 2 follows from Theorems 5.3.4, 5.3.6 and 5.3.7.

Next we consider the three cases of statement 3:

- First, we deal with the stability of the threshold value T.
  On the one hand, if $H > f(T) - T$, then T is asymptotically stable because F_{PTCC} is differentiable on an interval $(T-\varepsilon, T+\varepsilon)$, and $f'(T) = 0$.
  On the other hand, when $H = f(T) - T$, we distinguish several cases:
  - First, if $T > x_c$, then there exists $m_1 > 0$ such that $F_{PTCC}(x) = T$ for all $x \in [T, T+m_1)$, which, by continuity, implies that there exists $m_2 > 0$ such that $F^2_{PTCC}(x) = T$ for all $x \in (T-m_2, T)$; therefore T is asymptotically stable.
  - Next, if $\tilde{x} \leqslant T \leqslant x_c$, then T is the unique positive fixed point of F_{PTCC}, and it is globally stable (see Theorem 5.3.4).
  - When $T \in (0, \tilde{x})$, T is semi-stable because there is $\eta > 0$ such that $F_{PTCC}(x) = T$ for $x \in (T-\eta, T]$, $F_{PTCC}(x) \neq T$ for $x \in (T, T+\eta)$ and $F'_{PTCC}(T^+) > 1$.

- As for the smallest fixed point of g, if $x^*_- < x^*_+$, then $F_{PTCC}(x) = g(x)$ on a neighborhood of x^*_- and $x^*_- < \tilde{x}$. Hence, $F'_{PTCC}(x^*_-) = f'(x^*_-) > 1$ and we can assert that x^*_- is unstable. When x^*_- and x^*_+ collide, there is a smooth saddle-node bifurcation and x^*_- is semistable.

- Finally, we address the stability of $x^*_+ \in (\tilde{x}, 1)$. As $F_{PTCC}(x) = g(x)$ on a neighborhood of x^*_+, the local asymptotic stability of x^*_+ depends on $g'(x^*_+) = f'(x^*_+)$. Since $x^*_+ \in (\tilde{x}, K)$, it is clear that x^*_+ is asymptotically stable if $x^*_+ \leqslant \overline{x}$ (that is, $H \geqslant f(\overline{x}) - \overline{x}$), and unstable if $x^*_+ > \overline{x}$ (that is, $H < f(\overline{x}) - \overline{x}$). The global stability result follows from Theorem 5.3.5.

□

5.3.1.3 *Fixed points smooth and border-collision bifurcations*

The boundaries found in Subsection 5.3.1.1 and the stability results proved in Subsection 5.3.1.2 help us to analyze the possible local bifurcations of fixed points, using the bifurcation parameters H and T.

Since the map F_{PTCC} is piecewise-smooth continuous, the bifurcations can be smooth but most of them are border-collisions.

Smooth bifurcations occur for the bifurcation parameter H:

- A fold SB occurs if $H = f(\tilde{x}) - \tilde{x}$ and $T < \tilde{x}$: as H increases, the two coexisting fixed points of g (x^*_+ LAS and x^*_- unstable) collide at the critical point $\tilde{x}$ and then disappear.

- A flip SB occurs if $H = f(\overline{x}) - \overline{x}$ and $T < K$: as H decreases, the LAS fixed point x^*_+ becomes unstable and a LAS 2-cycle emerges.

Now, we describe the different types of border-collision bifurcations for PTCC. We first recall that F_{PTCC} is a piecewise-smooth map defined by f, g and the constant function T; as a consequence F_{PTCC} can have admissible or virtual fixed

points. For example, the fixed point T is admissible if and only if $T \leqslant K$ and $H \geqslant f(T) - T$; otherwise it is virtual since it is not a fixed point of F_{PTCC}. Recall that a BCB occurs when a fixed point transitioning from being virtual to admissible (or viceversa) collides with a break point and leads to a qualitative change in the long-term dynamics. For PTCC model (88) and a map f satisfying conditions **(A1)-(A2)**, these bifurcations can only occur when T becomes a boundary fixed point, that is, when $g(T) = T$ (equivalently, $H = f(T) - T$) or $f(T) = T$ (equivalently, $T = K$).

When $H = f(T) - T$, the first three BCBs described in Subsection 4.3 can occur as T or H change continuously. See Figure 19 for illustrations. In particular:

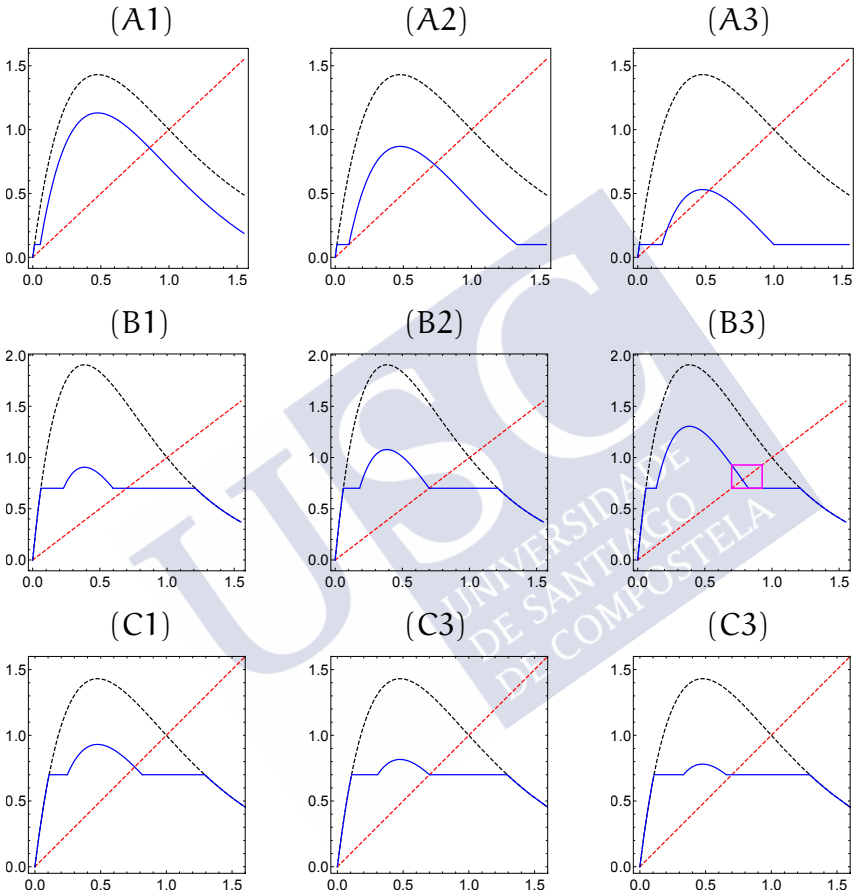

Figure 19: Illustrations of BCBs arising when $H = f(T) - T$ in (88). The Ricker map $f(x) = xe^{r(1-x)}$ is the black dashed curve, while the blue solid curve is the corresponding map F_{PTCC}. The red dashed line is $y = x$. Top row: fold BCB for $r = 2.1$ and $T = 0.1 < \tilde{x} \approx 0.353$. (A1): $H = 0.3 < f(T) - T \approx 0.562$; (A2): $H = f(T) - T$; (A3): $H = 0.9 > f(T) - T$. Center row: flip or period-doubling BCB for $r = 2.6$ and $T = 0.7 > \bar{x} \approx 0.485$. The attracting 2-cycle is represented by a magenta box in (B3). (B1): $H = 1 > f(T) - T \approx 0.827$; (B2): $H = f(T) - T$; (B3): $H = 0.6 < f(T) - T$. Bottom row: persistence BCB for $r = 2.1$ and $T = 0.7$ ($\tilde{x} < T < \bar{x} \approx 0.77$). (C1): $H = 0.5 < f(T) - T \approx 0.614$; (C2): $H = f(T) - T$; (C3): $H = 0.65 > f(T) - T$.

- A fold BCB occurs if $H = f(T) - T$ and $T < \tilde{x}$: T becomes a boundary fixed point as T decreases or H increases; after this critical value, two admissible fixed points arise: an attractor T, and a repeller x^*_-.

- A flip BCB occurs if $H = f(T) - T$, $T > x_c$, and x^*_+ is unstable for g: the attracting fixed point T becomes virtual after becoming a boundary fixed point as T or H decrease, while an unstable fixed point x^*_+ and an attracting 2-cycle $\{T, g(T)\}$ appear. Notice that the flat shape of F_{PTCC} to the right of the break point prevents the possibility of a period-multiplying BCB in our framework.

- A persistence BCB occurs if $H = f(T) - T$, $T \geqslant \tilde{x}$, and x^*_+ is asymptotically stable for g: as T or H increase, the virtual fixed point T and the admissible attractor x^*_+ interchange their roles.

In view of Theorem 5.3.8, for a Ricker map $f(x) = x\, e^{r(1-x)}$, with $r > 2$: a flip BCB occurs when $H = f(T) - T$ and $T > \bar{x}$, and a persistence BCB occurs when $H = f(T) - T$ and $\tilde{x} \leqslant T \leqslant \bar{x}$.

When T becomes a boundary fixed point at the critical value $T = K$, it only makes sense to choose T as the bifurcation parameter; in this case, persistence or flip BCBs can occur as T changes continuously. These bifurcations are typical of threshold harvesting (Hilker and Liz, 2020; Sinha, 1994). In particular:

- A persistence BCB occurs if $T = K$ and K is asymptotically stable for f: as T increases, the fixed point T becomes virtual and the attracting fixed point K becomes admissible.

- A flip BCB occurs if $T = K$ and K is unstable for f: as T increases, the fixed point T becomes virtual, K becomes admissible, and an attracting 2-cycle $\{T, f(T)\}$ emerges (see Figure 20).

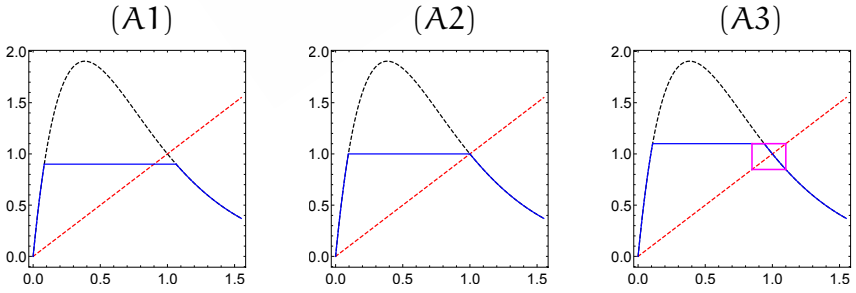

Figure 20: Illustration of a flip BCB in equation (88) when $T = K$. The Ricker map $f(x) = xe^{2.6(1-x)}$ is the black dashed curve, while the blue solid curve is the corresponding map F_{PTCC} with $H = 1.6$. The red dashed line is $y = x$. The attracting 2-cycle $\{T, f(T)\}$ is represented by a magenta box in panel (A3). (A1): $T = 0.9 < K = 1$; (A2): $T = K$; (A3): $T = 1.1 > K$.

For the Ricker map, a persistence BCB occurs if $T = 1$ and $0 < r \leqslant 2$, and a flip BCB occurs if $T = 1$ and $r > 2$.

In Figures 21 and 23, we use solid lines for BCBs of fixed points, and dashed lines for SBs of fixed points. Specifically, we use red color for fold bifurcations, orange for persistence BCBs, and brown for flip bifurcations.

5.3.2 *Complex dynamics: essential attraction and chaotic behavior*

The long-term dynamics of PTCC when the map f is compensatory are completely determined: every initial condition $x_0 > 0$ converges to a positive equilibrium. There are three regions of global asymptotic stability of x_+^*, T or K; and a region of bistability between T and x_+^*. For the overcompensatory Ricker map $f(x) = xe^{r(1-x)}$, $1 < r \leqslant 2$, whose positive equilibrium K is stable, we proved that asymptotic dynamics under PTCC scheme correspond to those for compensatory models. However, for general overcompensatory maps, asymptotic dynamics can become more complex.

In this section, for a general map $f : [0,\infty) \longrightarrow [0,\infty)$, we assume $f \in \mathcal{C}^3$ satisfies conditions **(A1)-(A2)** with $x_c < K$ and has negative Schwarzian derivative (S-unimodal). We consider the regions of the parameter plane (H,T) where complex dynamics are more likely to occur: $T < \tilde{x}$ and $H > f(T) - T$; or $H < f(T) - T$.

First, we consider the case $T < \tilde{x}$ and $H > f(T) - T$. Shifting the origin of coordinates from $(0,0)$ to (T,T), we show that the dynamics of (88) can be derived from the results obtained by Schreiber (2001) for constant quota harvesting models.

Theorem 5.3.9. *If F_{PTCC} has at least 2 positive fixed points, let*

$$x_-^* = \min\{x : x > 0,\ g(x) = x\} \ \text{ and } \ (x_-^*)^{-1} = \max g^{-1}(x_-^*).$$

Assume that $T < \tilde{x}$ and $H > f(T) - T$. Then, there are three generic categories for the dynamics of (88):

1. (Global attraction) *If $H > f(\tilde{x}) - \tilde{x}$, then T is the only positive fixed point of F_{PTCC}, and it is GAS.*

2. (Bistability) *If $H < f(\tilde{x}) - \tilde{x}$ and $g^2(x_c) > x_-^*$, then F_{PTCC} has three positive fixed points $T < x_-^* < x_+^*$.*
   T is asymptotically stable with basin of attraction $(0, x_-^*) \cup ((x_-^*)^{-1}, \infty)$; and x_-^* is unstable. Moreover,
   - *if $g'(x_+^*) \geqslant -1$, then x_+^* is asymptotically stable and attracts $(x_-^*, (x_-^*)^{-1})$ and, hence, every solution of (88) converges to a fixed point;*
   - *if $g'(x_+^*) < -1$, then the interval $[g^2(x_c), g(x_c)]$ is absorbing, with basin of attraction $(x_-^*, (x_-^*)^{-1})$.*

3. (Essential attraction) *If $H < f(\tilde{x}) - \tilde{x}$ and $g^2(x_c) < x_-^*$, then F_{PTCC} has three positive fixed points and T is an essential global attractor.*

Proof. It is clear that the long-term behavior of the solutions of (88) and equation $x_{n+1} = G(x_n)$, $n \geqslant 0$, is the same, where G was defined in (92). If we shift the origin of coordinates from $(0,0)$ to (T,T), then the map G satisfies assumptions (A1)-(A5) in (Schreiber, 2001). Thus, the proof follows from Lemma 1 and Theorem 1 therein. □

When H is the bifurcation parameter, the transition from bistability to global attraction of T occurs through a smooth fold bifurcation when x_-^* and x_+^* collide for $H = f(\tilde{x}) - \tilde{x}$. For this critical value, F_{PTCC} has two positive fixed points T and x_-^*; x_-^* is semi-stable with basin of attraction $[x_-^*, (x_-^*)^{-1}]$, and T attracts $(0, x_-^*) \cup ((x_-^*)^{-1}, \infty)$.
The transition between bistability and essential attraction occurs through a boundary-collision when $H < f(\tilde{x}) - \tilde{x}$ and $g^2(x_c) = x_-^*$ is considered at the end of this subsection.

We now deal with the case $H < f(T) - T$ (when T is a virtual fixed point). An important issue in this case is the relative position between $g^2(x_c)$ and T. If $g^2(x_c) > T$, then the long-term behavior of the solutions of (88) is governed by the map g; and we have two possibilities:

- if $g(x_c) \leqslant x_c$, then x_+^* is GAS by Lemma 4.2.2;
- if $g(x_c) > x_c$ then $I = [g^2(x_c), g(x_c)]$ is an absorbing interval whose basin of attraction is $(0, \infty)$.

When $g^2(x_c) = T$, two types of bifurcations can occur, a boundary-collision bifurcation or a persistence BCB. In the following, we provide further details about these bifurcations.

Boundary-collision bifurcations

The results stated in this subsection and the work by Schreiber (2001) help us to describe boundary-collision bifurcations for PTCC.

We first consider the case $T < \tilde{x}$, $H > f(T) - T$ and $g^2(x_c) = x_-^*$. Schreiber (2001) refers to the corresponding dynamics as *chaotic* semi-stability, because the interval $I = [g^2(x_c), g(x_c)] = [x_-^*, g(x_c)]$ is invariant and F_{PTCC} is chaotic in I. Actually, there is a homoclinic orbit containing the critical point x_c (see Appendix C in (Liz, 2010a) for further comments). Thus, the chaotic attractor collides with the unstable equilibrium x_-^* and, following the notation by Grebogi, Ott, and Yorke (1982), we can assert that the transition from bistability to essential attraction of T occurs through a boundary crisis. Therefore, this boundary-collision is not due to the non-smooth character of F_{PTCC}.

Let us consider the case $H < f(T) - T$ and $g^2(x_c) = T$. In this case, the bifurcations occur due to the discontinuity of F_{PTCC}.
If I does not contain any periodic attractor when $g^2(x_c) = T$, then the unique metric attractor of g consists of a finite union of intervals with a dense orbit (Thunberg, 2001, Section II.3), and a new form of boundary-collision bifurcation occurs at this point, when the metric attractor collides with the break point

T (see Figure 27). We will refer to this bifurcation as *discontinuity-induced crisis*. If g has an m-periodic attractor when $g^2(x_c) = T$, then a persistence BCB (for F^m_{PTCC}) occurs when this orbit collides with T, that is, when $g^m(T) = T$. In this case, a sequence of period-doubling and period-halving bifurcations giving rise to bubbles (Bier and Bountis, 1984) appear in the bifurcation diagram (see Figure 28).

5.3.3 *Impact of harvest parameters on population dynamics*

For a compensatory, overcompensatory or S-unimodal map f, the results obtained in the previous subsections give us a good description of long-term dynamics for the PTCC model (88).

In the case of compensatory models, the long-term dynamics are completely determined and we give a global picture of asymptotic dynamics in the 2-parameter bifurcation diagram in Figure 21. However, there are still some interesting features occurring in 1-parameter BDs (see Figure 22).

For overcompensatory models, the dynamics are richer than those exhibited by compensatory models. Moreover, the global picture of asymptotic dynamics depends on the expression of the unmanaged map f. Thus, we develop the study of global dynamics and construct 2-parameter and 1-parameter BDs for the Ricker map $f(x) = xe^{2.6(1-x)}$.

5.3.3.1 *Compensatory models*

We begin with the simple case of compensatory models. In the light of Theorem 5.3.8, analogous dynamics is exhibited by the overcompensatory Ricker map if $1 < r \leqslant 2$.

For illustrations, we consider the Ricker map $f(x) = x\, e^{r(1-x)}$, $r = 0.3 < 1$. The corresponding 2-parameter bifurcation diagram follows from Theorems 5.3.2 and 5.3.3, and it is shown in Figure 21.

We show in Figure 22 the three relevant possibilities for 1-parameter BDs as one of the harvesting parameters H or T changes.

The values of the bifurcation points are easily found. We first compute numerically the value $\tilde{x} \approx 0.4808$ such that $f'(\tilde{x}) = 1$.

We begin fixing two values of threshold T and we use the harvesting quota H as the bifurcation parameter.

For $T = 0.1$, a fold BCB occurs at $H = H_1 = f(T) - T \approx 0.031$, and a fold SB occurs at $H = H_2 = f(\tilde{x}) - \tilde{x} \approx 0.081$. Bistability between H_1 and H_2 induces hysteresis, which can have unexpected consequences for management: assume we increase the harvesting quota from a value slightly smaller than H_2; then, at $H = H_2$, the population falls abruptly to the threshold level $T = 0.1$. Then, we decrease again the quota, but relatively high levels of population abundance might not be recovered until $H < H_1$ (see Figure 22(A)).

If $T > \tilde{x}$, then there is always a GAS equilibrium, with a persistence BCB at $H = f(T) - T$; in Figure 22(B), we show the case $T = 0.6$, with $f(T) - T \approx 0.076$.

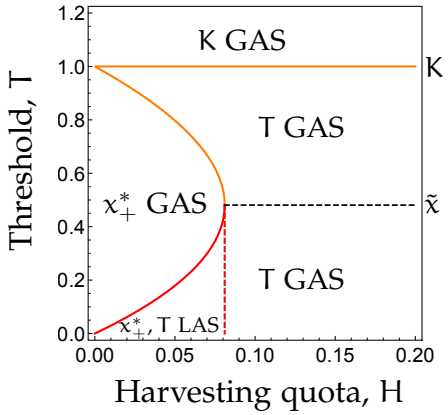

Figure 21: Stability diagram of PTCC with the Ricker map $f(x) = xe^{0.3(1-x)}$. There is a region of bistability, while in the others there is a unique equilibrium, which is GAS. We use orange color for persistence BCBs and red color for fold bifurcations (the solid curve corresponds to a fold BCB, and the dashed line to a fold SB).

When we use T as the bifurcation parameter, the most interesting case occurs when $H < f(\tilde{x}) - \tilde{x}$. For $H = 0.04$ and small T, there are three equilibria: T and the two positive fixed points $x_-^* \approx 0.135$ and $x_+^* \approx 0.846$ of g. T and x_+^* are LAS, and x_-^* is unstable. At the critical value $T = x_-^*$, x_-^* and T become virtual fixed points through a fold BCB, and x_+^* becomes GAS until $T = x_+^*$, where a persistence BCB occurs and T becomes GAS. A new persistence BCB occurs at $T = 1$, and, after that, the positive equilibrium $K = 1$ of f is GAS (Figure 22(C)).

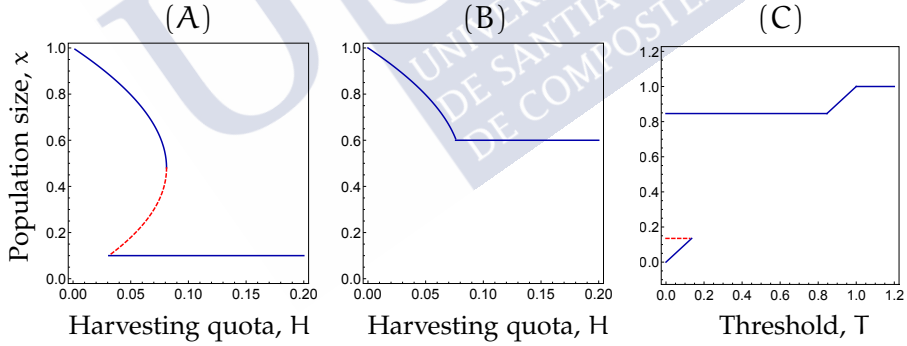

Figure 22: Bifurcation diagrams for the PTCC model (88) with the Ricker map $f(x) = x\,e^{0.3(1-x)}$. Red dashed lines correspond to unstable equilibria. (A): $T = 0.1 < \tilde{x}$: as harvesting quota increases, there is a fold BCB and a fold SB; bistability occurs between the two bifurcation points. (B): $T = 0.6 > \tilde{x}$: as harvesting quota increases, there is a persistence BCB. (C): $H = 0.04 < f(\tilde{x}) - \tilde{x}$: as the threshold increases, there is a fold BCB and two persistence BCBs. Bistability is observed until the first bifurcation point.

5.3.3.2 *Overcompensatory models*

In this section, we show some interesting phenomena that can be observed in (88) for overcompensatory maps. For that purpose, we consider the Ricker

map $f(x) = xe^{r(1-x)}$, $r = 2.6$, whose asymptotic dynamics are governed by an attracting 4-cycle. We have chosen this value for r because it has been used by Sinha and Parthasarathy (1996) and Schreiber (2001) for the CC rule, and by Hilker and Liz (2020) for TH, which can be seen as particular cases of PTCC. In this way, it is easier to relate our results with those in the previous references. Although we expect more complicated dynamics for larger values of r, for which f is chaotic, our case study also shows transitions between order and chaos. As shown by Schreiber (2001) (see also (Jiménez López and Liz, 2021)), maps with a periodic attractor can exhibit chaos when CC is applied.

We have seen that, for compensatory models, the dynamics of (88) are trivial in the sense that all solutions converge to an equilibrium. In the overcompensatory case, when $T < \tilde{x}$, boundary collisions can drive the system from a periodic or essential attractor to chaos as H increases. Moreover, the BCBs are not only determined by the pairs (H, T) for which T is a boundary fixed point; an important role is played by the pairs for which T is a boundary fixed point of F^2_{PTCC}. It may also occur that T is a boundary fixed point of F^4_{PTCC}, but for simplicity we restrict our analysis to bifurcations of 2-cycles. After the study of BCBs for F^2_{PTCC}, we devote some lines to describe the different bistability regions in Figure 23; then we plot some numerical 1-parameter BD, which help to understand the main features of the dynamics; and we finally discuss the influence of the threshold on the dynamics.

The 2-parameter bifurcation diagram in Figure 23 describes quite well the long-term dynamics and bifurcations of (88) in terms of the relevant parameters H and T. It follows from the stability results in Subsection 5.3.1.2; the smooth and border-collision bifurcations of fixed points in Subsection 5.3.1.3; the complex dynamics determined in Subsection 5.3.2 for $T < \tilde{x}$ and the local bifurcations for F^2_{PTCC} discussed in this subsection.

2-cycles smooth and border-collision bifurcations

In this section, we determine the local bifurcations of 2-cycles for F_{PTCC}, that is, those of fixed points for F^2_{PTCC}, first BCBs and then SBs.

Specific border-collision bifurcations for F^2_{PTCC} are determined by the solutions of $F^2_{PTCC}(T) = T$ (with $F_{PTCC}(T) \neq T$), so there are four cases:

1. If $T > K = 1$ and $f^2(T) = T$, then the 2-cycle $\{T, f(T)\}$ becomes attracting as T decreases for a fixed H, through a flip BCB.

2. If $T > K = 1$ and $g(f(T)) = T$, then the 2-cycle $\{T, f(T)\}$ emerges or disappears as H or T change continuously in a variety of BCBs (fold, persistence, flip).

3. If $T < K = 1$ and $f(g(T)) = T$, with $T < g(T)$, then the 2-cycle $\{T, g(T)\}$ emerges or disappears as H or T change continuously in a variety of BCBs (fold, persistence, flip).

4. If $T < K = 1$ and $g^2(T) = T$, with $T < g(T)$, then the 2-cycle $\{T, g(T)\}$ emerges or disappears as H or T change continuously, through a flip BCB.

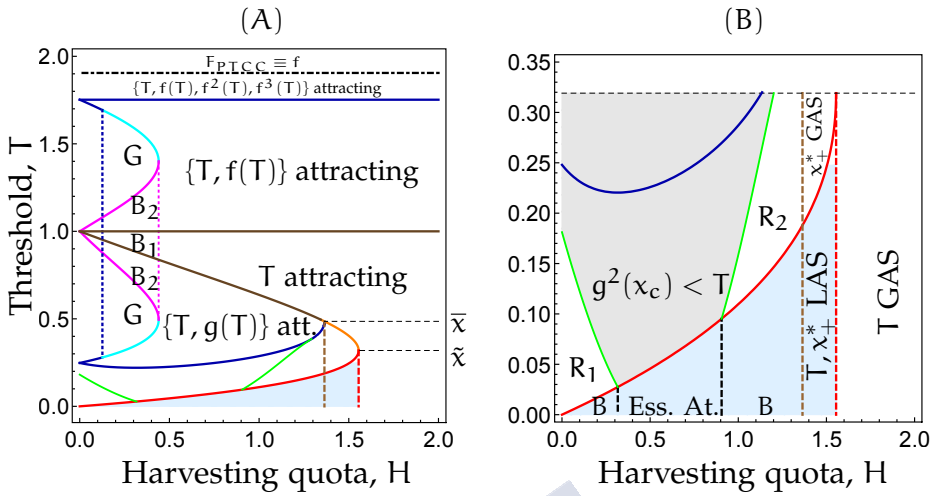

Figure 23: (A): Main bifurcation boundaries of PTCC control rule with the Ricker map $f(x) = xe^{2.6(1-x)}$. We use solid lines for border-collision bifurcations (BCBs) and dashed or dotted lines for smooth bifurcations (SBs). Bifurcations of fixed points: red for fold BCB, orange for persistence BCB, brown for flip BCB, brown dashed for flip SB, red dashed for fold SB. Bifurcations of 2-cycles: magenta for fold BCB, light blue for persistence BCB, dark blue for flip BCB, blue dotted for flip SB, magenta dotted for fold SB. The dot-dashed black line is defined by $T = f(x_c)$, so $F_{PTCC} \equiv f$ for larger values of T. Regions labelled with B_1 and B_2 exhibit bistability, while in regions labelled with G there is a 2-periodic attractor $p_1 \to g(p_1) = p_2 \to f(p_2) = p_1$ (see the text). The blue shadowed region and the green lines are explained in (B).
(B): Zoom of (A) for $0 < T < \tilde{x}$. According to the results in Subsection 5.3.2, when $f(T) - T < H < f(\tilde{x}) - \tilde{x}$ and $T < \tilde{x}$ (blue shadowed region), we find regions of bistability between T and a periodic or chaotic attractor (marked with B); bistability between T and other equilibrium x_+^*; and essential attraction to T. The green lines for $H < f(T) - T$ (where T is not a fixed point) are defined by $g^2(x_c) = T$. Complex behavior may be expected to appear in regions B, R_1 and R_2.

In Figure 23(A), we represent BCBs for F_{PTCC}^2 with solid lines: magenta color for fold BCBs, light blue for persistence BCBs, and dark blue for flip BCBs.

Figure 24 illustrates a fold BCB corresponding to case 2: as H increases and crosses the magenta bifurcation curve in Figure 23(A), the virtual cycle $\{T, f(T)\}$ becomes an admissible cycle of F_{PTCC} after collision with a virtual fixed point of F_{PTCC}^2 (a fixed point of $g \circ f$). After the bifurcation occurs, the cycle $\{T, f(T)\}$ coexists with two admissible stable and unstable 2-cycles (which are destroyed for a larger value of H through a fold smooth bifurcation for F_{PTCC}^2).

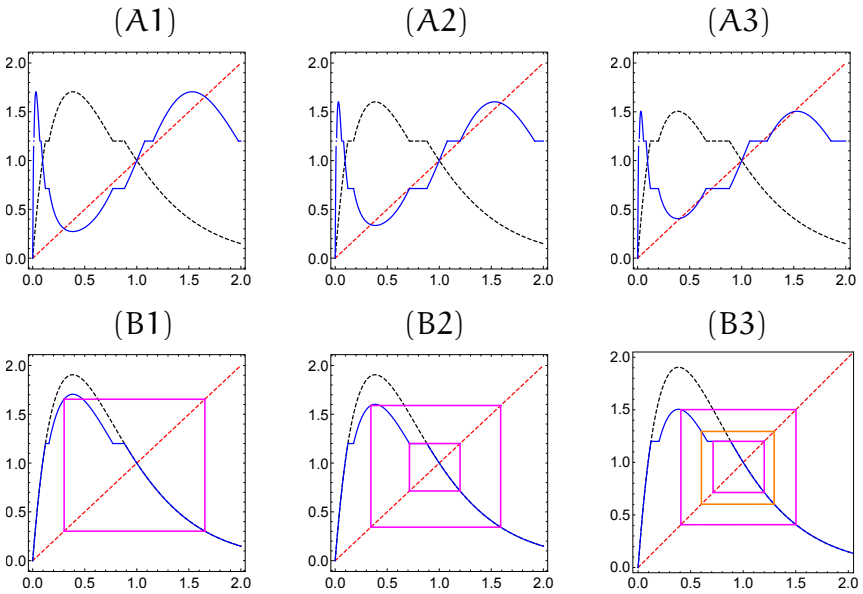

Figure 24: Illustration of a fold BCB for F^2_{PTCC} in equation (88) with the Ricker map $f(x) = xe^{2.6(1-x)}$ and $T = 1.2$. The red dashed line is $y = x$. Top row: the black dashed curve is the graph of F_{PTCC}, and the blue solid curve is the graph of F^2_{PTCC}. (A1): $H = 0.2$; (A2): critical value $H = 0.303$, when $F^2_{PTCC}(T) = g(f(T)) = T$; (A3): $H = 0.4$. Bottom row: the black dashed curve is the graph of f, while the blue solid curve is the graph of F_{PTCC}. Attracting or semistable 2-cycles of F_{PTCC} are represented by magenta boxes; unstable 2-cycles in orange boxes. (B1): $H = 0.2$ (one attracting cycle, corresponding to region G in Figure 23); (B2): $H = 0.303$ (the attracting 2-cycle persists, and a new 2-cycle $\{T, f(T)\}$ arises at the fold BCB and it is semistable; it corresponds to the magenta curve between regions G and B_2 in Figure 23); (B3): $H = 0.4$ (bistability between two attracting cycles, corresponding to region B_2 in Figure 23).

Now, we describe the smooth bifurcations which occur for the bifurcation parameter H:

- A fold SB occurs at $H_* \approx 0.44$: as H increases, the two coexisting stable and unstable fixed points of $f \circ g$ collide and then disappear.
- A flip SB occurs at $H^* \approx 0.126$: as H increases, the LAS 4-cycle of F_{PTCC} becomes unstable and a LAS 2-cycle of $f \circ g$ emerges.

The value H_* is numerically determined as the solution of system $f(g(x)) = x$, $f'(g(x))\, g'(x) = 1$; and H^* as the solution of $f(g(x)) = x$, $f'(g(x))\, g'(x) = -1$. In Figure 23(A) we use dotted lines for SBs of 2-cycles, magenta for fold and dark blue for flip.

Remark 9. We conjecture that T is GAS for equation (88) with the Ricker map $f(x) = xe^{2.6(1-x)}$ if (H, T) belongs to the region

$$R = \{(H, T) : H > H_*(r),\ H \geqslant f(T) - T,\ x_c < T < 1\}.$$

This would complete the global stability region shown in Figure 17.

The graph of the function $r \to H_*(r)$ can be plotted numerically, and it is an increasing function of r, with $H_*(2^+) = 0$. Recall that, by Theorem 5.3.8, F_{PTCC} does not have other 2-cycles than the fixed points if $r \leqslant 2$.

The reason why we think the conjecture is true is that F_{PTCC} is a continuous map and, once the 2-cycle is destroyed in the fold bifurcation, no other 2-cycles seem to appear. Hence, due to Lemma 4.2.1, T is a GAS equilibrium.

Bistability regions

As H or T change continuously, regions of bistability in the 2-parameter diagram shown in Figure 23 appear between two fold bifurcation curves, with the only exception of a region of essential attraction.

For small values of T, we find these regions between the curve $H = f(T) - T$ and the vertical line $H = f(\tilde{x}) - \tilde{x}$. The regions marked with B represent bistability between the attracting equilibrium T and a periodic or chaotic attractor; and there is a region where two attracting fixed points coexist. In the region of essential attraction, solutions converge to T with probability one, so there is not bistability. This dynamical behavior has already been observed for models of constant quota harvesting (Liz, 2010a; Schreiber, 2001) and it is explained in Section 5.3.2.

For larger values of T, we find a region of bistability between fold bifurcation branches for F^2_{PTCC}. We distinguish two types of regions labeled with B_1 and B_2 in Figure 23(A). In region B_1, the equilibrium T is attracting and it coexists with another periodic attractor $\mathcal{A}$, with period 2 or 4. In region B_2, the attracting 2-cycle $\{T, f(T)\}$ (if $T > K = 1$) or $\{T, g(T)\}$ (if $T < K = 1$) coexists with the attractor $\mathcal{A}$. The period of $\mathcal{A}$ is 4 if $H < H^* \approx 0.126$ and 2 if $H \geqslant H^*$.

1-parameter BDs varying T

In this subsection, we choose two particular values of the maximum allowed harvesting quota H and study the changes in the dynamics of (88) as the threshold harvesting T increases, that is, as the harvest rule PTCC becomes more conservative. As we can see in Figure 23(A), for sufficiently large values of H, there is a unique attractor, which is the periodic orbit of T (1, 2 or 4-periodic). For small values of H (in particular, for $H < H_* \approx 0.44$ (see Remark 9), the dynamics is more influenced by BCBs for F^2_{PTCC}. We plot the bifurcation diagrams in two cases: $H = 0.4 < H_*$ and $H = 1 > H_*$. We pay special attention to bifurcations (local and global) and long-term dynamics features. We find bistability and typical behaviors for maps with flat branches. However, the presence of consecutive flip bifurcations does not result in a bubbling effect, because the period halving bifurcation occurs before the period-doubling one.

We begin with $H = 0.4$. Since g does not depend on T, the fixed points of g are virtual or admissible fixed points of F_{PTCC} for every T. We obtain numerically that $x^*_- \approx 0.035 < x^*_+ \approx 0.852$. Since $g'(x^*_-) > 1$ and $g'(x^*_+) < -1$, both are

unstable. As T ranges from 0 to 2, there are ten border-collision bifurcations (see Figure 25). For small values of T, a zoom of the bifurcation diagram shows

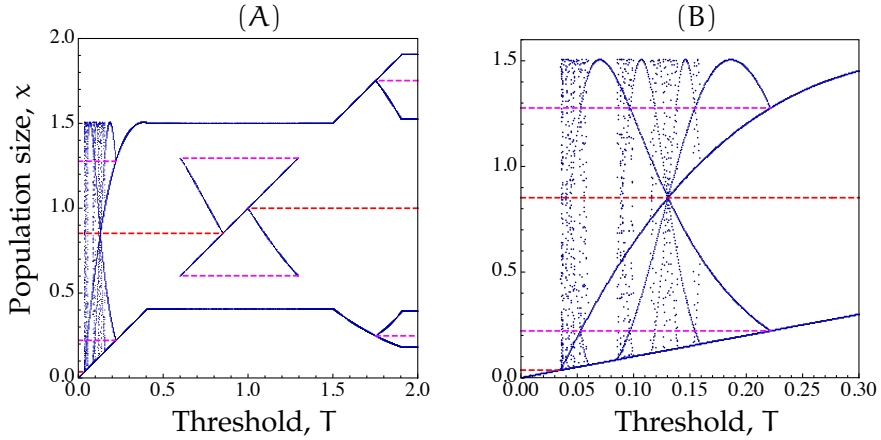

Figure 25: (A): Bifurcation diagram for (88) with the Ricker map $f(x) = x\,e^{2.6(1-x)}$, $H = 0.4$, and bifurcation parameter $T \in (0, 2)$. (B): Zoom of panel (A) for $0 < T < 0.3$. Red dashed lines represent unstable fixed points of F_{PTCC} ($x_-^* < x_+^* < K = 1$), and magenta dashed lines denote unstable 2-cycles of F_{PTCC}.

the first one, which occurs for $T = T_1 = p \approx 0.035$, in a fold BCB: the admissible fixed point T is an essential attractor for $T < T_1$; then it becomes virtual and a periodic attractor containing T arises. Between T_1 and $T_2 \approx 0.2216$, we can observe typical features of bifurcation diagrams for piecewise smooth maps with flat branches: intervals of effective chaotic behavior (periodic attractors with long periods) alternate with periodic windows and star-like structures (Sinha, 1994). For example, we can see a star for $T \approx 0.13$, when $g(T) = x_+^*$. At $T = T_2$ (satisfying $g^2(T_2) = T_2$), there is a flip BCB, and $\{T, g(T)\}$ becomes an attracting 2-cycle. After a persistence BCB at $T = T_3 \approx 0.407$ (where $f(g(T_3)) = T_3$), $\{T, g(T)\}$ is replaced by a 2-periodic orbit $\{p_1, p_2\}$, with $f(g(p_1)) = p_2$. There is bistability for $T \in (T_4, T_7)$, where $T_4 \approx 0.602$ and $T_7 \approx 1.294$ correspond to fold BCBs of F_{PTCC}^2; in particular, the fixed point T coexists with $\{p_1, p_2\}$ in (T_5, T_6), where $T_5 \approx 0.852$ and $T_6 = 1$ correspond to flip BCBs. At $T_8 \approx 1.5$, the 2-cycle $\{T, f(T)\}$ becomes attracting after a persistence BCB; this cycle becomes unstable at $T_9 \approx 1.75$, in a flip BCB, after which $\{T, f(T), f^2(T), f^3(T)\}$ becomes attracting. Finally, this 4-cycle is replaced by the attracting 4-cycle of f at $T_{10} \approx 1.9$.

Next we consider $H = 1$, which exhibits some new features; the corresponding bifurcation diagram is shown in Figure 26. The fixed points of g are now $x_-^* \approx 0.109 < x_+^* \approx 0.637$, and they are unstable. Since $H > H_*$, bistability is not observed for intermediate values of T. However, for small values of T, bistability occurs between the equilibrium T and a chaotic attractor of g. Bistability is observed for $T < x_-^*$; at $T = x_-^*$, the admissible fixed point T becomes virtual after a fold bifurcation. The chaotic attractor persists for $T \in (x_-^*, T^*)$, where $T^* \approx 0.158$ corresponds to a discontinuity-induced crisis, when the lower edge of the chaotic interval collides with T^* ($g^2(x_c) = T^*$); this bifurcation changes

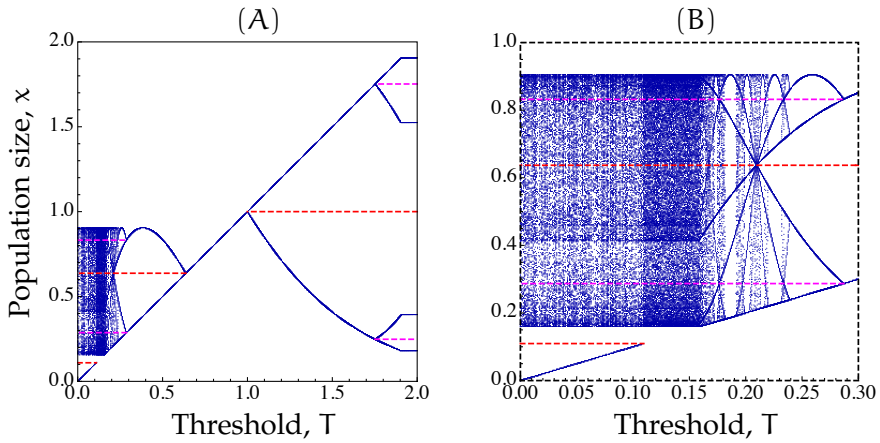

Figure 26: (A): Bifurcation diagram for (88) with the Ricker map $f(x) = x\,e^{2.6(1-x)}$, $H = 1$, and bifurcation parameter $T \in (0, 2)$. (B): Zoom of panel (A) for $0 < T < 0.3$. Red dashed lines represent unstable fixed points of F_{PTCC} ($x_-^* < x_+^* < 1$), and magenta dashed lines correspond to unstable 2-cycles.

abruptly the dynamics, from a chaotic attractor to a periodic attractor defined by the superstable orbit of T. After that, typical behavior of maps with flat intervals occur, as explained in the previous case. Notice that the equilibrium T is globally asymptotically stable for $T \in (x_+^*, 1)$ (see Theorem 5.3.4 and Figure 17); a sequence of two flip BCBs (period-halving and period-doubling) occurs as T increases and collides with x_+^* and $K = 1$, respectively. For $T > x_+^*$, the bifurcation diagram coincides with the bifurcation diagram of TH (compare with (Hilker and Liz, 2020, Fig. 3)).

1-parameter BDs varying H

As we have already mentioned, for $T = 0$ the PTCC rule becomes the CC harvesting strategy defined by the map $F_{CC}(x) = \max\{f(x) - H, 0\}$. For the Ricker map $f(x) = x\,e^{r(1-x)}$, the dynamics of F_{CC} depending on r and H was studied by Schreiber (2001). In particular, the bifurcation diagram for $r = 2.6$ corresponds to Figure 5**b** in that reference, and it is characterized by two intervals of bistability (where zero and an interval bounded away from zero are attracting), an interval of essential extinction, and total extinction for large values of H due to overharvesting. As explained in Section 5.3.2, for small values of $T > 0$, for which T is an admissible fixed point, a similar situation holds for (88), but extinction is not possible due to the positive minimum biomass level T. In this subsection, we consider three different values of T and plot the corresponding bifurcation diagrams as H increases; as expected, larger values of T not only help to avoid extinction, but also tend to simplify the dynamics.

Recall that there is a point $\tilde{x} \approx 0.32$ such that $f'(\tilde{x}) = 1$. If $T < \tilde{x}$, then a fold SB occurs at $H = \tilde{H} := f(\tilde{x}) - \tilde{x} \approx 1.555$, and T is a global attractor for $H > \tilde{H}$.

We begin with $T = 0.13 < \tilde{x}$. As H increases from zero, the curve defined by $g^2(x_c) = T$ is crossed twice (see Figure 23(B)). Looking at the 2-parameter bifurcation diagram in that figure, the dynamics starts in region R_1, where

the 4-periodic attractor of g for $H = 0$ undergoes a route of period-doubling bifurcations to chaos. After a first discontinuity-induced crisis at the quota value $H = H_1 \approx 0.086$ (green vertical line in Figure 27(B)), the dynamics is governed by the superstable periodic orbit of T. Notice that there are still

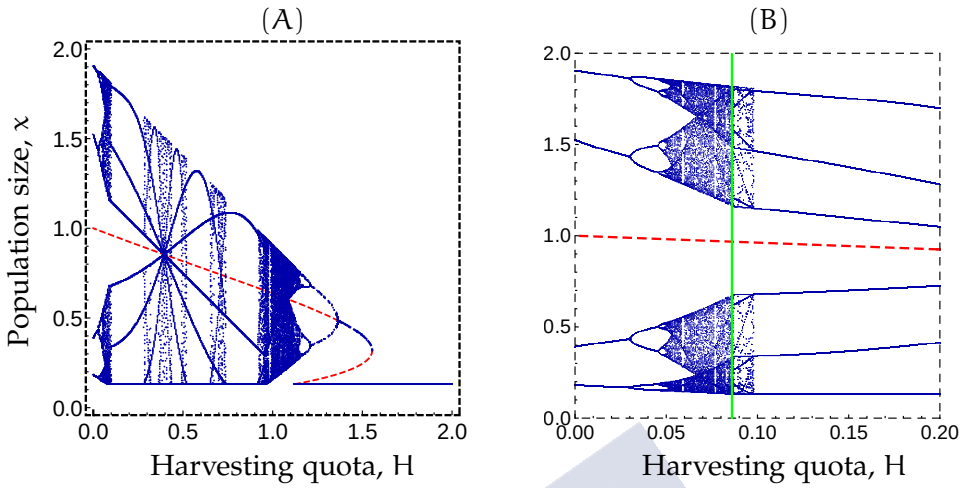

Figure 27: (A): Bifurcation diagram for (88) with the Ricker map $f(x) = xe^{2.6(1-x)}$, $T = 0.13$, and bifurcation parameter $H \in (0, 2)$. (B): Zoom of panel (A) for $0 < H < 0.2$. Red dashed lines represent unstable fixed points of F_{PTCC} ($x_-^* < x_+^* < 1$), and the green vertical line denotes a discontinuity-induced crisis (see the text).

periodic orbits with long periods until a 6-periodic window appears at the quota value $H \approx 0.098$, when $g^6(T) = T$.
Then we observe, as in the previous examples, a typical bifurcation diagram of maps with flat segments for $H \in (H_1, H_2)$ (see, for example, the star-like structure at $H \approx 0.394$, for which $g(T) = x_+^*$ is a fixed point of g), where at $H_2 \approx 0.959$ the second discontinuity-induced crisis occurs. We notice that at the first crisis, the metric attractor of g consists of two intervals, while in the second one it consists of only one interval; in both cases the bifurcation occurs when T collides with the smallest point of the attractor, that is, when $g^2(x_c) = T$. The dynamics is again chaotic in region R_2, until a series of period-halving bifurcations leads to an attracting fixed point at $H_4 \approx 1.364$. At $H_3 \approx 1.118$, T becomes an admissible fixed point in a fold BCB. There is bistability for $H \in (H_3, H_5)$, where $H_5 = \tilde{H}$.

For $T \geqslant \tilde{x}$, equation (88) does not exhibit complex behavior. In Figure 28, we show the bifurcation diagram in two particular cases: $T = \tilde{x}$, and $T = 0.8 > \tilde{x}$.

When $T = \tilde{x}$, we show the bifurcation diagram for $H \in (1, 1.6)$, where we underline two interesting features:

- first, as H decreases from $H = \tilde{H}$, the period-doubling bifurcation cascade that we observed in Figure 27 is broken. In this case, when the attracting 4-cycle of g collides with the superstable 4-cycle $\{T, g(T), g^2(T), g^3(T)\}$ at $H \approx 1.2$ for which $g^2(x_c) = T$ (persistence BCB for F_{PTCC}^4, represented by

a vertical green dashed line in Figure 28(A)). Thus, the sequence of flip bifurcations to chaos is replaced by a bubble in the bifurcation diagram;

- second, the fold SB that occurs at $H = \tilde{H}$ when $T < \tilde{x}$ does not take place. In this case, we observe a persistence BCB, since $g(T) = g(\tilde{x}) = \tilde{x} = T$.

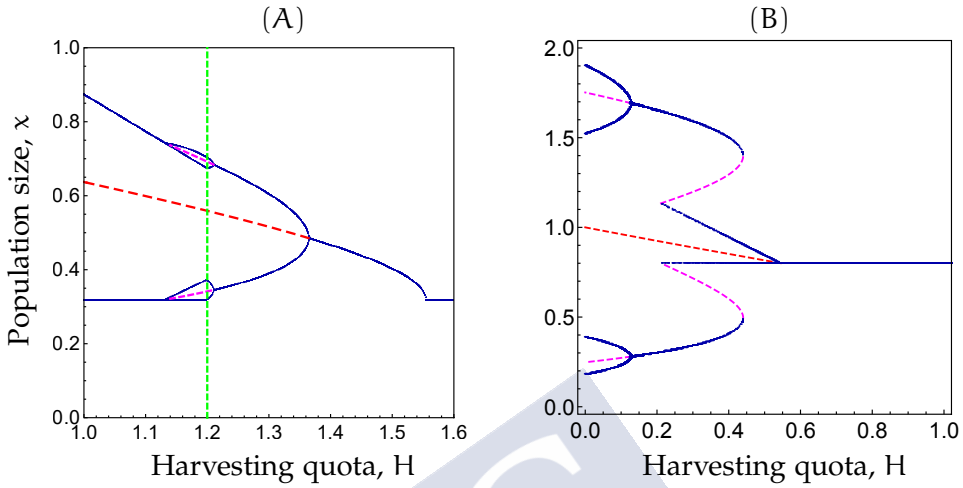

Figure 28: Bifurcation diagrams for (88) with the Ricker map $f(x) = x\,e^{2.6(1-x)}$ and bifurcation parameter H. (A): $T = \tilde{x} \approx 0.32$ and $H \in (1, 1.6)$; (B): $T = 0.8$ and $H \in (0, 1)$. In both cases, the red dashed line represents the unstable fixed point x_+^* of g, and the magenta dashed lines correspond to unstable 2-cycles. The green dashed vertical line in (A) denotes a persistence BCB for F^4_{PTCC}, giving rise to a bubble (see the text).

When $T = 0.8$, we distinguish four bifurcations as H ranges from 0 to 1. For $H < H_1 = H^* \approx 0.126$, there is an attracting 4-periodic cycle of F_{PTCC}; at $H = H_1$, a flip SB leads to an attracting 2-cycle of F_{PTCC}. At $H = H_2 \approx 0.211$, a fold BCB occurs when $f(g(T)) = T$, and $\{T, g(T)\}$ becomes attracting. These two attracting 2-cycles coexist until the first one disappears at $H = H_3 = H_* \approx 0.44$ in a fold SB for F^2_{PTCC}. The segment (H_1, H_2) corresponds to the region G in Figure 23(A), and (H_2, H_3) to region B_2. Finally, the 2-cycle $\{T, g(T)\}$ is destroyed in a flip BCB at $H = H_4 = f(T) - T \approx 0.545$, and T becomes an attractor for $H \geqslant H_4$.

The influence of threshold dynamics

In Figure 23, we can identify large regions where the dynamics of (88) is governed by the flat part of F_{PTCC}. In this situation, we do not expect complicated dynamics, since, with probability one, all orbits fall into a stable periodic attractor of the form $\{T, F_{PTCC}(T), \ldots, F^m_{PTCC}(T)\}$. The period m is the return period of the orbit to the flat part, starting at T.
In the case of threshold harvesting (TH), m can be determined as the least positive integer for which $f^m(T) \geqslant T$ (Sinha, 1994). The simplest case occurs when m is a power of 2: in this case, decreasing T leads to a sequence of period-halving bifurcations until T becomes a global attractor for $T \leqslant K$ (Hilker and

Liz, 2020). We observe this bifurcation scenario when $H + T \geqslant f(x_c)$, corresponding to the rightmost region in Figure 23(A) (in this case, PTCC becomes TH).

There are other parameters for which the orbit of T converges to an attractor that does not contain T. In these cases, it is possible that a single periodic orbit governs the long-term behavior of almost all solutions, as in regions marked with G in Figure 23(A) (see, e.g., Figure 24(B1)), but the attractor can also be chaotic. This complicated behavior can be expected for some values of (H, T) in regions marked with B, R_1, and R_2 in Figure 23(B). Increasing T tends to prevent chaotic behavior, but increasing H can either induce or prevent chaos, as it happens in a strategy of CC harvesting (see, e.g., (Schreiber, 2001, Fig. 5)).

For the PTCC rule (88), we have also found typical features of the bifurcation diagram for flat-topped maps that are also present in the dynamics of TH (Sinha, 1994). For example, ranges of effectively chaotic behavior (corresponding to periodic orbits of long period), periodic windows, and "star-like" intersections in the bifurcation diagram.

5.4 THRESHOLD CONSTANT CATCH (TCC)

We organize this section as follows: In Subsection 5.4.1, we study the existence and stability of fixed points, as well as the related bifurcations: SBs, BCBs and basin boundary metamorphoses. Then, Subsection 5.4.2 is devoted to prove the existence of intervals which do not contain any equilibrium but attract long-term complex dynamics. We additionally determine the parameter values where a boundary-collision may occur, that is, when the oscillatory attractor contained in one of those intervals (without fixed points) reaches one of the end points of the interval. The results in these two subsections are obtained for a general map f satisfying conditions **(A1)-(A2)** with $x_c = \infty$. In Subsection 5.4.3, we work with the Beverton-Holt model and we classify the local bifurcations of 2-cycles (SBs and BCBs of fixed points for F^2_{TCC}). In Subsection 5.4.4, we address a case study: we vary the harvest control parameters in (89) to obtain 1-parameter and 2-parameter bifurcation diagrams. In addition, we classify the asymptotic dynamics in the parameter plane (H, T) in different dynamical regimes; and we describe the long term behavior at bistability regions, which may not appear in the usual form, that is, between two fold bifurcations. We conclude this section with a more management-oriented perspective, by studying average yield and harvest frequency by means of analytical results and numerical simulations.

5.4.1 *Fixed points: location, stability and related bifurcations*

In this subsection, we study the fixed points of F_{TCC} depending on the parameter values H and T. We first focus on the number of fixed points, their location and stability; and we notice that the discontinuity in TCC modifies the fixed

point structure we had for PTCC. Then, we classify the local bifurcations of fixed points: smooth and border-collisions. Finally, we also use the information from the study of fixed points to determine basin boundary metamorphoses.

We recall that, for a map satisfying conditions **(A1)-(A2)** with $x_c = \infty$, there exists a unique $\tilde{x} \in (0, K)$ such that $f'(\tilde{x}) = 1$. The point $\tilde{x}$ plays an important role in the study of existence, stability and bifurcations of fixed points.

Existence, localization and stability of positive fixed points

In the following, we provide a theoretical result on the existence and stability of positive fixed points for the map F_{TCC} defined in (90). The proof follows similar arguments to those of the analogous results for PTCC (Proposition 5.3.1 and Theorem 5.3.3). We assume that $0 < T < \sup\{f(x) : x > 0\}$ and $H > 0$; for $H > T$, let $m = \inf\{x > 0 : F_{TCC}(x) = 0\}$ and $M = \sup\{x > 0 : F_{TCC}(x) = 0\}$. Recall that we denote by x_T the unique solution of $f(x) = T$.

Theorem 5.4.1. *Assume that f satisfies conditions **(A1)-(A2)** with $x_c = \infty$. Denote by x^*_- and x^*_+, when they exist, the positive fixed points of $g(x) = f(x) - H$, with $0 < x^*_- \leqslant \tilde{x} \leqslant x^*_- < K$. The following assertions hold:*

1. *If $T > K$, then K is the unique positive equilibrium. Moreover, for $H < T$, K is GAS; while, for $T \leqslant H$, K is LAS with basin of attraction $(0, m) \cup (M, \infty)$, and all initial conditions in $[m, M]$ converge to 0.*

2. *If $f(\tilde{x}) \leqslant T < K$ and $H \leqslant H_{10} := T - x^*_{+,T}$, where $f\left(x^*_{+,T}\right) = T$, then the unique positive fixed point is $x^*_+ \in \left[x^*_{+,T}, K\right)$. Moreover, if $H < H_{10}$, then x^*_+ is GAS; while, if $H = H_{10}$, then x^*_+ is a global attractor.*

3. *If $0 < T < f(\tilde{x})$, then:*

   a) *If $H < H_{12} := T - x^*_{-,T}$, where $f\left(x^*_{+,T}\right) = T$, then $x^*_+ \in [\tilde{x}, K)$ is the unique positive fixed point and it is GAS.*

   b) *If $H_{12} \leqslant H < H_{20} := f(\tilde{x}) - \tilde{x}$, then there are two positive fixed points $x^*_- < \tilde{x} < x^*_+$. Furthermore, x^*_- is unstable for all $H \neq H_{oscill} := f(T) - T$ and, $x^*_+ > \tilde{x}$ is LAS with (x^*_-, ∞) contained in its basin of attraction. In particular, if $0 < T < \tilde{x}$ and $H_{oscill} \leqslant H < H_{20}$, then x^*_+ is LAS and it attracts exactly (x^*_-, ∞).*

   c) *If $H = H_{20}$, then $\tilde{x}$ is the unique positive fixed point. It is at least semi-stable and $[\tilde{x}, \infty)$ belongs to its basin of attraction.*

Proof. We first prove the existence of positive fixed points. From the definition of the map F_{TCC} in (90), we have:
If $T > K = f(K)$ (as f is strictly increasing, $x_T > K$), then $F_{TCC}(x) = f(x)$ for all $x \in (0, x_T)$, and $F_{TCC}(x) = g(x) = f(x) - H < x - H < x$ for all $x > x_T$.
If $T < K = f(K)$ (as f is strictly increasing, $x_T < K$), then $F_{TCC}(x) = f(x) > x$ for all $x \in (0, x_T)$, and $F_{TCC}(x) = 0$ or $F_{TCC}(x) = g(x) = f(x) - H$ for all $x > x_T$.

Thus, we can conclude that K is a fixed point of F_{TCC} if and only if $T > K$, and for $T < K$ the positive fixed points of F_{TCC} are the ones of g.
Since $g'(x) = f'(x) > 0$ and $g''(x) = f''(x) < 0$, by the Mean Value Theorem, g can have at most two positive fixed points $x^*_- \leqslant \tilde{x} \leqslant x^*_+$. Now, the proof of statements 2 and 3 easily follows.

Next, we show that the stability results follow from Lemma 4.2.2.

To prove statement 1, we apply Lemma 4.2.2 to the map F_{TCC} in $(0, x_T)$. As $F_{TCC}(x) = f(x)$ for all $x \in (0, x_T)$, then K is a global attractor in $(0, x_T)$.
If $H < T$, then $0 < g(x_T) < F_{TCC}(x) = f(x) - H < x - H < x$ for all $x > x_T > K$ and $g(x_T) = f(x_T) - H = T - H < T$. Thus all initial conditions $x_0 > x_T$ enter $(0, x_T)$ in finite time and converge to K.
If $H \geqslant T$, then $g(x) = 0$ for all $x \in [x_T, M] = [m, M]$. Moreover, for all initial conditions $x_0 > M > x_T$, the proof follows as in the case $H < T$.

Now, we consider the statements 2 and 3-a). In both cases, we know that x^*_+ is the unique positive fixed point of F_{TCC}. In addition, $x^*_+ = x_T$ if $H = H_{10}$, since $F_{TCC}(x_T) = g(x_T) = f(x_T) - H_{10} = T - (T - x_T) = x_T$; and $x^*_+ \in (x_T, K)$ otherwise. The proof of case 2 with $H = H_{10}$ is a direct consequence of the following conditions fulfilled by f and g: $F_{TCC}(x) = f(x) > x$, for all $0 < x < x_T < K$; $F_{TCC}(x) = g(x) < x$, for all $x > x_T$; and $T = f(x_T) > F_{TCC}(x_T) = g(x_T)$. In the remainder cases, we apply Lemma 4.2.2 to the map F_{TCC} in (x_T, ∞). As $F_{TCC}(x) = g(x)$ for all $x \in (x_T, \infty)$, and we get that x^*_+ is GAS in (x_T, ∞). For all $x \in (0, x_T)$, $F_{TCC}(x) = f(x) > x$; and since $f(x_T) > g(x_T)$, we can conclude that all initial conditions in $(0, x_T)$ enter (x_T, ∞) in finite time, and thus converge to x^*_+. □

Figure 29 illustrates the number of fixed points in the parameter plane (H, T) for the PTCC model (88) and the TCC rule (89) with the Beverton-Holt map $f(x) = 3x/(1+x)$. We point out two main differences:

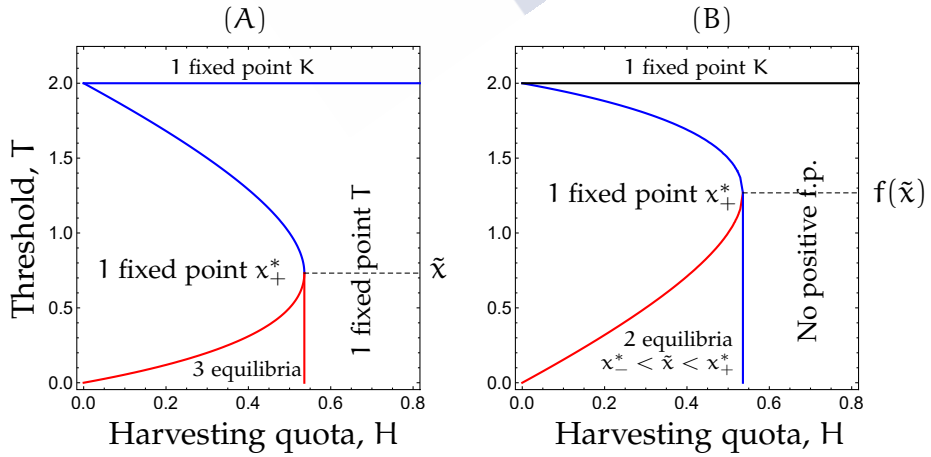

Figure 29: Number of positive fixed points of F_{PTCC} (panel (A)) and F_{TCC} (panel (B)) with the Beverton-Holt map $f(x) = 3x/(1+x)$. There are zero, one and two positive fixed points for the parameter values in the boundaries colored in black, blue and red, respectively.

- The parameter boundaries which determine the number of positive fixed points do not coincide at all.

- While T is an admissible positive fixed point of F_{PTCC} for all $T \leqslant K$ and $H \geqslant f(T) - T$, T is an admissible equilibrium of F_{TCC} if and only if it is a fixed point of g.

The critical quota values found in Theorem 5.4.1 help us to analyze bifurcations of fixed points and basin boundary metamorphoses. An interpretation of H_{10}, H_{12}, H_{oscill} can be found in Figures 30 and 32.

Fixed point smooth and border-collision bifurcations

For $0 < T < \sup\{f(x) : x \geqslant 0\}$ and $H > 0$, the map F_{TCC} is piecewise-smooth on $[0,\infty)\backslash\{x_T\}$ and x_T is a discontinuity point. As a consequence, the local bifurcations of fixed points are either SBs or specific BCBs of piecewise-smooth discontinuous models.

There is a fold SB when $0 < T < f(\tilde{x})$ and $H = H_{20} = f(\tilde{x}) - \tilde{x}$. The bifurcation occurs under variation of the harvesting quota H in the same manner as in CC (i.e., when $T = 0$) and PTCC harvesting strategies: the admissible fixed points of g collide and suddenly disappear as H increases.

Now we describe the possible dynamical scenarios at a BCB for F_{TCC}. Recall that, when a general map undergoes a BCB, an admissible or virtual fixed point collides with a break point. As the unique break point for F_{TCC} is the discontinuity point x_T, the BCBs can only occur when x_T becomes a boundary fixed point, that is, when $x_T = x^*_{-,T}$ (equivalently, $f(x^*_{-,T}) = T$ or $H = H_{12}$), $x_T = x^*_{+,T}$ (equivalently, $f(x^*_{+,T}) = T$ or $H = H_{10}$) or $x_T = K$ (equivalently, $T = K$).

When $0 < T < f(\tilde{x})$ and $H = H_{12}$, an existence BCB occurs as H increases or T decreases: the unstable fixed point x^*_- becomes admissible and bifurcation diagrams suggest that the GAS fixed point x^*_+ becomes an essential global attractor. See Figure 30, panels $(A1)$-$(A3)$.

When $f(\tilde{x}) < T < K$ and $H = H_{10}$, a period-adding BCB occurs as H or T increase: For $H < H_{10}$, the admissible fixed point x^*_+, with $g'(x^*_+) \in (0,1)$, is GAS in $(0,\infty)$. At $H = H_{10}$, the equilibrium x^*_+ collides with a break point and an attracting long-period cycle becomes admissible. See Figure 30, panels $(B1)$-$(B3)$.

When $x_T = T = K$, the threshold T becomes a boundary fixed point and the BCBs occur only under variation of the threshold parameter, as in PTCC. For $H < T$, there is a period-adding bifurcation; while, for $H > T$, an existence BCB occurs:

- If $T = K$ and $H < T$, then: For $T > K$, the admissible equilibrium K is GAS in $(0,\infty)$. At $T = K$, the virtual fixed point K, with $f'(K) \in (0,1)$, collides with a break point; and as T decreases, an attracting long-period cycle becomes admissible.

- If $T = K$ and $H > T$, then: The stable fixed point K of f becomes an admissible fixed point; and there is a transition, as T increases, from all initial conditions converging to the unstable equilibrium 0 to a bistable scenario in which initial conditions in $[m, M]$ converge to 0 and K is LAS.

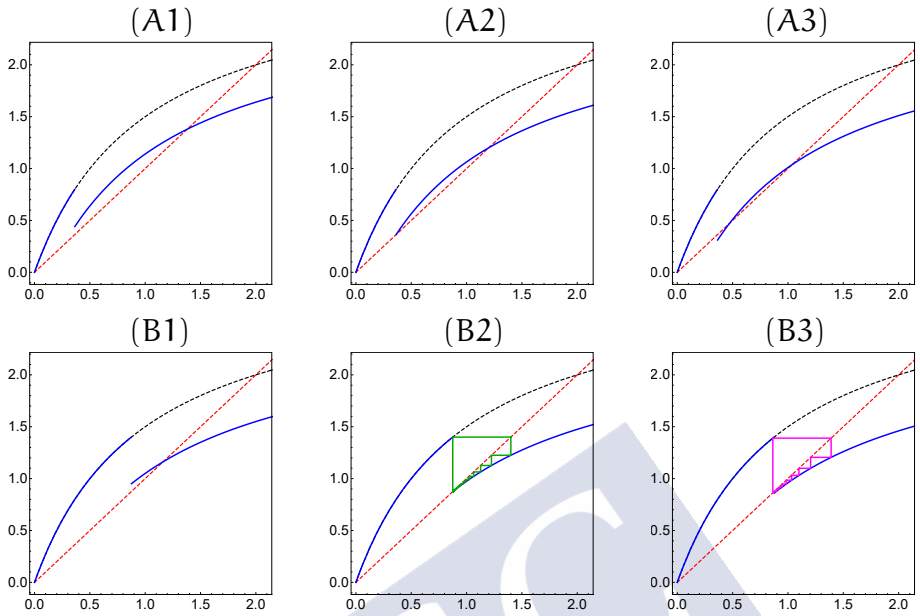

Figure 30: Illustrations of fixed point BCBs arising in the TCC rule (89). The Beverton-Holt map $f(x) = 3x/(1+x)$ is the black dashed curve, and the blue solid curve is the corresponding map F_{TCC}. The red dashed line is $y = x$. The attracting cycles $\{x_0, F_{TCC}(x_0), F^2_{TCC}(x_0), \ldots\}$ and homoclinic orbits are shown in magenta and green color, respectively. Top row: existence BCB for $T = 0.8 < f(\tilde{x}) \approx 1.27$. (A1): $H = 0.36 < H_{12} \approx 0.44$; (A2): $H = H_{12}$; (A3): $H = 0.49 > H_{12}$. Bottom row: flip or period-adding BCB for $f(\tilde{x}) < T = 1.4 < K = 2$. (B1): $H = 0.45 < H_{10} \approx 0.53$; (B2): $H = H_{10}$, homoclinic orbit; (B3): $H = 0.54 > H_{10}$, $F^9_{TCC}(x_0) = x_0$.

Basin boundary metamorphoses

The basin boundary metamorphoses that occur for the TCC rule and a strictly increasing map f are simple transitions from a simply-connected basin of attraction to a multiply-connected one. More precisely, there is a transition from coexistence of an essential global attractor $\mathcal{A}$ and an admissible repelling fixed point $\mathcal{R}$ of F_{TCC} to some sort of bistability between the attractor $\mathcal{A}$ and $\mathcal{R}$, in such a way that $\mathcal{R}$ is still repelling but some initial conditions converge to it. These bifurcations take place when:

- $0 < T < H_{20} = f(\tilde{x}) - \tilde{x}$, $H = T < H_{oscill}$: Bifurcation diagrams suggest that x^*_+ is an essential global attractor and 0 is an admissible unstable equilibrium for all $0 < H < T$. As H increases or T decreases through $H = T$, x^*_+ is LAS and the fixed point 0 is still unstable but the initial conditions in $[m, M]$ converge to it. See Figure 31, panels (A1)-(A3).

- $T > K$, $H = T$: K is GAS in $(0, \infty)$ and 0 is unstable for all $0 < H < T$. As H increases or T decreases through $H = T$, K becomes LAS and 0 is still repelling but the initial conditions in $[m, M]$ converge to it.

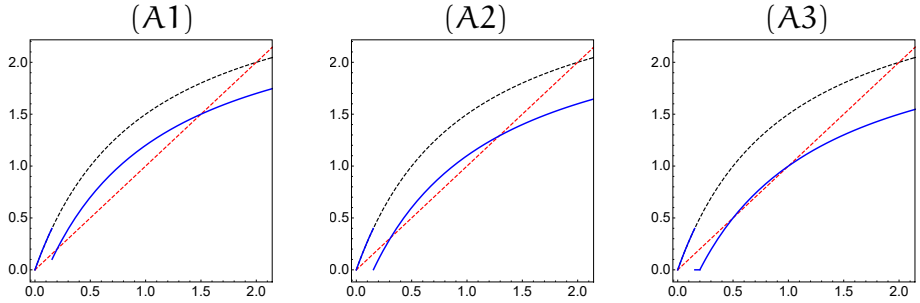

Figure 31: Basin boundary metamorphose arising in the TCC harvesting strategy (89) with the Beverton-Holt map $f(x) = 3x/(1+x)$ (black dashed curve) and $0 < T = 0.4 < \min\{H_{20}, H_{oscill}\} \approx 0.46$. The blue solid curve is the corresponding map F_{TCC} and the red dashed line is $y = x$. (A1): $H = 0.3 < T$; (A2): $H = 0.4 = T$; (A3): $H = 0.45 \in (T, H_{oscill})$.

5.4.2 *Complex dynamics: absorbing intervals*

The long-term dynamics of the TCC rule when the map f is compensatory with $x_c = \infty$ are not as simple as those of PTCC. While, for the PTCC strategy, every initial condition $x_0 > 0$ converges to a positive equilibrium, for TCC, there exist regions in the parameter plane (H, T) where there is an absorbing interval which does not contain any positive attracting or semi-stable fixed point.

Theorem 5.4.2. *Assume that f satisfies **(A1)-(A2)** with $x_c = \infty$ and $T \leqslant K$. Denote by x_-^* and x_+^*, when they exist, the positive fixed points of $g(x) = f(x) - H$, with $0 < x_-^* \leqslant \tilde{x} \leqslant x_-^* < K$. If any of the following conditions holds, then the interval $I = [\max\{0, T - H\}, T]$ is absorbing and does not contain any positive equilibrium:*

1. $T = K$, $H > 0$;
2. $f(\tilde{x}) \leqslant T < K$, $H > H_{10}$;
3. $0 < T < f(\tilde{x})$, $H > H_{20}$;
4. $0 < T < \tilde{x}$, $H \in (H_{oscill}, H_{20})$.

In cases 1, 2 and 3, all orbits of equation (89) enter the interval I in finite time. In case 4, orbits starting at $x_0 \in (0, x_-^*)$ enter I after a finite number of generations, but the positive fixed point $x_+^* > T$ attracts (x_-^*, ∞).

Proof. In all cases, since $T \leqslant K = f(K)$, we have $F_{TCC}(x) = f(x) > x$ for all $x \in (0, x_T)$. In addition, $F_{TCC}(x) = \max\{0, g(x)\}$, for all $x \geqslant x_T$. In cases 1, 2

and 3, for all $x \geqslant x_T$, $g(x) = f(x) - H < x$. However, in case 4, $g(x) < x$ if, and only if, $x \in [x_T, x^*_-) \cup (x^*_+, \infty)$.

Consequently, using that $f'(x) = g'(x) > 0$ for all $x > 0$, it is clear that there exists an invariant or strictly mapped into itself interval

$$I = [\max\{0, g(x_T)\}, f(x_T)] = [\max\{0, f(x_T) - H\}, T] = [\max\{0, T - H\}, T].$$

It also follows that all initial conditions enter I in finite time in cases 1, 2 and 3. However, in case 4 (see Figure 32(A) as an illustration), we can assert that just the initial conditions in $(0, x^*_-)$ enter I in finite time, since from Theorem 5.4.1 we have that (x^*_-, ∞) is the basin of attraction of x^*_+.

Finally, it remains to prove that I does not contain any positive fixed point. The cases 1, 2 and 3 are trivial since, under that conditions, the map F_{TCC} has no positive fixed points. In case 4, the positive fixed points of F_{TCC} are $x^*_- < x^*_+$, and the statement follows since $H > H_{oscill}$ implies that $T < x^*_-$. □

Boundary-collision bifurcations

When applying the TCC rule to a simple map as $f(x) = r\,x/(1 + x)$, $r > 1$, the asymptotic population dynamics can also change through a boundary-collision bifurcation, in which an oscillatory attractor, which is contained in the absorbing interval $I = [\max\{0, T - H\}, T]$, reaches the break points T or 0, and collides with an unstable equilibrium, x^*_- or 0. Avrutin et al. (2019, Subsection 1.8.3) mention that the boundaries of chaotic attractors of one-dimensional maps are determined by critical points, i.e., local extrema and break points, and their images. Therefore, if there is an oscillator attractor in I which is chaotic, then it necessarily reaches a critical point T or $\max\{0, T - H\}$ and the boundary-collision bifurcation occurs when $T = x^*_-$ or $\max\{0, T - H\} = 0$. These types of bifurcations take place when:

- $0 < T < \tilde{x}$, $H = H_{oscill} < T$: For all $H_{oscill} < H < \min\{T, H_{20}\}$, $I = [T - H, T]$ is an absorbing interval, such that all initial conditions in $(0, x^*_-)$ enter I in finite time. The oscillatory attractor contained in I collides with $T = x^*_-$ at $H = H_{oscill}$ and, as H decreases or T increases, bifurcation diagrams suggest that x^*_+ becomes an essential global attractor. See Figure 32 for an illustration.

- $0 < T < \tilde{x}$, $H = T \in (H_{oscill}, H_{20})$ or $0 < T < f(\tilde{x})$, $H = T > H_{20}$ or $f(\tilde{x}) \leqslant T < K$, $H = T = H_{10}$: For values of the harvesting quota H slightly smaller than T, the absorbing interval $I = [T - H, T]$ contains an oscillatory attractor, and the initial conditions in either $(0, x^*_-)$ or $(0, \infty)$ enter I in finite time. At $H = T$, the attractor in I collides with $T - H = 0$ and, as H increases or T decreases, at least some positive initial conditions in I converge to the unstable fixed point 0.
  In particular, for $0 < T < f(\tilde{x})$, $H = T > H_{20}$ or $f(\tilde{x}) \leqslant T < K$, $H = T = H_{10}$, bifurcation diagrams suggest that, as H increases or T decreases through

$H = T$, either there is some sort of bistability between an oscillatory attractor and the unstable equilibrium 0, or all initial conditions converge to 0 but there exist long transients.

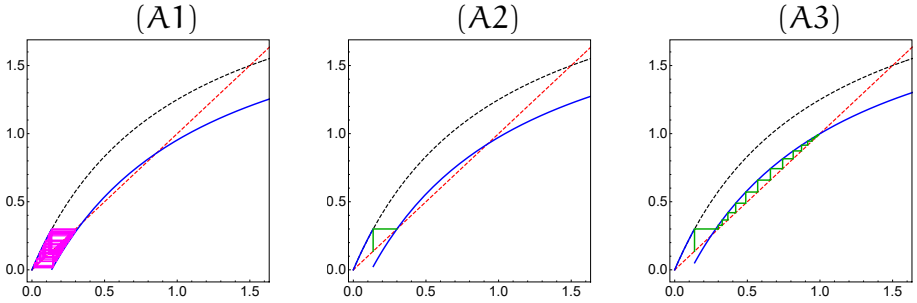

Figure 32: Illustration of a boundary-collision bifurcation for decreasing harvest quotas H in the TCC rule with the Beverton-Holt map $f(x) = 2.5x/(1+x)$ and the threshold value $T = 0.3 < \tilde{x} \approx 0.58$. The red dashed line is $y = x$. We plot the orbit of x_T such that $f(x_T) = T$ in magenta or green color if it converges to an oscillatory attractor or an equilibrium, respectively. $(A1) : H_{oscill} \approx 0.28 < H = 0.3 < T$, there is an oscillatory attractor contained in $I = [T-H, T]$. $(A2) : H = H_{oscill}$, the oscillatory attractor collides with the fixed point $T = x^*_-$. $(A3) : H = 0.25 < H_{oscill}$, as $f(x_T) = T > x^*_-$, the point $x_T < x^*_-$ belongs to the basin of attraction of the LAS equilibrium x^*_+.

5.4.3 *2-cycles smooth and border-collision bifurcations*

The local bifurcations of 2-cycles are BCBs or SBs of the fixed points for the piecewise-smooth map F^2_{TCC}. Here, we can classify them in the light of Theorem 4.4 in AlSharawi and Rhouma (2009) for the TCC harvesting strategy with $f(x) = rx/(1+x)$, $r > 1$. See Figure 33 for illustrations.

We focus our attention on the region of the parameter plane (H, T) where $H < T < K$. This is because numerical simulations suggest that for $H \geqslant T$ there might be oscillations in addition to the fixed point; but these oscillations could be complex attractors or long transients that eventually result in extinction.

The BCBs for F^2_{TCC} are determined by $F^2_{TCC}(T-H) = g \circ f(T-H) = T-H$ (with $F_{TCC}(T-H) \neq T-H$) or $F^2_{TCC}(T) = f \circ g(T) = T$ (with $F_{TCC}(T) \neq T$). At the outset, we fix some notations for relevant values of the harvesting parameters H and T. We define $H_{**} := (r-1)^2/(r+1)$, which is determined as the solution of the non-linear system $f(g(x)) = x$, $f'(g(x))g'(x) = 1$ and, $T_{**} > 0$ as the unique solution of the non-linear equation $g \circ f(T_{**} - H_{**}) = T_{**} - H_{**}$.

1. For $0 < T < T_{**}$ and $g \circ f(T-H) = T-H$, the unstable equilibrium of $g \circ f$ becomes admissible as H increases or T changes continuously through an existence BCB for F^2_{TCC}.

2. For $T_{**} \leqslant T < K$ and $g \circ f(T - H) = T - H$, the admissible stable fixed point of $g \circ f$ collides with a break point of F^2_{TCC}. At the collision point, there is a homoclinic orbit; after the collision, an attracting l-periodic cycle of F_{TCC} becomes admissible, as T or H increase, through a period-adding BCB for F^2_{TCC}.

3. For $H_{**} < T < K$ and $f \circ g(T) = T$, the stable fixed point of $f \circ g$ collides with a break point of F^2_{TCC} and becomes admissible as H or T are increased in a variety of BCBs. In view of some numerical bifurcation diagrams, period-adding BCBs for F^2_{TCC} are more likely to occur for $f(\tilde{x}) < T < K$. However, for $H_{**} < T < f(\tilde{x})$, we expect more complex bifurcations.

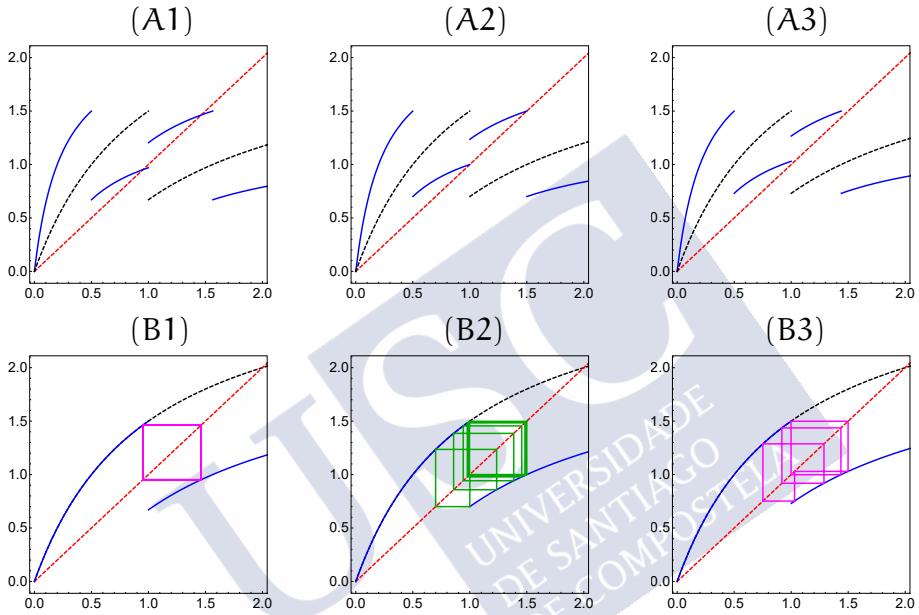

Figure 33: Illustration of a 2-cycle BCB. Panels in the top row show F_{TCC} as a black dashed curve and F^2_{TCC} as a blue solid curve. Panels at the bottom row show f as a black dashed curve and F_{TCC} as a blue solid curve. In all panels, the red dashed line is $y = x$, and the TCC rule (89) is applied to the Beverton-Holt map $f(x) = 3x/(1 + x)$ with $f(\tilde{x}) \approx 1.27 < T = T^{**} = 1.5 < K = 2$. Across the columns, parameter H decreases, giving rise to a homoclinic orbit and several period-adding BCBs. Left: $H = 0.83$, with the magenta box in panel (B1) representing an attracting 2-cycle. Middle: $H = 0.8$ such that $F^2_{TCC}(T) = f(f(T) - H) = T$, with a homoclinic orbit shown in green color in panel (B2); it appears when the attracting 2-cycle collides with a break point of F^2_{TCC} in a period-adding BCB. Right: $H = 0.77$, with an attracting 7-periodic orbit shown in magenta color.

The coexisting 2-cycles (stable and unstable fixed points of $f \circ g$) are destroyed when a fold SB for F^2_{TCC} occurs at H_{**}.

5.4.4 *Impact of harvest parameters on population dynamics*

The results obtained in the previous subsections for a strictly increasing map f under the TCC rule reflect that the presence of the discontinuity point of F_{TCC} provokes a huge change in the dynamics in comparison with PTCC. Recall that, for a population map f under conditions **(A1)-(A2)** with $x_c = \infty$, the dynamics of PTCC are trivial in the sense that all solutions converge to an equilibrium and the possible bifurcations are SB or BCB of fixed points. However, we know that for the TCC rule there exist absorbing intervals which do not contain any equilibrium and a larger variety of bifurcations, such as, basin-boundary metamorphoses, boundary-collisions, SBs and BCBs of fixed points and 2-cycles.

Our aim in this subsection is to better understand the role played by harvesting parameters H and T in the population dynamics of the TCC rule (89). For that purpose, we consider the unmanaged Beverton-Holt map $f(x) = 3x/(1+x)$.

We first plot a 2-parameter bifurcation diagram in Figure 34, which gives a global picture of the long-term dynamics and bifurcations of the TCC rule (89) in terms of the relevant control parameters H and T. The bifurcation curves have been obtained using the implicit or explicit expressions previously described. The colored areas correspond to different dynamical regimes for TCC. At each regime, there is a different effect of TCC in population dynamics in comparison with CC. After the description of the colored areas, we shortly describe the bistability regions marked with B1 and B2 in Figure 34.

In the remainder of the subsection, we present some 1-parameter BDs which show bifurcation scenarios that occur when varying one of the harvest control parameters H and T. The bifurcation scenarios exhibit some typical bifurcation sequences occurring in piecewise-smooth discontinuous maps, according to a specific regularity, such as a *Farey Tree* in a period-adding scenario or a slightly modified *truncated skew tent map scenario*; a detailed explanation of both scenarios is given in (Avrutin et al., 2019, Chapter 3). If we consider other threshold and quota values, for instance $T = 1$ and $H \in (H_{20}, T)$, we observe other features, such as the *bandcount incrementing scenario*. In all 1-parameter BDs, the background color indicates the dynamical regime corresponding to the two-parameter bifurcation diagram in Figure 34.

Dynamical regimes

For a general population map f satisfying conditions **(A1)-(A2)** with $x_c = \infty$, we define and identify the following dynamical regimes, which exist in certain parameter regions. For each dynamical regime, we additionally describe what the dynamics of CC would look like (see Proposition 5.2.1) and what effect TCC has in comparison with CC.

- *Unconditional persistence* (light blue): TCC guarantees persistence and convergence to an equilibrium for all initial conditions. This dynamical regime is not possible for the CC rule with $H > 0$ and $T = 0$. In compar-

ison with CC, TCC allows for unconditional persistence in the following ways:

- Bistability between extinction and the LAS equilibrium $x^*_+ > \tilde{x}$ in CC is replaced by the (essential) global attractor x^*_+ or K. This dynamics takes place when: $0 < T < f(\tilde{x})$, $0 < H < \min\{T, H_{oscill}, H_{20}\}$ (see the top row in Figure 30 and Figure 32(A3)); $f(\tilde{x}) \leqslant T < K$, $0 < H < H_{10}$ (see Figure 31(A1)) and; $K < T < \sup\{f(x) : x > 0\}$, $H < H_{20}$.
- Extinction in CC is replaced by global attraction to the fixed point K, when $K < T < \sup\{f(x) : x > 0\}$ and $H_{20} < H < T$.

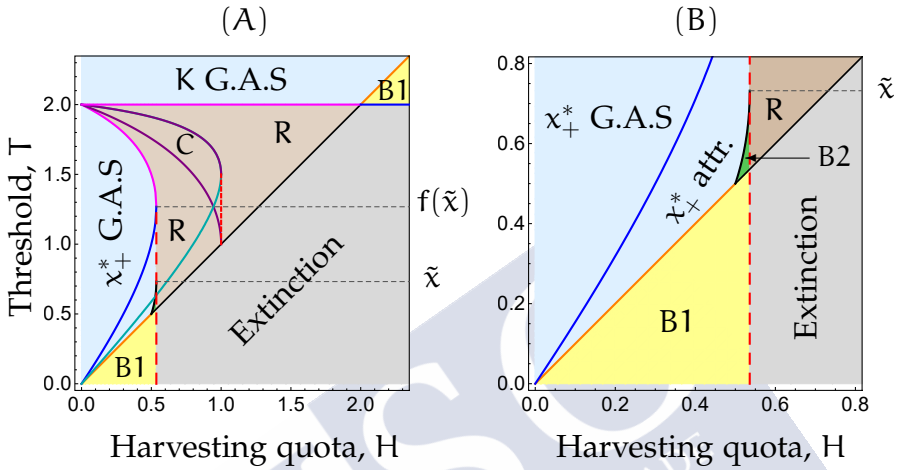

Figure 34: (A): Main bifurcation curves of the TCC rule with the Beverton-Holt map $f(x) = 3x/(1+x)$ in the two-parameter plane of the harvest control variables. Solid lines are for bifurcations involving break points, that is, border-collision bifurcations (BCBs), basin boundary metamorphoses and boundary-collision bifurcations. Dashed and dotted lines are for smooth-bifurcations (SBs) of F_{TCC} and F^2_{TCC}, respectively. Bifurcations of fixed points are shown in dark blue for existence BCBs, magenta for period-adding BCBs and red for fold SB. Bifurcations of 2-cycles are shown in light blue for existence BCBs, purple for period-adding or more complex BCBs, and red for fold SB. Basin boundary metamorphoses are shown in orange and boundary-collision bifurcations in black. Parameter regions labeled with B1 exhibit either bistability or tristability. Complex behavior (m-cycles with $m > 3$ or chaos) may be expected in regions marked with R. The region labeled with C has an attracting 2-cycle. In the region labeled with Extinction, there may exist long transients for some initial conditions ending in extinction or bistability between 0 and an oscillatory attractor. Colored areas indicate dynamical regimes that are explained in the main text. (B): Enlargement of (A) for $0 < T < \tilde{x}$. The region labeled with B2 exhibits bistability.

- *Conditional persistence* (yellow): Some initial conditions lead to population persistence, whereas other initial conditions lead to extinction. In compar-

ison with CC, TCC reduces the set of initial conditions which converge to 0 in several ways:

  - If $0 < T < f(\tilde{x})$ and $T \leqslant H < H_{oscill} < H_{20}$, then $T > x^*_-$ and some initial conditions in $(0, x^*_-)$ converge to the LAS equilibrium x^*_+ instead of being led to extinction.
  - If $0 < T < f(\tilde{x})$ and $\max\{H_{oscill}, T\} < H < H_{20}$, then $T < x^*_-$ and the interval $I = [0, T]$ is absorbing. Numerical bifurcation diagrams suggest that some initial conditions in $(0, x^*_-)$ converge to 0; but other initial conditions in $(0, x^*_-)$ may oscillate in I, at least during long periods of time before being led to extinction (see Figure 35(A)). All initial conditions in (x^*_-, ∞) converge to x^*_+ as in the CC rule.
  - If $K < T < \sup\{f(x) : x > 0\}$ and $T < H$, then all initial conditions in $(0, K]$ converge to the LAS equilibrium K instead of being led to extinction.

- *Unconditional oscillatory persistence of small populations* (green): TCC guarantees persistence for all initial conditions; there is bistability between x^*_+ and an oscillatory attractor. The latter attracts small population sizes. More specifically, all initial conditions in $(0, x^*_-)$ remain oscillating in $[T - H, T] \subset (0, x^*_-)$ instead of being led to extinction in the case of CC. This situation takes place when $0 < T < \tilde{x}$ and $H_{oscill} < H < \min\{H_{20}, T\}$ (see Figure 32(A1)).

- *Unconditional oscillatory persistence of all initial conditions* (brown): TCC guarantees persistence in the form of oscillatory attractors for all initial conditions. This dynamical regime does not exist in CC and occurs in TCC in the following ways:
  - If $0 < T < K$ and $H_{20} < H < T$, then extinction in CC is replaced by persistence in the interval $I = [T - H, T]$ for all initial conditions.
  - If $f(\tilde{x}) < T < K$ and $H_{10} < H < H_{20}$, then bistability between the LAS equilibria x^*_+ and 0 is replaced by persistence in $I = [T - H, T]$ for all initial conditions.

- *Extinction* (gray): All initial conditions eventually go extinct. This occurs in TCC if $0 < T < K$ and $\max\{T, H_{20}\} < H$. Numerical bifurcation diagrams suggest that either all initial conditions lead quickly to extinction; or that some positive initial conditions converge to 0 while others may oscillate in $I = (0, T]$, at least during long periods of time before being led to extinction. The dynamical regime of extinction for all initial conditions also exists in CC, but the possibility that some initial conditions lead to long oscillations before eventual extinction is due to TCC.

We can summarize the main characteristics of Figure 34 by distinguishing the threshold value relative to the maximum allowed quota. On the one hand, in

the case that $T > H$, the TCC strategy protects the population from extinction, for all initial conditions. We can broadly distinguish three different variations. First, if $T > K$, there will be no harvesting as the threshold is above the carrying capacity and K is GAS. Second, if $H < H_{20}$ and $\max\{\tilde{x}, H\} < T < f(\tilde{x})$, then x_+^* is an essential global attractor or GAS. Third, if $H > H_{20}$ so that the population would collapse under the CC rule, TCC guarantees persistence and there is an oscillatory attractor in the absorbing interval I, for all $H < T < K = 2$.

On the other hand, in the case that $T < H$, the TCC harvesting strategy is not protective enough that it guarantees persistence for all initial conditions. Indeed, if $H > H_{20}$ such that extinction is inevitable under CC, this is also the case under TCC unless $T > K$, in which case some initial conditions may persist. However, if $H < H_{20}$, CC leads to conditional persistence. TCC does not change this dynamical regime when $T < H$, but it makes extinction less likely because the set of initial conditions resulting in extinction decreases.

Bistability regions

In view of Theorems 5.4.1 and 5.4.2, there are different regions in the control parameter plane (H, T) where the long-term behavior of the solutions of TCC model (89) depends on the initial conditions. They do not appear in the usual form, that is, between two fold bifurcations. We observe in the 2-parameter bifurcation diagram in Figure 34 that they occur, when the harvesting quota H increases, after a bifurcation involving break points: basin-boundary metamorphosis or boundary-collision bifurcation. However, if $T < \tilde{x}$, they end when H increases through a fold SB at $H = H_{20}$.

The parameter regions labeled with B1 exhibit either "bistability" between the unstable fixed point 0 and the LAS equilibrium (x_+^* or K); or tristability if $T < K$ and there is an oscillatory attractor in the absorbing interval $I = [0, T]$ instead of long-transients ending in extinction. Thus, the simplest dynamics occur when $T > K$, where the basin of attraction of K is $(0, \infty)\backslash[m, M]$ and the initial conditions in $\{0\} \cup [m, M]$ converge to 0. When $T \in (0, \tilde{x})$, we distinguish two cases:

- If $H \in (\max\{T, H_{oscill}, H_{20}\})$, then the basin of attraction of x_+^* is exactly (x_-^*, ∞).
- If $H \in (T, \min\{H_{oscill}, H_{20}\})$, then the basin of attraction of x_+^* is larger and contains $(f^{-1}(x_-^*), T) \cup (x_-^*, \infty)$.

The region labeled with B2 exhibits bistability between the LAS fixed point x_+^* and an oscillatory attractor (m-periodic with $m > 3$ or chaotic) contained in the absorbing interval $I = [T - H, T] \subset (0, \infty)$.

1-parameter BDs varying H

Based on the 2-parameter bifurcation analysis, it is obvious that the impact of varying H depends on the value of T. Recall that, for $T = 0$, TCC becomes the

CC harvesting strategy. Here, we consider three different cases for $T > 0$. We first deal with small values of T ($0 < T < \tilde{x}$), where we can expect oscillations resulting from TCC. We then consider large values of T ($f(\tilde{x}) < T < K$), where increased quota values H lead from an equilibrium being an (essential) global attractor to complex dynamics. Last, we consider intermediate values of T ($\tilde{x} < T < f(\tilde{x})$), where the bifurcation sequence is more complex than for small or large thresholds. When $\tilde{x} < T < K$, there is a transition from (essential) global attraction of x_+^* to periodic or complex dynamics; the transition is to periodic dynamics if $f'(T) = g'(T-H) < 1$ at the bifurcation point; and it is to chaotic dynamics if $f'(T) = g'(T-H) > 1$ at the bifurcation point (see Bernardo et al., 2008, subsections 4.2.3 and 4.2.4).

First, let us begin with a small threshold value, $T = 0.52 < \tilde{x} \approx 0.73$. There are five bifurcation points as H increases from zero. For small to intermediate harvest quotas H, there is (essential) global attraction to the fixed point x_+^* of g (light blue background color in Figure 35(A)). At the bifurcation value $H_3 = H_{oscill} \approx 0.51$, there is a boundary-collision bifurcation, creating bistability between the equilibrium x_+^* and an oscillatory attractor contained in $I = [T-H, T]$ (green background color in Figure 35(A)). Their basins of attraction are separated by the unstable fixed point x_-^* of g. At $H_4 = T$, there is a boundary-collision bifurcation as the oscillatory attractor collides with the unstable fixed point 0; we then have a region of bistability between 0 and x_+^* (yellow background color in Figure 35(A)). Notice that, for quota values slightly greater than T, we observe oscillations which may be an oscillatory attractor or long transients; thus, there may be tristability between 0, x_+^* and (long) oscillations. At $H_5 = H_{20} \approx 0.54$, a fold SB occurs and, for $H > H_5$, apparently, all initial conditions converge to 0 (grey background color in Figure 35(A)). Furthermore, at $H_1 = H_{12} \approx 0.31$ and $H_2 \approx 0.45$, there are two existence BCBs for F_{TCC} and F_{TCC}^2, respectively; however, we do not plot the unstable 2-cycle in Figure 35(A) since it has not so much influence on the long-term dynamics.

Second, we consider a bifurcation sequence that occurs for large threshold values. This is shown in Figure 35(B) for $f(\tilde{x}) \approx 1.268 < T = T^{**} = 1.5 < K = 2$. At $H_1 = H_{10} \approx 0.5$, there is a period-adding BCB and, at $H_5 = T$, there is a border-collision bifurcation. In between these two bifurcations (brown background color in Figure 35(B)), we observe oscillatory dynamics. As H increases from H_{10} (where $f'(T) = g'(T-H) \in (0,1)$), we find a period-adding scenario. Between the period-adding BCBs at $H_2 \approx 0.8$ and $H_3 = H* = 1$, there is an attracting 2-cycle. For some values of the quota $H \in (H_2, H_3)$, we see that the average population size is bigger than the GAS equilibrium x^* at $H_1 = H_{10}$; this means that an increased harvesting quota elevates the average population size, which is know as hydra effect. At $H_4 \approx 1.36$, there is a transition from an attracting 3-cycle to chaotic dynamics through a fold SB for $F_{TCC}^3 = f^2 \circ g$.

Finally, we consider a bifurcation sequence that occurs for intermediate threshold values. This is shown in Figure 36(A) for $H^{**} = 1 < T = 1.1 < f(\tilde{x}) \approx 1.27$. As in Figure 35(B), we observe a region of oscillatory dynamics (brown back-

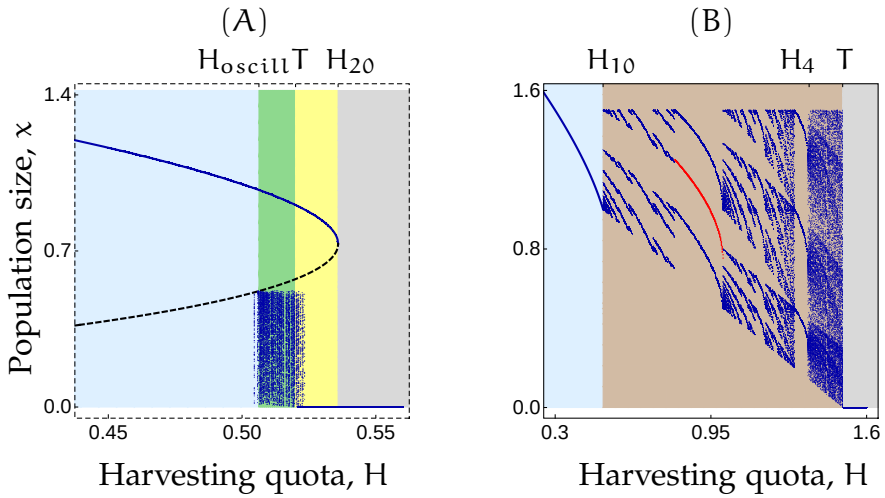

Figure 35: Bifurcation sequences for increased harvesting quotas H in the TCC rule (89) with the Beverton-Holt map $f(x) = 3x/(1+x)$. (A) : Case for a small threshold value $T = 0.52 < \tilde{x} \approx 0.73$. The black dashed curve represents the unstable equilibrium x^*_- of g. (B) : Case for a large threshold value $f(\tilde{x}) \approx 1.268 < T = T^{**} = 1.5 < K = 2$ and $H \in (0.3, 1.6)$. The red solid curve represents the average population size in the parameter region where the 2-cycle of $f \circ g$ is an attractor.

ground color) between the two bifurcation points at $H_1 = H_{20} \approx 0.536$ (fold SB) and $H_4 = T$ (border-collision bifurcation). But now we find a different bifurcation sequence for this oscillatory parameter region. At $H_1 = H_{20}$, since $f'(T) = g'(T-H) > 1$, there is a transition from the globally attracting fixed point $x^*_+ < \tilde{x}$ to complex dynamics as H increases (see Figure 36(A)). For even larger values of H, the complex dynamics are replaced by a period-adding scenario (see Figure 36(B)). When further increasing H, we observe a sequence of bifurcations similar to those in a truncated skew tent map scenario, giving rise to an exchange between cyclic and more complex dynamics (see Figure 36(C)-(D)). More precisely, at $H_3 = H^{**} = 1$, there is a fold SB for $F^2_{TCC} = f \circ g$: as H decreases, an unstable and a stable 2-cycle are created; then, at $H_2 \approx 0.992$, the stable 2-cycle becomes virtual, and after the BCB we observe complex dynamics. If we continue decreasing H (see Figure 36(C)), the unstable orbit plays a role in the dynamics; between two collisions of the bands of the chaotic attractor with the unstable 2-cycle, the chaotic attractor does not fill the absorbing interval $I = [T-H, T]$. Note that the two boundary-collision bifurcation are interior crises.

1-*parameter BDs varying* T

Now we consider T as a bifurcation parameter while keeping the quota H fixed. Before doing so, we note that, according to the two-parameter bifurcation diagram in Figure 34, the dynamics are strongly influenced by the relative position of H with respect to the critical value H_{20}. We summarize this in the following way. First, consider aggressive harvesting with thresholds smaller than the

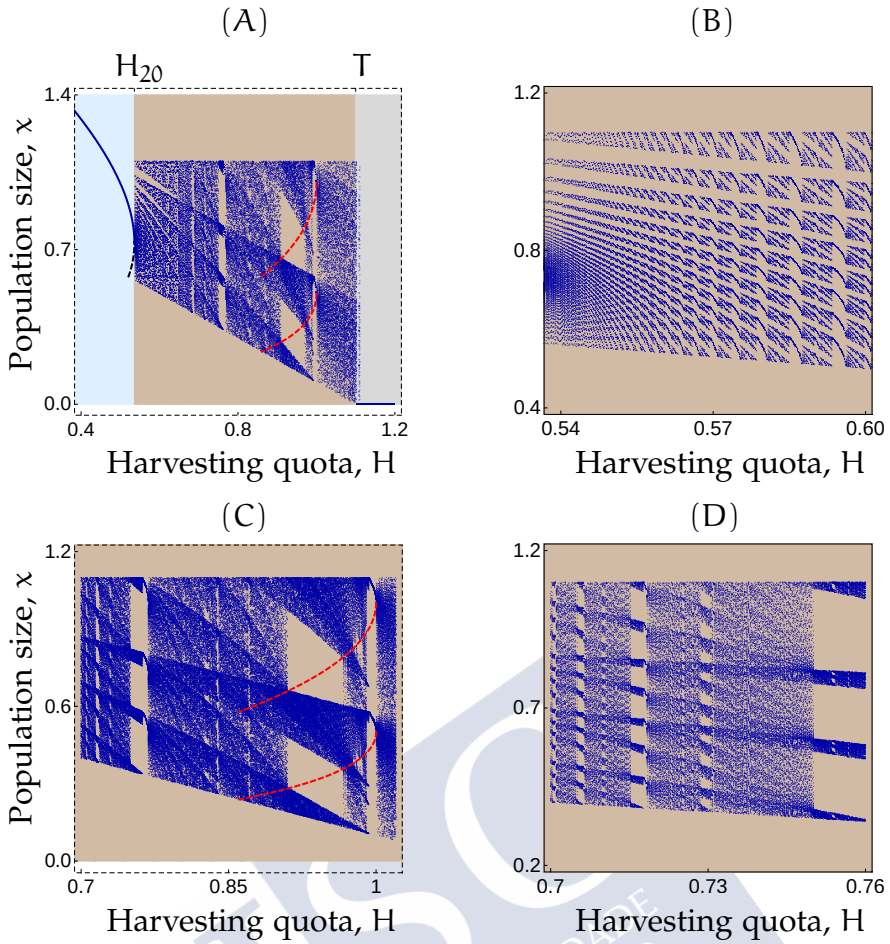

Figure 36: Bifurcation sequence for the TCC harvesting strategy (89) with the Beverton-Holt map $f(x) = 3x/(1+x)$ and an intermediate threshold value $H^{**} = 1 < T = 1.1 < f(\tilde{x}) \approx 1.268$ when increasing the harvest quota H. The black dashed curve in (A) corresponds to the unstable fixed point x_-^* of g. The red dashed curves represent the unstable 2-cycle of $f \circ g$. The panels show repeated zooms into the bifurcation parameter H.

maximum allowed quota, i.e., $T < H$. On the one hand, if $H > H_{20}$, then 0 might attract all initial conditions. On the other hand, if $H < H_{20}$, then sufficiently large initial conditions converge to the LAS equilibrium x_+^*. Second, consider more protective harvesting with thresholds larger than the maximum allowed quota. On the one hand, if $H_{20} < H$ and $T < K = 2$, then there is an oscillatory attractor in the absorbing interval I. On the other hand, if $H < H_{20}$ and $\max\{\tilde{x}, H\} < T < f(\tilde{x})$, then x_+^* is an essential global attractor or GAS.

It is also worth mentioning that, for $H < H_{20}$, a continuous variation (increasing or decreasing) of the threshold T can be either stabilizing and destabilizing (see Figure 37(A)). However, for $H > H_{20}$, an increment on the threshold T is always stabilizing (see Figure 37(B)), but the stable fixed point is the virgin stock K and exists for $T > K$, that is, for a very protective harvest rule that leads to no harvesting. Notice that, for threshold values slightly smaller than K

and $H < T$, there is always a period-adding scenario, since, for $T \approx K$, we have $f'(T) = g'(T - H) \in (0, 1)$.

We illustrate the above comments in two numerical bifurcation diagrams (see in Figure 37), namely for $H = 0.52 < H_{20} \approx 0.54$ and $H = 1.1 > H_{20}$.

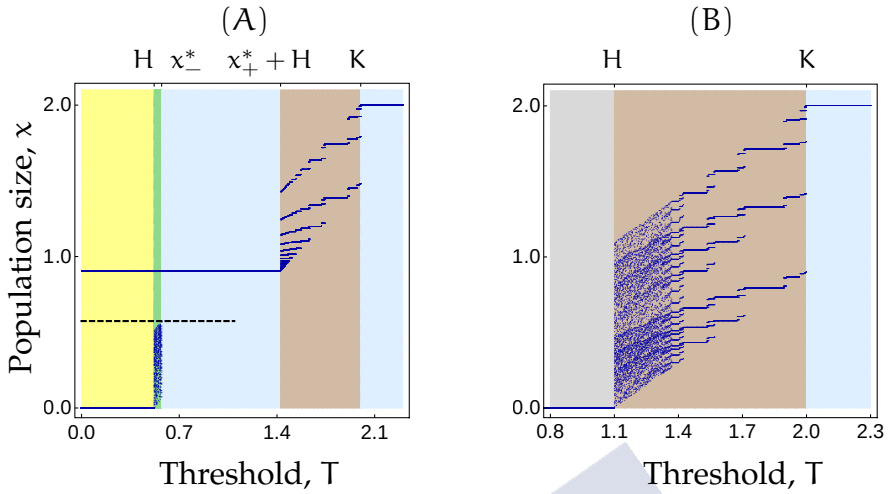

Figure 37: Bifurcation sequences when varying the harvest threshold for the TCC rule (89) with the Beverton-Holt map $f(x) = 3x/(1 + x)$. The black dashed curve in (A) corresponds to the unstable fixed point x^*_- of g. (A): Case with modest harvest quota $H = 0.52 < H_{20} \approx 0.54$. (B): Case with large harvest quota $H = 1.1 > H^{**} = 1$. We find a small region of transition from apparent chaos to a period-adding scenario.

We begin with the case $H = 0.52 < H_{20}$ shown in Figure 37(A). For small, protective thresholds values $T < H$, there is bistability between extinction and $x^*_+ \approx 0.9$ (yellow background). At $T_1 = H$, a boundary-collision bifurcation occurs and replaces the extinction equilibrium, to which initial conditions in $[m, M]$ converge, by an oscillatory attractor contained in I (green background). Hence, there are two regions of bistability for $T < T_2 = x^*_- \approx 0.57$. For $T \in (x^*_-, x^*_+ + H)$, we observe that the equilibrium x^*_+ is GAS. Finally, there are two period-adding BCBs at $T_3 = x^*_+ + H \approx 1.43$ and $T_4 = K = 2$; the first one destabilizing the dynamics and the second one stabilizing dynamics at the virgin stock level where no harvesting takes place anymore.

Finally, let us consider the case $H = 1.1 > H_{20}$ in Figure 37(B). For small thresholds $T < H$, all initial conditions converge to the extinction equilibrium (grey background). For very protective thresholds $T > K$, harvesting is ceased and the virgin stock size K is GAS (light blue background). In between these two extremes (brown background), there are oscillatory population dynamics. More specifically, they emerge at $T = H$ in a boundary-collision bifurcation, which replaces extinction by complex dynamics. As T increases, we observe a transition from apparently chaotic dynamics to a period-adding scenario. At $T = K$, the transition from oscillations to the GAS equilibrium K occurs in a period-adding BCB.

5.4.5 *Average yield and harvest frequency*

Here, we consider a more exploitation-oriented perspective by studying the average yield and harvest frequency, as functions of the harvest control parameters. We first recall and extent some theoretical results, before turning to numerical simulations. For that purpose, let us consider $T \geqslant 0$ and $H > 0$, then the catch or yield obtained in generation $n \in \mathbb{N}$ with the CC rule (86) ($T = 0$) or the TCC harvesting strategy (89) ($T > 0$) develops according to

$$Y_n = \begin{cases} 0, & f(x_n) < T; \\ \min\{f(x_n), H\}, & f(x_n) \geqslant T. \end{cases} \tag{93}$$

A rigorous theoretical study on the MSY for the CC rule and the TCC rule, in the particular case of the Beverton-Holt model (80), can be found in (AlSharawi and Rhouma, 2009). Assuming that the management objective is the indefinite survival of the population, they conclude that, for the CC rule, the MSY is $H_{20} = f(\tilde{x}) - \tilde{x}$ and can be attained if and only if $x_0 \geqslant \tilde{x}$. However, if $x_0 < \tilde{x}$, then the optimal catch is $H_{opt} = f(x_0) - x_0 < H_{20}$. Note that $\tilde{x}$ is the population size that sustains the MSY. That is, even for the optimal choice of the harvesting quota H, the MSY can be attained only for initial conditions exceeding the critical biomass level $\tilde{x}$ corresponding to MSY. For the TCC strategy with $T = f(\tilde{x})$, AlSharawi and Rhouma (2009) show that the MSY is equal to H_{20} and attainable for all initial conditions. In the following, as an expansion of the work by AlSharawi and Rhouma (2009), we study the average yield $\overline{Y}$ and harvest frequency HF for the TCC rule applied to the Beverton-Holt model $f(x) = r\,x/(1+x)$, $r > 1$.

Analytical results

In some particular cases, it is possible to carry out an analytical study of both the average yield and the harvest frequency. For instance, when an equilibrium or a 2-cycle is an (essential) global attractor. First, assume that $T > K$ and $H < T$, then K is GAS. So, for all initial conditions, after removing transients, we have $\overline{Y} = 0$ and $HF = 0$. That is, there is no harvesting in the long run. However, if $T \in [\tilde{x}, f(\tilde{x})]$ and $H = H_{20} < T$, then the equilibrium $\tilde{x}$ is an (essential) global attractor. In this case, for almost all initial conditions we have $\overline{Y} = H_{20}$ and $HF = 1$. That is, we can harvest at MSY all the time.

Now, we consider (H, T) values such that F_{TCC} has a 2-cycle which is an (essential) global attractor (see the region labeled with C in Figure 34(A)). The 2-cycle $\{x_1, x_2\}$ satisfies $f(x_1) < T < f(x_2)$, thus $\overline{Y} = H/2$ and $HF = 1/2$. In this case, the average yield attains a local supremum at $H = H^{**} = (r-1)^2/(r+1)$ and $T = T^{**}$ (with $g \circ f(T^{**} - H^{**}) = T^{**} - H^{**}$). It is easy to prove that $H^{**} < H_{20} = (\sqrt{r}-1)^2$, for all $r > 1$, which means that the MSY is not attainable. However, numerical simulations show that, in spite of having harvest

moratoria every other generation, the average yield can be close to H_{20} (see Figure 38(B)).

Numerical results

The presence of more complex dynamics or bistability makes it difficult to develop a rigorous analytical study of the average yield and harvest frequency. Thus, we study some numerical simulations for the Beverton-Holt population map $f(x) = 3x/(1+x)$, which help us to better understand the influence of T and H on $\overline{Y}$ and HF.

We begin by considering two different values of the threshold, namely $T = 0$ and $T = f(\tilde{x})$ (see Figure 38). For each of the fixed threshold values, we choose a random initial condition x_0 in $[0, \max\{F_{TCC}(x), x > 0\}]$. Then, we vary the fixed quota and for each value of H we run the system of equations (89)-(93) 650 times. After removing transients (600 iterations), we compute the average yield and harvest frequency for the last 50 iterations as follows:

$$\overline{Y} = \frac{1}{50}\sum_{n=601}^{650} Y_n, \quad HF = \frac{1}{50}\sum_{n=601}^{650} HF_n,$$

where, at generation $n \in \mathbb{N}$, $HF_n := 1$ if harvesting takes place and $HF_n := 0$ if there is no harvesting.

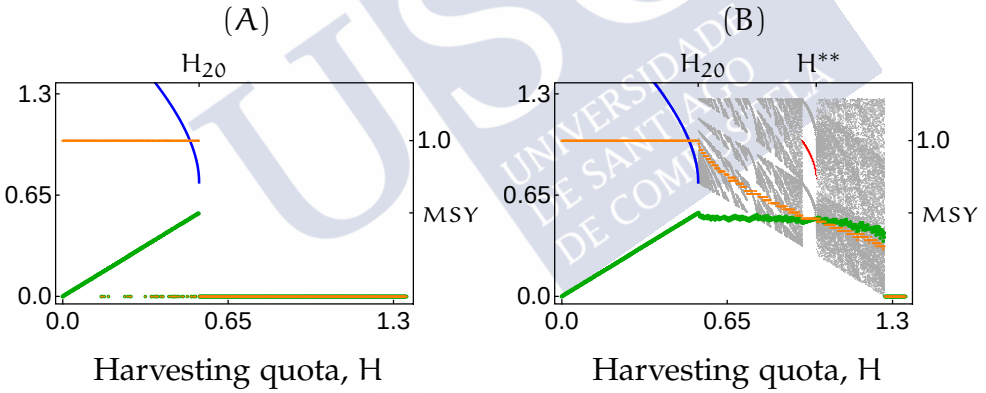

Figure 38: Average yield (green lines) and harvest frequency (orange lines) for (A) : the CC rule with $T = 0$ and (B) : the TCC rule with $T = f(\tilde{x})$. The blue curve represents the LAS equilibrium x^*_+. The red curve is the mean population size of the 2-cycle. The population bifurcation diagram is shown in gray color. Simulations are for (89)-(93) with the Beverton-Holt map $f(x) = 3x/(1+x)$; see the main text for more details.

First, the case $T = 0$ (CC rule) is presented in Figure 38(A). For quota values $H \leqslant H_{20}$ we observe bistability. If $x_0 < x^*_-$, the population perishes in a finite number of generations, so after removing transients $\overline{Y} = 0$ and $HF = 0$. If $x_0 > x^*_-$, the population converges to the LAS equilibrium x^*_+, so $\overline{Y} = H$ and $HF = 1$. When $H > H_{20}$, as 0 is GAS, after removing transients we have $\overline{Y} = 0$ and $HF = 0$. Therefore, Figure 38(A) illustrates that H_{20} is the MSY for the CC rule.

Second, the case $T = f(\tilde{x})$ is presented in Figure38(B). We observe two main improvements in comparison with the CC rule. For $H \leqslant H_{20}$, the equilibrium x^*_+ is a global attractor and, for all positive initial conditions, $\overline{Y} = H$ and $HF = 1$ (after removing transients). For $H \in (H_{20}, T)$, the population persists in an oscillatory manner and the average yield is smaller but quite close to MSY. Notice that for the CC rule ($T = 0$) it is quite risky to harvest at MSY, because $\overline{Y} = 0$ for all $H > H_{20}$. However, for $T = f(\tilde{x})$ and $H \in (H_{20}, H^{**})$, $\overline{Y}$ remains very close to MSY and harvesting takes place at least every other generation as $HF \geqslant 1/2$.

Now, we vary the threshold and fix the quota value $H = H_{20}$, which is the MSY for $T \in [0, f(\tilde{x})]$. In Figure 39, we show the average yield and harvest frequency as the threshold T increases, that is, as the harvesting strategy becomes more protective. If $T \in (0, \tilde{x})$, we observe bistability as for the CC rule, but the set of positive initial conditions for which $\overline{Y} = H_{20}$ and $HF = 1$ increases with increasing T (not explicitly illustrated in Figure 39). Moreover, for $T \in [H_{20}, \tilde{x})$, $\overline{Y} > 0$ for all positive initial conditions. The MSY is attainable for all positive initial conditions, if and only if $T \in [\tilde{x}, f(\tilde{x})]$, since $H_{20} < \tilde{x}$. For $T \in (f(\tilde{x}), K)$, the population persists in an oscillatory manner, and there are some generations of harvest moratoria and average yields smaller than H_{20}. When T is close to $K = 2$, the harvesting strategy is very conservative and the average yield is almost null.

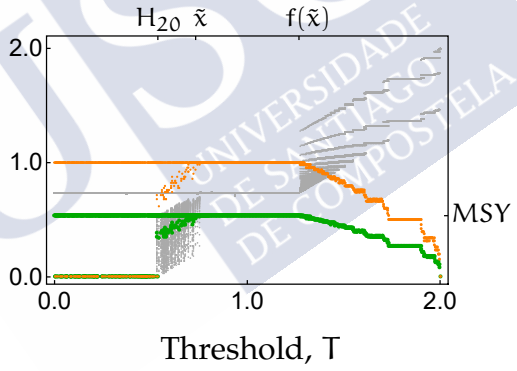

Figure 39: Average yield (green lines) and harvest frequency (orange lines) for the TCC rule with a fixed quota $H = H_{20}$ and increasing harvesting thresholds. The population bifurcation diagram is shown in gray color. Simulations are for (89)-(93) with the Beverton-Holt map $f(x) = 3x/(1+x)$; see the main text for more details.

5.5 DISCUSSION

Here, we summarize our main achievements and connect our research work with other related studies. As usual, we organize the contents in paragraphs with a explanatory headline.

Interests to study piecewise smooth dynamical systems

Piecewise smooth dynamical systems are undergoing an increasing interest for two main reasons: on the one hand, they find applications in various fields, like economics, social sciences, electronics, mechanics, population management, and control, among others (Agliari et al., 2011; Bernardo et al., 2008; Radi and Gardini, 2018; Segura, Hilker, and Franco, 2020); on the other hand, they exhibit rich dynamics, including new bifurcations different from the well known bifurcations for smooth maps. In this chapter, we have presented two new examples of piecewise maps which come from a threshold constant catch harvesting strategy (TCC) and a precautionary alternative (PTCC).

Influence of CC and TH in the dynamics of PTCC and TCC

PTCC and TCC can be seen as combinations of constant catch harvesting (CC) and threshold harvesting (TH) rules. The maps governing these two strategies are piecewise smooth: the graph of the map for constant harvesting has a flat part at the bottom (Schreiber, 2001), and the corresponding map for TH is flat-topped (Hilker and Liz, 2020). The dynamics of PTCC are strongly influenced by both maps: results valid for CC help to understand the dynamics of PTCC for small values of T (see Subsection 5.3.2), and typical features of the bifurcation diagrams of TH are present in those of PTCC (see Figures 25(B) and 26). As a result, the dynamics of PTCC is richer than and qualitatively different from the dynamics of TH and other threshold-based control rules as proportional threshold harvesting (PTH, for short), see, e.g., (Hilker and Liz, 2019). By contrast, we show that the dynamics of the TCC rule differ substantially to those of these three strategies.

General description of long-term dynamics of PTCC and TCC

We have combined analytical and numerical results to provide a thorough overview of the dynamics of PTCC and TCC. For simple cases (compensatory models), when applying the continuous control rule PTCC, the dynamics and bifurcations are thoroughly described analytically, and all initial conditions converge to a positive equilibrium. By contrast, the application of TCC gives rise to rich and complex dynamics ranging from boundary-collision bifurcations and basin boundary metamorphoses over multistability and homoclinic orbits to BCBs. For some parameter values we can assert that a positive equilibrium is GAS. In some dynamical regimes, we know for sure that oscillations exist (see Figure 32(A1)), while in other cases there may be long transients (see Figure 35(A)). If the long transients are actually oscillatory attractors, there is tristability. In practice, it might not matter whether the oscillations are transient when they are on a long time scale (Hastings et al., 2018). In parameter regions with an attracting 2-cycle (see Figure 35(B)), we find a hydra effect. This effect

cannot occur in non-oscillatory mode (for $T < K$), since the attracting fixed points decrease as harvesting parameters increase. The border-collision bifurcations come in the form of existence and period-adding BCBs. The boundary-collision bifurcations come in the form of both boundary crises (Figures 35(A)-(B), 36(A) and 37(A)-(B)) and interior crises (Figure 36(C)). Bischi, Lamantia, and Tramontana (2014) also studied a discontinuous one-dimensional map without harvesting below a threshold, but with proportional (rather than constant catch) harvesting above the threshold. They found BCBs as well. We recall that related control rules like pure threshold harvesting, CC, proportional harvesting or PTCC are continuous, so their dynamical behavior (e.g., AlSharawi and Rhouma, 2009; Hilker and Liz, 2020) is less rich.

As expected, overcompensatory models under the PTCC strategy exhibit more complicated dynamics; in this case, some regions of the 2-parameter plane (H, T) can be completely understood; for example, some global stability results (see Subsection 5.3.1.2), and regions where bistability or essential attraction occur (see Subsection 5.3.2). We have chosen as case study a Ricker model which in the absence of harvesting is oscillatory but not chaotic. This choice allows us to provide good 2-parameter bifurcation diagrams (see Figure 23) and also to compare our results with those obtained for CC by Schreiber (2001) and for TH by Hilker and Liz (2020). Selected numerical bifurcation diagrams illustrate the main dynamical features of PTCC, which include bistability regions created and destroyed by fold bifurcations or boundary collisions, sudden transitions between chaos and periodic attractors, and bubbles, among others. In contrast with other continuous threshold harvesting rules (TH, PTH), the fixed point of F_{PTCC} does not need to be unique for the usual unimodal maps. When two stable equilibria coexist, we observe a phenomenon similar to the so-called Allee effect: too low or too high population densities asymptotically approach the threshold value T, while intermediate population densities tend to a higher equilibrium.

Significant dynamical characteristics of PTCC and TCC

An important characteristic of the map associated to PTCC is that it is a continuous piecewise-smooth map that has flat branches. In this situation, border-collision bifurcations play an essential role. For compensatory models, there are just two types of BCBs, persistence and fold bifurcations of fixed points (see Figure 21). For overcompensatory population models, some additional types of BCBs appear, such as: flip BCBs of fixed points and fold, persistence and flip BCBs of 2-cycles. For the Ricker model with $r = 2.6$ under PTCC, we observe that the variety of BCBs is wider than that corresponding to other continuous piecewise-smooth models with flat branches, e.g., TH or CC. For TH, we can deduce from Proposition 5.2.2 that the BCBs are either persistence or flip; while for CC there are not BCBs, see Proposition 5.2.1. It is worth mentioning that the boundary-collision bifurcations are not due to the non-smoothness of F_{PTCC}.

In some cases, the presence of flat branches leads to superstable attractors and other typical features of flat-topped maps, such as the essential global attraction of the orbit of T, ranges of effectively chaotic behavior, periodic windows and star-like intersections. Piecewise-smooth maps with flat branches appear in different applications, ranging from chaos control (Corron, Pethel, and Hopper, 2000; Glass and Zeng, 1994; Sinha, 1994) to economic models (Agliari et al., 2011; Brianzoni, Michetti, and Sushko, 2010), and sustainable harvest rules (Hilker and Liz, 2020).

Probably the most notorious feature of the TCC rule from a dynamical systems point of view is the discontinuity at the harvesting threshold. This makes the TCC rule a discontinuous piecewise-smooth map. In order to show the influence of the discontinuity point, we recall that, in the absence of harvesting, models with compensatory population growth like the Beverton-Holt map always yield stable dynamics and not even damped oscillations. Besides, we have already mentioned that, when applying PTCC to general compensatory models, all initial conditions converge to an equilibrium; moreover, we are not aware of many simple control rules like TCC that can destabilize Beverton-Holt dynamics. By contrast, for certain control parameter values, TCC can induce oscillations in population size. The oscillations could be formed by alternating phases of population size decay (overharvesting above threshold) and recovery (population growth below threshold). Hence, TCC induces an effect similar to overcompensation, i.e., reduced population growth at large population sizes, which is well-known to induce oscillations. Regarding non-smooth bifurcations in discontinuous piecewise-smooth one-dimensional dynamical systems, we also find some interesting features. Firstly, it is mentioned in (Avrutin et al., 2019) that, although we usually study bifurcations of attractors, bifurcations of other invariant sets can also essentially influence the dynamics and are worth to be investigated. This is the case for the existence BCB of the unstable 2-cycle in Figure 36(C). However, we observe in Figure 35(A) that, for smaller values of the threshold T, the same type of bifurcation does not have a significant influence on the dynamics. Secondly, there are non-smooth bifurcations for F_{TCC} which appear in a different manner to the one described by Avrutin et al. (2019). For instance, basin boundary metamorphoses and boundary-collision bifurcations occur without the existence of a homoclinic orbit (we find homoclinic orbits at period-adding BCBs, see Figures 31 and 33). Basin boundary metamorphoses are simple, that is, they do not involve fractal basins of attraction as in Grebogi, Ott, and Yorke (1983). Boundary-collision bifurcations are due to the non-smoothness of the TCC map, which is not the case for PTCC (see Subsection 5.3.2). There are also some BCBs different to those described by Avrutin et al. (2019), for instance the existence BCB. Thirdly, we observe typical sequences of bifurcations in one-parameter bifurcation diagrams, the period-adding scenario (see Figures 35, 36 and 37) and an apparent truncated skew tent map scenario (see Figure 36). The last scenario does not exactly follow the

structure defined by Avrutin et al. (2019, Section 3.2), because it is not possible to have a degenerated flip bifurcation, since $(F_{TCC}^{2k})'(x) > 0$ for all $x > 0$.

PTCC and TCC as sustainable control rules based on thresholds

The PTCC rule is a precautionary strategy with multiple biomass reference points, such that the escapement is at least as large as the threshold. However, the TCC control rule has a unique reference point and it is possible that the population size after harvesting falls below the threshold. This could seem strange if the threshold is viewed as a minimum below which the population size should not fall. However, our results show that despite this possibility TCC is still beneficial for both population conservation and sustained yield. Only when the harvesting quota is so high that it exceeds the threshold ($H > T$), population extinction is possible.

PTCC and TCC overcome some concerning problems of traditional control rules

From a biological point of view, PTCC and TCC are harvesting strategies that help preventing some undesirable consequences of traditional control rules. On the one hand, we have shown in this chapter that both PTCC and TCC are, not surprisingly, protective strategies in the sense of promoting population persistence, where CC harvesting would lead to sudden collapses due to overexploitation. The constant catch strategy is risky because the MSY quota is at a fold bifurcation point; increasing the quota slightly moves the fishery into the extinction regime. On the other hand, the main drawback of a threshold approach is the fisheries moratoria associated with low stock size. A combined strategy like PTCC or TCC also helps to overcome this weakness of threshold harvesting rules. In this direction, a manager would be interested in situations where the long-term dynamics is governed either by g (usual constant harvesting) or by g and the threshold T in PTCC. The reason is that periods without harvesting only appear when f plays a role in the definition of F_{PTCC} or F_{TCC}. As it is expected, this undesirable situation corresponds to a combination of high values of T and small values of H (more conservative strategies). For the threshold constant catch rule, we have studied the (long-term) average yield complementing some previous work: with TCC, the MSY is still obtained for the same quota value that for CC, as already shown by AlSharawi and Rhouma (2009), but for thresholds $T > H_{20}$ there is a "buffer" for harvest quotas $H \in (H_{20}, T)$ guaranteeing population persistence for all initial conditions even if the quota is beyond the MSY value that would lead to collapse under CC harvesting (e.g., Figures 35(A), 36 and 37). Remarkably, the average yield has been found to be almost as high as the MSY in this buffer range (see Figure 38(B)). Also, the harvest frequency remains close to 100% near the MSY value (see Figures 38(B) and 39). This observation coincides with a similar finding in a specific model for Baltic Sea cod (Hjerne and Hansson, 2001). TCC therefore seems viable for

adaptive management, allowing quotas around and beyond the MSY, which typically comes with many problems for fisheries (Sinclair, Fryxell, and Caughley, 2006). Therefore, TCC remedies many of the well-known and notorious problems of pure threshold harvesting, such as high yield variability and fishery closures, as it provides high yields with almost no fishing moratoria.

Population destabilization by increasing harvesting

There are two different forms of increasing harvesting effort in PTCC or TCC: increasing the harvesting quota H or decreasing the threshold value T.

For simple compensatory population models, a variation of harvesting parameters does not modify the stability of fixed points.

Thus, we have focused on the effects of PTCC applied to overcompensatory models. For large H, PTCC becomes TH, and therefore a stable equilibrium cannot be destabilized increasing harvesting by decreasing the threshold (Hilker and Liz, 2020). However, fixing a lower value of H, decreasing T can produce several stability switches, some of them destabilizing. For the Ricker map, increasing H cannot destabilize a stable equilibrium. However, it might occur for other population models governed by unimodal maps with negative Schwarzian derivative. Examples of such situations for a strategy of constant quota harvesting are provided by Jiménez López and Liz (2021).

USC
UNIVERSIDADE
DE SANTIAGO
DE COMPOSTELA

6 LASOTA DISCRETE MODEL FOR BLOOD CELL PRODUCTION

This chapter comprises the contents of the research article (Liz and Lois-Prados, 2020a)[1], where we develop a detailed qualitative study of the discrete-time blood cell model proposed by Lasota. The chapter is divided into four different sections.

We begin with an Introduction in Section 6.1, where we first include the model formulation; then we motivate the usefulness of the model as a representation of several clinical cases and as a population model including adult survivorship; finally we summarize our contributions to the previous study of the dynamics in (Lasota, 1977).

The analytical results and numerical simulations we use to determine the asymptotic dynamics appear in Sections 6.2 and 6.3, respectively. We first provide fixed points existence and stability results, that allow to describe the associated local SBs. Then, we fix $c = 0.47$ and obtain a 2-parameter BD in the parameter plane (γ, σ), where we summarize the results from Section 6.2. We conclude Section 6.3 by showing some numerical 1-parameter BD, which illustrate the rich dynamics of equation (95) and help to complete the information given in the 2-parameter BD. We find different types of bubbles, hydra effect and features typical of models with Allee effect, that is, extinction windows and several mechanisms of essential extinction.

Finally, in Section 6.4, we first consider the model as Lasota did, that is, as a discrete-time representation of the blood cell production process. In this case, we revisit the conclusions obtained by Lasota on the influence of the destruction rate σ, giving extra details or advising of some mistakes found in (Lasota, 1977). We additionally interpret the influence of the degree of disturbance γ, which was not covered by Lasota. We conclude the section emphasizing the relevance of the study in the framework of population dynamics, in particular for $\sigma \in (0, 1)$ and $\gamma \neq 1$.

1 Eduardo Liz (Departamento de Matemática Aplicada II, Universidade de Vigo, Spain) & Cristina Lois-Prados (Instituto de Matemáticas, Universidade de Santiago de Compostela, Spain), "A note on the Lasota discrete model for blood cell production", *Discrete and Continuous Dynamical Systems Series B (ISSN: 1553524X, 15313492)*, **25**, pp. 701-713, 2020. The final authenticated version was published online at: http://doi.org/10.3934/dcdsb.2019262
JCR 2019 (category; impact factor; relative position; quartile): Applied Mathematics; 1.27, 115/261, Q2.
SJR 2019 (category; impact factor; quartile; H index): Discrete Mathematics and Combinatorics; 0.82; Q1; 45.
PhD student contributions: An outline of the manuscript had been previously conceived by my supervisor E. Liz, then the authors have equally contributed to the development of the final version.

6.1 INTRODUCTION AND MODEL DESCRIPTION

In this section, we include the formulation of the discrete model for blood cell production studied in this chapter, as well as a summary of our research study. We use headlines to outline the contents comprised within each paragraph.

Formulation of the discrete model by Andrzej Lasota

Based on experimental results, the Polish mathematician Andrzej Lasota proposed in 1977 (Lasota, 1977) a discrete model for the production of red blood cells (erythrocytes). If x_n denotes the number of cells at time n, and σx_n is the number of cells destroyed in the time interval $[t_n, t_{n+1}]$, then the dynamics is governed by equation

$$x_{n+1} - x_n = -\sigma x_n + p_n, \tag{94}$$

where p_n is the number of cells which are produced in the bone marrow during the same period. The bone marrow has the ability to change production when the number of blood cells changes, so $p_n = p(x_n)$. Based on experimental results, the form $p(x) = (cx)^\gamma e^{-x}$ was proposed for the production function, thus leading to the difference equation

$$x_{n+1} = (1-\sigma)x_n + (cx_n)^\gamma e^{-x_n}, \tag{95}$$

where $\sigma \in (0,1)$ and c, γ are positive constants.

The model as a representation of different clinical cases

As indicated by Lasota, equation (95) provides a flexible model that explains the behavior of the blood cell population in many clinical cases. For example, if $\gamma > 1$, then there is a critical value of the population size such that populations below it cannot survive in the long term. In population dynamics, such effect is known as a strong Allee effect (Courchamp, Berec, and Gascoigne, 2008). In the model under consideration, it means that, if the number of cells is too small (for example, after a heavy hemorrhage), then the organism eventually dies. Cell populations above the critical value usually persist and they can approach a stable positive equilibrium (which is considered the normal behavior), but its number can oscillate when there is a disease affecting the blood cell production, and even behave in an erratic (aperiodic) way in the case of a severe disease. As the examples in (Lasota, 1977) show, an increasing value of σ leads to severe disease (because a large proportion of cells are destroyed). Even though this model assumes that the blood production is not a continuous process (a more accurate model seems to be a delay differential equation (Lasota, 1977; Wazewska-Czyzewska and Lasota, 1976)), it is quite intuitive and displays a very rich dynamics.

Interpretation as a discrete-time model for iteroparous populations

On the other hand, equation (95) can also be considered as a discrete model for iteroparous populations (which means that, part of the population survives the reproductive season) whose recruitment function is defined by a gamma-Ricker map (Liz, 2018a). In this context, equation (95) is a flexible model for populations with discrete reproductive seasons, adult survivorship, overcompensating density dependence, and Allee effects.

Overview of the research study

In this chapter, we show some interesting aspects of the dynamics of (95) that can help to understand the potential effects of increasing either the destruction rate of cells (in the erythropoietic model), or the adult mortality rate (in the population model). We proceed as follows:
We provide a detailed study of the fixed points stability and associated local SBs. Then we fix the parameter $c = 0.47$ and summarize the long-term dynamics and bifurcations in a 2-parameter BD. In order to complete this information, we plot some 1-parameter BDs, which we also use to revisit the results obtained by Lasota (1977). We find several features which he did not observed, such as the possibility of a bubbling effect, destabilizing and then stabilizing the cell population, as the destruction rate σ increases. In the discussion section we also include an interpretation of the results in the framework of population dynamics.

6.2 FIXED POINTS: LOCATION, STABILITY AND BIFURCATIONS

In this section, we study the fixed points of the map associated to Lasota's equation (95), depending on the parameter values σ, γ and c. By contrast with the research study carried out in Chapter 5, where we require the stock-recruitment function to fulfill conditions **(A1)-(A2)**, here we consider a case study given by the function in (95) and we shall start by determining some basic properties in Subsection 6.2.1. We continue to study the number of fixed points, their location and stability. We first consider the case $0 < \gamma \leqslant 1$ and then $\gamma > 1$; in the former case we obtain a sharp global stability condition. Finally, in Subsection 6.2.3, we classify the local bifurcations of fixed points, all of them smooth (flip, fold and pitchfork).

6.2.1 *Preliminary results*

We first introduce the maps $f : [0,\infty) \to [0,\infty)$ and $F_{BC} : [0,\infty) \to [0,\infty)$ defined by

$$f(x) = (cx)^{\gamma} e^{-x}, \quad F_{BC}(x) = (1-\sigma)x + (cx)^{\gamma} e^{-x} = (1-\sigma)x + f(x), \qquad (96)$$

where $\sigma \in (0,1)$, $c, \gamma > 0$. Notice that equation (95) can be written in the form $x_{n+1} = F_{BC}(x_n)$.

Some useful properties of the map f have been recently proved in (Liz, 2018a), and they will be useful in our analysis. Now, we state the intervals of monotonicity of F_{BC} depending on the parameters. We prove that F_{BC} can be either strictly increasing or bimodal (see Figure 40).

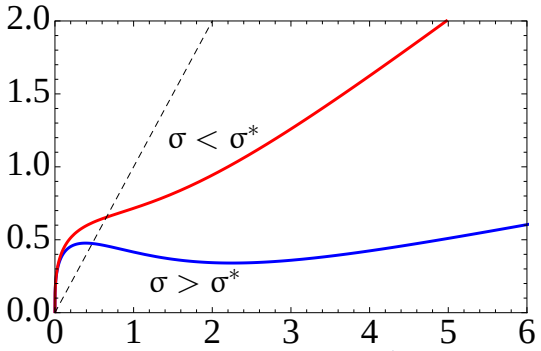

Figure 40: Graphs of the map F_{BC} for $\gamma = 0.3$, $c = 0.6$, and different values of σ: $\sigma = 0.6 < \sigma^* \approx 0.774$ in red (F_{BC} is strictly increasing), and $\sigma = 0.9 > \sigma^*$ in blue (F_{BC} has two critical points). The dashed line is the graph of $y = x$.

Theorem 6.2.1. *The map F_{BC} defined in (96) has the following properties:*

1. $F_{BC}(0) = 0$ *and* $\lim_{x\to\infty} F_{BC}(x) = \infty$.
2. F_{BC} *is differentiable in* $(0,\infty)$, $F'_{BC}(0^+) = 1-\sigma$ *if* $\gamma > 1$, $F'_{BC}(0^+) = 1-\sigma+c$ *if* $\gamma = 1$, *and* $F'_{BC}(0^+) = \infty$ *if* $0 < \gamma < 1$. *In any case,* $\lim\limits_{x\to\infty} F'_{BC}(x) = 1-\sigma > 0$.
3. *Define* $H(\gamma) = \sqrt{\gamma}(\gamma+\sqrt{\gamma})^{\gamma-1}e^{-\gamma-\sqrt{\gamma}}$. *The following statements hold:*
   a) *If* $c^\gamma H(\gamma) < 1$ *and* $0 < \sigma \leqslant \sigma^* := 1 - c^\gamma H(\gamma)$, *then* F_{BC} *is strictly increasing on* $(0,\infty)$.
   b) *If* $c^\gamma H(\gamma) \geqslant 1$, *or* $c^\gamma H(\gamma) < 1$ *and* $\sigma > \sigma^*$, *then* F_{BC} *has two positive critical points* $c_1 < c_2$. *Moreover,* F_{BC} *attains a local maximum at* c_1 *and a local minimum at* c_2.

Proof. The proof of items 1 and 2 is elementary, so we only provide the proof of 3.

The first and second derivatives of F_{BC} on $(0,\infty)$ are, respectively:

$$\begin{aligned} F'_{BC}(x) &= (1-\sigma) + c^\gamma x^{\gamma-1}e^{-x}(\gamma - x); \\ F''_{BC}(x) &= c^\gamma e^{-x}\, x^{\gamma-2}(x^2 - 2\gamma x + \gamma^2 - \gamma). \end{aligned} \tag{97}$$

We distinguish two cases according to the zeros of F''_{BC} on $(0,\infty)$ (see Figure 41).

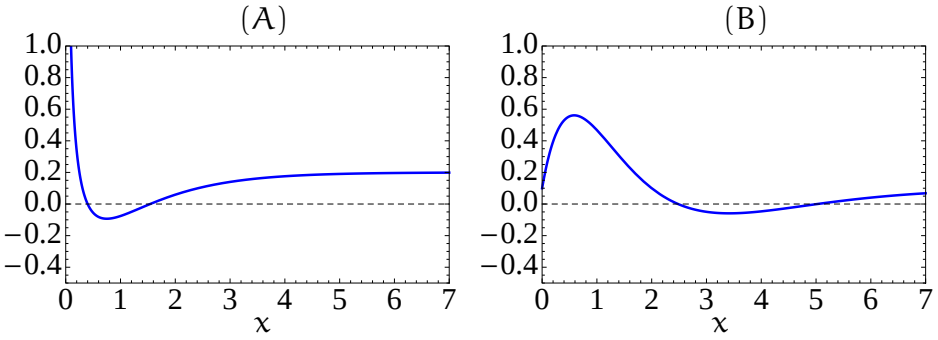

Figure 41: Graphs of the map F'_{BC} (solid, blue) and the line $y = 0$ (dashed, black), with $c = 1$. (A): $\gamma = 0.25 < 1$, $\sigma = 0.8 > \sigma^* \approx 0.707$; (B): $\gamma = 2 > 1$, $\sigma = 0.9 > \sigma^* \approx 0.841$. In both cases, there are two intersection points, that determine the critical points of F_{BC}.

If $\gamma \leqslant 1$, then F'_{BC} has a unique critical point at $d^+ = \gamma + \sqrt{\gamma}$; moreover, F'_{BC} is decreasing on $(0, d^+)$ and strictly increasing on (d^+, ∞).

If $\gamma > 1$, then $F''_{BC}(d^+) = F''_{BC}(d^-) = 0$, with $d^+ = \gamma + \sqrt{\gamma} > d^- = \gamma - \sqrt{\gamma} > 0$. In this case, $F'_{BC}(0^+) > 0$, F'_{BC} is strictly increasing on $(0, d^-) \cup (d^+, \infty)$, and decreasing on (d^-, d^+).

In both cases, it is clear that $F'_{BC}(x) \geqslant 0$ for all $x > 0$ if and only if $F'_{BC}(d^+) \geqslant 0$, and F'_{BC} has two positive zeros $c_1 < c_2$ if $F'_{BC}(d^+) < 0$. Moreover, it follows from the sign of F'_{BC} that c_1 corresponds to a local maximum of F_{BC}, and c_2 to a local minimum.

Finally, it is easy to check that condition $F'_{BC}(\gamma + \sqrt{\gamma}) \geqslant 0$ is equivalent to $\sigma \leqslant 1 - c^\gamma H(\gamma)$. □

6.2.2 *Existence and stability*

We begin by studying the existence and local stability of positive fixed points. In this regard, we first address the case $0 < \gamma \leqslant 1$, for which the map F_{BC} can have at most one positive equilibrium. Then, we consider the case $\gamma > 1$, where F_{BC} can have 0, 1, or 2 positive fixed points. Let us note that, in general, the fixed points of F_{BC} are the solutions of equation $f_1(x) = f_2(x)$, where $f_1(x) = \sigma x^{1-\gamma}$ and $f_2(x) = c^\gamma e^{-x}$.

Theorem 6.2.2. *Assume that* $0 < \gamma \leqslant 1$.

1. *If* $\gamma < 1$, *then* F_{BC} *has a unique positive fixed point* p. *Moreover,* $F_{BC}(x) > x$ *if* $0 < x < p$, *and* $F_{BC}(x) < x$ *if* $x > p$.

2. *If* $\gamma = 1$, *then* F_{BC} *has a unique positive fixed point* p *if* $c > \sigma$ *and no positive fixed points if* $c \leqslant \sigma$. *In the former case,* $F_{BC}(x) > x$ *if* $0 < x < p$, *and* $F_{BC}(x) < x$ *if* $x > p$.

3. *Assume that* $0 < \gamma < 1$, *or* $\gamma = 1$ *and* $c > \sigma$. *Then the unique positive equilibrium* p *is locally asymptotically stable for the Lasota equation* (95) *if the following condition holds:*

$$c^\gamma < G(\gamma, \sigma) := \sigma \left(\gamma + \frac{2}{\sigma} - 1\right)^{1-\gamma} e^{\gamma + \frac{2}{\sigma} - 1}. \tag{98}$$

If $c^\gamma > G(\gamma, \sigma)$, *then* p *is unstable.*

Proof. We only prove the case $\gamma < 1$, since the proof for $\gamma = 1$ is very similar.

The existence and uniqueness of p follows from the fact that $f_1(x) = \sigma x^{1-\gamma}$ is strictly increasing, with $f_1(0) = 0$, and $f_2(x) = c^\gamma e^{-x}$ is decreasing, with $f_2(0) > 0$, $f_2(\infty) = 0$. A simple graphical analysis shows that $F_{BC}(x) > x$ if $0 < x < p$, and $F_{BC}(x) < x$ if $x > p$.

The derivative of F_{BC} at the fixed point p is

$$F'_{BC}(p) = 1 - \sigma + \gamma c^\gamma p^{\gamma-1} e^{-p} - c^\gamma p^\gamma e^{-p} = 1 + \sigma(\gamma - 1 - p). \tag{99}$$

Since $\gamma < 1$, it is clear that $F'_{BC}(p) < 1$. On the other hand, it follows from (99) that

$$F'_{BC}(p) > -1 \iff p < \gamma + \frac{2}{\sigma} - 1.$$

Using the statement 1, it is clear that the last inequality holds if and only if

$$F_{BC}\left(\gamma + \frac{2}{\sigma} - 1\right) < \gamma + \frac{2}{\sigma} - 1,$$

and this inequality is equivalent to (98). □

Remark 10. We notice that equation (95) is *uniformly permanent* if either $\gamma < 1$ or $\gamma = 1$ and $\sigma < c$. This means that there exists a compact interval $[A, B]$ such that $0 < A \leqslant \liminf_{n\to\infty} F^n_{BC}(x) \leqslant \limsup_{n\to\infty} F^n_{BC}(x) \leqslant B$, for all $x > 0$. Indeed, if F_{BC} is strictly increasing then the unique positive equilibrium p is a global attractor, and we can choose $A = B = p$; if F_{BC} is bimodal, then elementary arguments show that we can choose $A = F_{BC}(c_2)$, $B = F_{BC}(c_1)$, where c_1, c_2 are the critical points of F_{BC} ($0 < c_1 < c_2$).

Theorem 6.2.3. *Assume that* $\gamma > 1$, *and define*

$$c^* := \left(\sigma\,(\gamma - 1)^{1-\gamma}\, e^{\gamma-1}\right)^{1/\gamma}. \tag{100}$$

Then the map F_{BC} *defined in* (96) *has two positive fixed points if* $c > c^*$, *one positive fixed point if* $c = c^*$, *and no positive fixed points if* $c < c^*$. *Moreover:*

- *If* F_{BC} *has only one fixed point* q, *then* $q = \gamma - 1$, $F'_{BC}(q) = 1$ *and* q *is semi-stable.*

- *If* F_{BC} *has two positive fixed points* q, p, *then* $q < \gamma - 1 < p$, $F'_{BC}(q) > 1$, *and* $F'_{BC}(p) < 1$. *The fixed point* q *is unstable, while* p *is asymptotically stable if* (98) *holds.*

- *If* $c < c^*$, *then all solutions of* (95) *converge to* 0.

Proof. Since $f_1(0^+) = \infty$, $f_2(0) = c^\gamma$, f_1 and f_2 are decreasing and convex, and $\lim_{x\to\infty}(f_1(x)/f_2(x)) = \infty$, it follows from elementary arguments that F_{BC} can have at most two positive fixed points.

Assume that there is at least one positive fixed point of F_{BC}, and denote by q the smallest one. It follows from the properties of f_1 and f_2 that $f_1'(q) \leqslant f_2'(q)$. This inequality, together with the equality $f_1(q) = f_2(q)$, leads to $q \leqslant \gamma - 1$. If $q = \gamma - 1$, then $f_1'(q) = f_2'(q)$ and $\gamma - 1$ is the unique positive fixed point of F_{BC}. However, if $q < \gamma - 1$, then $f_1'(q) < f_2'(q)$. Since $\lim_{x\to\infty}(f_1(x)/f_2(x)) = \infty$, there exists another fixed point $p > q$. Moreover, $f_1'(p) > f_2'(p)$, which is equivalent to $p > \gamma - 1$. Thus,

- there is a unique positive fixed point of F_{BC} if and only if $q = \gamma - 1$, that is, if $f_1(\gamma - 1) = f_2(\gamma - 1)$, which is equivalent to $c = c^*$;

- there are two positive fixed points q and p of F_{BC} if and only if the following inequality holds $f_1(\gamma - 1) < f_2(\gamma - 1)$, which is equivalent to $c > c^*$;

- F_{BC} does not have positive fixed points if $c < c^*$.

In the first case, by using the properties of f_1 and f_2, it is easy to check that $F_{BC}(x) < x$ for all $x > 0$, $x \neq q$. Therefore all solutions of (95) starting at an initial condition $x_0 \in (0, q)$ converge to zero. Moreover, if $F_{BC}(x) \geqslant q$ for all $x > q$, then all solutions starting at $[q, \infty)$ converge to q. If there are points $x > q$ such that $F(x) < q$, then the immediate basin of attraction of q is $[q, r]$, where r is the smallest point in $F_{BC}^{-1}(q) \setminus \{q\}$. Therefore, q is semistable.

In the second case, we have that $F'_{BC}(p) < 1 < F'_{BC}(q)$. Thus, q is unstable. If (98) holds, then $F'_{BC}(p) > -1$, implying that the equilibrium p is asymptotically stable.

Finally, if $c < c^*$, then $F(x) < x$ for all $x > 0$ and therefore all solutions of (95) converge to 0. □

Figure 42 shows the three different possibilities considered in the statement of Theorem 6.2.3.

Figure 41 illustrates that the map F_{BC} can have two critical points either if $\gamma = 0.25 < 1$ or $\gamma = 2 > 1$; and it is well known that a discrete dynamical system generated by a map with two critical points can lead to the coexistence of several attractors. However, if $\gamma < 1$ or $\gamma = 1$ and $\sigma < c$, we will prove that the unique positive fixed point p is a global attractor of all positive solutions of (95) when it is asymptotically stable. Moreover, we get that the parameter region of global asymptotic stability includes the nonhyperbolic case, thus extending condition (98) to $c^\gamma \leqslant G(\gamma, \sigma)$. The proof follows from Lemma 4.2.7 by taking $h(x) = F_{BC}(x)$ and $f(x) = (cx)^\gamma e^{-x}$.

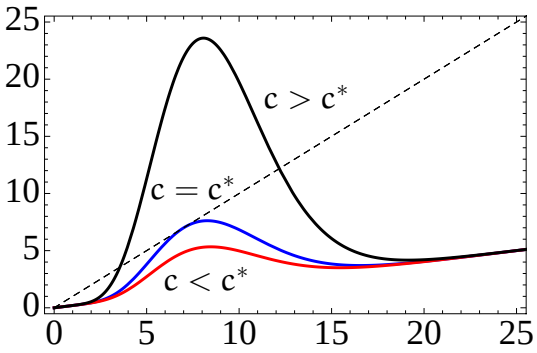

Figure 42: Graphs of the map F_{BC} for $\gamma = 8$, $\sigma = 0.8$, and different values of c: $c = c^* \approx 0.425$ in blue (one positive fixed point), $c = 0.4 < c^*$ in red (no positive fixed points), and $c = 0.5 > c^*$ in black (two positive fixed points). The dashed line is the graph of $y = x$.

Corollary 6.2.4. *Assume that* $0 < \gamma < 1$, *or* $\gamma = 1$ *and* $c > \sigma$. *Then, the unique positive equilibrium* p *for the Lasota equation* (95) *is globally asymptotically stable if and only if* $c^\gamma \leqslant G(\gamma, \sigma)$, *where* $G(\gamma, \sigma)$ *is defined in* (98).

Proof. It is clear from the proof of Theorem 6.2.2 that condition $c^\gamma \leqslant G(\gamma, \sigma)$ is equivalent to (84). Thus, in order to use Theorem 4.2.7, we only need to check conditions 1-4.

Conditions 1 and 2 follow from elementary arguments, and 4 was proved in (Liz, 2018a, Proposition 2). Hence, it remains to prove statement 3. From the proof of Theorem 6.2.1, we know that $f''(x) < 0$ for all $x \in (0, \gamma + \sqrt{\gamma})$. Since the unique critical point of f is $z = \gamma < \gamma + \sqrt{\gamma}$, then 3 follows. □

6.2.3 *Bifurcations of fixed points*

The properties of F_{BC} studied in statement 2 of Theorem 6.2.1, together with the existence and stability results found in Subsection 6.2.2 allow us to analyze the fixed points local bifurcations of the Lasota model (95), using the bifurcation parameters σ, γ and c. Since the map F_{BC} is smooth, then all local bifurcations are also smooth.

We first consider some properties of c^*, which can be seen as a function of the parameters $\gamma > 1$ and $\sigma \in (0, 1)$:

$$\lim_{\gamma \to 1^+} c^*(\gamma, \sigma) = \sigma \quad \text{and} \quad \lim_{\gamma \to 1^+} c^{*\prime}(\gamma, \sigma) = \infty.$$

Second, we remark that, if $\gamma = 1$ and $c \leqslant \sigma$, then $c^\gamma < G(\gamma, \sigma)$. The proof of these properties is elementary. Now, we are in a position to describe the existing bifurcations:

- A flip SB occurs if $\gamma > 0$ and $c^\gamma = G(\gamma, \sigma)$: if $c^\gamma < G(\gamma, \sigma)$, the fixed point of F_{BC} is GAS ($0 < \gamma \leqslant 1$) or LAS ($\gamma > 1$), but it becomes unstable for $c^\gamma > G(\gamma, \sigma)$ and a LAS 2-cycle emerges.

- A fold SB occurs if $\gamma > 1$, $c^\gamma < G(\gamma, \sigma)$ and $c = c^*$: as c decreases, the two coexisting fixed points of F_{BC} collide and disappear.
- A pitchfork SB occurs if $c > \sigma$ and $\gamma = 1$: as γ increases, the unstable extinction equilibrium becomes LAS and the unstable fixed point q emerges.

6.3 IMPACT OF PARAMETERS VARIATION ON LONG-TERM DYNAMICS

In this section, we combine the rigorous analysis from the previous sections with numerical bifurcation diagrams to show the potential rich dynamics of the solutions to the Lasota equation (95) and the role of the parameters γ and σ. For parameter c, we fix the value $c = 0.47$ already used by Lasota (1977). Although his study is restricted to $\gamma = 8$ and three different values of σ ($\sigma = 0.1, 0.4, 0.8$), we will consider more cases to give an idea of the more relevant dynamical phenomena. In particular, we will revisit the cases studied by Lasota.

We begin by displaying in Figure 43 a 2-parameter bifurcation diagram for $c = 0.47$, which shows in the parameter plane (γ, σ) the stability and extinction boundaries provided in Section 6.2. In this case, condition $c^\gamma \leqslant G(\gamma, \sigma)$ holds for all $\gamma \in (0, 1]$, and therefore Corollary 6.2.4 implies that the unique positive equilibrium is globally asymptotically stable in this parameter range (if $\gamma = 1$, this equilibrium exists only for $\sigma < 0.47 = c$).

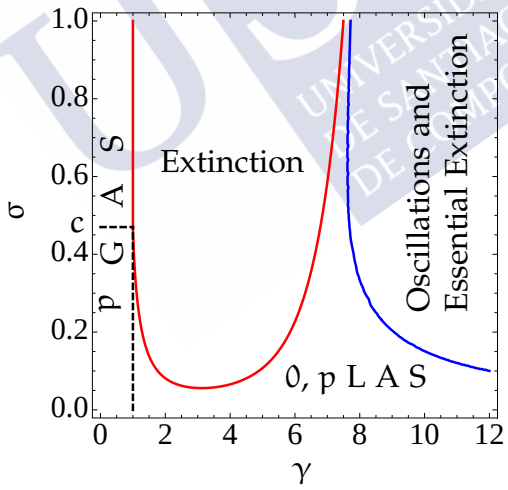

Figure 43: Main bifurcation boundaries and regions with different dynamical behavior for equation (95) with $c = 0.47$, in the parameter plane (γ, σ). The two solid lines represent the extinction boundary (red color) and the stability boundary of the largest positive equilibrium (blue color). The vertical dashed line $\gamma = 1$ (from $\sigma = 0$ to $\sigma = c = 0.47$) is the border between global stability of the unique positive equilibrium and a bistability region, in which both the largest positive equilibrium and the extinction equilibrium are asymptotically stable.

The red solid line is given by equation (100) when $\gamma > 1$. According to Subsection 6.2.3, this line corresponds to a fold bifurcation and represents the boundary between extinction and bistability. In the bistable case, there are solutions that converge to the extinction equilibrium and others that converge to the largest positive equilibrium, so permanence depends on the initial condition. For $\sigma > c$, the red line $\gamma = 1$ represents the boundary between global stability of the positive equilibrium and extinction, according to Subsection 6.2.3 it also corresponds to a pitchfork bifurcation.

The blue solid line represents the boundary of local asymptotic stability of p, which loses its stability at a flip bifurcation, so the region to the right of this line corresponds to more complicated dynamics, which includes periodic attractors, chaotic attractors, and essential extinction, as we show below in some numerical bifurcation diagrams. We recall that essential extinction means that almost all solutions (in a sense of Lebesgue measure) converge to zero (Schreiber, 2001, 2003). Essential extinction usually occurs after a boundary collision between the basins of attraction of a chaotic attractor and the extinction equilibrium 0; however, we report below different transitions from bistability to essential extinction.

In the remainder of this section, we show some relevant numerical bifurcation diagrams to illustrate the rich behavior of equation (95). In some cases (Figures 44 and 45), we fix a value of γ and use σ as a bifurcation parameter, while in Figure 46 we do the opposite.

Bubbles

A first interesting phenomenon is the existence of the so-called bubbles, which are characteristic in bifurcation diagrams of population models where some adults survive more than one reproduction period. A primary bubble is shown

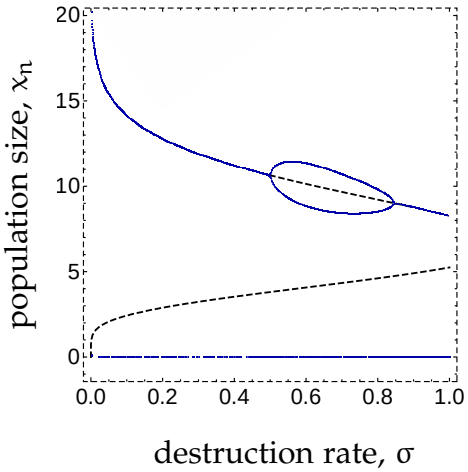

Figure 44: Bifurcation diagram showing a bubble for equation (95) with $c = 0.47$, $\gamma = 7.65$, using σ as the bifurcation parameter. Black dashed lines correspond to unstable equilibria.

in Figure 44: the largest positive equilibrium loses its asymptotic stability in a period-doubling bifurcation as the destruction rate σ increases, but stability is regained at the next bifurcation point for a larger value of σ, after a period-halving bifurcation occurs. This phenomenon shows that increasing the mortality rate can be either stabilizing or destabilizing. More complex bubbling effects can be observed in Figure 45(C). In this case, the equation can reach a chaotic regime inside the bubble (see (Liz and Ruiz-Herrera, 2012) for more details and related references).

Hydra effect

It is easy to check that the largest equilibrium of (95) decreases as σ increases. However, the average population size of the nontrivial attractor can increase with σ when the largest equilibrium loses its asymptotic stability. This phenomenon can be observed in Figure 45(B), where the average of the 2-periodic attractor is represented by a red solid line.

Sudden collapses

A typical feature of population models with Allee effects, where population cannot survive in the long term if its abundance is below a critical size, is the possibility of sudden collapses. Sudden collapses typically occur when the basins of attraction of the zero equilibrium and another attractor collide (boundary collisions). See, e.g., (Liz, 2010a; Schreiber, 2001, 2003).

There are two main mechanisms leading to sudden collapses. The simplest one is a fold bifurcation, which leads from bistability to extinction when the two positive equilibria of (95) collide and then disappear (see Figure 42). A bifurcation diagram showing this first case is given in Figure 45(A), for $c = 0.47$ and $\gamma = 7$. A more complex mechanism for sudden collapses is a catastrophe bifurcation, which takes place when a chaotic attractor collides with the basin of attraction of zero. This situation is represented in Figure 45(B), for $c = 0.47$ and $\gamma = 8$. We emphasize that these are the values chosen by Lasota (1977) to investigate the dynamics of (95) as σ increases. Although he found chaotic orbits for $\sigma = 0.8$, it seems he did not observe the sudden collapse, which occurs at $\sigma \approx 0.87$, when $F^2(c_1) = q$. As before, c_1 and q are the smallest critical point and the smallest positive fixed point of F, respectively.

The two above mentioned mechanisms are well known and have been rigorously explained (see, e.g., Schreiber, 2001); however, we have found a different situation. For $c = 0.47$, $\gamma = 8.5$, essential extinction would be expected to begin at $\sigma = \sigma_1 \approx 0.86$, when $F^2(c_1) = q$. However, at a previous value $\sigma = \sigma_2 \approx 0.8315$, an attracting 3-cycle disappears in a fold bifurcation for F^3, in such a way that the transition from bistability to essential extinction occurs at $\sigma = \sigma_2$ (see Figure 45(C) − (D)).

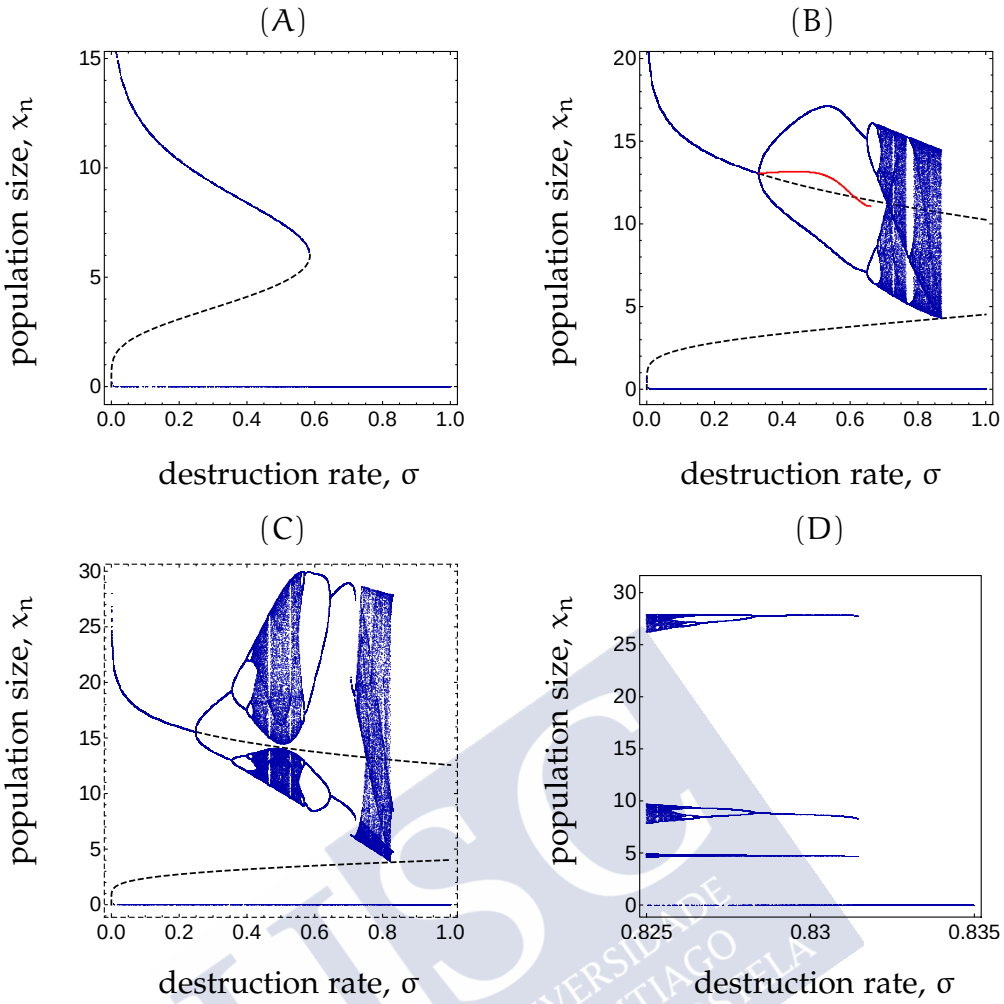

Figure 45: Bifurcation diagrams for equation (95) with $c = 0.47$, using σ as the bifurcation parameter. Black dashed lines correspond to unstable equilibria. For more details, see the text. (A): $\gamma = 7$; (B): $\gamma = 8$; (C): $\gamma = 8.5$ and $\sigma \in (0, 1)$; (D): magnification for $\gamma = 8.5$.

The three examples shown in Figure 45 illustrate that there are multiple possibilities for the transition to extinction or essential extinction in equation (95).

Extinction windows

The influence of parameter γ on the dynamics of (95) is quite interesting, as it can be observed in the 2-parameter diagram in Figure 43 for $c = 0.47$. For small values of σ, there is a transition from global stability of the positive equilibrium to bistability as γ passes the critical value $\gamma = 1$. This dynamical change occurs after a pitchfork bifurcation, where a new branch of (unstable) fixed points is born; see (Liz, 2018a), where this bifurcation is explained for the gamma-Ricker map, which corresponds to (95) with $\sigma = 1$. This case is shown in Figure 46(A) for $\sigma = 0.05$.

For larger values of σ, there are extinction windows, which were also observed in other models with Allee effects (Liz, 2010a; Schreiber, 2001, 2003). A simple extinction window originated by two fold bifurcations as γ increases (two positive equilibria disappear at the first one, but are created again in the second one) is shown in Figure 46(B) for σ = 0.1. Since the map F governing the dynamics of (95) is bimodal for larger values of σ (see Theorem 6.2.1), there can be multiple extinction windows, as it has been reported in (Liz, 2010a) for a population model with harvesting also governed by a bimodal map. These complicated dynamics are shown in Figure 46(C) for σ = 0.9. Thus, a thorough analysis of the influence of γ on the dynamics of (95) in the parameter region where oscillations and essential extinction can occur seems to be a very difficult task.

It is worth noticing that, in some population models, γ is a cooperation parameter (Avilés, 1999; Courchamp, Berec, and Gascoigne, 2008), and extinction windows are related to a kind of "rescue effect". That is to say, populations that go to extinction when cooperation rates are small can persist at intermediate population levels due to high cooperation intensity. However, larger rates of cooperation can lead to chaos and essential extinction. For related discussions, see (Liz, 2018a,b).

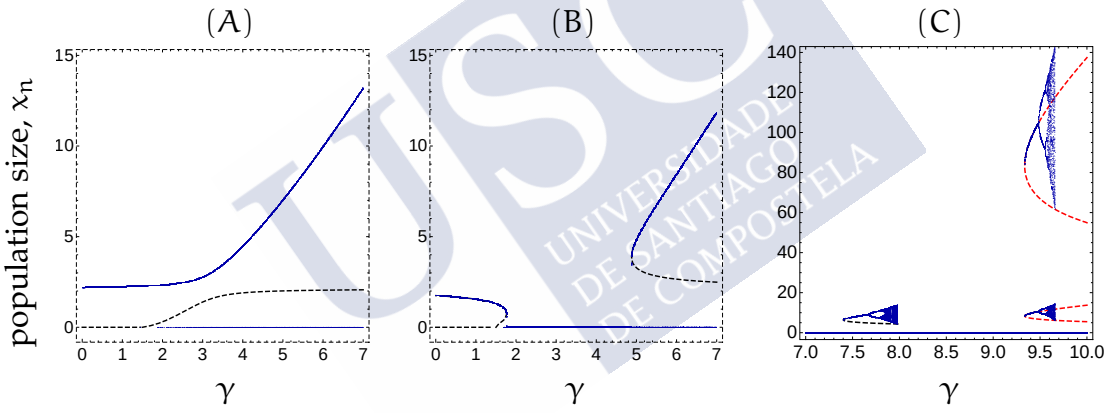

Figure 46: Bifurcation diagrams for equation (95) with c = 0.47 and different values of σ, using γ as the bifurcation parameter. Black dashed lines correspond to unstable equilibria, and red dashed lines to unstable 2-periodic orbits. (A): There are neither oscillations nor extinction windows for σ = 0.05. (B): An extinction window for σ = 0.1. (C): Multiple extinction windows for σ = 0.9.

6.4 DISCUSSION

Here, we review the research work developed in this chapter and compare it with the previous study due to Lasota. Moreover, we interpret the obtained results in the framework of population dynamics. We use headlines to organize the contents.

Interests leading to the further study of Lasota's blood cell production model

Some months before starting to study the dynamics of equation (95), my supervisor Eduardo Liz contacted Dr. Paweł J. Mitkowski to discuss about a model of delay differential equations for blood cell production, and he sent us a copy of the paper (Lasota, 1977). In this paper, the beautiful equation (95) was proposed as a simple one-dimensional discrete-time model for the production of blood cells. To explain the influence of the destruction rate σ on the behavior of the solutions of (95), Lasota fixed $c = 0.47$ and $\gamma = 8$. Then, he considered three values of σ, which were enough to explain the dynamics of blood cell production in some relevant clinical cases.

Our main motivation to write this paper was to carry out a much more detailed analysis of the dynamics of (95). We have combined an analytical study in Section 6.2 with a numerical approach in Section 6.3. While in the latter section we have fixed $c = 0.47$ as in (Lasota, 1977), our theoretical results (Theorems 6.2.1, 6.2.2, 6.2.3 and Corollary 6.2.4) show the strong influence of c on the dynamics. In particular, very small values of c lead the system to extinction (see Figure 42).

Revision of the conclusions exposed by Lasota

The main purpose of Lasota (1977) was showing chaotic behavior in some biological models, including (95); this fact explains the choice $\gamma = 8$ in (Lasota, 1977). Indeed, Figure 43 shows that, if $c = 0.47$ and $\gamma < 7.5$, then the dynamics of (95) is much simpler, as illustrated in Figure 45 for $\gamma = 7$.

The three cases studied in (Lasota, 1977) correspond to $c = 0.47$ and $\gamma = 8$, which are the parameters used in Figure 45(B). We are in a position to discuss these cases in more detail. Lasota distinguished three situations:

1. Normal conditions in blood cell production are assumed to correspond to small values of σ ($\sigma = 0.1$ in (Lasota, 1977)). In this case, the number of blood cells tends to remain constant, but the organism dies if the number of cells is too small. This situation corresponds to the case when (95) has three equilibria $0 < q < p$, and 0 and p are asymptotically stable. In this example, this occurs for $\sigma \in (0, \sigma_1)$, where $\sigma_1 \approx 0.331$ is the value at which p loses its asymptotic stability after a period-doubling bifurcation.

2. Intermediate values of σ would lead to a (non-severe) disease. For $\sigma = 0.4$, Lasota observed a 2-periodic attractor, explaining some oscillations in the number of blood cells that are typical of such diseases. The 2-periodic attractor corresponds to σ in the interval $(\sigma_1, \sigma_2) \approx (0.331, 0.651)$.

   An interesting remark of Lasota is that the ill system is able to adapt to a larger destruction rate, because the average value of the 2-periodic orbit for $\sigma = 0.4$ (about 13.1) is not much worse than the value of the attracting positive equilibrium (about 15.4) for $\sigma = 0.1$. Actually, we observe a

hydra effect, characterized by the fact that the average population can even increase as σ increases. For example, the average is 13.05 for $\sigma = 0.33$, and 13.074 for $\sigma = 0.5$ (see the thick red line in Figure 45(B)).

3. Larger values of σ in Lasota's example lead to chaotic behavior. The typical route of period-doubling bifurcations to chaos is observed in Figure 45. Lasota used the value $\sigma = 0.8$, for which a 3-periodic orbit can be found, and he reported a bistability scenario: solutions starting from an invariant interval $[A, B]$ converge to the chaotic attractor, while solutions starting at an initial point $x_0 \in (0, A)$ converge to zero. However, he did not mention that the basins of attraction of these two attractors collide at a larger value $\sigma \approx 0.87$, leading the population of cells to essential extinction.

One of the main conclusions of Lasota's example is that increasing σ is destabilizing. However, this is not always the case: our results show that a bubbling phenomenon is possible. For example, in Figure 44, we observe that the larger positive equilibrium p is asymptotically stable for $\sigma = 0.9$ but unstable for $\sigma = 0.7$. Figure 45(B) shows that the chaotic behavior can also be reversed by moving σ to a larger value. We refer to (Liz and Ruiz-Herrera, 2012) for further details and relevant references on bubbling.

New results on the influence of parameter γ

Another interesting aspect not covered by Lasota (1977) is the influence of parameter γ in the dynamics of (95). Although the meaning of this parameter was not explained in (Lasota, 1977), for a related model, Mitkowski (2011) argued that γ can be interpreted as the degree of disturbance from the normal response in the feedback loop that regulates the production of cells in the bone marrow: when $\gamma = 0$, the answer is correct, but when $\gamma > 0$, the response is inhibited and the greater is the inhibition, the greater is the value of γ. For example, extinction is not possible for $\gamma < 1$ (see Remark 10). For $\gamma > 1$, the dynamics strongly depend on the interaction between σ and γ: while for small values of σ the changes in γ do not affect the dynamics (see Figure 43), for larger values of σ there are extinction windows which can alternate with chaotic attractors (see Figure 46).

Overview of the research study in the framework of population dynamics

To finish, we emphasize that equation (95) is also of interest in population dynamics. When $\sigma = 1$, (95) is equivalent to the gamma stock-recruitment model used in fisheries (Quinn and Deriso, 1999), and has been also used in other contexts such as cooperation interactions in a group of individuals (Avilés, 1999) and populations with Allee effects (Courchamp, Berec, and Gascoigne, 2008). An important feature of this model is its flexibility, allowing different forms of density dependence (compensatory, overcompensatory, depensatory). For re-

cent results and discussions in this direction, see (Liz, 2018a,b; Liz and Buedo-Fernández, 2019). In this context, equation (95) is a relevant generalization of the classical Ricker model.

On the one hand, the usual discrete-time models with Allee effects assume that adults cannot survive the reproductive season (Schreiber, 2003), but this assumption is not realistic for many populations. The introduction of a positive adult survivorship rate $1-\sigma$ ($0<\sigma<1$) increases the generality of the model and induces some new dynamical phenomena in comparison with the classical gamma model. The most relevant ones are hydra effects, period-doubling reversals (bubbling), multiple extinction windows, and new mechanisms leading to essential extinction.

On the other hand, although the Ricker model with adult survivorship (corresponding to (95) with $\gamma=1$) has been considered before (see, e.g., (Liz, 2010a; Liz and Ruiz-Herrera, 2012; Yakubu et al., 2011) and references therein), the introduction of the parameter γ makes the model more flexible. For example,Yakubu et al. (2011) showed that equation (95) with $\gamma=1$ fits well the Atlantic cod fishery data, but the Pacific Halibut data are best fitted with $\gamma=2$. For $\gamma>1$, the recruitment function $f(x)=(cx)^{\gamma}e^{-x}$ combines both negative and positive density dependence. The parameter γ represents the strength of cooperation, and its influence on the stability and the size of the positive equilibria has been studied in (Liz, 2018a).

The above discussion highlights the importance of studying equation (95) in the framework of population dynamics. In particular, for $\gamma>1$, our analysis points out the subtle interplay between adult survivorship rates and Allee effects.

CONCLUSIONS AND FUTURE PROSPECTS II

In our opinion, the qualitative study of asymptotic dynamics carried out in this part of the thesis could be of potential interest in the framework of (piecewise-smooth) discrete one-dimensional dynamical systems, but also in fisheries management. In the following, we first include a section with conclusions, where we mention the knowdledge acquired during the PhD period in order to reach the objectives of this part of the thesis. Then, we describe some other ideas for future research, which we consider that could increase the value of our work.

A. Conclusions

Through Chapters 5 and 6 within Research Line II, the reader can find our contributions to the qualitative study of discrete dynamical systems that model the performance of single species populations. Both chapters finish with a discussion section, where we compare our work with some related research studies. In this section, we also talk about our achievements, but from a different perspective, mentioning what we have learned working in goals G3 and G4.

We start with Chapter 6, where we have included the contents of the research article (Liz and Lois-Prados, 2020a) devoted to attain objective G4. Although I had started to work in objective G3 before, it was the first objective we achieved in the framework of Research Line II. In my opinion, it has a justified reason, that is, the map associated to the model is more regular, so we could use the classical theory for smooth dynamical systems. However, depending on the values of the three distinct parameters, the map could be strictly increasing or have two critical points. Thus, the study was not so simple and, to understand the rich dynamics, the student was introduced in results ensuring that LAS implies GAS, as well as conditions for local and global bifurcations, representation of the main dynamics in a 2-parameter BD and interpretation of 1-parameter BD. Another important aspect of the model into consideration is that it can describe either the dynamics of red blood cells, or the dynamics of a single-species populations with adult survivorship and different forms of density dependence.

In Chapter 5, we included the contents of two articles devoted to attain objective G3. The presence of the threshold level reduces the regularity of the map, therefore, as a first step to achieve this goal, the PhD student needed to go in depth into the qualitative theory of piecewise-smooth one-dimensional difference equations, which incorporate many new dynamical behaviors with respect to the smooth ones. Moreover, since the considered discrete-time equations model the performance of populations subject to protective harvesting strategies, reading several fisheries management oriented works helped us to

understand the possible interdisciplinary potentials of our study, as well as to come up with new ideas for future research.

B. Future prospects

In the following, we give a brief description of three main research topics that we would like to carry out in the near future.

i. comparison of threshold-based harvesting strategies for compensatory and overcompensatory models

In the Introduction section in Chapter 5, we have compiled different reasons to consider control rules combining threshold reference points and constant catches. To our knowledge, there are not current harvest policies using these types of control rules. However, we have found in the literature that some species have been managed by means of harvest policies making use of fixed escapement (Bristol Bay sockeye salmon) or combinations of threshold reference points with fixed mortality rates (U.S. west coast ground-fish).

One reason, for the minor or no presence of TH and CC control rules combinations in harvest policies, might be the reduced research studies of their performance or possibilities to meet some management objectives. In this regard, our aim is to use an analytical approach to compare the performance of PTCC, TCC, TH and PTH (applied to compensatory and overcompensatory stock recruitment models). A similar study was developed by Hjerne and Hansson (2001) and Steiner, Criddle, and Adkinson (2011), they followed a non-analytical approach and recommended to use combinations of CC and TH control rules rather than TH, PH and PTH.

To accomplish this goal, we aim to complement the research study in Chapter 5 with the aspects mentioned below.

TCC asymptotic dynamics on overcompensatory population models

An equivalent study has been previously developed for the other three strategies: PTCC (Liz and Lois-Prados, 2020b), TH (Hilker and Liz, 2020) and PTH (Hilker and Liz, 2019).

As TCC is a discontinuous piecewise-smooth model, it may be difficult to develop a complete analytical study of the dynamics for general overcompensatory models. For that reason and in order to compare the results obtained for the four different control rules, as a case study, we would initially consider the Ricker model $x_{n+1} = x_n e^{r(1-x_n)}$ with $r = 2.6$ for the unmanaged population, since it had already been used in the above mentioned references.

Apart from the interest of the study in fisheries management, the qualitative study of the distinct bifurcations is also significant. We observed, in the 2-parameter BD representing the long-term dynamics of PTCC and TCC for

compensatory models (i.e., Figures 21 and 34), that the discontinuity of TCC induces complex dynamics, while for PTCC all initial conditions converge to a positive equilibrium. In the overcompensatory case, we expect even richer dynamics, since it is the case for the continuous model given by PTCC (see Figure 23). In order to carry out this part of the study, we plan to continue studying some references describing BCBs in discontinuous piecewise-smooth models. We have found interesting literature in some references cited by Bischi, Lamantia, and Tramontana (2014), such as (Gardini et al., 2010).

Average yield and harvest frequency

Once we have determined the long-term behavior of the population, we continue by studying the potential of the different strategies to provide high $\overline{Y}$ and low-variable HF.

We can reuse the research carried out in (Hilker and Liz, 2019, 2020; Lois-Prados and Hilker, submitted) for TH, PTH and TCC, but for TH and PTH we have to incorporate the harvest frequency to the study. In addition, we have to develop a similar study for PTCC applied to compensatory models and for both PTCC and TCC applied to overcompensatory models. Although we may be able to compare the performance of some harvest strategies for general models in some particular parameter regions, we predict that to obtain more precise results we would have to consider some particular case studies for the Beverton-Holt and Ricker models.

II. QUALITATIVE STUDY OF PROTECTIVE HARVESTING STRATEGIES WITH TWO THRESHOLD REFERENCE POINTS

In the Future Prospect I, we have cited the works by Enberg (2005) and Hjerne and Hansson (2001), whose simulation results support the use of different precautionary strategies, since they help to overcome the fisheries moratoria problem of simple threshold-based control rules. We recall that these precautionary strategies incorporate two different threshold levels $0 < T_1 < T_2$, rather than a unique reference point $T > 0$. The decision taken at the smallest level is allowing or forbidding to harvest, while at the highest threshold they determine the fishing intensity. Hjerne and Hansson (2001) proposed to use two alternative constant quota levels, the reduced quota been half of the normal one. Enberg (2005) considered two different mortality rates in two types of harvesting strategies: one removing a constant proportion of the excess, i.e., the stock biomass above the threshold; other removing a constant fraction of the total biomass. In this PhD monograph we have already studied a precautionary strategy, the PTCC rule formulated in Subsection 5.2.3. The distinct reference points in (88) are $T_1 = T$ and $T_2 = T + H$. When population is above the highest threshold, we remove a constant quota H; if biomass is below the smallest threshold, then

harvesting is forbidden; and for intermediate values of the stock, we apply TH removing all the surplus population above T_1.

The research carried out in (Enberg, 2005; Hjerne and Hansson, 2001) assesses the performance of precautionary strategies which are applied to particular simulation models for the Baltic Sea cod and the Norwegian spring spawning herring "Clupea harengus" populations. By contrast, to study the performance of the PTCC strategy, we have considered deterministic compensatory and overcompensaroty models; as well as the generic Ricker model as a particular case. We are not aware of other analytical studies of precautionary control rules. Therefore, we find interesting to develop a similar analytical study of other precautionary strategies.

Precautionary control rule using PH *and* CC *strategies*

The harvesting strategies used by Enberg (2005) and Hjerne and Hansson (2001) correspond to threshold-based rules that include different harvesting intensities, but they only use one control rule: CC or PH. We have already mentioned that PTCC also includes different harvesting intensities, but uses two distinct control rules: TH and CC. We have seen that this control rule prevents extinction for all values of the harvesting parameters, and it seems that the application of CC harvesting for high stock levels reduces the yield variability typical of TH. The use of the TH strategy at intermediate values of the population pretends to reduce harvesting moratoria, but we guess that the use of PTH rather than TH may improve the performance of the precautionary control rule, because the population would have a faster recovery to higher values where CC takes place. Thus, it may be significant to study this control rule, we refer to it as *precautionary proportional threshold harvesting constant catch* (PPTHCC).

For the formulation of this strategy, let us consider a map $f : [0,\infty) \longrightarrow [0,\infty)$, two threshold levels $0 < T_1 < T_2 < \sup\{f(x) : x \in [0,\infty)\}$, and the intervention parameters $H > 0$ and $0 < q < 1$, their dynamics are governed by:

$$x_{n+1} = F_{PPTHCC}(x_n) = \begin{cases} f(x_n), & f(x_n) \leqslant T_1; \\ (1-q)f(x_n) + qT_1, & T_1 < f(x_n) \leqslant T_2 + H; \\ f(x_n) - H, & T_2 + H < f(x_n). \end{cases} \quad (101)$$

If we consider the particular value of $q = H/(H + T_2 - T_1)$, then the map F_{PPTHCC} is continuous and it facilitates the study of the dynamics. Moreover, the parameters of the harvesting strategy are reduced, because q is expressed as a function of the other parameters. It would also be beneficial for managers, since they just have to determine the threshold levels and the constant quota H. There are also some reasons to consider the biomass reference point $T_2 + H$ instead of T_2. If the threshold was set at T_2, then after removing the constant quota H, the stock between T_2 and $T_2 + H$ would reduce to levels below T_2 and the map would be discontinuous. In that case, if we wanted to obtain a

continuous map, we would have to choose $q = H/(T_2 - T_1)$, and apply TH for population levels in the interval $(T_2, T_2 + H]$.

It would be interesting to study the potential of the continuous strategy given by (101) to provide high $\overline{Y}$ and low-variable HF. In particular, a comparison of this strategy with other threshold-based strategies, such as the "40-10" control rule currently utilized to manage the U.S. west coast ground-fish population, seems to be particularly significant from a fisheries management point of view. Notice that the "40-10" control rule is a particular case of a precautionary strategy studied by Enberg (2005).

III. ASYMPTOTIC DYNAMICS OF THE PTCC RULE ON POPULATION MODELS INCLUDING ADULT SURVIVORSHIP

In the Discussion section of Chapter 6, we provide reasons to study models including adult survivorship and cooperation of the population. We recall that the model into consideration does not include exploitation parameters, for $\gamma = 1$ (no cooperation), it reads as:

$$x_{n+1} = (1 - \sigma)x_n + cx_n e^{-x_n},$$

where $\sigma \in (0, 1)$ and $c > 0$. This is a Ricker model including adult survivorship, which represents a type of iteroparous population with overcompensatory density dependence. A general formulation of these types of models can be found in (Liz, 2010a), where they carry out a qualitative study of the asymptotic dynamics when the CC control rule is applied. They compare the results obtained with those in (Schreiber, 2001) for the semelparous case.

Thus, we consider interesting to follow the ideas in (Liz, 2010a) to complement the research developed in Section 5.3 of Chapter 5. The introduction of the threshold reference point in the model managed with CC might complicate the study of the dynamics, making the study interesting from a dynamical systems point of view.

This future prospect would be also relevant in the framework of fisheries management, since it would provide a wider knowledge to the literature on threshold-based control rules.

USC
UNIVERSIDADE
DE SANTIAGO
DE COMPOSTELA

Abrams, P. A. (2009). "When does greater mortality increase population size? The long story and diverse mechanisms underlying the hydra effect." In: *Ecology Letters* 12:5, pp. 462–474.

Agliari, A., P. Commendatore, I. Foroni, and I. Kubin (2011). "Border collision bifurcations in a footlose capital model with first nature firms." In: *Computational Economics* 38:3, pp. 349–366.

AlSharawi, Z. and M. B. H. Rhouma (2009). "The Beverton–Holt model with periodic and conditional harvesting." In: *Journal of Biological Dynamics* 3:5, pp. 463–478.

Aulbach, B. and B. Kieninger (2001). "On three definitions of chaos." In: *Nonlinear Dynamics and Systems Theory* 1:1, pp. 23–37.

Avilés, L. (1999). "Cooperation and non-linear dynamics: An ecological perspective on the evolution of sociality." In: *Evolutionary Ecology Research* 1:4, pp. 459–477.

Avrutin, V., L. Gardini, I. Sushko, and F. Tramontana (2019). *Continuous and Discontinuous Piecewise-Smooth One-Dimensional Maps*. Singapore: World Scientific.

Banerjee, S., M. S. Karthik, G. Yuan, and J. A. Yorke (2000). "Bifurcations in one-dimensional piecewise smooth maps-theory and applications to switching circuits." In: *IEEE Transactions on circuits and systems I: Fundamental Theory and Applications* 47:3, pp. 389–394.

Bernardo, M., C. J. Budd, A. R. Champneys, and P. Kowalczyk (2008). *Piecewise-smooth Dynamical Systems: Theory and Applications*. Vol. 163. Applied Mathematical Sciencies. London: Springer-Verlag.

Beverton, R. J. H. and S. J. Holt (1957). *On the Dynamics of Exploited Fish Populations*. Vol. II. Fishery Investigations. Ministry of Agriculture, Fisheries and Food.

Bier, M. and T. C. Bountis (1984). "Remerging Feigenbaum trees in dynamical systems." In: *Physics Letters A* 104:5, pp. 239–244.

Bischi, G. I., F. Lamantia, and F. Tramontana (2014). "Sliding and oscillations in fisheries with on–off harvesting and different switching times." In: *Communications in Nonlinear Science and Numerical Simulation* 19:1, pp. 216–229.

Blackwood, J. C., A. Hastings, and P. J. Mumby (2012). "The effect of fishing on hysteresis in Caribbean coral reefs." In: *Theoretical Ecology* 5:1, pp. 105–114.

Braverman, E. and E. Liz (2012). "Global stabilization of periodic orbits using a proportional feedback control with pulses." In: *Nonlinear Dynamics* 67:4, pp. 2467–2475.

Brianzoni, S., E. Michetti, and I. Sushko (2010). "Border collision bifurcations of superstable cycles in a one-dimensional piecewise smooth map." In: *Mathematics and Computers in Simulation* 81:1, pp. 52–61.

Butterworth, D. S. (1987). "A suggested amendment to the harvesting strategy used at ICSEAF to specify hake TAC levels." In: *Coll. scient. Pap. int. Commn SE Atl. Fish.* 14, pp. 101–108.

Clark, W. G. and S. R. Hare (2004). "A conditional constant catch policy for managing the Pacific halibut fishery." In: *North American Journal of Fisheries Management* 24:1, pp. 106–113.

Coppel, W. A. (1955). "The solution of equations by iteration." In: *Mathematical Proceedings of the Cambridge Philosophical Society* 51:11, pp. 41–43.

Corron, N. J., S. D. Pethel, and B. A. Hopper (2000). "Controlling chaos with simple limiters." In: *Physical Review Letters* 84:17, pp. 3835–3838.

Courchamp, F., L. Berec, and J. Gascoigne (2008). *Allee effects in ecology and conservation*. New York: Oxford University Press.

Cull, P. (2007). "Population models: stability in one dimension." In: *Bulletin of Mathematical Biology* 69:3, pp. 989–1017.

Cull, P. and J. Chaffee (2000). "Stability in discrete population models." In: *AIP Conference Proccedings* 517:1, pp. 263–276.

Deriso, R. (1985). "Risk averse harvesting strategies." In: *Resource Management*. Ed. by Marc Mangel. Vol. 61. Lecture Notes in Biomathematics. Berlin: Springer, pp. 65–73.

Deroba, J. J. and J. R. Bence (2008). "A review of harvest policies: Understanding relative performance of control rules." In: *Fisheries Research* 94:3, pp. 201–233.

Devaney, R. L. (1989). *An introduction to chaotic dynamical systems*. Advanced book program. United States of America: Addison-Wesley Publishing Company.

El-Morshedy, H. A. and V. Jiménez López (2008). "Global attractors for difference equations dominated by one-dimensional maps." In: *Journal of Difference Equations and Applications* 14:4, pp. 391–410.

Enberg, K. (2005). "Beneficts of threshold strategies and age-selective harvesting in a fluctuating fish stock of Norwegian spring spawing herring *Clupea harengus*." In: *Marine Ecology Progress Series* 298, pp. 277–286.

Engen, S., R. Lande, and B. E. Sæther (1997). "Harvesting strategies for fluctuating populations based upon uncertain population stimates." In: *Journal of Theoretical Biology* 186:2, pp. 201–212.

Franco, D. and F. M. Hilker (2013). "Adaptive limiter control of unimodal population maps." In: *Journal of Theoretical Biology* 337, pp. 161–173.

— (2014). "Stabilizing populations with adaptive limiters: prospects and fallacies." In: *SIAM Journal on Applied Dynamical Systems* 13:1, pp. 447–465.

Franco, D., J. Perán, and J. Segura (2020). "Stability for one-dimensional discrete dynamical systems revisited." In: *Discrete and Continuous Dynamical Systems - B* 25:2, pp. 635–650.

Gardini, L., F. Tramontana, V. Avrutin, and M. Schanz (2010). "Border-collision bifurcations in 1d piecewise-linearmaps and Leonov's approach." In: *International Journal of Bifurcations and Chaos* 20:10, pp. 3085–3104.

Glass, L. and W. Zeng (1994). "Bifurcations in flat-topped maps and the control of cardiac chaos." In: *International Journal of Bifurcation and Chaos* 4:4, pp. 1061–1067.
Granados, A., L. Alsedà, and M. Krupa (2017). "The period adding and incrementing bifurcations: from rotation theory to applications." In: *SIAM Review* 59:2, pp. 225–292.
Grebogi, C., E. Ott, and J. A. Yorke (1982). "Chaotic attractors in crises." In: *Physical Review Letters* 48:22, pp. 1507–1510.
— (1983). "Metamorphoses of basin boundaries in nonlinear dynamical systems." In: *Physical Review Letters* 56:10, pp. 1011–1014.
Hastings, A., K. C. Abbott, K. Cuddington, T. Francis, G. Gellner, Y. C. Lai, A. Morozov, S. Petrovskii, K. Scranton, and M. L. Zeeman (2018). "Transient phenomena in ecology." In: *Science* 361:6406, doi: 10.1126/science.aat6412.
Hilborn, R. (2012). "The evolution of quantitative marine fisheries management 1985–2010." In: *Natural Resource Modeling* 25:1, pp. 122–144.
Hilborn, R. and C. J. Walters (1992). *Quantitative Fisheries Stock Assessment: Choice, Dynamics and Uncertainty*. London: Chapman and Hall.
Hilker, F. M. and E. Liz (2019). "Proportional threshold harvesting in discrete-time population models." In: *Journal of Mathematical Biology* 79:5, pp. 1927–1951.
— (2020). "Threshold harvesting as a conservation or exploitation strategy in population management." In: *Theoretical Ecology* 13:4, doi: 10.1007/s12080–020–00465–8.
Hjerne, O. and S. Hansson (2001). "Constant catch or constant harvest rate?: The Baltic Sea cod (*Gadus morhua* L.) fishery as a modelling example." In: *Fisheries Research* 53:1, pp. 57–70.
Jiménez López, V. and E. Liz (2021). "Destabilization and chaos induced by harvesting: Insights from one-dimensional discrete-time models." In: *Journal of Mathematical Biology* 82:1, pp. 1–28.
Lasota, A. (1977). "Ergodic problems in biology." In: *Asterisque* 50, pp. 239–250.
Liz, E. (2010a). "Complex dynamics of survival and extinction in simple population models with harvesting." In: *Theoretical Ecology* 3:4, pp. 209–221.
— (2010b). "How to control chaotic behaviour and population size with proportional feedback." In: *Physics Letters A* 374:5, pp. 725–728.
— (2018a). "A global picture of the Gamma-Ricker map: a flexible discrete-time model with factors of positive and negative density dependence." In: *Bulletin of Mathematical Biology* 80:2, pp. 417–434.
— (2018b). "A new flexible discrete-time model for stable populations." In: *Discrete and Continuous Dynamical Systems - B* 23:6, pp. 2487–2498.
Liz, E. and S. Buedo-Fernández (2019). "A new formula to ger sharp global stability criteria for one-dimensional discrete-time models." In: *Qualitative Theory of Dynamical Systems* 18:3, pp. 813–824.

Liz, E. and D. Franco (2010). "Global stabilization of fixed points using predictive control." In: *Chaos: An Interdisciplinary Journal of Nonlinear Science* 20:2, doi: 10.1063/1.3432558.

Liz, E. and C. Lois-Prados (2020a). "A note on the Lasota discrete model for blood cell production." In: *Discrete and Continuous Dynamical Systems - B* 25:2, pp. 701–703.

— (2020b). "Dynamics and bifurcations of a family of piecewise smooth maps arising in population models with threshold harvesting." In: *Chaos: An Interdisciplinary Journal of Nonlinear Science* 30:7, pp. 1–16.

Liz, E. and A. Ruiz-Herrera (2012). "The hydra effect, bubbles, and chaos in a simple discrete population model with constant effort harvesting." In: *Journal of Mathematical Biology* 65:5, pp. 997–1016.

Lois-Prados, C. and F. M. Hilker (submitted). "Bifurcation sequences in a discontinuous piecewise-smooth map combining constant-catch and threshold-based harvesting strategies." In: *SIAM Journal on Applied Dynamical Systems*.

Ludwig, D. (1998). "Management of stocks that may collapse." In: *Oikos* 83, pp. 397–402.

Melbourne, I. (1991). "An example of nonasymptotically stable attractor." In: *Nonlinearity* 4:3, pp. 835–844.

Mitkowski, P. J. (2011). *Chaos in the Ergodic Theory Approach in the Model of Disturbed Erythropoiesis*. Cracow: PhD Thesis, AGH University of Science and Technology.

Nusse, H. E. and J. A. Yorke (1992). "Border-collision bifurcations including "period two to period three" for piecewise smooth systems." In: *Physica D: Nonlinear Phenomena* 57:1-2, pp. 39–57.

Podvigina, O. and P. Ashwin (2011). "On local attraction properties and a stability index for heteroclinic connections." In: *Nonlinearity* 24:3, pp. 887–929.

Punt, A. E. (2010). "Harvest control rules and fisheries management." In: *Handbook of Marine Fisheries Conservation and Management*. Ed. by R. Quentin Grafton, Ray Hilborn, Dale Squires, Maree Tait, and Meryl J. Williams. Oxford University Press, pp. 582–594.

Quinn, T. J. and R. B. Deriso (1999). *Quantitative Fish Dynamics*. New York: Oxford University Press.

Radi, D. and L. Gardini (2018). "A piecewise smooth model of evolutionary game for residential mobility and segregation." In: *Chaos: An Interdisciplinary Journal of Nonlinear Science* 28:5, doi: 10.1063/1.5023604.

Ricker, W. E. (1954). "Stock and recruitment." In: *Journal of the Fisheries Research Board of Canada* 11:5, pp. 559–623.

— (1975). *Computation and Interpretation of Biological Statistics of Fish Population*. Canada: Bulletin of Fisheries Research Board of Canada.

Schreiber, S. J. (2001). "Chaos and population disappearances in simple ecological models." In: *Journal of Mathematical Biology* 42:3, pp. 239–260.

— (2003). "Allee effects, extinctions, and chaotic transients in simple population models." In: *Theoretical Population Biology* 64:2, pp. 201–209.

Segura, J., F. M. Hilker, and D. Franco (2016). "Adaptive threshold harvesting and the suppression of transients." In: *Journal of Theoretical Biology* 395, pp. 103–114.
— (2020). "Degenerate period adding bifurcation structure of one-dimensional bimodal piecewise linear maps." In: *SIAM Journal on Applied Mathematics* 80:3, pp. 1356–1376.
Sinclair, A. R. E., J. M. Fryxell, and G. Caughley (2006). *Wildlife Ecology, Conservation, and Management*. Oxford: Blackwell.
Singer, D. (1978). "Stable orbits and bifurcation of maps of the interval." In: *SIAM Journal on Applied Mathematics* 35:2, pp. 260–267.
Sinha, S. (1994). "Unidirectional adaptative dynamics." In: *Physical Review E* 49:6, pp. 4832–4842.
Sinha, S. and S. Parthasarathy (1996). "Unusual dynamics of extinction in a simple ecological model." In: *Proceedings of the National Academy of Sciences* 93:4, pp. 1504–1508.
Steiner, E. M., K. R. Criddle, and M. D. Adkinson (2011). "Balancing biological sustainability with the economic needs of Alaska's sockeye salmon fisheries." In: *North American Journal of Fisheries Management* 31:3, pp. 431–444.
Sushko, I., L. Gardini, and K. Matsuyama (2014). "Superstable credit cycles and U-sequences." In: *Chaos, Solitons and Fractals* 59, pp. 13–27.
Thunberg, H. (2001). "Periodicity versus chaos in one-dimensional dynamics." In: *SIAM Review* 43:1, pp. 3–30.
Wazewska-Czyzewska, M. and A. Lasota (1976). "Mathematical problems of the red blood cell system." In: *Matematyka Stosowana* 6, pp. 25–40.
Wiggins, S. (1990). *Introduction to applied nonlinear dynamical systems and chaos*. Texts in Applied Mathematics. New York: Springer-Verlag.
Yakubu, A. A., N. Li, J. M. Conrad, and M. L. Zeeman (2011). "Constant proportion harvest policies: Dynamic implications in the Pacific halibut and Atlantic cod fisheries." In: *Mathematical Biosciences* 232:1, pp. 66–77.

USC
UNIVERSIDADE
DE SANTIAGO
DE COMPOSTELA

GLOSSARY

RESEARCH LINE I

Abbreviation/symbol	Meaning
(X, d) or (I, d)	metric spaces
$B(x, \varepsilon)$	open ball of center $x \in X$ and ratio $\varepsilon > 0$
$\overline{D}$	closure of a set D, $D \subset X$
$\alpha(A)$	Kuratowski measure of noncompactness of A, $A \subset X$
$\operatorname{diam}(B)$	$\sup\{d(x, y) : x, y \in B\}$, $B \subset X$
$(X, \|\cdot\|)$ or $(I, \|\cdot\|)$	Banach spaces
$\|\cdot\|$	absolute value in $\mathbb{R}$
$(\mathcal{C}(I, \mathbb{R}^n), \|\cdot\|_\infty)$	Banach space of continuous functions from I to $\mathbb{R}^n$ with $\|x\|_\infty = \max_{i=1,\dots,n} \max_{t\in I} \|x_i(t)\|$, $x = (x_1, \dots, x_n)$
$\mathcal{C}(I, \mathbb{R}_+)$	set of continuous functions from I to the non negative real numbers $\mathbb{R}_+$
$\mathcal{C}^1(I, \mathbb{R}^n)$	set of continuous differentiable functions from I to $\mathbb{R}^n$
$\left(\mathcal{C}_\omega\left(\mathbb{R}, \mathbb{R}^2\right), \|\cdot\|_\omega\right)$	Banach space of pairs (x, y), where $x, y \in \mathcal{C}(\mathbb{R}, \mathbb{R})$ are ω-periodic functions, with $\|(x, y)\|_\omega := \|x\|_\infty + \|y\|_\infty$
$\operatorname{co}(A)$	convex hull of A, $A \subset X$
T or N	operators between subsets of metric or Banach spaces
C	cone in a Banach space X
$C_{r,R}$	$\{x \in C : r \leqslant \|x\| \leqslant R\}$, with $0 < r < R$
B_r	$\{x \in C : \|x\| \leqslant r\}$
S_r	$\{x \in C : \|x\| = r\}$
(V1)-(V2)	vector version compression-expansion conditions
(H,E1)-(H,E2)	homotopy version expansion conditions
E	x_0-star convex set ($x_0 = 0$, star convex set)
F	boundary of E
β_x	unique positive real number such that $\beta_x x \in F$, $x \in E$
∂	continuous map from $E\backslash\{0\}$ to F, $\partial(x) \equiv \beta_x x$
β	continuous map from $E\backslash\{0\}$ to $[1, \infty)$, $\beta(x) \equiv \beta_x$
∂^C, β^C	extensions of ∂, β to $C\backslash\{0\}$

Abbreviation/symbol	Meaning
(C1)-(C2)	compression conditions in $C \cap (E_2 \backslash \mathring{E}_1)$
(E1)-(E2)	expansion conditions in $C \cap (E_2 \backslash \mathring{E}_1)$
φ, ψ	functionals from a Banach space X into $[0, \infty)$
E_r	$\{x \in X : \varphi(x) \leqslant r\}$
F_r	$\{x \in X : \varphi(x) = r\}$
x	prey population
y	predator population
a	percapita intrinsic growth of preys
b	percapita mortality rate of predators
λ	attack rate of predators
c	conversion efficiency
g	general prey growth
$g(x) \equiv 1$	linear prey growth
$g(x) \equiv 1 - x/K$	logistic prey growth
K	carrying capacity of preys population
φ	general functional response of predators
φ_I, φ_{II}	particular expressions of φ including cooperation between predators
α	hunting cooperation
ω	period of the functions in the Lotka-Volterra models
(G1)-(G2)	conditions required to φ
η, ψ	auxiliary functions in **(G1)-(G2)**

Abbreviation/symbol	Meaning
x_n	population size at generation n
ICs	initial conditions
h	map defining a general discrete-time dynamical system $x_{n+1} = h(x_n)$
h_s	auxiliary S-unimodal mapping in $h(x) = (1-\sigma)x + \sigma h_s(x)$, $\sigma \in (0,1)$
x^*	fixed point of a general map
f	production or stock-recruitment curve
K	fixed point of the map f satisfying **(A1)**
x_c	critical point of a map f satisfying **(A2)**
$\tilde{x}$	point such that $f'(\tilde{x}) = 1$ of a map f satisfying **(A2)**
$\overline{x}$	(smallest) point such that $f'(\overline{x}) = -1$ of a map f satisfying **(A2)** with $x_c < \infty$
LAS	locally asymptotically stable
GAS	globally asymptotically stable
BD	bifurcation diagram
SB	smooth bifurcation
BCB	border-collision bifurcation
H	(maximum) harvesting quota
T	threshold harvesting parameter
g	$g(x) := f(x) - H$
x^*_-, x^*_+	positive fixed points of g ($0 < x^*_- \leqslant \tilde{x} \leqslant x^*_+ < K$)
CC	constant catch harvesting
F_{CC}	map defining the CC rule
TH	(pure) threshold harvesting rule
F_{TH}	map defining the TH rule
TCC	threshold constant catch harvesting
F_{TCC}	map defining the TCC rule
PTCC	precautionary TCC
F_{PTCC}	map defining the PTCC rule
Y_n	yield or catch at generation n
$\overline{Y}$	average yield
MSY	maximum sustainable yield
HF	harvest frequency

Abbreviation/symbol	Meaning
σ	blood cell destruction rate
$1-\sigma$	adult population survivorship rate
γ	degree of disturbance in the blood cell production process or strength of population cooperation
F_{BC}	map defining the Lasota blood cell production model
p, q	positive fixed points of F_{BC}

TRANSFER OF COPYRIGHT / PUBLISH AGREEMENT

In order to accomplish the requirements stated in the document *Reglamento de los estudios de doctorado en la USC* published in the *Diario Oficial de Galicia* on September 16th , 2020, we include here the authorizations of the different journals, signed in the transfer of copyright or publish agreement documents, to use the contents of the published articles in the present thesis document:

Proceedings of the Royal Society of Edinburgh, Section A: Mathematics

"You may reproduce the article or an adapted version of it in any volume of which you are editor or author subject to normal acknowledgment."

Journal of Fixed Point Theory and Applications

"Author(s) retain the following non-exclusive rights for the published version provided that, when reproducing the Article or extracts from it, the Author(s) acknowledge and reference first publication in the Journal:
to reproduce, or to allow a third party Licensee to reproduce the Article in whole or in part in any printed volume (book or thesis) written by the Author(s)."

Nonlinear Analysis: Real World Applications

"The Author Rights include the right to use the Preprint, Accepted Manuscript and the Published Journal Article for Personal Use and Internal Institutional Use. They also include the right to use these different versions of the Article for Scholarly Sharing purposes.
In the case of the Accepted Manuscript and the Published Journal Article the Author Rights exclude Commercial Use (unless expressly agreed in writing by Elsevier Ltd), other than use by the author in a subsequent compilation of the author's works or to extend the Article to book length form or re-use by the author of portions or excerpts in other works (with full acknowledgment of the original publication of the Article)."

Chaos: An Interdisciplinary Journal of Nonlinear Science

"Each Copyright Owner may:
Reprint the Version of Record (VOR) in print collections written by the Author, or in the Author's thesis or dissertation. It is understood and agreed that the

thesis or dissertation may be made available electronically on the university's site or in its repository and that copies may be offered for sale on demand."

Discrete and Continuous Dynamical Systems - B

"The Author(s) shall, without limitation, have the non-exclusive right to use, reproduce, distribute, create derivative works including update, perform, and display publicly, the Work in electronic, digital or print form in connection with the Author(s)' teaching, conference presentations, lectures, other scholarly works, and for all of Author(s)' academic and professional activities, provided any electronic reproduction faithfully renders the appearance and functionality of each page in its entirely exactly as published online in the Journal."

USC
UNIVERSIDADE
DE SANTIAGO
DE COMPOSTELA

USC
UNIVERSIDADE
DE SANTIAGO
DE COMPOSTELA